Technische Universität München

Fakultät für Chemie

Professur für Siliciumchemie

Experimental and Theoretical Investigations concerning the Reactivity of low-valent Silicon and Aluminium Species

Amelie Simona Porzelt

Vollständiger Abdruck der von der Fakultät für Chemie der Technischen Universität München zur Erlangung des akademischen Grades eines

Doktors der Naturwissenschaften (Dr. rer. nat.)

genehmigten Dissertation.

Vorsitzender: Prof. Dr. Job Boekhoven

Prüfende der Dissertation:

1. Prof. Dr. Shigeyoshi Inoue

2. Prof. Dr. Max C. Holthausen

3. Lecturer Dr. Michael Cowley

Die Dissertation wurde am 06.05.2020 bei der Technischen Universität München eingereicht und durch die Fakultät für Chemie am 25.08.2020 angenommen

Kurzfassung

Die Chemie der Hauptgruppenelemente hat in den letzten Jahrzehnten durch die Erkenntnis, dass niedervalente Hauptgruppenverbindungen Reaktivitäten besitzen, die bisher nur für Übergangsmetalle bekannt waren, eine Renaissance erfahren. Die zugrundeliegenden Struktur-Reaktivitätsbeziehungen sind jedoch noch zu wenig erforscht. Diese Arbeit befasst sich mit der fundamentalen Forschung von niedervalenten Silicium und Aluminium Verbindungen in einem kombinierten experimentellen und theoretischen Ansatz. Das übergreifende Ziel ist es die Grundlagen für eine zukünftige Anwendung in der Katalyse zu legen. Dazu werden Kombinationen von sterisch-anpassbaren Aryl- oder elektropositiven Silylliganden mit *N*-heterozyklischen Iminen oder Carbenen als Elektronendonor verwendet, um diese Verbindungen isolieren zu können. Verschiedene Methoden der Bindungsanalyse ermöglichen den Einblick in ihre elektronische Struktur, die eine starke Abhängigkeit von der Art der Liganden aufweist. Dies ermöglicht im Folgenden die Reaktivität der Verbindungen durch die Wahl der Liganden zu beeinflussen. Die Anwendung der Verbindungen in der Aktivierung kleiner Moleküle, wie z.B. Wasserstoff, Kohlenstoffmonoxid oder Schwefelwasserstoff, wird unter Einbeziehung theoretischer Studien untersucht. Im Rahmen dieser Arbeit wurden diverse neue Strukturmotive erhalten, wie z.B. isolierbare Dialumene, bei Raumtemperatur stabile Silanone sowie Siliciumcarbonyle, die die Möglichkeit hervorheben Hauptgruppenelemente wie Übergangsmetalle einzusetzen.

Abstract

Main group chemistry has experienced a renaissance in the last decades with low-valent main group compounds resembling transition-metal reactivity. However, detailed insight to the fundamental structure-reactivity relation is mostly missing. This thesis aims to address this gap, through the development of low-valent silicon and aluminium compounds in a combined experimental and theoretical approach. The overarching aim is to set the stage for future catalytic application. Combinations of sterically tuneable aryl or electropositive silyl ligands together with electron-donating *N*-heterocyclic imines or carbenes are employed to enable the isolation of acyclic silylenes, silyliumylidene ions and dialumenes. Different bonding analysis methods are employed to provide insight into their electronic structure, revealing high dependency of the nature of the attached ligands. This enabled the possibility of tuning the reactivity *via* new molecular design. The application of these species in the activation of small molecules, such as dihydrogen, carbon monoxide or hydrogen sulphide, is explored and assisted by theoretical mechanistic evaluations. In the course of this work a variety of new structural motifs were achieved, such as the first isolable dialumenes, room-temperature stable silanones and silicon carbonyl complexes, further highlighting the ability of main group elements to act as transition-metals.

Diese Arbeit wurde in der Zeit von Mai 2016 bis April 2020 in der Arbeitsgruppe von Prof. Dr. S. Inoue an der Technischen Universität München angefertigt.

Das Leben ist schön.

Lotte Porzelt

Acknowledgements

Mein besonderer Dank gilt Herrn Professor Dr. Shigeyoshi Inoue für die Möglichkeit in seiner Gruppe zu niedervalenter Hauptgruppenchemie an äußerst spannenden und gleichzeitig sehr aktuellen Fragen der Silicium-/Aluminiumchemie zu forschen. Bedanken möchte ich mich insbesondere für die zahlreichen Diskussionen im Labor, für dein schier unendliches Ideenreichtum und deine unermüdliche Energie neues zu entdecken. Außerdem danke ich dir für die umfassende Unterstützung diese Arbeit in einer Kombination aus theoretischen Rechnungen und Experimenten schreiben zu dürfen.

Des Weiteren möchte ich mich bei Herrn Professor Dr. Max C. Holthausen bedanken. Die Kooperation mit dir und deiner Arbeitsgruppe hat mir die Möglichkeit gegeben, sehr viel tiefer in die theoretische Chemie einzusteigen, als ich es am Anfang meiner Promotionszeit für möglich hielt. Mehrere Forschungsaufenthalte in Frankfurt sowie deine konstruktive Kritik führte stets dazu, Ideen weiter zu entwickeln und zu verbessern. Ganz besonders möchte ich mich für das Vertrauen und die Bereitschaft bedanken in laufende Projekte einzusteigen.

Danken möchte ich darüber hinaus allen aktiven, ehemaligen und temporären Mitgliedern der Arbeitsgruppe Inoue. Insbesondere danke ich allen denjenigen, die mit ihren experimentellen Arbeiten die Grundlage für theoretische Untersuchungen geliefert haben. Außerdem bedanke ich mich bei allen Postdocs Dr Daniel Franz, Dr. Vitaly Nesterov, Dr. Prasenjit Bag, Dr. Samuel Powley, Dr. Catherine Weetman und Dr. Shiori Fujimori für ihre Unterstützung, ihren Rat und das Teilen ihrer Erfahrung. Ganz besonderer Dank geht an den „AK Inoue Lunch Club“, Gizem, Cath und Daniel (und Shiori). Cath und Gizem: Die gemeinsame Laborzeit mit euch war einfach spitze!

Außerdem danke ich Richard Wetzel und Anika Kwiatkowski für ihre Unterstützung bei der Bewältigung (nicht-)alltäglicher Probleme innerhalb und außerhalb der Uni. Darüber hinaus danke ich Ben für die unzähligen Diskussionen zu theoretischen Fragestellungen.

Der Gruppe von Max Holthausen an der Goethe Universität Frankfurt (Dr. Julia Schweizer, Dr. Lioba Meyer, Uhut Karacas sowie dem Concept Manager Ammo) danke ich für ihre „temporäre“ Aufnahme in ihre Gruppe, die Unterstützung bei meinen eigenen Forschungsfragen und für die gemeinsamen Konferenzbesuche.

Dem XRD-Team, Dr. Philipp J. Altmann, Dr. Daniel Franz, Daniel Henschel und Philipp Frisch, danke ich für die Messungen meiner Kristalle.

Für das unermüdliche Korrigieren dieser Arbeit in der Endphase danke ich meinen Korrekturlesern Cath, Ben und Ulli mit Andi ;-).

List of Abbreviations

12C4 12-crown-4 ether
2c-2e bond two-centre two-electron bond
3c-2e bond three-centre two-electron bond
3c-4e bond three-centre four-electron bond
4-PPy 4-pyrollidinopyridine
Ad 1-adamantyl
AO atomic orbital
Bbp 2,6-$(CHTMS_2)_2$-C_6H_3
Bbt 2,6-$(CHTMS_2)_2$-4-$CTMS_3$-C_6H_2
BCF $B(C_6F_5)_3$
BCP bond critical point
*c*AAC cyclic alkyl(amino)carbene
CC couples cluster
CCP cage critical point
CGMT Carter-Goddard-Malrieu-Trinquier
CI configuration interaction
COT 1,3,5,7-cyclooctratetraene
cp critical point
Cp cyclpentadienyl
Cp* Me_5-Cp
Cp^{tBu3} 1,3,5-tri-^{t}Bu-cyclopentadienyl
Cy cyclohexyl, C_6H_{11}
d days
DFT density functional theory
Dipp 2,6-^{i}Pr$_2$-C_6H_3
DMAP 4-*N,N*-dimethylaminopyridine
DME dimethoxyethane
EDA energy decomposition analysis
Eind 1,1,3,3,5,5,7,7-octaethyl-s-hydrindacen-4-yl
EMind 1,1,7,7-tetraethyl-3,3,5,5,-tetramethyl-s-hydrindacen-4-yl
EPR Electron paramagnetic resonance
GGA generalized gradient approximation
GIAO Gauge-Independent Atomic Orbitals
IDipp :C[N(2,6-^{i}Pr$_2$-C_6H_3)CH]$_2$
IDippN NC[N(2,6-^{i}Pr$_2$-C_6H_3)CH]$_2$
IEt_2Me_2 :C[NEtCMe]$_2$
$I^iPr_2Me_2$:C[N^{i}PrCMe]$_2$
IMe_2H_2 :C[NMeCH]$_2$
IMe_4 :C[NMeCMe]$_2$
IRC intrinsic reaction coordinate
I^{t}BuN NC[N^{t}BuCH]$_2$
LCAO linear combination of atomic orbitals
LDA local density approximation
LSD local spin-density approximation
Mes Mesityl (2,4,6-Me_3-C_6H_2)
Mes* 2,4,6-^{t}Bu$_3$-C_6H_2
MP Møller-Plesset
*m*Ter 2,6-Mes_2-C_6H_3
*m*Ter^{Dipp} 2,6-$Dipp_2$-C_6H_3
NAO natural atomic orbital
NBO natural bond orbital
NCP nuclear critical point
NHBO $[OB(NDippCH)_2]^-$, *N*-heterocyclic boryloxy
NHC *N*-heterocyclic carbene
NHI *N*-heterocyclic imines
NHO *N*-heterocyclic olefin
NHOs natural hybrid orbitals
NHSi *N*-heterocyclic silylene
NLMO natural localized molecular orbital
NNA non-nuclear attractor
NON 4,5-bis(2,6-diisopropylanilido)-2,7-di-^{t}Bu-9,9-dimethylxanthene
NRT Natural Resonance Theory
OTf triflate, trifluoromethanesulfonate
PBE *Perdew-Burke-Ernzerhof*
PES potential energy surface
PGTO primitive *Gaussian* type orbitals
QTAIM Quantum Theory of Atoms in Molecules
RCP ring critical point
rt room temperature
SCF self-consistent field approach
SC-XRD Single Crystal X-ray Diffraction
$SiTMS_3$ hypersilyl group
Tbb 2,6-$(CHTMS_2)_2$-4-^{t}Bu-C_6H_2
Tbt 2,4,6-$(CHTMS_2)_3$-C_6H_2
^{t}Bu *tert*-butyl
TD-DFT time-dependent DFT
THF tetrahydrofuran
Tipp 2,4,6-^{i}Pr$_3$-C_6H_2
TMS trimethylsilyl, $SiMe_3$
TNL Total non-*Lewis*
tol toluene
TS transition state
UEG uniform electron gas
UNEP United Nations Environment Programme
UNESCO United Nations Educational, Scientific and Cultural Organization
VSCC valence shell charge concentration
WBI *Wiberg* bond index
WCA weakly coordinating anion
WEEE waste electronic and electric equipment
Xyl 2,6-Me_2-C_6H_3
ΔE_{ST} singlet-triplet gap

Table of Contents

1. Introduction

To celebrate the 150th birthday of the periodic table, introduced by Dmitri I. Mendeleev in 1869,[1-2] the United Nations Educational, Scientific and Cultural Organization (UNESCO) designated 2019 as the International Year of the Periodic Table of Elements. Mendeleev and Lothar Meyer separately developed the classification of elements dependent on their atomic weight.[3-5] This classification arranged the elements into groups, taking into account chemical similarities, as well as into periods, according to their ascending molecular weight. The periodic table used nowadays is a modified version of the one proposed 150 years ago. Newfound elements, some of which were originally proposed to exist by Mendeleev, have been added and the sorting changed from atomic weight to atomic number, and hence the periodic table is the world's widest spread chemical tool nowadays.[6]

In light of the international festivities all around the world, a descriptive version of the periodic system showing the natural abundance of each element was designed (Figure 1). With regard to limited resources available for an increasing global population, it explicitly highlights elements, which are in danger of running out for the next generations. This situation is aggravated by the fact that resources are not equally split around the globe and some critical elements are mined under conditions not in agreement with human rights (conflict minerals in Figure 1). Unambiguously, an alternative source could be recycling of those elements. However, critical elements like tantalum, gallium or arsenic, nowadays are widely used in standard mobile devices (also marked in Figure 1) and have an end-of-life recycling rate below 1% according to a report from the United Nations Environment Programme (UNEP).[7-8]

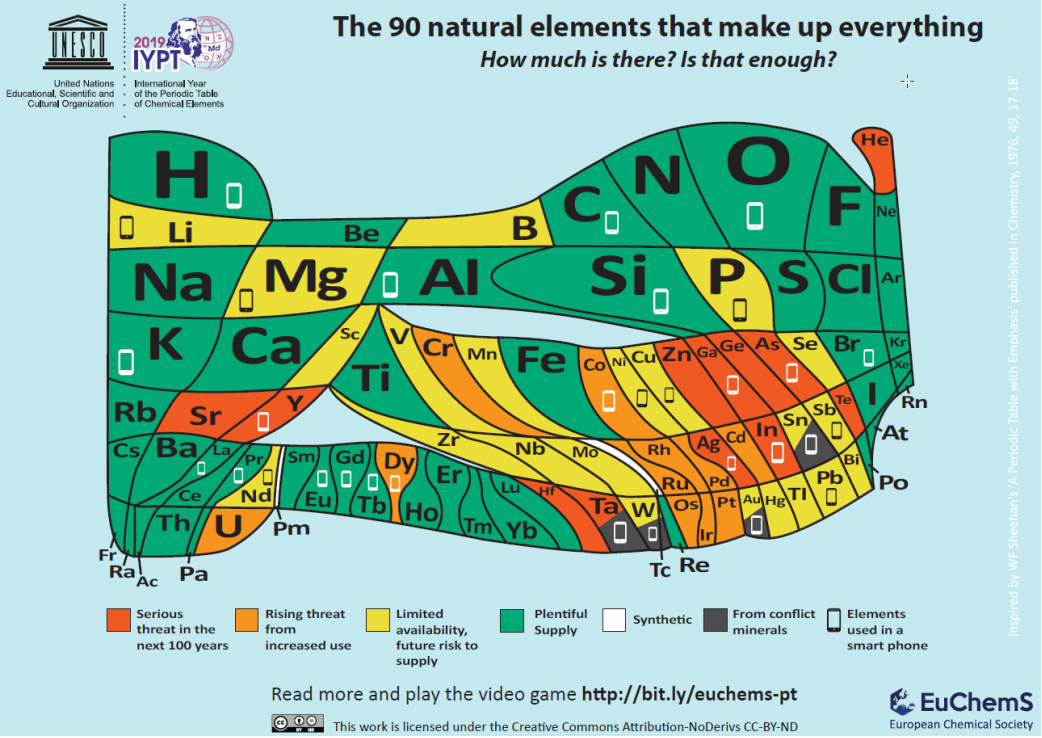

Figure 1: Periodic table of elements illustrating element scarcity. Elements in grey are harvested in conflict minerals and elements, which are used in a standard smart phone, are marked with a phone.[9]

Low recycling rates are due to different reasons: economical - as existing recycling methods are too expensive to be applied on a huge scale - or technological - because there are currently no methods to recycle some elements effectively. Thus, chemical research is required to develop environmentally benign and energy-efficient methods to boost recycling of those resources.[10] Besides technical reasons, one aim for the development and spread of Figure 1 in social media was to raise awareness in the limited supply

of elements. This particularly highlights elements present in waste electronic and electric equipment (WEEE) and therefore encourages an increase in recycle rates.[11]

Aside from the concerns of limited resources for everyday objects, another important issue arises upon examination of transition-metal groups 8 to 10, as these metals are widely used across diverse applications in industry. In Figure 1, this group is mainly marked orange, with the exception of iron as being abundant within the Earth's crust (Figure 2a), and nickel, which however is already marked yellow. These groups are furthermore highly important for chemical industry, as they are widely used in catalytic processes. To address a few examples: the so-called "Monsanto Process"[12] - a rhodium-catalysed carbonylation of methanol to yield acetic acid -, hydroformylation reactions originally discovered by Otto Roelen[13] - carbonylation of unsaturated hydrocarbons *via* rhodium or cobalt based catalysts - or the "second Wacker process"[14] - selective ethylene oxidation *via* a combined palladium/copper catalytic cycle.[15-18] In light of their limited availability, their uses as homogenous catalysts faces further problems: incomplete recycling of the catalyst from the reaction medium as well as residual toxic transition-metals contained in the obtained products.[15-16,18]

Recent years have brought forward different concepts to overcome the use of expensive transition metals and replace them with cheaper and more ecologically friendly resources by using either non-precious metal or non-metal based catalysts.[19-24] Beyond these developments, fundamental research in low-valent main group compounds has succeeded in the resemblance of transition-metal reactivity (Figure 2b-d), although catalytic applications are still limited to few examples.[25-29]

Besides oxygen, silicon and aluminium are the most abundant elements found within the Earth's crust (Figure 2a), they are environmentally benign and thus ideal candidates to replace transition metals in catalysis. Different to transition-metal compounds which enable the activation of H_2 *via* strong back-donation from the metal d-orbitals to the σ*-orbitals of H_2 (Figure 2b), main group elements lack these d-orbitals. However, this can be compensated by the ambiphilicity of low-valent main group species (Figure 2c,d).

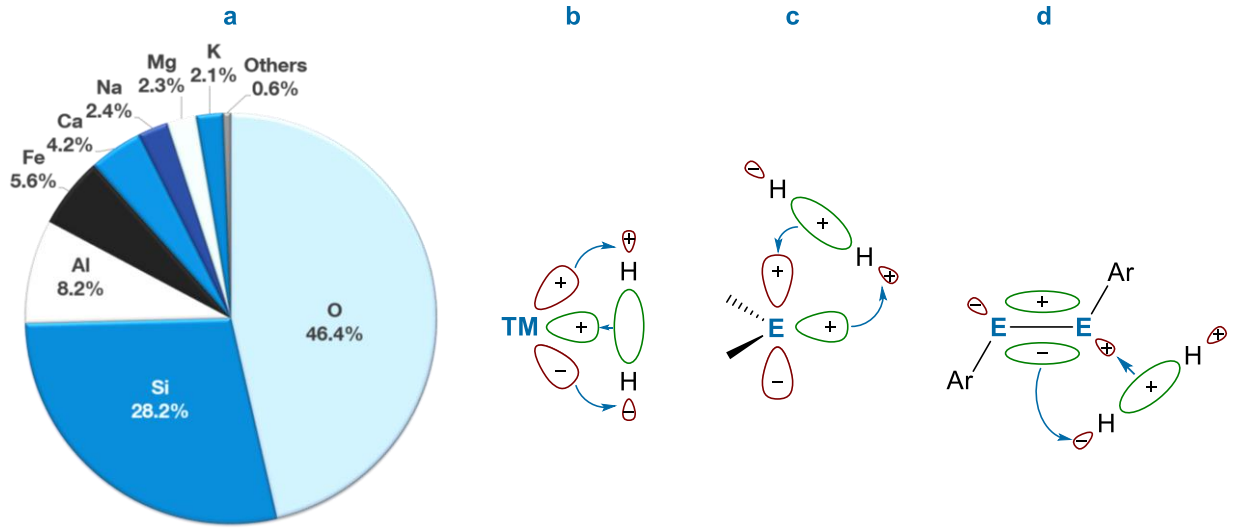

Figure 2: (**a**) Abundance of chemical elements in the Earth crust;[30] Interaction of the frontier orbitals of H_2 with (**b**) transition metals, (**c**) singlet main group species (like tetrylenes) and (**d**) main group multiple bonds.

This thesis develops the fundamental research of low-valent silicon and aluminium compounds in a combined experimental and theoretical approach, with the overarching aim to set the stage for their future catalytic application.

2. Low-Valent Silicon Chemistry

Although belonging to the same group (group 14), the properties of carbon and its heavier homologue silicon diverge drastically: the electronegativity (Pauling electronegativity scale) decreases from 2.55 to 1.90, silicon is more polarizable and its atomic radius is significantly increased (C: 0.70 Å, Si: 1.10 Å).[31] This results in completely different characteristics, for example, upon comparison of the simplest alkane CH_4 and silane SiH_4: the silane decomposes explosively upon contact with air whilst methane is stable. This difference is rationalized by the inversion of polarity for $C^{\delta-}$–$H^{\delta+}$ and $Si^{\delta+}$–$H^{\delta-}$ bonds.[32] On comparison of the sizes of the s- and p-orbitals for C and Si, there is a 20% increase in size difference for the latter. This reduces the orbital overlap which gives rise to decreased hybridisation for Si.[33]

The high reactivity of silicon species is also apparent upon comparison of silylium ions R_3Si^+ with the lighter homologues, carbenium ions R_3C^+ (Figure 3). The carbon version is an intermediate in S_N1 reactions, isolable and used as hydride abstraction reagent, e.g. $[Ph_3CBF_4]$,[34] whereas the silicon version was only isolated by Lambert in 1997.[35] The silicon centre with its unoccupied p-orbital exhibits an enormous electrophilicity, which possesses reactivity towards any available nucleophile including inert solvents and even counter anions.[36] Lambert used the mesityl (Mes = 2,4,6-Me_3-C_6H_2) group to sterically protect the silicon centre in his silylium ion $[Mes_3Si][B(C_6F_5)_4]$. However, structural verification *via* SC-XRD (Single Crystal X-ray Diffraction) analysis required anion exchange to the *closo*-carborane anion $[HCB_{11}Me_5Br_6]^-$.[37]

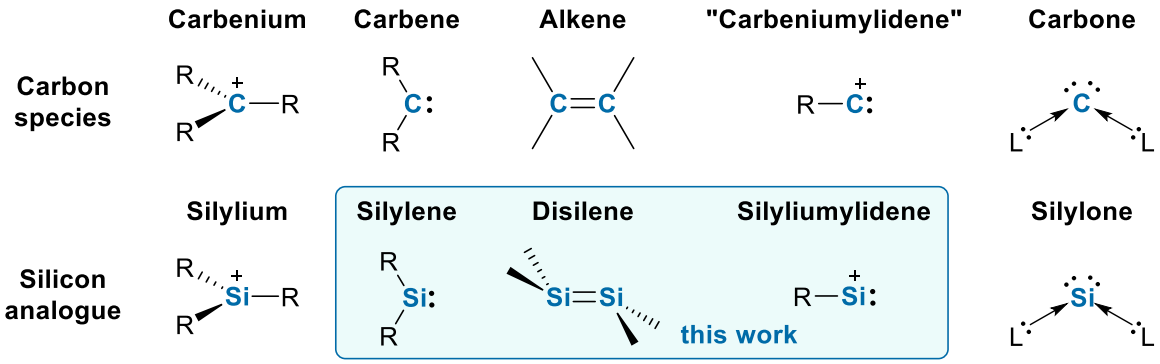

Figure 3: Overview of low-valent carbon and silicon species.

In nature silicon is only found in oxidation state +IV, as it bears an increased tendency to undergo disproportion reactions from oxidation state +II in comparison to carbon.[32] On further descending the group 14, the preference for lower oxidation states increases again, which is reflected in mostly lead +II compounds found in nature. This is a consequence of further reduced hybridisation as well as additional relativistic effects and is termed “inert-pair” effect.[32-33,38] Going down the group 14, the preferred electronic ground state for the parent tetrylene H_2E (E = C, Si, Ge, Sn, Pb) changes from the triplet state for carbon to a singlet ground state for silicon and the heavier congeners (Figure 4).[32] This schematic view also nicely depicts the ambiphilic character of silylenes: they feature a vacant p-orbital representing the highly reactive *Lewis* acidic site, as well as a nucleophilic, although rather inert, *Lewis* basic lone pair. The lone pair has substantial s-character due to decreased hybridisation as discussed previously.

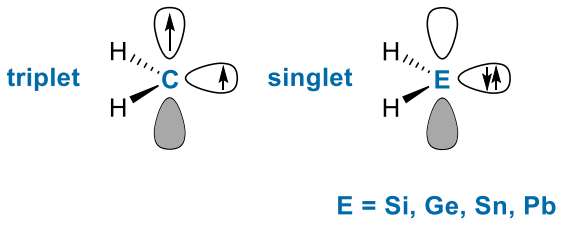

Figure 4: Frontier orbitals of carbenes and the heavier homologues.

To enable the isolation of reactive species like silylenes, two main concepts can be applied: (i) intra- or intermolecular electron donors, which partially occupy the empty p-orbital and/or (ii) kinetic stabilisation *via* sterically demanding groups to shield the empty p-orbital from the attack of nucleophiles (see chapter 2.1). The use of sterically demanding groups bears a second important feature: it prohibits the dimerisation of silylenes to disilenes (Figure 3, see chapter 2.2). Ligand removal from carbenes or silylenes yields their cationic form, called "carbeniumylidenes" or silyliumylidenes ions. The carbon version has been subject to studies in astrophysics,[39] gas-phase spectroscopy[40-41] and theoretical chemistry[42-43] for the diatomic $X–C^+$ with X = H, F, Cl, but to the best of our knowledge an isolable "carbeniumylidene" ion has not been reported to date. By contrast, the silicon version is isolable applying the concepts discussed above (see chapter 2.3). To complete the series of low-valent species, the so-called carbones and silylones, where the central atom is in the formal oxidation state of zero, should be noted. These species are however not part of this thesis.

2.1. Silylenes

As already stated above, silylenes exhibit a singlet electronic ground state (Figure 4), giving rise to a highly reactive species due the *Lewis* acidic lone pair and high tendency to undergo oligiomerisation reactions. Thus, silylenes require specific tuning of the electronic and steric effects of the ligands to enable their isolation. Generally, electron-withdrawing groups increase the s-character of the silicon lone pair *via* inductive effects. In combination with π-donor properties, e.g. as being the case for nitrogen-, phosphorous- or sulphur-based ligands, the empty p-orbital at the silicon centre becomes partially occupied, thereby reducing the *Lewis* acidity of the respective silylene. The opposite holds true for electropositive substituents, e.g. silyl- or boryl groups, as they lack π-donor properties and thus yield even higher reactivity.

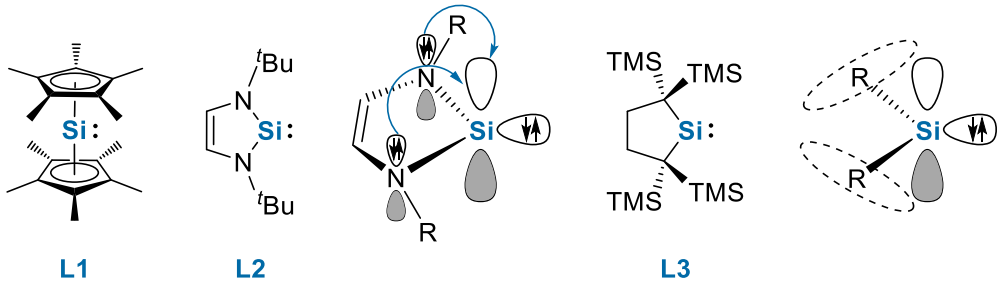

Figure 5: Important examples of the first isolable silylenes including the schematic orbital interactions for stabilisation *via* intramolecular electron donation or steric protection of the empty p-orbital, ^{t}Bu = *tert*-butyl , TMS = trimethylsilyl, $SiMe_3$.

The first isolable monomeric silylene, decamethylsilicocene **L1** (Figure 5), was synthesized by Jutzi in 1986.[44] SC-XRD analysis revealed two independent units: one exhibiting coplanar orientation of the Cp* ligands (Cp* = Me_5-Cp, Cp = cyclpentadienyl) and the second bearing an angle of 25.3° between the two Cp*-planes. Although representing the first example of an isolable divalent silicon species, it is generally not considered a typical silylene as it exhibits a rather nucleophilic character and a high coordination number due to η^5-arrangement of both Cp* units.[45-46] Denk *et al.* succeeded in the isolation of the first di-coordinate silylenes **L2**,[46] belonging to the group of *N*-heterocyclic silylenes (NHSi). Stabilisation in **L2** is achieved by the two amino groups attached to the silicon atom in a heterocycle (∢NSiN = 90.5°), which yields effective electron donation from the nitrogen lone pairs into the empty p-orbital at the silicon centre. This concept had already been proven useful for the carbon congener N-heterocyclic carbenes (NHC), which were isolated by Arduengo in 1991.[47] Kira succeeded in the isolation of the carbocyclic bis(alkyl)silylenes **L3**, proving π-donors attached to silicon centre not being necessary for stabilisation of this silylene. It is solely stabilised by steric shielding of the silicon centre by the flanking trimethylsilyl (TMS) groups, which however results in decomposition to a cyclic silene *via* 1,2-silyl migration above 0 °C even in the solid state.[48] After those pioneering studies, a plethora of NHSis with varying substituents at the

nitrogen atoms (called "wingtips") as well as modification of the backbone were described.[36] In 2006, Driess and Roesky introduced two new types of cyclic silylenes in a conjugated six-membered heterofulvene ring[49] as well as a chloro-silylene possessing a N,N-di(^{t}Bu)amidinato ligand,[50] both of which have been extensively studied concerning their reactivity as well as their application as transition-metal ligands.[51-52]

Donor-stabilised Silylenes

Upon switching to acyclic silylenes, stabilisation *via* intermolecular electron donors seemed to be crucial for quite some time. The previously mentioned NHCs possess various possibilities to tailor their properties. They are strong σ-donors and bear tuneable π-acceptor properties upon exchange of one amino group by different atoms as well as different ring sizes being possible. Furthermore, they bear a tremendous variety in their steric demand, which is tailorable *via* different groups at the wingtips.[53] Additionally, the backbone can be saturated or unsaturated, with the latter allowing for an alternate coordination mode through the C^4 as an "abnormal" carbene.[54-55] Exchange of one amino group to an alkyl group gives the so-called cyclic alkyl(amino)carbenes (*c*AAC),[56] which were introduced by Bertrand in 2005.[57]Thus, they are ideal candidates to stabilise otherwise elusive species, as shown by Robinson in 2008 upon isolation of a neutral Si_2 core with silicon in oxidation state zero, which is stabilised by two IDipp (:C[N(2,6-^{i}Pr$_2$-C$_6$H$_3$)CH]$_2$) moieties (**L4** in Figure 6).[58]

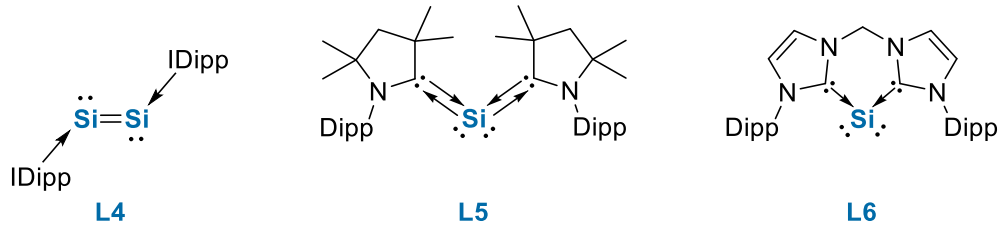

Figure 6: Examples of low-valent NHC-stabilised silicon species; Dipp = 2,6-^{i}Pr$_2$-C$_6$H$_3$.

In 2009, Filippou[59] and Roesky[60] were successful in the isolation of dihalo-substituted NHC-stabilised silylenes **L7**/**L8** (Figure 7) and published their results back to back. The two silylenes are however accessed *via* two different routes. Firstly, the di(bromo)-substituted **L8** is obtained stepwise *via* initial coordination of the NHC to the silicon centre in $SiBr_4$, with one bromide leaving as the counter anion and then subsequent reduction with KC_8. Alternatively, treatment of tri(chloro)-silane with two equivalents of IDipp yields the di(chloro)-substituted **L7** and the imidazolium salt of the carbene *via* reductive dehydrochlorination.

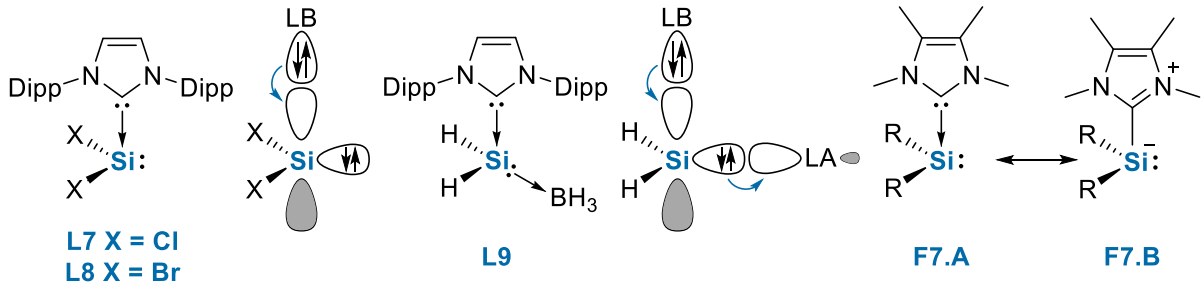

Figure 7: Silylenes stabilised *via Lewis* base coordination or *push-pull*-stabilisation and different *Lewis* representations for donor-stabilised acyclic silylenes (**F7.A**/**F7.B**).

The isolation and characterisation of dihalo-substituted silylenes, an intermediate in the industrial preparation of silicon, are outstanding results, which have paved the way for a variety of other low-valent silicon species.[61-62] For example, they provided access to a silylone (**L6**, Figure 6), which was isolated by

Driess in 2013 upon treatment of a bis-carbene with **L7** (yielding silyliumylidene ion **L49**, discussed in chapter 2.3 and Figure 17) and followed by reduction with sodium naphthalenide.[63] In comparison, the analogue cAAC-substituted **L5**, reported by Roesky, features π-back-donation from the silicon centre to the ligand in addition to solely σ-donation from the NHC to the silicon centre present in **L6**.[64]

SC-XRD analysis of compounds **L7**/**L8** revealed long Si–C^{NHC} bonds of 1.985(4)/1.989(3) Å, which are elongated in comparison to typical Si–C single bond lengths. In general, *Lewis* base-stabilised silylenes exhibit a trigonal pyramidal geometry, with the degree of pyramidalisation dependent on the s-character of the stereochemically active lone pair at the silicon centre. Based on recent debates in literature concerning the graphical representation of E–C^{NHC} bonds (E: central atom, exemplified in **F7.A**/**F7.B**, Figure 7),[65-67] Si–C^{NHC} and Al–C^{NHC} bonds will be represented as arrows within this work, provided it is not misleading. Furthermore, it should be noted that a single *Lewis* representation is not able to correctly illustrate the characteristics of a specific bond. Further discussion and possibilities to reveal a leading *Lewis* representation for specific compound are given in chapter 4.4 and 4.5.

After the pioneering work by Roesky and Filippou, the number of reported NHC-stabilised silylenes increased significantly[53] with examples relevant to this thesis given in Figure 8. The aryl-chloro-silylene **L10**, again described by Filippou in 2010,[68] was prepared by the carbene induced dehydrochlorination from *m*TerSiHCl$_2$ (*m*Ter = 2,6-Mes$_2$-C$_6$H$_3$) silane. This chloro-silylene can be converted into the corresponding silyliumylidene *via* treatment with an additional equivalent of IMe$_4$ (:C[NMeCMe]$_2$) (see chapter 6.6). Sekiguchi published the first NHC adduct of a solely silyl-substituted acyclic silylene **L11**, obtained *via* reductive dehalogenation of di(bromo)-silane (^{t}Bu$_3$Si)SiBr$_2$ with KC$_8$ in the presence of IMe$_4$, which was published together with its radical cation.[69]

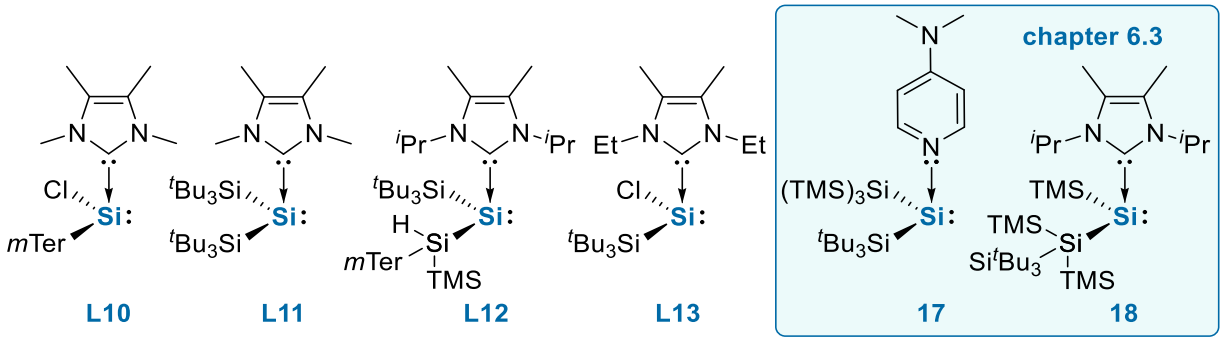

Figure 8: Selected examples of donor-stabilised acyclic silylenes (**L10-L13)** and the base-stabilised silylenes studied within this thesis (**17** and **18**).

Compound **L12** was reported by Cowley and Holthausen and can further be obtained as the 4-pyrollidinopyridine (4-PPy) adduct.[70] These are the rearrangement products of a base-stabilised disilene and will be discussed in the disilene chapter (2.2) in more detail. In comparison to the IMe$_4$- and supersilyl-substituted silylene hydride published in 2013,[71] the silyl-substituted silylene chloride **L13** requires the increased steric demand of the IEt$_2$Me$_2$ (:C[NEtCMe]$_2$) carbene to enable its isolation.[72] It is of note, that a silyl-substituted bromo-silylene, stable in tetrahydrofuran (THF) solution at room temperature (rt), was reported in 2001. However, this compound lacked structural verification, thus no assignment as free silylene, THF adduct or bridged dimer was possible.[73] Compounds **17** and **18** were studied within this thesis and are discussed in chapter 6.3.

Dependent on the substituents, stabilisation of an acyclic silylene as a highly reactive species might not be sufficient by simple coordination of an NHC, based on the enhanced nucleophilic character of the lone pair due to the coordinated *Lewis* base. Further stabilisation can be obtained by making use of the ambiphilicity of silylenes though coordination of the lone pair to an additional *Lewis* acid as exemplified in **L9** (Figure 7), resulting in a *push-pull*-stabilised silylene. This is achieved *via* conversion of **L7** with

BH_3•THF to reach the NHC-stabilised chloro-silylene borane adduct and followed by treatment with $LiAlH_4$ for chloride-hydride substitution.[74-75] These types of *push-pull*-stabilised silylenes are currently known with the *Lewis* acid represented by boranes or transition-metal carbonyl complexes.[75-81]

Upon consideration of other electron donating groups to stabilise acyclic silylenes, e.g. 4-*N*,*N*-dimethylaminopyridine (DMAP) as used in **17**, one important example bearing isocyanides as a milder *Lewis* base was published by the groups of Okazaki and Tokitoh already in 1997.[82-83] They described the isocyanide-silylene complex **L14**, bearing two different aryl-substituents (Figure 9). On the experimental side, it was accessible *via* thermal dissociation of the disilene, MesTbtSi=SiTbtMes **L32** (Tbt = 2,4,6-$(CHTMS_2)_3$-C_6H_2) (Figure 14), into its monomers followed by reaction with different isocyanides. Moreover, thermal dissociation of the disilene in benzene also led to the first example of silylene addition to the aromatic benzene ring in a [1+2] cycloaddition.[84] Thus, **L14** represents a trapped monomer of the thermally controlled monomer-dimer equilibrium of the disilene, which is further discussed in chapter 2.2.

One major point of interest within this thesis is the bonding situation of the silicon version of a ketamine, as being the case for **L14** (Figure 9). The carbon version of the valence isoelectronic CO derivative, named ketenes, bear a planar structure of type **F9.A** (Figure 9) and have been studied by Staudinger as early as 1905.[85-86] Transition-metal complexes bearing CO or isocyanide ligands are applied as catalysts in a huge variety of reactions, e.g. hydroformylation,[87] Reppe chemistry[88], Pausen-Khand reaction,[89] hydrosilylation and cross-coupling reactions like Suzuki-Miyaura or Sonogashira coupling.[90-91] Heavier ketenes and ketimines both feature potential for back-bonding from the silylene to the ligand analogue to transition-metal complexes. Thus, they could enable access to new reactivity profiles. Silylenes have already proven their ability to reductively couple carbon monoxide.[92-94] However, carbonyl silylene complexes have not been isolated until recently.[95]

The research concerning valence-isoelectronic silylene isocyanide complexes was initiated by an early study of Weidenbruch, who reported a bridged dimer of silylene isocyanides.[96] Nevertheless, only three examples of monomeric silylene isocyanide complexes are described in literature to date: **L14** (*vide supra*), which was characterised by calculated NMR shifts as well as experimentally through onwards reactivity. The second example, **L15** (Figure 9), is accessible *via* addition of isonitriles to silylene **L3**[97] and the third example **L17** was reported just recently.[95]

Matrix isolation studies play an important role in the identification of reactive intermediates, as they enable spectroscopic analysis of otherwise elusive species. Therefore, theoretical calculations are often used in combination with IR-data to enable the identification of the obtained species. This was also the case for CO-adducts of silylenes, with several groups studying silylenes bearing only small ligands (R = H, Me, Ph) in a CO atmosphere.[98-102] They revealed silylene-CO adducts bearing a bent structure (**F9.B**-**F9.D**, E = Si, X = O), which highly contrasts the corresponding ketenes. Furthermore, silaketenes (**F9.A**, E = Si, X = O) are not even a minimum on the potential energy surface. Additionally, the monomer of West's disilene **L31** (Figure 14) as well as silylene **L1** were examined in matrix isolation studies concerning their potential to form stable adducts with carbon monoxide, but the adducts were found to dissociate upon warming of the matrix.[103-104]

From the *Lewis* structural point of view, the bent silicon carbonyls/isocyanides can either bear a single dative bond from the CX moiety to the silicon centre (**F9.B**), a donor-acceptor type interaction (**F9.C**) or a bent silaketene with two covalent bonds (**F9.D**). Formulation of type **F9.C** is reminiscent of transition-metal carbonyl/isocyanide complexes, bearing π-back donation from the metal centre to the carbonyl/isocyanide unit.[32] In Figure 9, all complexes are given in the *Lewis* representation as published in the original reports. A systematic study of the bonding situation present in tetrylene isocyanide complexes covering silicon, germanium and tin, was reported by Power, Tuononen and Mansikkamäki in 2013.[105] They revealed a linear dependency between the magnitude in shift of the characteristic CN-band

in IR spectra and back-bonding contributions within energy decomposition analysis (EDA), thus emphasizing the importance of *Lewis* structure representations **F9.C**/**F9.D**.

Stable silylene CO adducts were unknown until isolation of **L16**,[95] which was published during submission of this thesis. Silicon carbonyl complex **L16** bears a bent structure and a Si–C bond length of 1.865(6) Å, which is closer to commonly observed Si–C single bonds (1.87–1.93 Å) than Si=C double (1.70–1.76 Å) bonds.[106] Calculations on **L16** revealed the structural motive **F9.B** as the most appropriate, although electron donation from the silicon lone pair to the carbonyl unit is present. In terms of reactivity, **L16** was shown to act as a masked silylene in the activation of H_2 (requiring heating to 60 °C) and ligand exchange of the carbonyl moiety for isocyanide CNCy (Cy = cyclohexyl) was possible to give **L17**.

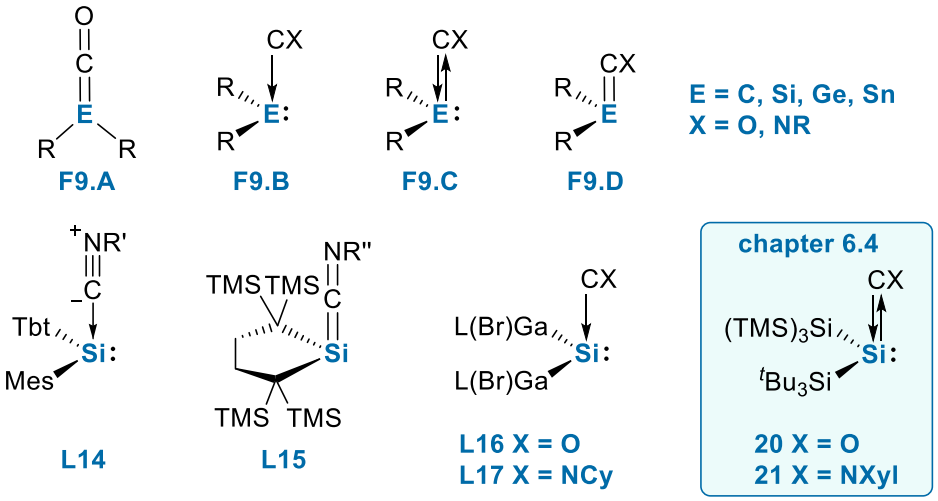

Figure 9: Possible structures and *Lewis* representations for ketenes/ketimines and their heavier analogues; R' = Tbt, Tipp, Mes*, Tipp = 2,4,6-^{i}Pr$_3$-C$_6$H$_2$, Mes* = 2,4,6-^{t}Bu$_3$-C$_6$H$_2$; R'' = Dipp, Ad; Ad = 1-adamantyl, L = HC[C(Me)N(2,6-^{i}Pr$_2$-C$_6$H$_3$)]$_2$, Cy = cyclohexyl, C$_6$H$_{11}$, Xyl = 2,6-Me$_2$-C$_6$H$_3$.

Chapter 6.4 discusses the synthesis, reactivity and bonding situation of bis(silyl)silylene carbonyl complex **20**. Analogous to **L16**, compound **20** also undergoes ligand exchange reactions with isocyanides to yield the bis(silyl)-substituted silicon isocyanide complex **21**.

Donor-Free Acyclic Silylenes

In the case of donor-free acyclic silylenes, the frontier orbitals highly resemble those of transition-metals (Figure 2b) and should therefore enable the activation of enthalpically strong bonds as present in H_2 (Figure 2c). Early studies featuring a bis(amino)-substituted silylene were hampered due to lack of steric protection, which led to reversible dimerisation (see chapter 2.2 for further discussion), whereas the presence of a silylene was proven by trapping reactions with aryls, olefins, acetylenes or silanes.[107-108] In 2003, Lee *et al.* synthesized bis[bis(TMS)amino]silylene **L18** (Figure 10), which exhibits a limited stability at –20 °C for 12 h.[109] Characterisation *via* SC-XRD was not provided, however, calculated ^{29}Si shifts as well as trapping reactions clearly revealed successful isolation of **L18**.

In 2012, the group of Power and the Aldridge concomitantly succeeded in the isolation of the first acyclic, donor-free silylenes **L19**[110] and **L20**,[111] which showed different structural features. Compound **L19** bears a rather tight angle at the silicon centre (∢SSiS = 90.519(19)°), comparable to that of cyclic silylenes, and a ^{29}Si NMR shift at 285.5 ppm. In comparison to this, the amino- and boryl-substituted **L20** revealed a widened interligand angle (∢RSiR) of 109.7(1)° in SC-XRD analysis and the ^{29}Si resonance shifted downfield (δ = 439.7 ppm). This remarkable structural difference also effects the reactivity of these silylenes: the former **L19** shows reversible coordination of ethylene[112] but no reaction with H_2, whereas the latter **L20**

activates H_2 below rt and has shown to enable reductive coupling of CO accompanied by Si–B insertion, as found in 2019.[92] It is important to note that increasing the steric bulk of the aryl groups attached to sulphur led to decreasing interligand angles attributed to dispersion forces.[113]

In 2013, Protchenko *et al.* reported **L21** with the boryl group replaced by a hypersilyl ($SiTMS_3$) group, which resulted in an opening of the interligand angle to 116.91(5)° and a ^{29}Si shift at 438/467 ppm (based on two rotational isomers).[114] In a one-pot synthetic protocol, two equivalents of potassium hypersilanide ($(TMS_3SiK(THF)_2)$) are added to the amido-substituted tri(bromo)-silane to yield **L21** *via* reductive dehalogenation. Interestingly, **L21** possesses an activation barrier for H_2 comparable to that of **L20** and decomposes *via* C-H activation at the Dipp (2,6-$^{i}Pr_2$-C_6H_3) group instead of TMS group migration at 80 °C over a prolonged time of five days (d). Later, it was also shown that **L21** reacts with ethylene to give the corresponding siliran, which at elevated temperatures undergoes migratory insertion of the ethylene moiety into the Si–Si bond followed by reaction with a second ethylene molecule.[115-116]

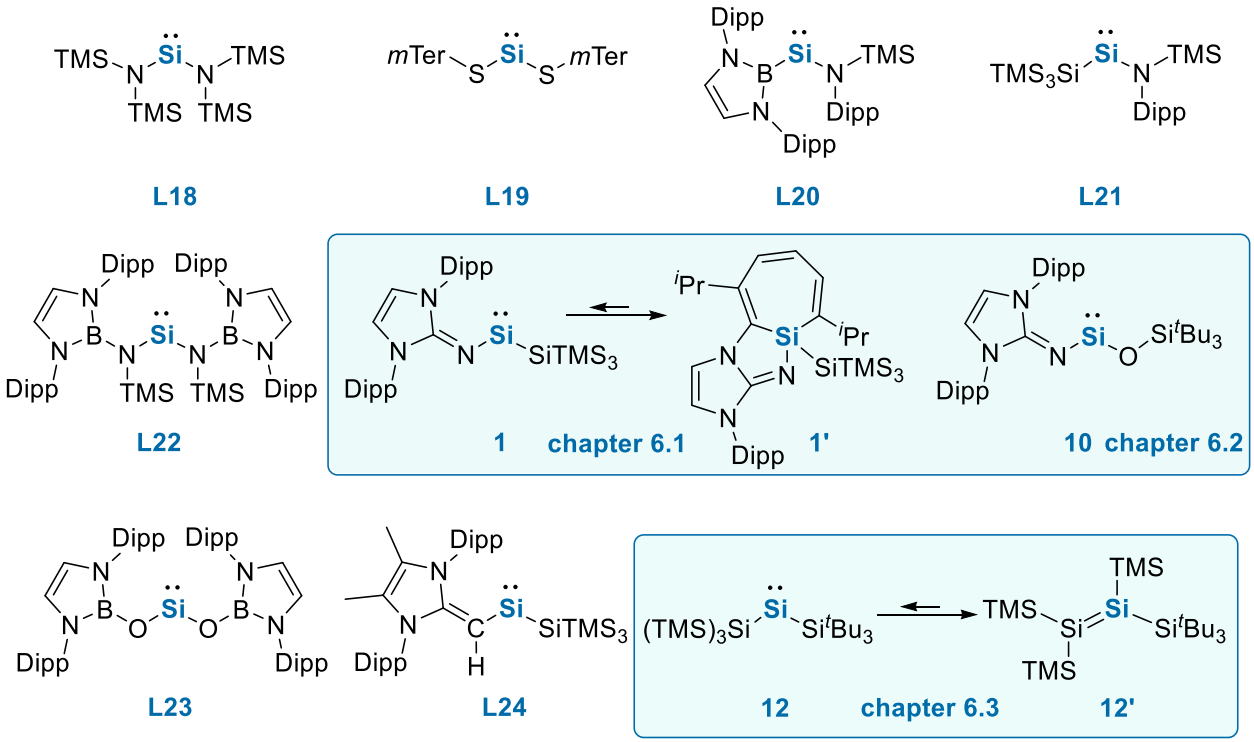

Figure 10: Reported examples of acyclic silylenes including the ones studied in this thesis.

Heavier analogues have been known since Lappert and Harris in 1974,[117] however it wasn't until 2016 that isolable acyclic di(amino)-substituted silylenes were accessible due to use of an extremely bulky boryl-amide ligand [N(TMS{B(DippNCH$_2$)}] (**L22**).[118] Owing to the steric demand of the ligand, donation of the nitrogen lone pair to the empty p-orbital at the silicon centre is limited by the spatial arrangement. In terms of reactivity, **L22** shows no reaction with H_2, neither at elevated temperature nor at elevated pressure. The diamino-silylene however reacts with O_2, followed by C-H activation at the Dipp group to yield the corresponding silanol, as well as with ammonia under cleavage of one Si–N bond and addition of a second equivalent of NH_3.

A different type of ligand used in low-valent main group chemistry is a variant of the established NHC ligands, namely *N*-heterocyclic imines (NHI).[119] The monoanionic ligands with an electron lone pair at the exocyclic nitrogen atom are strong electron donors (2σ+4π) (Figure 11, **F11.A**- **F11.C**). They are, therefore, ideal candidates to stabilise the electron-deficient low-valent silicon centre. The steric demand is adjustable *via* modification of the wingtips in the imidazoline moiety with the ability to delocalise a

positive charge within this ring being an additional advantage of NHIs over amine ligands. The anionic ligand was introduced by Kuhn in 1995[120] and has found application as a ligand to stabilise low-valent main group species in a variety of isolated compounds.[119]

Besides initial studies of Bertrand, which were focused on the stabilisation of phosphorous-centred radicals, radical cations and phosphinonitrenes,[121-123] NHI-substitution allowed for the isolation of else elusive compounds containing a boron-sulphur or aluminium-tellurium double bond by the Inoue group.[124-125] Switching to silylenes, acyclic silylene **L25** (Figure 11) was reported by Inoue in 2012, with the Cp* ligand adopting a η^2-coordination. Further examples of low-valent silicon compounds **L26** and **L27** were obtained in 2016, dependent on the equivalents BCF ($B(C_6F_5)_3$) added to the TMS-substituted NHI.[126] Attempts by Rivard to access a bis(NHI)-substituted silylene *via* reduction of $(IDippN)_2SiBr_2$ (IDippN =NC[N(2,6-^{i}Pr$_2$-C$_6$H$_3$)CH]$_2$)with KC_8, as it was possible for the germanium analogue, gave compound **L28**.[127] This is the result of cleavage of the N-aryl bonds which was attributed to over-reduction to Si(I) and Si(0) species by density functional theory (DFT) methods. Interestingly, similar problems arose for the synthesis of **L25**, with the achieved yield *via* reductive dehalogenation of di(bromo)-silane ($IDippNCp^*SiBr_2$) amounting to less than 10% However, it was improved to 57% *via* an alternative salt-metathesis route by treatment of silyliumylidene ion **L46** (Figure 17) with the lithium salt of the NHI ligand.[128]

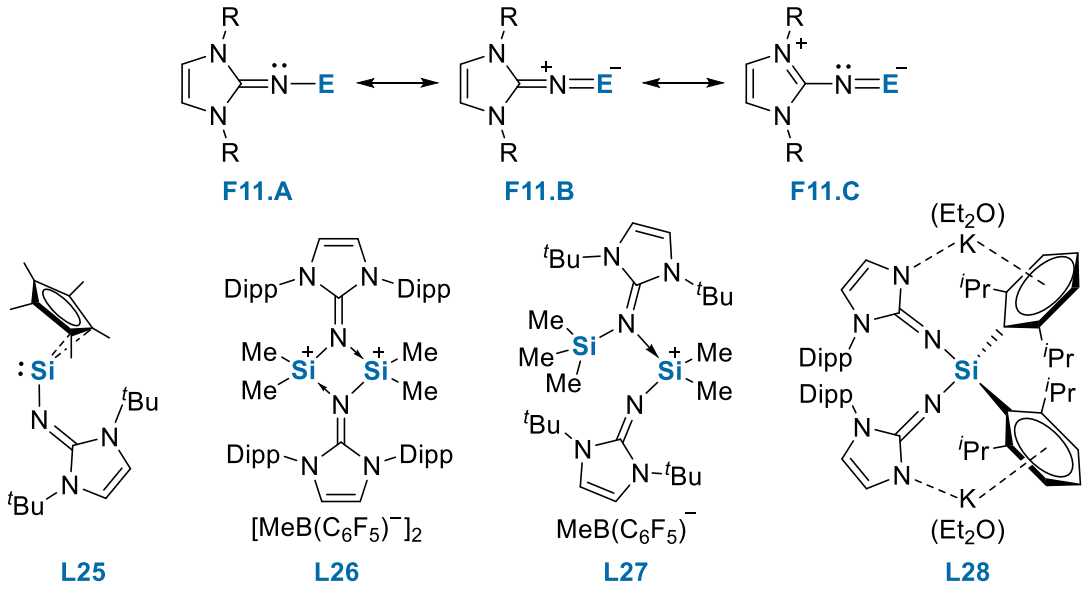

Figure 11: Selected resonance structures for a model complex of the anionic imidazolin-2-iminato ligand with E^+ (**F11.A**-**F11.C**) and selected examples of reported NHI-stabilised silicon compounds (**L25**-**L28**).

The limited number of reports on donor-free, acyclic silylenes encouraged us to tackle this topic using a combination of silyl- and NHI-substituents. Reductive dehalogenation of the corresponding NHI-tri(bromo)-silane with hypersilyl potassium allowed to access silylene **1** (Figure 10) with the silepin **1'** representing the isolable resting state (see chapter 6.1). Moreover, this also enabled the isolation of imino-siloxy-silylene **10** *via* rearrangement of a silanone (see chapter 6.2).

In 2019, Aldridge introduced a new *N*-heterocyclic boryloxy ligand (NHBO = $[OB(NDippCH)_2]^-$), where replacement of the amino group in **L22** with oxygen renders the NHBO ligand isoelectronic to NHIs.[129] The bis-oxy-substituted acyclic silylene **L23** (Figure 10) possesses an interligand angle of 100.02(8)°, comparable to that in **10** (103.56(8)°). Besides the silylene, the group also described all heavier homologues with the same substitution. However, no reactivity of **L23** or the heavier homologues was specified, presumably due to its high stability counteracting inherent reactivity.

In the same year, the group of Rivard reported the *N*-heterocyclic olefin- (NHO) and silyl-substituted silylene **L24** (Figure 10).[130] The monoanionic NHO ligands bears strong donor abilities (2σ+2π) comparable to NHIs, but their uncharged form can also be used as organocatalysts for CO_2 capture or polymerisation reactions.[131-132] Attempts towards the bis(NHO)-substituted silylene were precluded due to the corresponding di(bromo)-silane not being accessible. Compound **L24** was obtained in a manner similar to the corresponding NHI-substituted silylenes. In contrast to **1**, **L24** is isolable at rt as well as stable in solution under inert atmosphere for prolonged periods, and according to SC-XRD analysis this exhibits an interligand angle of 101.59(7)°. DFT calculations revealed an enhanced C=Si double bond character, demonstrating the stabilisation by the NHO ligand *via* its high π-donor ability. Initial reactivity studies focused on the oxidative addition of MeOTf, HBpin, $HSiCl_3$ and P_4. Reactivity tests of **L24** with N_2O did not yield the corresponding silanone, as was the case for **1**. However, the group of Rivard was able to show the first example of the rt activation of a primary C-H bond in ^{t}Bu-NC (*tert*-butyl isocyanide) by silylenes, yielding a silyl-cyanide.

Table 1: Summary of important properties and reactivity of reported acyclic silylenes **L19**-**L24** in literature.

Compound	L19	L20	L21	L22	L23	L24
∢RSiR [°]	90.519(19)	109.7(1)	116.91(5)	110.94(5)	100.02(8)	101.59(7)
λ_{max}[nm]	382	-	-	385/300	348	416
^{29}Si NMR [ppm]	285.5	439.7	438/467	204.6	35.5	432.9
Activation of H_2	no	yes	yes	no	n.r.	n.r.
Activation of Ethylene	reversible	n.r.	yes.	n.r.	n.r.	n.r.
Other reported reactivity	n.r.	red. coupling of CO	migratory insertion 2nd eq C_2H_4	O_2, NH_3	n.r.	P_4, ^{t}BuCN

n.r. = not reported

The literature-reported examples of donor-free acyclic silylenes and their reactivity show that they unambiguously posses great potential to replace transition-metals in terms of activation of strong bonds. However, this represents only the first step of a catalytic cycle, as reductive elimination of these activated bonds still remains the bottleneck in catalytic applications.[26,133]

Triplet Silylenes

As described in the beginning of this section, a major difference between carbon and silicon in oxidation state II is the electronic ground state for the parent :EH_2 (E = C, Si): triplet for carbene and singlet for silylene, which is closely related to the energy difference between the lone pair (HOMO) and the empty p-orbital (LUMO). The energy difference can however be influenced *via* the stabilising ligands: Electropositive substituents, like silyl groups or alkali metals, effectively reduce the energy difference between the singlet and the triplet state (ΔE_{ST}). Moreover, bulky substituents can also influence ΔE_{ST} due to widening of the interligand angle.

Initial calculations on the ground state multiplicity of the smallest possible silylene :SiH_2 were performed more than 50 years ago.[134] Connected to the establishment of theoretical chemistry, the development of new theoretical approaches, as well as the increasing accuracy of the applied methods, several theoretical groups have studied the potential energy surface of different silylenes in singlet and triplet ground state.[135-139] These studies revealed different interligand angles for intersection of the potential energy surfaces of the singlet and the triplet state as well as different sterically demanding silyl groups predicted to bear a triplet ground state. At the beginning of this century, several groups also addressed

this topic experimentally but were not able to undoubtedly clarify the multiplicity of their compounds,[136] e.g. triplet species should undergo nonstereospecific [2+1] cycloaddition reactions *via* a di-radical mechanism corresponding to the Skell rule.[140] Furthermore, previously predicted triplet ground state silylenes were experimentally proven to be singlet species.[138,141-142] In 2003, Sekiguchi finally succeeded in accessing the triplet state silylene **L29** (Figure 12) by photolysis of the corresponding silacyclopropene in a methylcyclohexane glass matrix.[143] Electron paramagnetic resonance (EPR) spectroscopy revealed a broad signal at 845 mT with the intensity being inversely proportional to the measurement temperature. Further analysis focused on the products obtained after annealing of the matrix, with the resulting C–H activated product taken as further proof for the triplet silylene. However, in 2013 Apeloig revealed that the activation barrier for the intramolecular C-H activation is significantly lower from the singlet than the triplet state[141], thus the C–H activation product does not serve as an indicator for an triplet species. The related alkali metal-substituted silylenes **L30** were described in 2008, with comparable EPR signals at 790 and 780 mT.[144]

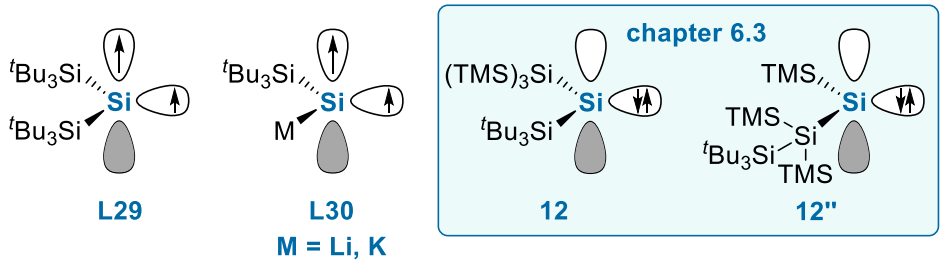

Figure 12: Reported triplet silylenes **L29** and **L30** and singlet ground state bis(silyl)silylenes **12** and **12''** studied in this work.

With only these three examples of triplet silylenes being reported, compounds **12** and **12''** were investigated concerning a potential triplet ground state within this thesis (see chapter 6.3). Interestingly, high level calculations (DLPNO-CCSD(T)[145-146]/cc-pVQZ[147-148] single point calculations on PBEh-3c[149] optimized structures) by Holthausen[150] revealed a very tight ΔE_{ST} for **L29** with the triplet state favoured by only 1.2 kcal/mol, which is significantly lower than predicted prior to isolation.[135]

2.2. Disilenes

The year 1981 was an important year for low-valent main group chemistry. In this particular year the so-called "Double-bond rule",[151-152] stating that elements bearing a principal quantum number > 2 should not be able to form π bonds *via* overlap of two p-orbitals either with themselves or with other elements, was proven wrong within four independent reports. Becker *et al.* reported the first phospha-alkyne, which bears a triple bond between phosphorous and carbon.[153] The group of Brook described the first silaethene containing a silicon carbon double bond[154] and the Yoshifuji group successfully obtained a phosphor-benzene, containing a P=P double bond.[155] The fourth report, possessing the highest relevance for this thesis, included the isolation of the first disilene exhibiting a silicon-silicon double bond in **L31** (Figure 14) by West.[156] Key to accessing these reactive species was the high steric demand of the surrounding ligands, which provide the necessary kinetic stability to enable their isolation.

Since this important breakthrough, multiple bonds between main group compounds, especially of group 14, are quite common nowadays with numerous reports on low-valent multiple bonded systems. They display significant structural difference to the carbon analogue, which can be described *via* the Carter-Goddard-Malrieu-Trinquier (CGMT) model[157-160] exemplified in Figure 13A. The structural difference is again connected to the increased stability of the singlet going down the group and the inert pair effect. The double bond in ethylene is built *via* two triplet fragments and thus exhibits a planar structure. In contrast, the Si=Si double bond is best represented by two dative bonds bridging the two silylene units. This gives rise to *trans*-bent (*trans*-bent angle θ defined in Figure 13, angle between the SiR_2 plane and the Si=Si axis) and/or twisted structures (given by twist angle τ in Figure 13, angle between the two SiR_2 planes), which results in a weaker bonding.

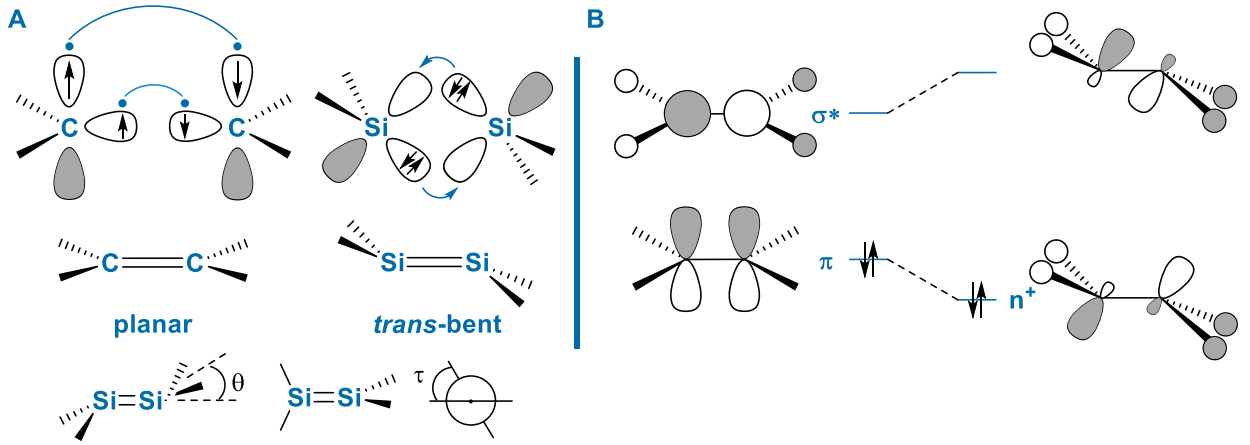

Figure 13: (**A**) CGMT model for the dimerisation of triplet carbenes and singlet silylenes with definition of *trans*-bent (θ) and twist angle (τ) and (**B**) 2nd order Jahn-Teller distortions.

A different explanation for the weakened bonding is the second-order Jahn-Teller distortion occurring due to decreased energy difference of the π- and σ*-orbitals (Figure 13B).[161-162] Going down group 14, mixing between the π-bond and the σ*-orbital increases, which destabilises the π bond due to enhanced lone pair character present in the double bond.[163-164] This also allows for an explanation of the structural differences upon ligand exchange. Electropositive ligands stabilise the π-bond, thus favour more planar structures, which results in a shortened central bond length. For electronegative ligands the π- and σ*-orbitals become closer in energy, with increased interference of these promoting *trans*-bent or twisted structures and an increased bond length. Moreover, the steric demand of the ligand also highly influences the structure, well exemplified for a tetra(^{t}Bu$_2$MeSi)-substituted distannene by Sekiguchi.[165] This compound minimizes the high steric pressure of the attached ligands by adopting a highly twisted but not *trans*-bent structure. Reported Si=Si double bond lengths are in the range from 2.14 Å to 2.29 Å.[53,166]

Since the seminal work of West, a huge variety of disilenes have been described.[167-170] Their reactivity resembles that of alkenes, e.g. they show 1,2-addition, cycloaddition or coordination to metal complexes. In the following only disilenes relevant to this thesis are discussed, e.g. tetrasilyl-substituted disilenes and amino- or imino-substituted disilenes (Figure 14). Moreover, disilenes featuring a disilene-silylene equilibrium or rearrangement are also included.

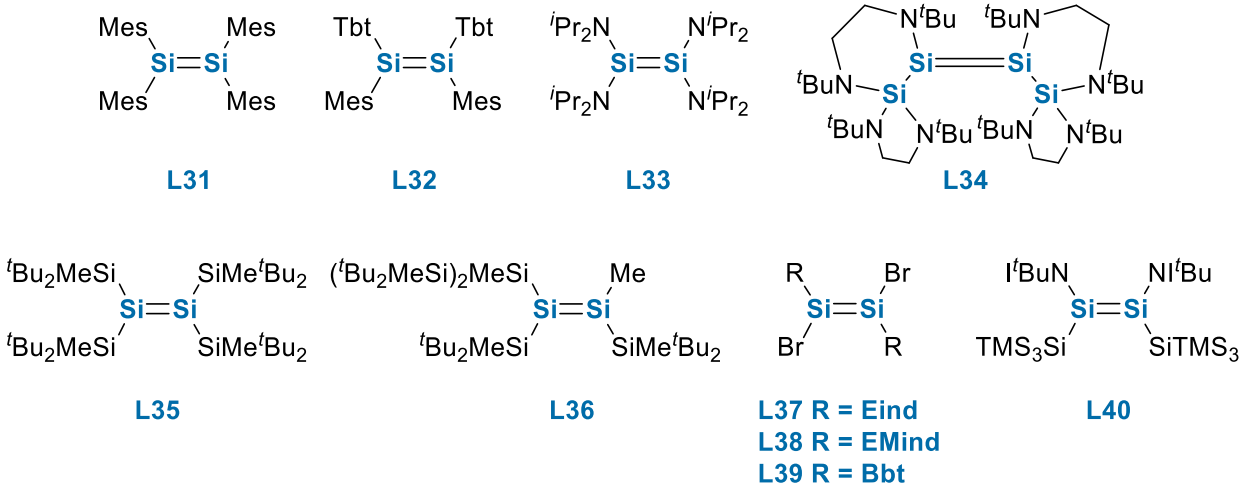

Figure 14: Selected examples of tetrasilyl-, aryl-/bromo- and NHI/silyl-substituted disilenes; Eind = (1,1,3,3,5,5,7,7-octaethyl-s-hydrindacen-4-yl, EMind = 1,1,7,7-tetraethyl-3,3,5,5,-tetramethyl-s-hydrindacen-4-yl, Bbt = 2,6-(CHTMS$_2$)$_2$-4-CTMS$_3$-C$_6$H$_2$.

The group of Okazaki described Tbt-/Mes-substituted disilene **L32**, which was the precursor to isocyanide adduct **L14** (Figure 9).[82-84] Kira *et al.* reported a tetra-amino disilene **L33** in 1998, which is proposed to be in equilibrium with its monomer (see chapter 2.1) according to a temperature-dependent UV study. However, in both cases no structural characterisation *via* SC-XRD was provided.[108] Apeloig, West and coworkers succeeded in the isolation of **L34**, which is the tetrameric product of the unsaturated analogue of **L2** (Figure 5), with a long Si=Si bond length of 2.289 Å.[171] In their study, reversibility of the tetramerisation was shown again by UV/vis spectroscopy. Furthermore, the methanol-trapping product of the dimeric silylene was isolated.

The tetra(^{t}Bu$_2$MeSi)-substituted disilene (**L35**) was obtained *via* the general approach of reductive coupling of the respective di(bromo)-silanes.[172] This compound is highly related to triplet silylene **L29**, which possesses two supersilyl groups. This nicely reflects the high influence of the ligands on the low-valent silicon centre: the replacement of one ^{t}Bu group by a Me group results in changing the reactivity from a highly reactive triplet silylene to an isolable disilene. Different to other tetrasilyl disilenes, which either bear twist angles up to 28° or *trans*-bent angles up to 15°,[169] its structure is highly twisted (τ = 54.5°) but not bent. This disilene shows very interesting redox chemistry, with both the disilene radical cation as well as disilene radical anion being reversibly accessible.[172-173]

The bond strength of disilenes show a broad range dependent on the substituents and their steric demand. Thus, also the monomeric silylenes can be accessible, for example as discussed in chapter 2.1, Tokitohs Tbt- and Mes-substituted disilene **L32**[82] as well as EMind- (1,1,7,7-tetraethyl-3,3,5,5,-tetramethyl-s-hydrindacen-4-yl)/Eind- (1,1,3,3,5,5,7,7-octaethyl-s-hydrindacen-4-yl) and bromo-substituted disilenes **L37**/**L38** as shown by the group of Tamao and Matsuo.[174]

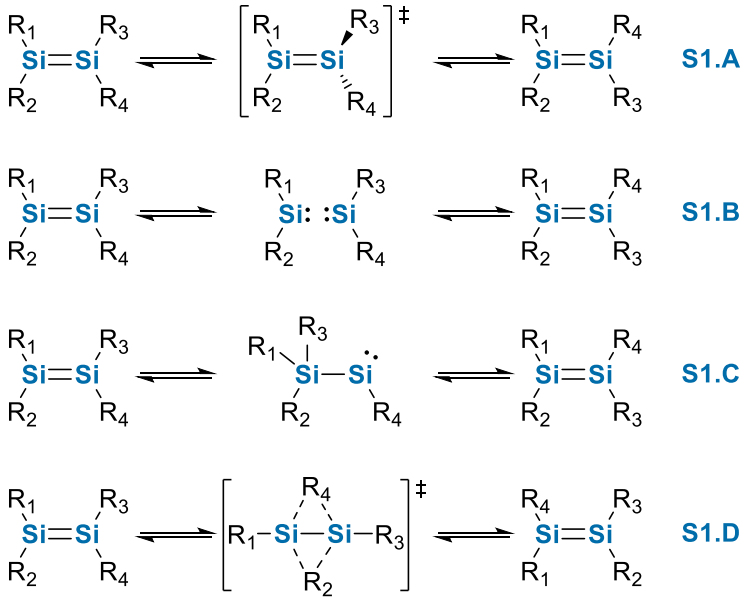

Scheme 1: Possible isomerisation pathways for disilenes.

With the different substituents being present at the disilene, different rearrangement/isomerisation mechanisms are possible (Scheme 1). In literature, the following possibilities are discussed: rotation around the Si-Si bond (**S1.A**), monomerisation to silylenes and re-association (**S1.B**), migration of one ligand to give an intermediary silyl-silylene, rotation around the Si–Si single bond followed by back-migration of one ligand (**S1.C**) and a dyotropic rearrangement (**S1.D**). Interestingly, mixing of disilenes **L37** and **L38** in C_6D_6 at rt yields the crossover product with one Emind and one Eind aryl-substituent most probably *via* mechanism **S1.B**. In contrast, the likewise bis(aryl)-bis(bromo)-substituted disilene **L39** was shown to exhibit a rather high thermal stability (up to 60 °C) with no sign of dissociation into the corresponding monomers. Heating to higher temperatures results in the C-H activation product at the Bbt

ligand (Bbt = 2,6-(CHTMS$_2$)$_2$-4-CTMS$_3$-C$_6$H$_2$), most likely induced *via* bromide migration to a silyl-silylene (mechanism **S1.C**).[175]

The first example of a *trans*-bent and twisted disilene was reported by Sekiguchi in 2003, upon reduction of the sterically demanding di((^{t}Bu$_2$MeSi)$_2$MeSi)-dibromo-silane followed by silylsilylene-disilene rearrangement (pathway **S1.C** in Scheme 1), which gave **L36** as the first stable disilene with a methyl-substituent.[176] The second example of a disilene bearing a *trans*-bent and twisted structure was achieved in an analogous experimental approach upon exchange of the sterically demanding IDippN group in **1** with I^{t}BuN (I^{t}BuN = NC[N^{t}BuCH]$_2$) to obtain **L40** in its dimeric Z-constitution.[177] Compound **L40** represents the first example of a disilene able to activate H_2 and shows interesting reactivity upon treatment with ammonia. Here, the product depends on the reaction temperature with lower temperatures yielding the disilene addition product and higher temperatures giving the silylene addition product.[177-178]

Interestingly, disilenes are capable of NHC coordination, as shown first in a joint report by the groups of Jutzi and Scheschkewitz.[179] Hence, cyclotrisilene **L41** (Figure 15), bearing solely carbon-based ligands and the Cp* ligand in a η^3-coordination, forms a reversible adduct **L42** with I^{i}Pr$_2$Me$_2$ (:C[N^{i}PrCMe]$_2$). It bears a Si–Si bond of 2.2700(5) Å, which is located at the upper end for reported disilenes, and the Cp* ligand only bears η^1 coordination. Change of the Cp*-substituent to Tipp (Tipp = 2,4,6-^{i}Pr$_3$-C$_6$H$_2$) in cyclotrisilene **L41** analogously results in a reversible coordination, however in the latter case, rearrangement to the silyl-/aryl-substituted and NHC-stabilised silylene **L43** occurs.[180]

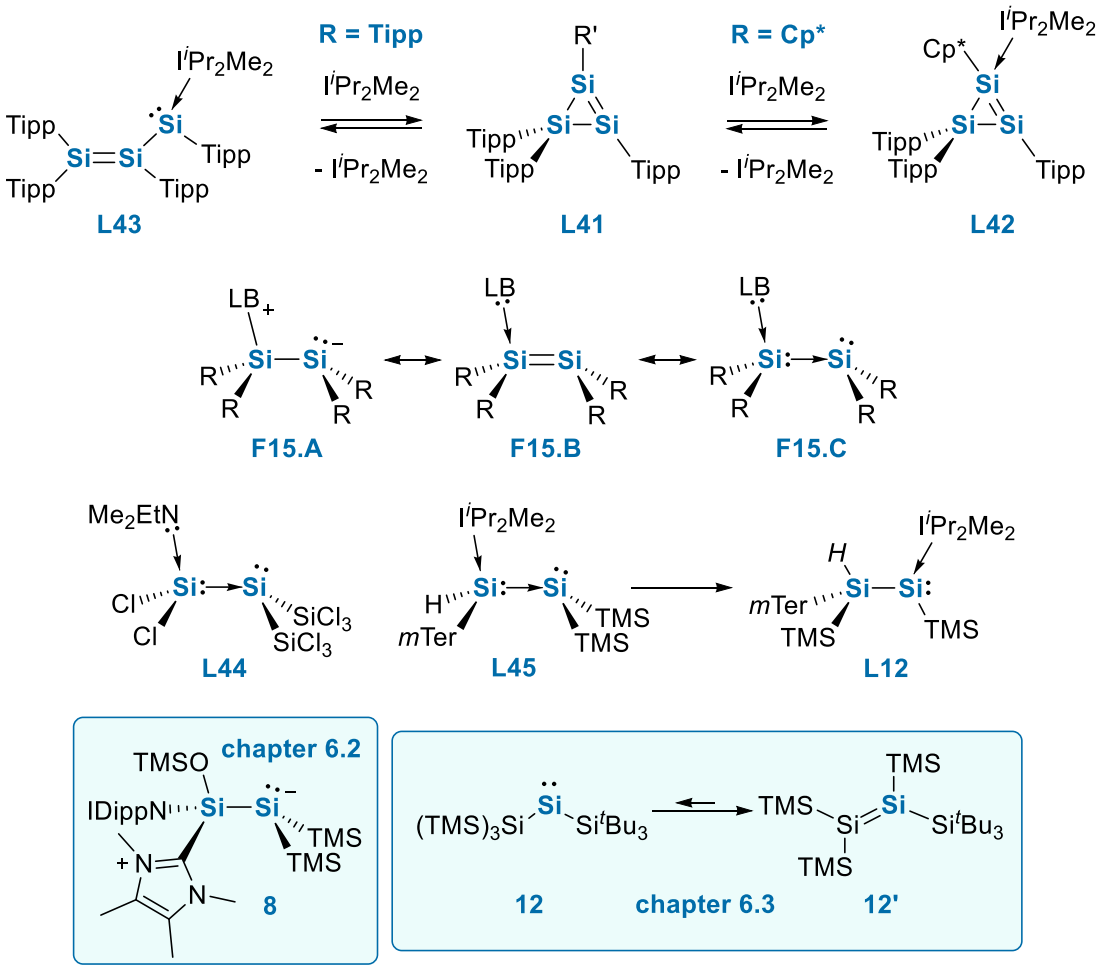

Figure 15: NHC-coordination at a disilene, NHC-stabilised disilene-silylsilylene interconversion, different *Lewis* structure representations of donor-stabilised disilenes and selected examples of donor-stabilised disilenes with the corresponding rearrangement product.

An different example of a base-stabilised disilene (**L44** in Figure 15), with the ligands in a rarely observed cis arrangement, was reported by the group of Holthausen in 2016.[181] Several *Lewis* structure representations are possible: a zwitterionic disilene (**F15.A**), a base stabilised disilene (**F15.B**) or a disilene possessing a dative Si–C as well as dative Si–Si bond (**F15.C**). For compound **L42**, detailed bonding analysis revealed a dative Si–Si bond as the most appropriate structure (**F15.C**) (see chapter 4.5). The concept of dative Si–Si bonds was further investigated in collaboration with the Cowley group,[70] with **L45** revealing similar characteristics in bonding analysis. Rearrangement from **L45** to NHC-stabilised bis(silyl)silylene **L12** occurs *via* $I^iPr_2Me_2$ dissociation, TMS-migration and $I^iPr_2Me_2$ re-association, representing the first example of a bis(silyl)silylene-disilene equilibrium. This can directly be observed *via* NMR spectroscopy starting from a slightly modified version of **L45** bearing the weaker electron donor 4-PPy. The influence of the ligand was also investigated, revealing the Cp*-substituted analogue of **L45** not being capable of a disilene-silylsilylene interconversion as shown for *m*Ter-substituted **L45**. Different to **L44** and **L45**, the NHC-stabilised silanone rearrangement product **8** bears no *cis* arrangement of the ligands and is further discussed in chapter 6.2 including bonding analysis, which revealed the zwitterionic representation as most appropriate description. Compounds **12** and **12'** (Figure 15 and chapter 6.3), studied in this thesis, feature a silylene-disilene interconversion and are thus closely related to the disilene-silylsilylene pair **L45**/**L12**.

2.3. Silyliumylidene Ions

Silyliumylidene ions combine properties of silylenes and silylium ions in one molecule: a high electrophilicity due to two vacant p-orbitals representing the *Lewis* acidic side as well as a lone pair of electrons as the *Lewis* basic site. These properties give rise to enhanced reactivity compared to both silylium ions and silylenes. Thus, it is unsurprising that these species exist only as a short-lived intermediate in the gas phase as well as being observable in the solar spectrum in a donor-free configuration (Figure 16).[182-186]

To enable their isolation in the condensed phase, donor stabilisation by *Lewis* base is essential to mitigate the electrophilicity of silyliumylidene ions by partially occupying the empty p-orbitals. Dependent on the applied donors, the choice of counter anion can also affect the stability of the corresponding silyliumylidene. Weakly coordinating anions (WCA) assist the stability of these complexes due to steric shielding of the reactive centre at the anion.

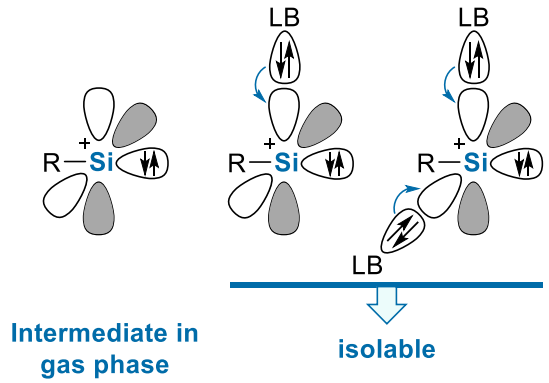

Figure 16: Orbital situation of silyliumylidenes dependent on the presence and number of donors.

The fact of donor-free silyliumylidene ions not being isolable was demonstrated by the group of Müller in 2013 (Scheme 2).[187] Accordingly, thermal dissociation of anthracene from dibenzosilanorbonadienyl cation **S2.A** yield silylium ion **S2.B**. Detailed DFT calculations revealed a mechanistic scenario, which includes the benzene adduct of the donor-free silyliumylidene ion **S2.C**. This experimentally not detectable intermediate (note: the silyliumylidene ion without benzene coordination is not observed either) activates the used solvent benzene under release of H_2 to give **S2.B**.

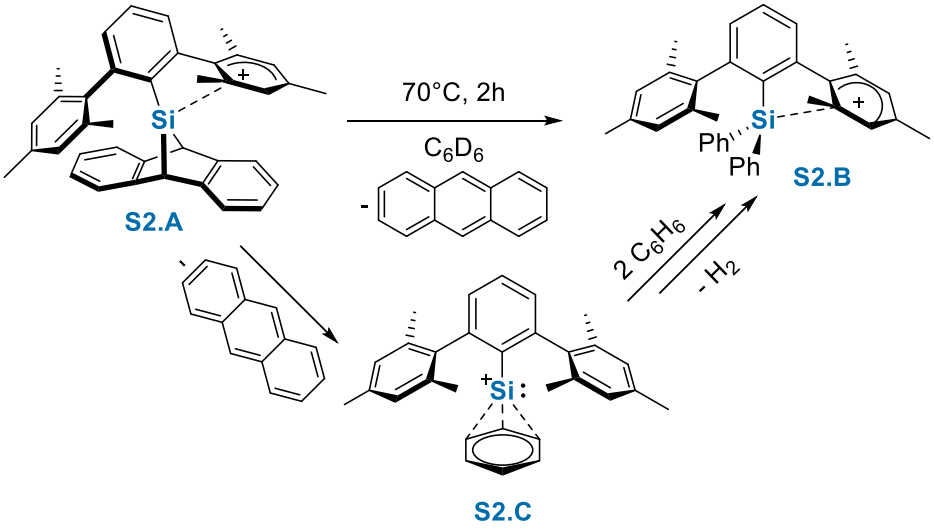

Scheme 2: Formation of donor-free silyliumylidene as benzene adduct **S2.C** and its further conversion to silylium ion **S2.B** by thermal dissociation of **S2.A**.

Isolable Silyliumylidene Ions

The first isolable silyliumylidene ion **L46** (Figure 17) was reported by Jutzi in 2004 *via* treatment of silylene **L1** with the salt $[Cp^*H_2B(C_6F_5)_4]$ under release of Cp*H.[188] Stabilisation is associated with π-complexation of the Cp* ligand and a high η^5 coordination number. Two years later, Driess succeeded in the isolation of compound **L47**, stabilised by aromatic 6π-electron delocalisation and intramolecular donation of the sterically encumbered β-diketiminate ligand.[189] Interestingly, it represents the sole example of an isolable two-coordinate silyliumylidene ion outside of a metal sphere to date. Analogous to the application of NHCs in the stabilisation of silylenes, the application of NHCs to stabilise silyliumylidene ions led to an increased variety of isolable species.

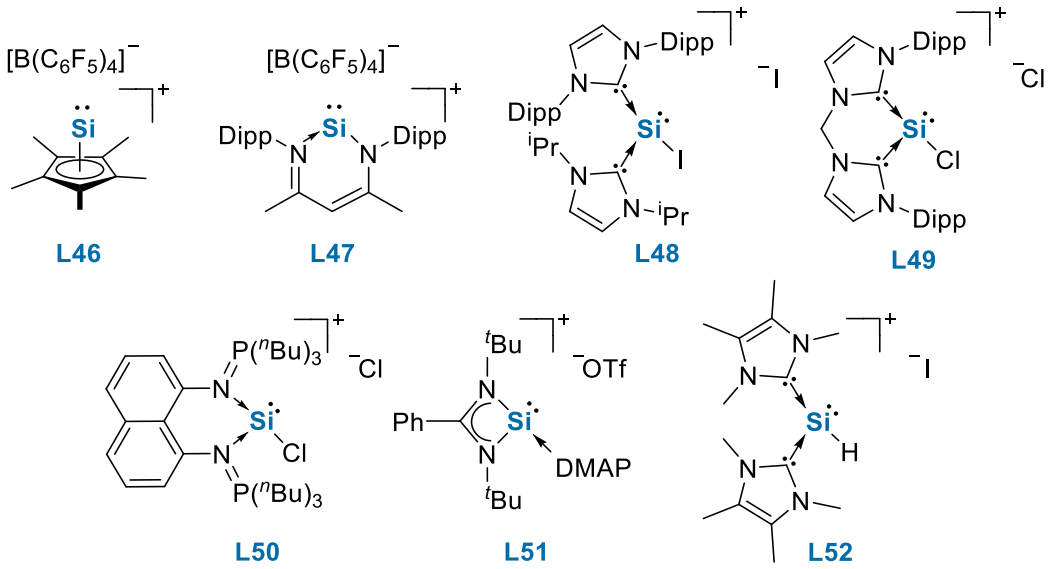

Figure 17: Selected examples of isolated silyliumylidene ions.

The group of Driess described the bis-carbene stabilised chloro-silyliumylidene ion **L49**, which can be converted to silylone **L6** (Figure 6) *via* treatment with sodium napthalenide.[63] The first example of a silyliumylidene ion stabilised by two different NHCs was reported by the group of Filippou.[190] The bis-

NHC-stabilised iodo-silyliumylidene ion **L48** is obtained in a stepwise approach by coordination of IDipp to SiI_4, reduction with KC_8 and further addition of $I^iPr_2Me_2$. Other examples of isolable silyliumylidene ions include the chelated bis(iminophosphorane)-stabilised chloro-silyliumylidene ion **L50**[191] and DMAP-stabilised, amindinate-substituted silyliumylidene **L51**.[192]

This thesis focuses on NHC-stabilised aryl-substituted silyliumylidene ions, thus a general overview of aryl ligands used in low-valent main group is given in Figure 18. Aryl ligands of type **F18.A** (2,4,6-trialkyl-phenyl ligands) still bear free rotation of the alkyl groups attached to the phenyl ring and have enabled the isolation of the first disilene **L31** (Figure 14). Although officially belonging to the same 2,4,6-trialkyl-phenyl ligands, **F18.B** bear increased steric demand due to the silyl groups attached at the benzylic position. This is easily exemplified by the isolation of a bis(Bbt)-substituted disilyne by the group of Tokitoh, which represents the sole example of an aryl-stabilised Si≡Si triple bond to date.[175,193] In contrast, 2,6-bis(2,6/2,4,6-di/tri-alkyl-phenyl)phenyl ligands of type **F18.C** possess hindered rotation around the C–C bond in the *ortho*-position and have the additional possibility of stabilizing a low-valent element by interaction with the flanking phenyl groups.[194] This type of ligand has been widely used in low-valent main group chemistry.[106,195-196] However, they have a tendency to coordinate group one cations to the flanking aryl rings, which is discussed further in chapter 3. The last group **F18.D** is based on a rigid fused-ring s-hydrindacenyl skeleton bearing the possibility to tune the steric demand at the benzylic positions. The rotation of substituents in ortho position discussed previously for **F18.A-C** is effectively frozen in aryl groups of type **F18.D**.[197]

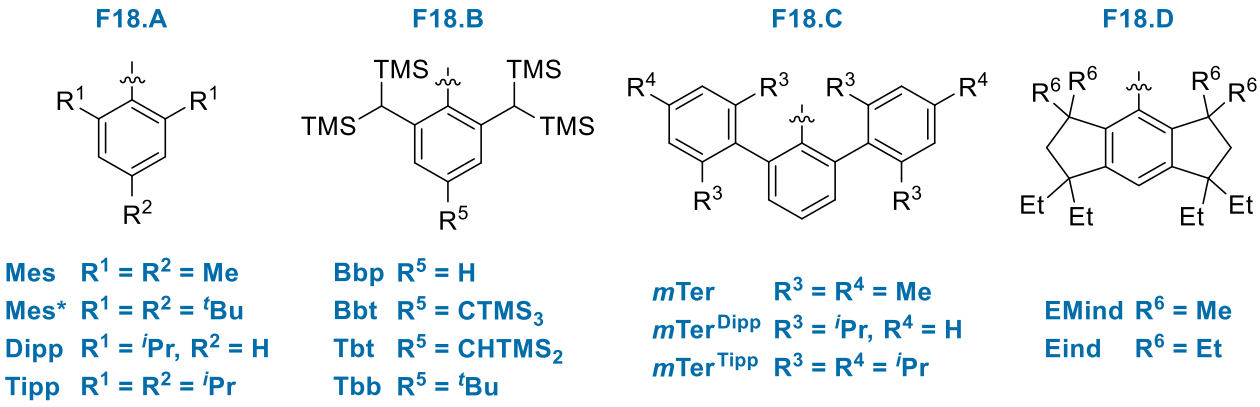

Figure 18: Overview of aryl ligands used in low-valent main group chemistry.

An overview of reported NHC-stabilised aryl-substituted silyliumylidene ions and connected chloro-silylenes including their synthetic routes is given in Figure 19. The groups of Sasamori, Matsuo and Tokitoh jointly received silyliumylidene ions **L53** and **L54** *via* treatment of their bromo- and aryl-substituted disilenes **L57** and **L38** with four equivalents of IMe_4.[198] In the same report, NHC-stabilised aryl-bromo-silylenes **L58** and **L59** were obtained *via* treatment with two equivalents of the NHC, whereas the corresponding silyliumylidene ion bearing the Bbt ligand was not accessible. Concurrently, the Inoue group was able to obtain the *m*Ter- and Tipp-substituted **32** and **33** *via* treatment of the corresponding aryl-di(chloro)-silane Si(IV) precursor with three equivalents of IMe_4. This resulted in formation of the imidazolium salt IMe_4·HCl along with the desired compounds **32** and **33** as orange and yellow compounds, respectively.[199] It should be noted, that this synthetic procedure has been used by Filippou to access **L10** using only two equivalents of NHC, whereby the formation of an orange compound was observed but could not be identified.[68] In 2018, the groups of Sasamori, Matsuo and Tokitoh expanded on both approaches, the disilene route as well as the Si(IV) route. The Eind-substituted silyliumylidene ion **L55** is also accessible from the Si(IV) route, albeit synthesis *via* the disilene route gives the product in higher purity.[200] Furthermore, the bromo-silylene **L60** was isolated. Frisch and Inoue quite recently extended the Si(IV) route to the Mes-substituted silyliumylidenes **L56**, whereas also silyl-substituted silyliumylidene ions (R = $^tBu_3Si$, $^tBu_2MeSi$) were shown to be accessible *via* the Si(IV) route.[201] The group of So contributed

the parent silyliumylidene ion [H-Si(IMe$_4$)$_2$I] **L52** (Figure 17), formed *via* treatment of NHC-stabilised iodosilicon(I) dimer with four equivalents of IMe$_4$. The proposed mechanism includes the initial formation of a cationic, NHC-stabilised silicon(I) radical which is able to abstract a proton from the solvent toluene.[202]

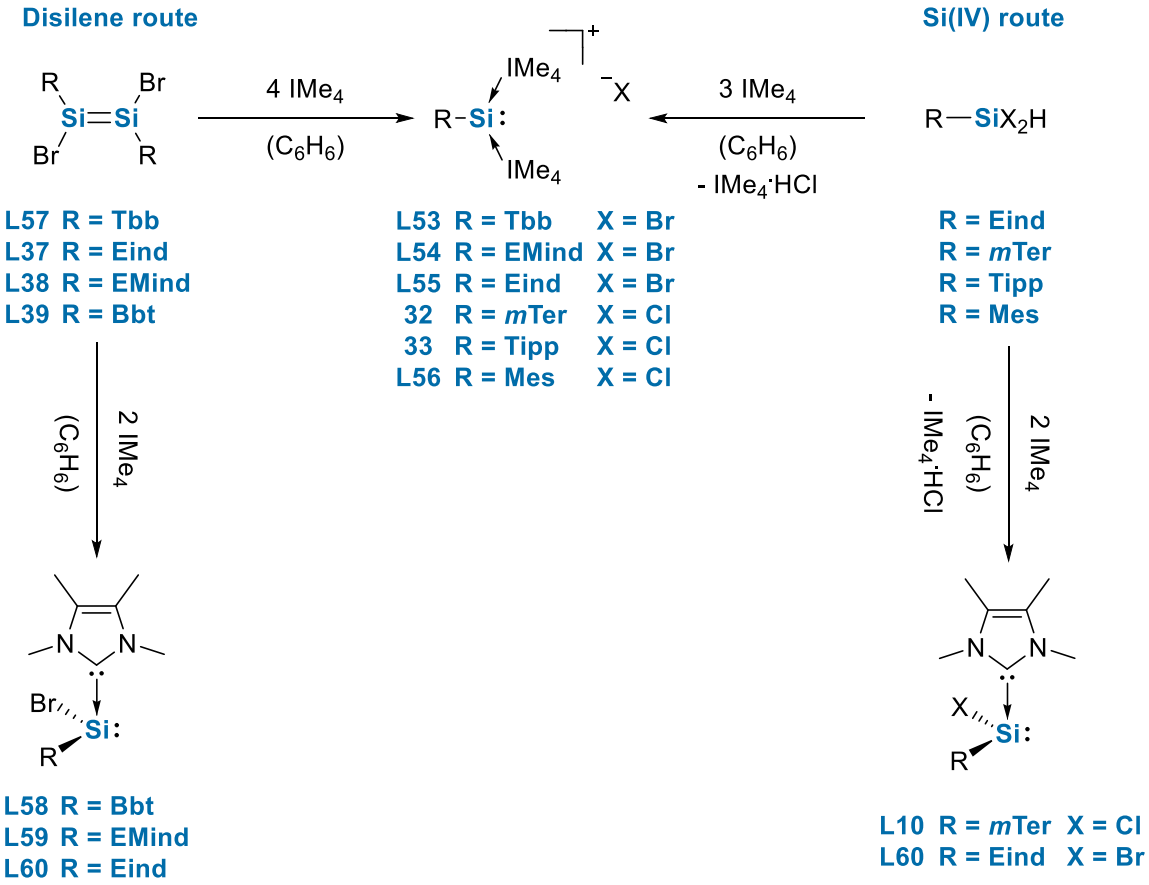

Figure 19: Reported NHC-stabilised aryl-substituted silyliumylidene ions bearing two identical NHC units and accessible NHC-stabilised aryl-substituted chloro-silylenes; Tbb = 2,6-(CHTMS$_2$)$_2$-4-^{t}Bu-C$_6$H$_2$.

Reactivity of NHC-stabilised Silyliumylidene Ions

Based on their ambiphilicity, silyliumylidene ions bear two reactive sites: a lone pair and (potential) vacant p-orbitals, dependent on the donors applied. However, the discussion concerning the usage of dative bonds, as already stated for the NHC-stabilised silylenes, also comes into play for NHC-stabilised silyliumylidene ions. The two discussed *Lewis* representations are given in Figure 20: (i) two covalent silicon–carbene bonds, the positive charge delocalized in the NHCs and thus the silicon centre bears a negative charge or (ii) two dative silicon–carbene bonds with the positive charge residing on the silicon centre.

Reactivity studies of silyliumylidenes were mainly limited to their use as synthons for asymmetric silylenes, e.g. silylene **L25** in Figure 11 was obtained from **L46** and LiNIDipp.[128,203] Furthermore, silylene-like reactivity was reported for **L50** and **L51** in the activation of elemental sulphur.[191-192] The group of Inoue further demonstrated the C-H activation of terminal alkynes, namely phenylacetylene, to give **L61** (Figure 20) as the Z isomer only.[199] In 2015, isolation of the NHC-stabilised silaacylium ion **L62** was accomplished *via* reaction with carbon dioxide and elimination of CO.[204] It is of note, that decreased kinetic stabilisation of the Tipp ligand in **33** prevented the isolation of the corresponding silaacylium ion due to decomposition occurring at temperatures above –30 °C. However, it was characterized *via* low-temperature NMR measurement. The heavier analogues **L63-L65** were isolated in a similar approach, where the possibility

of chalcogen transfer as well as conversion back to the silyliumylidene ion, by treatment with AuI, was presented.[205] The originally stated double bonding character between silicon and the chalcogens, especially oxygen, is still debateable due to the high electronegativity differences of silicon and oxygen. The decreasing tendency to form multiple bonds on descending the group, in addition to the positive charge of the complexes, renders multiple bond formation unlikely. Thus, **L62-L65** are depicted without carbene–silicon dative bonds and the Si–E (E = O, S, Se, Te) bonds are depicted as a single bond, although some multiple bond character could be anticipated based on negative hyperconjugation.[206]

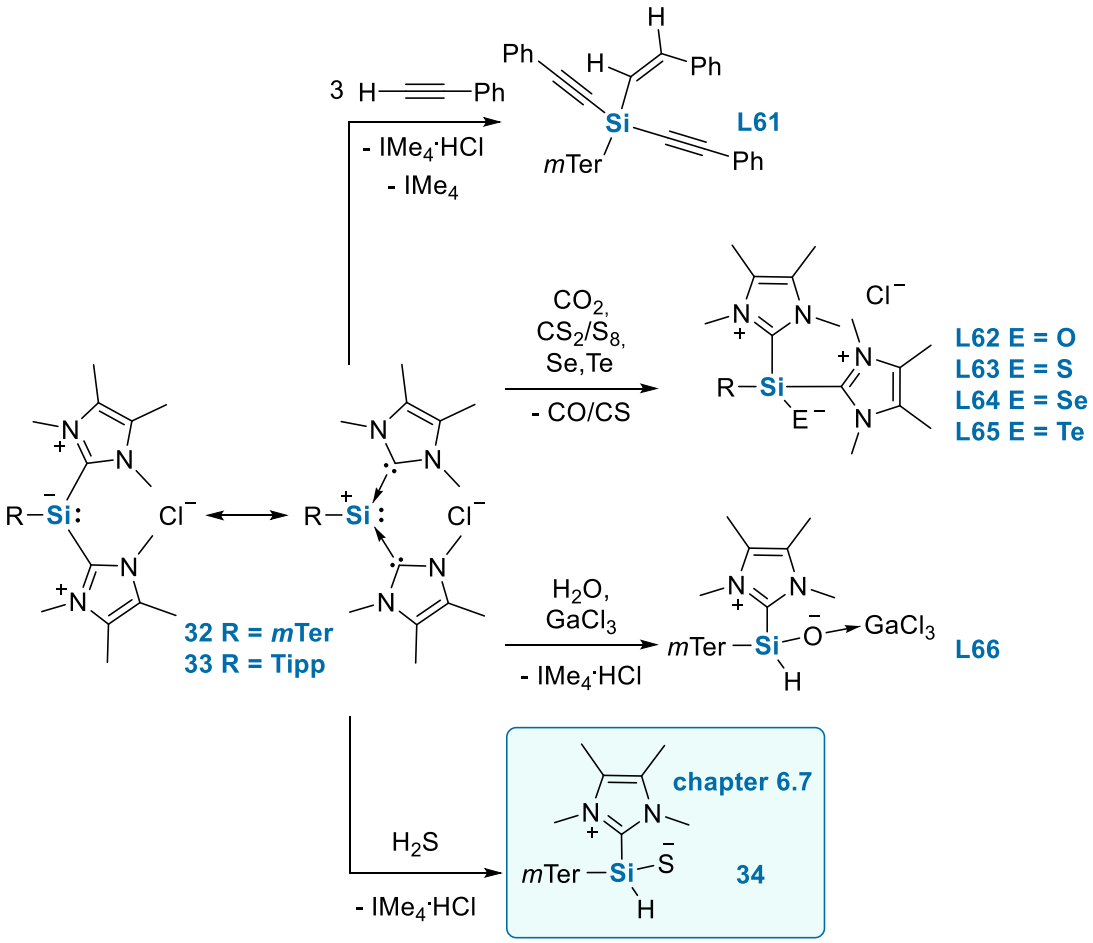

Figure 20: Reported reactivity of NHC-stabilised silyliumylidene ions **32** and **33** towards small molecules.

The conversion of **32** and **33** with hydrogen sulphide, yielding **34,** was successfully studied in a combined experimental and theoretical approach (see chapter 6.7). Furthermore, clean conversion of **32** with water was possible with additional *Lewis* acid stabilisation necessary to obtain a donor-acceptor stabilised silaaldehyde **L66**.[207] Beside the activation of small molecules, application of NHC-stabilised silyliumylidene ions as ligands in transition-metal complexes were also explored and reviewed recently.[208]

Silyliumylidene Ions in Catalysis

At the beginning of this thesis, the solely known catalytic application of low-valent silicon was the **L46** catalysed degradation of oligoethylenglycol ethers (Scheme 3A) reported by the group of Jutzi in 2011.[209] The calculated mechanism proceeds *via* initial coordination of two molecules of dimethoxyethane (DME) to the silicon centre which enables the conversion to dioxane and dimethyl ether *via* rearrangement of the σ-bonds and lone pairs. This was experimentally verified *via* SC-XRD of the DME adduct of **L46**, which revealed rather weak Si–O interactions but a change in coordination of silicon to the Cp* ligand to η^3. The adduct is not particularly stable and decomposes within several days in solution to yield dioxane and

dimethyl ether, whilst reforming the catalyst. However, the catalysis experiments required rather high catalyst loadings of 5-10 mol% and required up to 20 days to reach full conversion. This paper remained the sole example of low-valent silicon in catalysis until October 2019, where the publications of Fritz-Langhals and So manifested the usability of silyliumylidene ions in catalysis.[210-211]

In the former report again silyliumylidene ion **L46** was used, which was shown to be accessible from bis(Cp*)-substituted silylene **L1** (Figure 5) with the more convenient and readily available hydride abstraction agent $[Ph_3CB(C_6F_5)_4]$ under release of tetra-methyl fulvene. Fritz-Langhals revealed this silyliumylidene ion to be an active catalyst in the hydrosilylation of terminal olefins (Scheme 3B) with a variety of silanes or siloxanes yielding the anti-Markovnikov products as well as internal olefins and terminal alkynes (not shown).

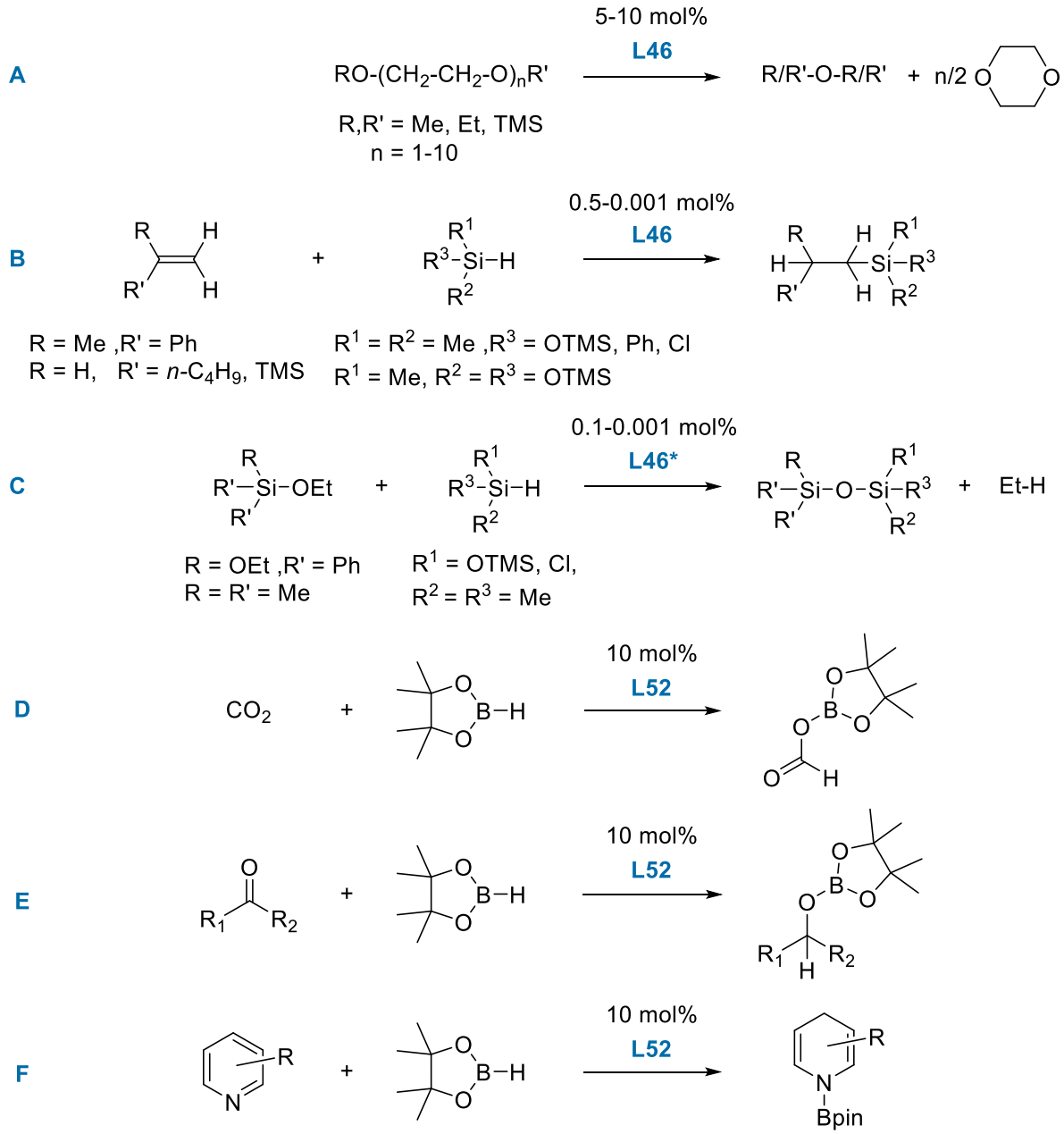

Scheme 3: Reported examples of silyliumylidene as catalyst, **L46*** = **L46** with a different anion, namely $HB(C_6F_5)_3^-$.

The suggested mechanism includes coordination of the silane to the silicon centre *via* the hydride - thus the silicon centre acts as a *Lewis* acid - followed by insertion of the substrate and subsequent release of

the product. This so-called “cationic” mechanism was proposed in the case of electron-deficient borane-catalysed hydrosilylation reactions[212-214] and was further evidenced by coalescence of the Si-H proton in Et_3SiH after addition of 0.10 mol% of **L46**. The catalysis proceeds at rt with low to very low catalyst-loadings (0.1-0.001 mol%). Reaction times vary from ten minutes up to one day depending on the substrate and silane. Furthermore, catalytic crosslinking of hydrido-siloxanes and vinyl-siloxanes was obtained, although higher temperatures are necessary for this type of catalysis.

In the second part of this paper, **L46** was examined concerning its properties in Piers-Rubinsztajn reactions (Scheme 3C): the conversion of silyl ethers and silanes to give siloxanes and alkanes, which was hitherto only possible with BCF.[215] Compound **L46*** (**L46*** = **L46** with $HB(C_6F_5)_3^-$ anion) was shown to effectively catalyse this reaction, resulting in formation of industrially relevant siloxane copolymers as well as branched silicones. However, an increased reaction temperature of 55 °C and use of a small amount of solvent is necessary, to overcome the catalyst blocking *via* coordination of the oxygen of the siloxane to the silicon centre. This further allows for a reversible inhibition of the silyliumylidene ion in hydrosilylation catalysis *via* addition of small amounts of alkoxy-silanes.

Concomitantly, the group of So reported their application of silyliumylidene ion **L52** in hydroboration of CO_2 and a variety of aldehydes, ketones and amines (Scheme 3D, E and F).[211] The catalytic hydroboration of CO_2, ketones and amines was performed with high catalyst loadings of 10 mol% as well as high temperatures (90 °C) to ensure complete conversion. Only in the case of aldehydes, the hydroboration can be performed at rt. Their calculated mechanism (only given for the reaction of CO_2 and pinacolborane (HBpin)) relies on coordination of the carbon atom in CO_2 to the silicon centre, which enables the conversion with HBpin, thus representing a *Lewis* base catalytic cycle. Furthermore, it was stated that catalytic reduction of CO_2, with HBpin, is possible under air and in “wet” C_6D_6 (78 ppm H_2O). This is intriguing considering the known instability of silyliumylidene ions in air and water. However, it is of note that no comment concerning the stability of **L52** at higher temperatures was provided, thus raising questions about the identity of the active catalyst. Nevertheless, it was clearly shown that silyliumylidene ions are effective (pre-)catalysts in a variety of hydroboration reactions, with the actual catalytically active species yet to be identified.

3. Low-Valent Aluminium Chemistry

Aluminium is the most abundant metal within the earth crust (Figure 2a) but is contained almost exclusively in oxides and hydroxide minerals in nature.[32] In its metallic form, it is highly used in packaging, transportation and construction due to its low density and good manufacturing properties. Another advantage of aluminium, especially in comparison to iron, is its corrosion resistance as it forms a closed and durable oxide surface layer, which is industrially obtained *via* anodisation processes.

The differences between atoms belonging to the same group but a different period, like carbon and silicon discussed in chapter 2, are revisited upon comparison of boron and aluminium. Belonging to group 13, their preferential oxidation state is +III with an empty p-orbital residing on the boron/aluminium centre (Figure 21 **F21.A** for Al), representing the *Lewis* acidic site. Thus, in comparison to group 14 compounds in oxidation state +IV, trivalent aluminium compounds are electrophilic in nature.[32] Aluminium centres are highly polarized due to the combination of a high charge and a small cation radius (0.68 Å).[216] In going from B to Al the electronegativity decreases (B: 2.01, Al: 1.47 on Pauling scale) and descending group 13, the tendency to build π bonds decreases whereas the tendency for coordination increases (Figure 21 **F21.B**).[32] Hence, access to isolable low-valent aluminium species is enabled by high steric bulk of the attached ligands to kinetically protect the small aluminium centre and/or coordination of internal/external electron donors (exemplified for alumylenes **F21.C**/**F21.D**/**F21.E** Figure 21) to prevent oligiomerisation as well as disproportionation. Alumylenes are isolobal to silylenes as well as isoelectronic to silyliumylidenes. Thus, the HOMO of alumylene **F21.C** is a lone pair, with the two empty p-orbitals reflecting the ambiphilicity present in this compound.

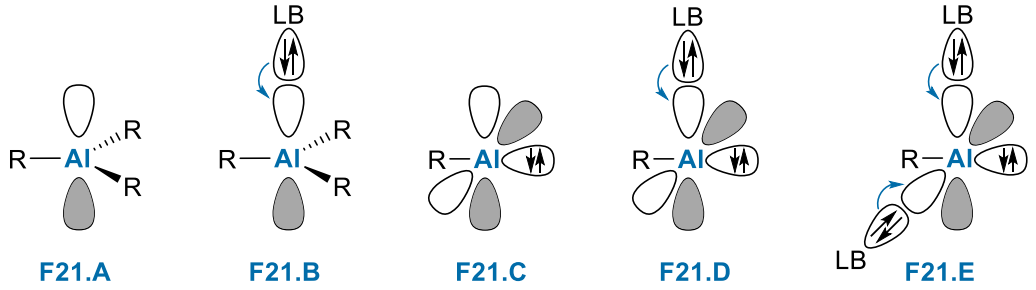

Figure 21: Frontier orbitals of Al(III) **F21.A**/**F21.B** and Al(I) **F21.C**/**F21.D**/**F21.E** compounds.

The first structurally characterized aluminium–aluminium bond in **L67** (Figure 22) was described by Uhl in 1988,[217] starting the "renaissance" of aluminium chemistry.[218] Following the Si/Al comparison, the increased importance of the steric protection for a Al(I) species is easiest explained by the Cp*-substituted compounds: the bis(Cp*)-substituted silylene **L68** as well as Cp*-substituted silyliumylidene ion **L46** are isolable compounds, whereas the corresponding Cp*Al: tetramerizes in the solid state to give **L68**.[219] However, a ^{27}Al NMR signal at higher temperatures was ascribed to the monomeric species, revealing only a minor barrier for the dissociation from the tetramer in solution.[220]

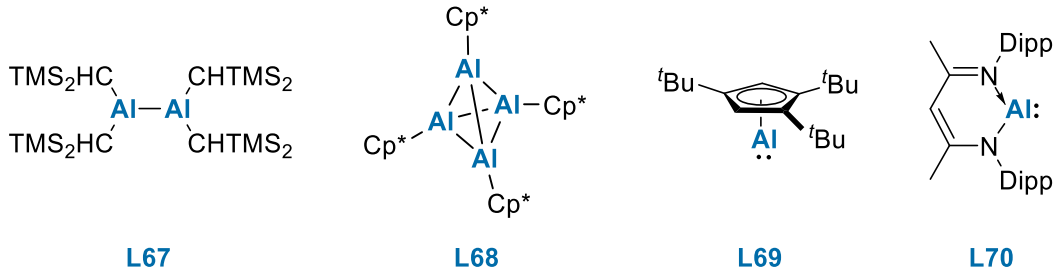

Figure 22: Selected examples of reported low-valent aluminium compounds.

Several different varieties of substituted Cp-ligands have been studied and have been shown to influence this monomer-tetramer equilibrium, depending on the steric demands of the Cp ligand. In 2019, the group of Braunschweig synthesised the monomeric complex, **L69**, using the highly sterically demanding Cp^{tBu3} ligand (Cp^{tBu3} = 1,3,5-tri-^{t}Bu-cyclopentadienyl).[221] However, a modified experimental approach involving multiple steps was necessary, highly connected to Fischer's as well as Cowley's studies on the redox equilibrium between Al(I) and Al(III) dependent on ligand coordination.[222-223] The group of Roesky contributed **L70** as the first isolated monomeric Al(I) compound in 2000,[224] which has been studied extensively since then.[218,225] Similar to Driess' compound **L47** in silyliumylidene chemistry, **L70** occupies a special position in low-valent aluminium chemistry as being the sole reported monomeric twofold coordinate Al(I) compound to date. An overview on the development of low-valent aluminium compounds can be found in Wehmschulte's review on Al(I) and Al(II) compounds.[226]

Literature concerning NHC-stabilised low-valent aluminium compounds is relatively rare. The group of Jones described the NHC-adduct of the parent dialane bearing Al(II) centres in **L71** (Figure 23), which is accessible *via* treatment of the adduct $IDippAlH_3$ with their well-known Mg(I) reagent.[227] Li *et al.* succeeded in the isolation of an asymmetric substituted Al-Al bond bearing one Al(I) and one Al(III) centre, with the latter stabilised by a coordinated cAAC moiety.[228] Only three examples of NHC-stabilised alumylenes have been reported to date. As such compounds **L72** and **L73** were isolated by the group of Driess, originally attempting to access a bis-NHC and acceptor-stabilised Al(I) hydride.[229] However, treatment of **L72** with potassium hydride in THF resulted in the formation of H_2 and **L73**. Quite recently, the Braunschweig group were able to isolate the parent alumylene :Al-H in **L74** *via* stabilisation with two cAAC moieties, this however bears considerable diradical character.[230]

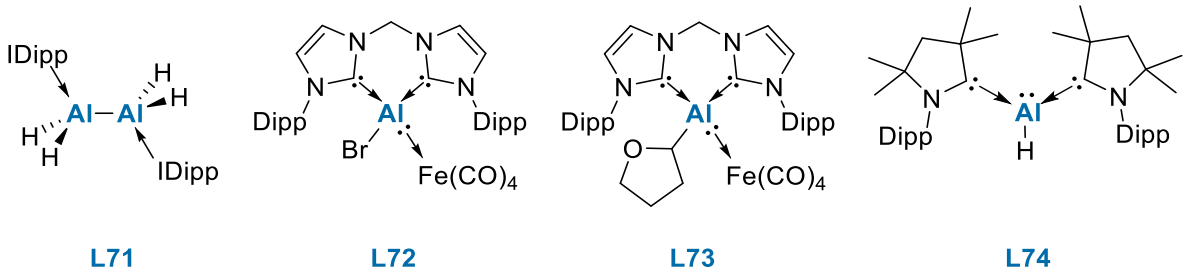

L71 **L72** **L73** **L74**

Figure 23: Reported low-valent NHC-stabilised aluminium compounds.

Turning to the dimeric compounds, namely dialumenes, the concepts discussed in chapter 2 are revisited. The CGMT model[157-160] as well as 2nd order Jahn-Teller distortions[161-162,164] are applicable to dialumenes. This is shown for only one ligand attached to the central atom (as per typical group 13 coordination) in Figure 24, yielding *trans*-bent and/or twisted structures. The same holds true for the electronic effect of the ligands attached to the aluminium centre: electropositive groups facilitate planarisation and electronegative groups promote *trans*-bent/twisted structures.

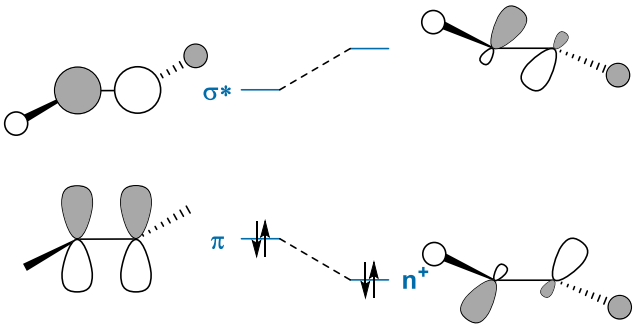

Figure 24: 2nd order Jahn-Teller distortions responsible for observed *trans*-bent geometries.

The isolation of the dimeric unit of alumylenes posed a challenge for some time, even though a series of compounds bearing a bond order higher than one could be isolated (Figure 25).[231] In 1993, the group of Uhl and the group of Pörschke succeeded in isolation of the K/Li salts of the radical mono-anionic compounds **L75**.[232-233] These compounds exhibit a planar structure, based on the additional electron occupying the empty p-orbital on aluminium, which is delocalized on both centres as a π-type orbital. Power *et al.* described the Tipp-substituted version **L76** shortly afterwards.[234] The group of Power pursued the dialumene challenge and reported di-anionic dialumene **L77**, obtained *via* treatment of *m*Ter^{Dipp}AlI$_2$ (*m*Ter^{Dipp} = 2,6-Dipp$_2$-C$_6$H$_3$) with elemental sodium, in 2006.[235] The aluminium centres are 2.428(1) Å apart and the sodium cations are coordinated to the flanking phenyl groups. Similar to Robinson's analogue gallium compound,[236] there had been a considerable debate if the central bond bears triple bond character, as stated in the original publication, or only a bond order > 1. Remarkably, usage of the less bulky *m*Ter group resulted in a tri-anionic and trimeric structure.

Furthermore, four different masked dialumenes **L78**-**L81** were isolated and characterized. Power *et al.* were successful in the trapping of the intermediary dialumene (**L78**, Figure 25), as the toluene adduct upon reduction of *m*Ter^{Dipp}AlI$_2$ with KC$_8$ in a stepwise approach.[237] Following a similar procedure under supplementary addition of bis(TMS)acetylene, the group of Cui isolated **L79**.[238] Tokitoh *et al.* contributed **L80** and **L81** bearing the sterically demanding Bbp (Bbp = 2,6-(CHTMS$_2$)$_2$-C$_6$H$_3$) or Tbb (Tbb = 2,6-(CHTMS$_2$)$_2$-4-^{t}Bu-C$_6$H$_2$) group in 2012 and 2015,[239-240] respectively. Compound **L80** showed reversible exchange of the benzene unit with C$_6$D$_6$ as well as exchange with naphthalene, anthracene and bis(TMS)acetylene. In a follow-up report, Tokitoh's group evinced **L80** and **L81** being able to activate H$_2$, whereas the anthracene adducts are not capable of this.[241]

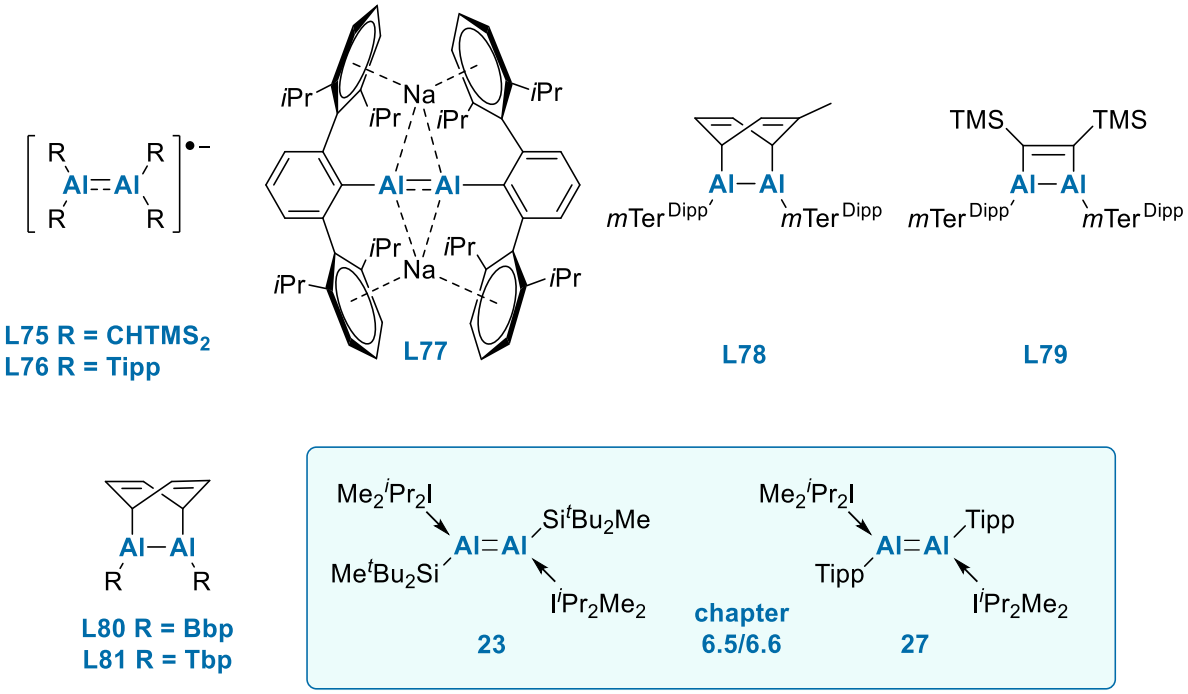

Figure 25: Reported examples of compounds containing an aluminium-aluminium bond with bond order > 1; *m*Ter^{Dipp} = 2,6-Dipp$_2$-C$_6$H$_3$, Bbp = 2,6-(CHTMS$_2$)$_3$-C$_6$H$_3$.

On the theoretical side, different group 13 dimetallenes REER (E = Al, Ga, In, Tl, R= H, Me, ^{t}Bu, Ph) were systematically investigated with a variety of different methods in 2010 by Moilanen, Power and Tuononen.[242] They revealed dialumenes bear considerable singlet diradical character, which becomes even more important in the case of digallenes. The group of Frenking and the group of Jones jointly performed a study on NHC-stabilised trielanes, NHC-stabilised ditrielanes, NHC-stabilised ditrielenes and NHC-stabilised ditrielyne bearing hydride, chloride or no substituents and IMe$_2$H$_2$ (:C[NMeCH]$_2$) as the

NHC.[243] Accordingly, (HAl $IMe_2H_2)_2$ bears a *trans*-planar and (ClAl $IMe_2H_2)_2$ exhibits a *trans*-bent structure. Depending on the substituent, the interaction energies of the NHC as the donor and the Al_2X_2 core (X = H, Cl) as the acceptor diverge: In the case of the chloride-substituent, a π-type orbital at the Al_2Cl_2 is the acceptor for electrons donated from the NHC, whereas in the hydride case a low-lying empty σ-orbital is the accepting orbital. Thus, it is apparent that NHC-stabilised dialumenes are isostructural to disilenes.

Inspired by the successful isolation of a variety of silyl-substituted disilenes, the combination of NHC-stabilisation and the bulky silyl group $SiMe^tBu_2$ enabled the isolation of the first dialumene **23**, discussed in chapter 6.5 with initial reactivity studies. In a follow-up report, this dialumene was shown to react with CO_2, N_2O and O_2, as well as catalysing the hydroboration of CO_2.[244] Furthermore, the effect of the stabilising ligand in dialumenes was studied *via* exchange to aryl-substituted **27** with the results discussed in chapter 6.6.

A rather new chapter in low-valent aluminium chemistry are anionic aluminyls (Figure 26). Aldridge, Goicoechea and co-workers started this type of chemistry, with the isolation of **L82** in 2018.[245] Stoichiometric reduction of (NON)AlI (NON = 4,5-bis(2,6-diisopropylanilido)-2,7-di-^{t}Bu-9,9-dimethylxanthene) with KC_8 gives the dimeric $[Al(NON)]_2$, whereas conversion with excess KC_8 yields **L82**. Based on the increased anionic character, the aluminium centres bears enhanced nucleophilicity, which enables this compound to undergo C–H activation with benzene as well as activation of H_2. Furthermore, reactions with electrophilic reagents, like CH_3OTf or MeI, result in the formation of new aluminium-element bonds, whereas in the case of electrophilic Al(I) centres the formation of the corresponding Al(III) halide product was observed.

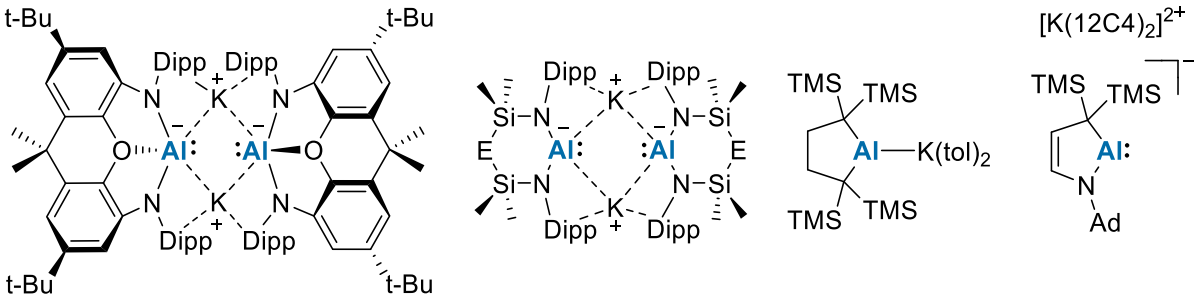

L82 **L83 E = O** **L84 E = CH_2CH_2** **L85** **L86**

Figure 26: Reported anionic aluminyl compounds; tol = toluene, 12C4 = 12-crown-4 ether.

The group of Coles and the group of McMullin successfully isolated **L83** and **L84**, bearing a comparable nucleophilic aluminium centre but a reduced coordination number compared to **L82**.[246-247] In terms of reactivity, **L83** can reduce 1,3,5,7-cyclooctratetraene (COT), which features its potential as a reducing agent, although the potassium cation plays an important role in the reactivity of those compounds. Compound **L84** gives access to the magnesium and calcium alumanyl compounds, which can be further converted with COT to give hetero-bimetallic inverse sandwich complexes. The group of Yamashita contributed compound **L85** as the first alkyl-substituted aluminyl, bearing a rather short aluminium–potassium bond.[248] Despite, nucleophilic reactivity of the aluminium centre was demonstrated similar to **L82** and additionally a series of [1+2] and [1+4] cycloaddition reactions towards unsaturated hydrocarbons was shown.[249] Koshino and Kinjo reported cyclic (alkyl)(amino)aluminyl anion **L86**, as the aluminium version of the isoelectronic cAACs.[250] Its ambiphilicity was evinced by oxidative addition to Si–H, N–H and non-polar C–C bonds. Furthermore, a B–B coupling reaction to yield a triangle AlB_2 unit was presented.

4. Theoretical Background

In this thesis, density functional theory (DFT) in combination with Natural Bond Orbital (NBO) and Quantum Theory of Atoms in Molecules (QTAIM) analysis was used to explore the bonding situation of unprecedented bonding motifs to allow for choosing an appropriate *Lewis* representation. Moreover, these methods were used for identification of non-isolable intermediates *via* calculation of NMR shifts or UV/vis bands. In the following, all methods applied in chapter 6 are briefly discussed. This overview is based on several books and journal articles addressing the general concepts of computational chemistry[251-253], NBO[254-256] and QTAIM.[257-259]

All quantum chemical approaches have one aim in common: a description of the electronic structure of atoms and molecules to describe the properties of a molecular system. To this end, the time-independent, non-relativistic *Schrödinger* equation (1) needs to be solved, or more precisely, needs to be approximately solved: $\hat{H}$ applied to the wave function Ψ maps to the wave function times its eigenvalue E, the energy of the system.

$$\hat{H}\Psi = E\Psi \tag{1}$$

$\hat{H}$ is the Hamilton operator for a molecule, bearing M nuclei and N electrons, which consists of the kinetic energy of electrons and nuclei ($\hat{T}_e$ and $\hat{T}_N$), the potential energy of electrons and nuclei among themselves ($\hat{V}_{ee}$ and $\hat{V}_{NN}$) as well as Coulomb attraction between electrons and nuclei ($\hat{V}_{Ne}$):

$$\hat{H} = \hat{T}_e + \hat{T}_N + \hat{V}_{Ne} + \hat{V}_{ee} + \hat{V}_{NN} \tag{2}$$

Thus, the complete expression of $\hat{H}$ in atomic units is

$$\hat{H} = -\frac{1}{2}\sum_{i=1}^{N}\nabla_i^2 - \frac{1}{2}\sum_{A=1}^{M}\frac{\nabla_A^2}{M_A} - \sum_{i=1}^{N}\sum_{A=1}^{M}\frac{Z_A}{r_{iA}} + \sum_{i=1}^{N}\sum_{j>i}^{N}\frac{1}{r_{ij}} + \sum_{A=1}^{M}\sum_{B>A}^{M}\frac{Z_A Z_B}{R_{AB}} \tag{3}$$

Further simplification is obtained by the *Born-Oppenheimer* approximation, taking advantage of the high mass difference between nuclei and electrons, which in a good approximation considers only electrons moving in the field of fixed nuclei. Thus, kinetic energy of the nuclei $\hat{T}_N$ becomes zero and the potential energy $\hat{V}_{NN}$ a constant, to yield the electronic Hamiltonian:

$$\hat{H}_{elec} = -\frac{1}{2}\sum_{i=1}^{N}\nabla_i^2 - \sum_{i=1}^{N}\sum_{A=1}^{M}\frac{Z_A}{r_{iA}} + \sum_{i=1}^{N}\sum_{j>i}^{N}\frac{1}{r_{ij}} = \hat{T} + \hat{V}_{Ne} + \hat{V}_{ee} \tag{4}$$

Hence, the total energy of a system is given by the electronic *Schrödinger* equation (5), depending solely on the electron coordinates.

$$(\hat{H}_{elec} + \hat{V}_{NN})\Psi_{elec} = (E_{elec} + V_{NN})\Psi_{elec} \tag{5}$$

Thus, if Ψ_{elec} is known (or at least a good approximation) eq. (5) can be solved to access the energy of the considered system. However, this is only possible for one-electron systems like H_2^+ in reasonable calculation time. Further simplification is necessary to allow for calculations of multi-electron systems, starting with the *Hartree-Fock* approximation. Here, the unknown N electron wave function is replaced by *N* one-electron wave functions to obtain the so-called *Slater* determinant Φ_{SD} in eq. (6), also fulfilling *Pauli* principle.

$$\Psi_{elec} \approx \Phi_{SD} = \frac{1}{\sqrt{N!}}\det\{\chi_1(\vec{x}_1)\,\chi_2(\vec{x}_2)\,\cdots\,\chi_N(\vec{x}_N)\} \tag{6}$$

Here the one-electron functions consist of linear combinations of atomic orbitals (LCAO-approach), which are obtained by analytical solution of the wave function within the *Born-Oppenheimer* approximation for the hydrogen atom. The *N* one-electron wave functions contain a spin function $\sigma(s)$ and a spatial orbital $\phi(\vec{r})$ and are called spin orbitals, thus dependent on the coordinates ($\vec{r}$) of the electron as well as its spin state:

$$\chi(\vec{x}) = \phi(\vec{r})\,\sigma(s), \qquad \sigma = \alpha, \beta \tag{7}$$

Separation of the wave function Ψ into those orthonormal spin orbitals further allows for simplification of the *Hamiltonian* to the sum of N one-electron *Hamilton* operators $\hat{f}_i$, so-called *Fock* operators, in eq.(8). Application of the *Fock* operator on a spin orbital yields the eigenvalue ε_i, representing the orbital energy.

$$\hat{H}_{elec} = \sum_{i}^{N} \hat{f}_i \tag{8}$$

with

$$\hat{f}_i = -\frac{1}{2}\nabla_i^2 - \sum_{A}^{M} \frac{Z_A}{r_{iA}} + V_{HF}(\vec{x}_i) \tag{9}$$

and

$$V_{HF}(\vec{x}_i) = \sum_{j}^{N} \left(\hat{J}_j(\vec{x}_i) - \hat{K}_j(\vec{x}_i) \right) \tag{10}$$

The *Fock* operator is defined according to eq. (9), with the first two terms representing the kinetic and potential energy due to electron-nucleus attraction. The third term, also referred as *Hartree-Fock* potential, represents a *mean field potential*, thus the average repulsive potential experienced by electron i from the remaining N-i electrons. This can be further divided into the repulsive Coulomb interaction of the electrons $\hat{J}$ and the exchange operator $\hat{K}$ according to eq. (10). Application of the *Rayleigh-Ritz principle* yields minimisation of the total energy *via* appropriate choice of the spin orbitals. By use of the self-consistent field approach (SCF) the best coefficients for the molecular orbitals are obtained by iterative algorithms (Scheme 4).

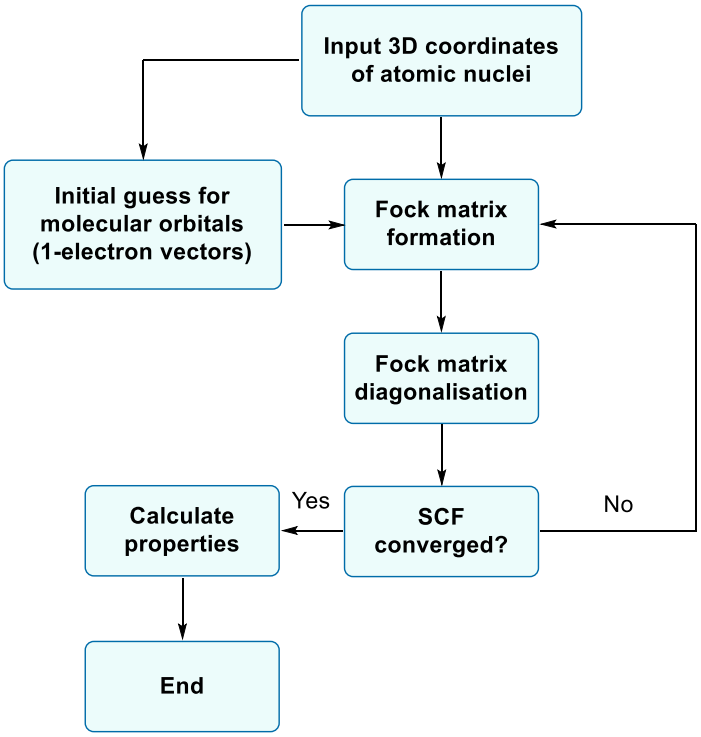

Scheme 4: Schematic representation for the calculation of the electronic ground state of a molecule.

With these equations on hand, the simplest method of computational chemistry - HF calculations - can be implemented after choosing suitable basis sets (see chapter 4.2). Inclusion of particular electron correlation gives post-HF *ab inito* methods, such as Møller-Plesset (MP) perturbation theory, configuration interaction (CI) and coupled cluster (CC) approaches. They offer improved accuracy of the calculation, however costs increase with the increasing calculation time and required computational resources. DFT represents a rather inexpensive approach in computational chemistry. It is applicable for complex and huge systems whilst yielding satisfactory results. The concepts of DFT are introduced in the following chapter.

4.1. Density Functional Theory

As a different approach to the one discussed previously, DFT replaces the 4N-dimensional wave function Ψ by the observable electron density $\rho(\vec{r})$ which depends only on the spatial variable $\vec{r}$. Thus, $\rho(\vec{r}_1)$ gives the probability to find one of the N electrons with arbitrary spin inside of the volume element $d(\vec{r}_1)$.

$$\rho(\vec{r}) = N \int \cdots \int |\Psi(\vec{x}_1, \dots, \vec{x}_N)|^2 d\vec{s}_1 d\vec{x}_2 \dots d\vec{x}_N \tag{11}$$

The electron density has to fulfil three physical boundary conditions: (i) integration over the complete space yields the total number of electrons, (ii) it decreases to zero for infinite distances and (iii) it exhibits a cusp at the position of the nuclei.

The DFT approach relies on two important theorems by *Hohenberg* and *Kohn*. The first theorem reveals the unambiguous connection between electron density and an external potential $\hat{V}_{ext}(N, R_A, Z_A)$. Thus, the Hamilton operator as well as its wave function is uniquely determined.

$$\rho_0 \Rightarrow \{N, Z_A, R_A\} \Rightarrow \hat{H} \Rightarrow \Psi_0 \Rightarrow E_0 \tag{12}$$

The second theorem yields a variational principle, with E being an upper bound to the true ground state energy E_0.

$$E_0 = E_0[\rho_0(r)] \leq E[\rho(r)] \tag{13}$$

Thus, the electronic ground state energy is given as a functional of the electron density (eq. (14)) consisting of the kinetic energy of electrons T, the potential energy for the electron interaction V_{ee} and the Coulomb attraction between electrons and nuclei V_{Ne}.

$$E_0[\rho_0] = T[\rho_0] + V_{ee}[\rho_0] + V_{Ne}[\rho_0] \tag{14}$$

As V_{Ne} is independent of the wave function generating the density and known, it is separated and the two other parts are combined to the so–called *Hohenberg-Kohn* functional $F_{KH}[\rho_0]$. The *Hohenberg-Kohn* theorems give justification for DFT, they however do not provide any description for the functionals or any practical application. This was enabled by the *Kohn-Sham* equations, with division of the kinetic energy into a calculable term of non-interacting electrons T_s and the residual kinetic energy of the real system (eq.(15)). Moreover the potential energy of the electron-electron interactions is split into the Coulomb functional $J[\rho]$ and a non-classical part $E_{nc}[\rho]$. All unknown contributions are summed together in the exchange-correlation functional $E_{XC}[\rho]$ in eq. (17).

$$T[\rho] = T_s[\rho] + T_c[\rho] \tag{15}$$

$$V_{ee}[\rho_0] = J[\rho] + E_{nc}[\rho] \tag{16}$$

$$E_{XC}[\rho] = T_c[\rho] + E_{nc}[\rho] \tag{17}$$

Thus, HF and DFT both treat electrons as independent particles moving in the average field of all others, but DFT includes correlation by virtue of the functional. Until this point DFT represents an exact theory, however, as the formulation of $E_{XC}[\rho]$ is unknown, it needs to be approximated. As analogy, the exchange-correlation functional is obtainable at various levels and complexity ascending the "Jacobs ladder" from the *Hartree-Fock* level towards heaven corresponding to chemical accuracy.[260-262] The first group of functionals is achieved *via* local density approximation (LDA), estimating the exchange-correlation functional from homogenous electron gas, as it is the case in ideal metals. Including the spin of electrons then yields the local spin-density approximation (LSD).

$$E_{XC}^{LDA} = \int \rho(\vec{r})\varepsilon_{XC}(\rho(\vec{r}))d\vec{r} \tag{18}$$

In equation (18) ε_{XC} can be further divided, with the exchange part being highly related to the previously mentioned *mean field* but differing in a pre-factor. The correlation part is not known, but was analytically determined by *Vosko*, *Wilk* and *Nusair* based on high-precision Monte-Carlo simulations.[263] The LDA functionals use an expression for $E_{XC}[\rho]$ originally developed for homogenous electron densities, thus representing the bottleneck of this type of functionals, as electron density typically shows huge variety within one molecule.

Further improvement of the exchange-correlation functional is obtained by including the gradient of the electron density. This yields the generalized gradient approximation (GGA) functionals according to the general expression:

$$E_{XC}^{GGA}[\rho_\alpha, \rho_\beta] = \int f(\rho_\alpha, \rho_\beta, \nabla\rho_\alpha, \nabla\rho_\beta)\, d\vec{r} \tag{19}$$

Meta-GGA functionals possess increased accuracy by introducing additional dependence on the Laplacian $\nabla^2\rho(\vec{r})$ as well as kinetic energy density of Kohn-Sham orbitals τ:

$$E_{XC}^{MGGA}[\rho_\alpha, \rho_\beta] = \int f(\rho_\alpha, \rho_\beta, \nabla\rho_\alpha, \nabla\rho_\beta, \nabla^2\rho_\alpha, \nabla^2\rho_\beta, \tau_\alpha, \tau_\beta)\, d\vec{r} \tag{20}$$

All three levels of functionals described until now are called local functionals, because they are depending on the local spin density, its gradient and the Laplacian. The next step on the Jacobs ladder are non-local functionals based on coupling of *Hartee-Fock* theory with local DFT yields so-called hybrid exchange correlation functionals expressed by:

$$E_{XC}^{Hybrid} = (1-a)E_X^{GGA} + aE_X^{HF} + E_C^{GGA} \tag{21}$$

Hybrid functionals highly increase the necessary calculation time in comparison to the functional types as explained beforehand, which makes them more expensive especially for large and complex systems. The last spoke on the Jacobs ladder is represented by double hybrid functionals, which include an additional perturbation theory based correlation part. With this general overview, only a short recap is given. A tremendous variety of DFT functionals is available to date. The used combination of functional and basis set is crucial with regard to reliability of achieved results for a specific molecular system. The functionals and basis sets used within this thesis are presented in the following chapter.

4.2. Used Functionals and Basis Sets

B3LYP

One of the most popular functionals in theoretical chemistry is the hybrid functional B3LYP, named after their contributors *Becke*, *Lee, Yang* and *Parr* as well as its contained 3 parameters in equation (22) (a = 0.2, b = 0.72, c= 0.81).[264-266] These three parameters are optimized to atomisation, ionisation energies

and proton affinities in the G2 database. Thus, the functional combines exact *Hartree-Fock* exchange with the LSD exchange of *Vosko, Wilk* and *Nusair*[263] and gradient correction of *Beckes* B88[265] functional to the LSD. The correlation functional part is represented by a combination of LSD and gradient correction of the LYP[266] functional.

$$E_{XC}^{B3LYP} = (1-a)E_X^{LSD} + aE_X^{HF} + bE_X^{B88} + cE_C^{LYP} + (1-c)E_C^{LSD} \quad (22)$$

The B3LYP functional paved the way for DFT calculations to become a popular tool in computational chemistry. However, some major drawbacks of this functional are the underestimation of barrier heights in reactions, which is ascribed to (i) self-interaction error of the electrons and (ii) inability of describing medium-range interactions (~2-5 Å), thus also failing in the description of non-covalent interactions such as *Van-der-Waal* interactions.[267] This can be reduced in parts by inclusion of *Grimme's* empirical dispersion GD-3.[268] However this does not provide a complete solution, as London dispersion forces can play a major role depending on the system.[269-270]

Minnesota Density Functionals M06-L and M06-2X

The group of Truhlar have developed a whole range of different functionals, the Minnesota density functionals, with M06-L representing a meta-GGA functional and M06-2X a hybrid meta-GGA functional. The exchange functional of M06-L represents a linear combination of the M05[271] and VSXC[272-273] exchange functional as given in equation (23), incorporating the exchange energy density of *Perdew-Burke-Ernzerhof* (PBE).[274] The correlation functional is again a combination of M05 and VSXC, but contains a different treatment of the opposite spin and parallel spin correlation (eq. (24)). In equation (25) and (26), $e_{\alpha\beta}^{UEG}$ and $e_{\sigma\sigma}^{UEG}$ represent the uniform-electron gas (UEG)[275] correlation energy density for antiparallel and parallel spin cases and D_σ the self-interaction correction factor. The complete description of the functional with all 37 parameters, which were optimized to 314 data sets (including databases of barrier heights, noncovalent interactions, bond length, frequencies…), can be found in Truhlar's and Zhao's original publication from 2006.[276]

$$E_X^{M06-L} = \sum_\sigma \int dr\left[F_{X\sigma}^{PBE}(\rho_\sigma, \nabla\rho_\sigma) f(w_\sigma) + \varepsilon_{X\sigma}^{LSDA} h_X(x_\sigma, z_\sigma)\right] \quad (23)$$

$$E_C = E_C^{\alpha\beta} + E_C^{\alpha\alpha} + E_C^{\beta\beta} \quad (24)$$

$$E_C^{\alpha\beta} = \int e_{\alpha\beta}^{UEG}\left[g_{\alpha\beta}(x_\alpha, x_\beta) + h_{\alpha\beta}(x_{\alpha\beta}, z_{\alpha\beta})\right] dr \quad (25)$$

$$E_C^{\sigma\sigma} = \int e_{\sigma\sigma}^{UEG}[g_{\sigma\sigma}(x_\sigma) + h_{\sigma\sigma}(x_\sigma, z_\sigma)] D_\sigma dr \quad (26)$$

Although further work of the Truhlar group provided other local functionals, e.g. M11-L, the M06-L functional is one of the most broadly used Minnesota functionals.[277] The M06-2X, with its formula given in equation (27), combines the M06-L functional (shortened as E^{DFT} here) with 54% *Hartree-Fock* exchange. This gives an improved performance concerning main group thermochemistry as well as barrier heights and noncovalent interactions.[267,277]

$$E_{XC}^{M06-2X} = \frac{54}{100} E_X^{HF} + \left(1 - \frac{54}{100}\right) E_X^{DFT} + E_C^{DFT} \quad (27)$$

The M06-L and M06-2X functionals have proven to be an effective tool in low-valent silicon chemistry, as used by several theoretical chemistry groups active in this field.[70,181,278-279] As these functionals are optimized to training data sets including dispersion interactions, they do not need additional empirical dispersion corrections. The M06-L functional, although being a local, meta-GGA functional allows for fast and reliable calculations also for increased system sizes. The M06-2X, representing a hybrid functional, needs more computational resources and computing time. Beside their generally good performance in

main group chemistry, all calculations using the M06 suite of functionals should be performed on an ultrafine grid in numerical integration (which is the default in G16, but not in G09), avoiding occurrence of interfering imaginary frequencies.[280]

Pople Basis Sets

Besides the important choice of the functional, also the basis set is crucial in achieving representative results from DFT calculations. Within this thesis, all used basis sets rank to the *Pople* style basis sets.[281-284] They are given in a specific form, e.g. for the split valence, triple zeta basis including diffuse functions as well as polarisation function on all atoms: 6-311++G(2d,2p). The numbers in the front represent the split valence basis with the core orbitals represented by a contraction of six primitive *Gaussian* type orbitals (PGTO) and the valence orbitals split into three functions of three, one and one PGTO. Gaussian type orbitals (GTO) are exemplified in terms of Cartesian coordinates in eq.(28).

$$\chi_{\zeta,n.l.m}(x,y,z) = Nx^{l_x}y^{l_y}z^{l_z}e^{-\zeta r^2} \tag{28}$$

They bear zero slope at the nucleus, which is problematic for a proper description near the nucleus, and have a too fast fall off at the "tail" (far from the nucleus). Thus, several of them are necessary to achieve an accurate description. Generally, the contraction of basis sets reduces the number of variational coefficients determined in the calculation and thus improves computational efficiency. Especially, the inner core electrons change only very little depending on the bonding situation. Hence they can be described by less PGTOs in a decent way. The valence electrons, which determine the reactivity of a molecule, are treated more flexible based on the higher number of PGTOs representing them. The two following plus signs "++" stand for the addition of diffuse functions to PGTOs, with the first representing the addition of diffuse s and p functions on heavy atoms and the second addition of diffuse s functions also to hydrogen. The term G(2d,2p) gives the polarisation of 2d-orbitals added on heavy atoms and 2p-orbitals added to hydrogen, which allows for an improved description of polarisation present in the molecule. It should be noted, that geometry optimisation (introduced in the following chapter) on the double zeta basis 6-31+G(d,p) most of the time meets all requirements for the correct description of the geometry, but bonding analysis should be performed on a higher basis set afterwards.

4.3. Geometry Optimisation and other Types of Calculations

Until now, only the energy dependency on the electrons was discussed. However, the energy also depends on the coordinates of the nuclei. The solution of the *Schrödinger* equation for different assemblies of the nuclei yields the potential energy surface (PES). Within the PES, the assembly of the nuclei representing stationary points, i.e. the first derivatives equal to zero as being the case for a minimum or a first-order saddle point (transition state (TS)), are of chemical interest. In the geometry optimisation the potential energy around a starting point x_0 is approximated in a Taylor series

$$E(x) \approx E(x_0) + F^T(x - x_0) + \frac{1}{2}(x - x_0)^T H(x - x_0) \tag{29}$$

including the gradient vector F (i.e. the first derivative of E) and the *Hesse* matrix H (i.e. the second derivative of E). This is called the *Newton-Raphson* method with ^{T} representing the transposed version of a particular matrix. Depending on the type of calculation, the hessian is approximated with valence force fields (used in standard geometry optimisation as implemented in the *Berny* algorithm[285-286] in the Gaussian programs[287-289]) or explicitly calculated for the determination of transition states at the beginning of the calculation (Scheme 5). As the gradient needs to equal to zero at a stationary point, the optimisation step is given by:

$$(x - x_0) = -H^{-1}F \tag{30}$$

All Hessian eigenvalues are positive by definition near a minimum, thus giving the step direction opposite to the direction of the gradient, hence the optimisation proceeds in the direction of the searched for minimum. For one negative eigenvalue of the Hessian, the step direction follows the gradient component to end in a stationary point with one negative eigenvalue, the first-order saddle point representing a TS on the PES. The step size needs to be updated during optimisation especially if a minimum is very close, which is implemented in the so-called “trust radius”.

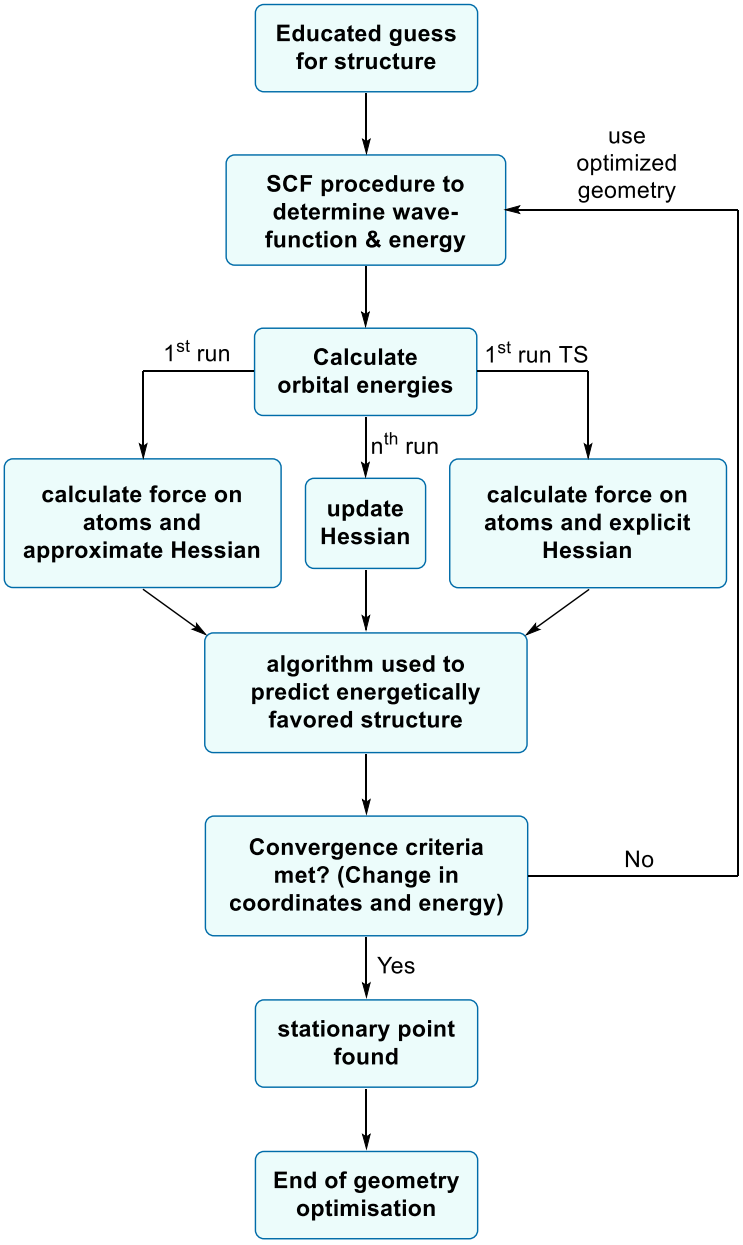

Scheme 5: Schematic representation for the geometry optimisation of a molecular structure.

The explicit calculation of the Hessian matrix is expensive and recalculation in each step would be incredibly time and memory consuming. Thus, the approximated or explicit Hessian is updated based on the energy and first derivatives calculated along the optimisation pathway, called pseudo-*Newton Raphson* method. To obtain the explicit Hessian, the storage and diagonalisation of it requires sufficient memory allocation especially for larger systems. It scales $(3N)^3$ in Cartesian coordinates with N representing the number of nuclei in the molecule. Some important features of the optimisation procedure are: (i) it will converge to the “nearest” stationary point on the PES, thus the user should be

able to give an "educated" guess of the molecular geometry to reach the searched for stationary point and (ii) the method does not give any information about the characteristics of a found stationary point. To assess the nature of a stationary point, the calculation of the Hessian matrix need to be done analytically. This starts with determination of the force constants with respect to the Cartesian nuclear coordinates, transformation into mass-weighted coordinates and calculations of the resulting vibrational frequencies. These allow assessment of a stationary point as a minimum (zero imaginary frequencies) or a TS (one imaginary frequencies). Moreover, thermochemistry data are obtained at this point, which give the corresponding enthalpies and *Gibb*s free energies to compare different structures with respect to their relative energies in a reaction mechanism. Furthermore, bond dissociation energies D_0, defined according to

$$D_0 = D_e - E_{ZPE} \tag{31}$$

get accessible, with D_e representing the difference in electronic energy and E_{ZPE} the difference in zero-point correction. Although being the official IUPAC definition,[290] the use of *Gibbs* free energy of bond dissociation is more common nowadays.[68,181] To assess the connectivity of a TS with other minima on the PES, the intrinsic reaction coordinate (IRC)[291] approach was used as implemented in the Gaussian programs.

NMR chemical shifts are achieved using the Gauge-Independent Atomic Orbital (GIAO)[292-293] method implemented in the Gaussian programs, which are referenced to calculated shifts of tetramethylsilane (for ^{29}Si and ^{13}C shifts). Another type of calculation used within this thesis is time-dependent DFT (TD-DFT), i.e. the calculation of excited states to obtain information about the orbitals involved in experimentally observed UV/vis bands. As standard DFT is not able to describe excited states, the formulation of the wave function needs to be extended to a time-dependent form, obtained from the *Runge-Gross* Theorem. Further boundary conditions and approximations are necessary to enable the determination of absorption-induced transition of electrons from the bonding to non-bonding orbitals. Further details can be found in Dreuw's and Head-Gordon's TD-DFT review.[294] Within this thesis, TD-DFT was used as implemented in the Gaussian versions[287-289] without modification or referencing.

4.4. Natural Bond Orbital Analysis

The generally used term NBO analysis refers to the program NBO of *Glendening*, *Landis* and *Weinhold*, which transforms the canonical orbitals - delocalized over the whole molecule - into localized natural bond orbitals (NBOs). This enables the description of a molecule with core electrons (CR), lone pairs (LP) and bonding electron pairs localized on two atoms (BD(n), with n representing the bond order) within the molecule. With this in hand, one can deduce a whole series of properties from the molecular structure, method and basis given to the program, including:

- A representative *Lewis*-like structure of the molecule
- Atomic charge as well as charge transfer within the molecule
- Bond orders
- Bond types
- Hybridisation
- Resonance structures
- Donor-acceptor interactions

To enable this *Lewis*-like description, the NBO program executes a series of similarity (T) (i.e. $A' = B^{-1}AB$ holds true) and unitary (U) transformations (i.e. $\hat{U}^{-1} = \hat{U}^{\dagger}$) starting from the atomic orbitals (AO), *via* natural atomic orbitals (NAO) and natural hybrid orbitals (NHOs) to give NBOs and natural localized molecular orbitals (NLMO). The transformations are depicted in Scheme 6. Important measures, which are discussed within NBO analysis, are highlighted. The historical and mathematical background for those transformations can be found in specialized books of *Landis* and *Weinhold*.[295-296]

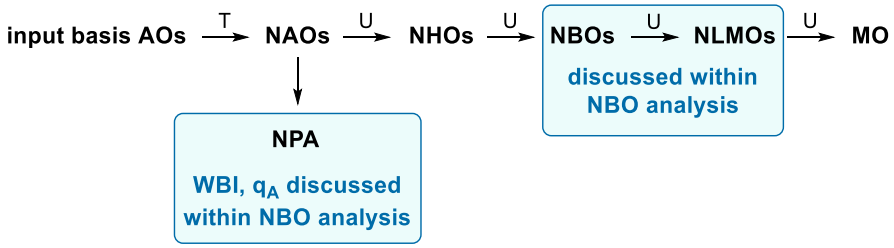

Scheme 6: Overview of transformations within NBO analysis.

One of the first properties achieved within transformation of atomic orbitals into atom-centred orthonormal NAOs, is the NPA charge q_A defined within NAO formulism as

$$q_A = Z_A - \sum_i q_i \tag{32}$$

where Z_A denotes the atomic number of atom A and q_i represents the quantified orbital population. One important difference to several other charge partitioning concepts, is satisfaction of the Pauli principle based on the requirement $0 \leq q_i \leq 2$ holding true. The sum of all q_i corresponds to the total number of electrons in the molecule. The second important property obtained from NAO formalism is the *Wiberg* bond index (WBI), as a measure of the bond order.[297] Due to orthonormality of the NAO basis, it is obtained from the density matrix elements with the sum of all WBI of an atom giving its total valence.

Further mathematical transformations and the linear combination of NHOs yield NBOs as the bond-localized orbitals (eq. (33)). Within the NBO formulation, the occupied orbitals (core and valence orbitals) are only a subset of all accessible orbitals. The residual electron density, not attributed to occupied orbitals, is summed into Valence and Rydberg non-*Lewis* parts, which together give the Total non-*Lewis* (TNL) electron density. The algorithm within the NBO program searches for the occupancy of all orbitals yielding the minimum energy. If the TNL value is low (i.e. only a small quantity of the total electron density is located in non-*Lewis* orbitals), a satisfactory and representative *Lewis* structure is received within NBO analysis. However, further tests *via* modification of the bonds and lone pairs present in the molecule, i.e. testing other possible fitting *Lewis*-like representations, should be performed to check the obtained results.

$$\sigma_{AB} = c_A h_A + c_B h_b \tag{33}$$

(note: generally, only two-centre two-electron (2c-2e) bonds are represented at this point, three-centre four-electron bonds (3c-2e, hypovalent bonds) have to be explicitly requested in the input and three-centre four-electron bonds (3c-4e, hypervalent bonds) are achieved in a later step). Thus, NBOs provide insight to the electron density of atom A and atom B contributing to the bond/or non-bonding interaction between A and B. In addition, the allocation of s-and p-orbitals contributing to a bonding, filled orbital (CR, LP or BD(n)) as well as non-bonding, unfilled orbitals (LV or BD*) are obtained.

The next step considers interaction between NBOs in terms of electron donors and electron acceptors, or in other words conjugation or hyperconjugation of electrons occurring within one molecule to lower these orbitals in energy. This is approximated by second order perturbation theory, with highly occupied NBOs representing the donors and low occupied NBOs acting as acceptors. Depending on the donor-acceptor interaction of a NBO pair $\sigma_{AB}/\sigma^*_{CD}$, which is quantified by overlap of those NBOs, the filled orbital ε_- is lowered in energy by $\Delta E^{(2)}_{\sigma_{AB} \rightarrow \sigma^*_{CD}}$ (Figure 27). Very strong donor-acceptor interactions (3c-4e, e.g. A=B-C: vs. :A-B=C, with : representing a lone pair of electrons) are termed hyperbonds within this analysis.

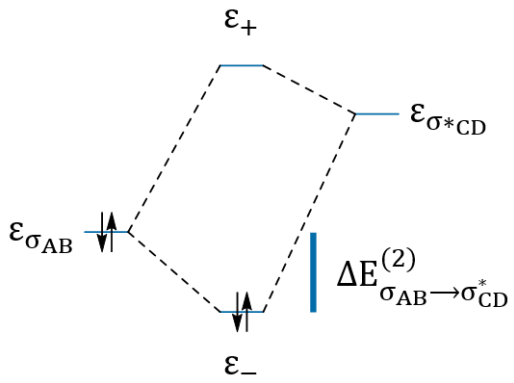

Figure 27: Stabilising interaction between filled donor orbital σ_{AB} and vacant acceptor orbital σ^*_{CD}, adapted from [296]

These donor-acceptor interactions are, by definition, already included in the NLMO perspective, with NLMOs representing the least delocalized orbitals with full double-occupancy. The NBO program outputs the percentage contribution of all centres incorporated for the formation of a corresponding NLMO. With this said, the major difference between NBOs and NLMOs are: (i) varying occupancy vs. fixed occupancy of two electrons and (ii) 2nd order perturbation theory results necessary to depict effects of delocalisation within a molecule vs. delocalisation included by definition. It is, therefore, apparent why NLMOs are the preferred representation for orbital depiction in publications. However, they are less transferable due to the interaction features included based on specific molecular environment. Graphical representations of NBOs/NLMOs are accessible with the ChemCraft program.[298]

The last important feature of the NBO program, used within this thesis, is the Natural Resonance Theory (NRT) analysis.[299-301] This provides further insight into electron delocalisation occurring within a molecule for multiple resonance structures (defined *Lewis* representations) contributing to the full description of a molecule. This is performed *via* initial identification of different resonance structures, called reference structures that can also be given by the user. These reference structures are weighted using root-mean-square optimisation of the resonance-weighted NBO occupancies to represent the electron density obtained from the wave function as best as possible. Thus, a percentage for a resonance structure contribution to the full description of a molecular structure is achieved. Moreover, the resonance-averaged NRT bond orders, an alternative bond order to the forehand mentioned WBI, are calculated including a partition into covalent and ionic contributions.

4.5. Quantum Theory of Atoms in Molecules

QTAIM represents another possibility for bonding analysis, which uses the electron density ρ(r). This different approach was developed by *Richard Bader* and investigates the topology of ρ(r) obtained from high resolution SC-XRD experimentally or theoretical calculations. As the electron density of a molecule is non-homogenous, analysis of its topology reveals the so-called critical points (cp) at $\nabla\rho(r_c) = 0$, which are divided into different classes upon examination and diagonalisation of the *Hesse* matrix with the description of type (ω, σ). The Hessian is the square matrix of second-order partial derivatives of a twice continuously differentiable functional (here the electron density ρ(r)), with ω representing the rank (the number of non-zero curvatures of ρ at a cp) and signature σ (the algebraic sum of the signs of the curvature at the cp). For a molecule in its equilibrium geometry, four types of critical points are possible with each type connected to an element within the chemical structure:

- (3,-3): all curvatures < 0 thus the cp is a local maximum of ρ; nuclear critical point (NCP) coinciding with the nuclear coordinates or non-nuclear attractor (NNA) if the maxima is not connected with a nuclear position.
- (3,-1): two curvatures < 0, but a minimum along one axis; bond critical point (BCP).
- (3,1): two curvatures > 0, but maximum along one axis; ring critical point (RCP).
- (3,3): all curvatures > 0; cage critical point (CCP).

For an isolated molecule, the following *Pointcaré-Hopf* relationship givens the strict connection for the number n of co-existing cp's:

$$n_{NCP} + n_{NNA} - n_{BCP} + n_{RCP} - n_{CCP} = 1 \quad (34)$$

If two atoms are bound (to be exact the description of *Bader* only states a "bonding interaction", which will be used equivalently to a bond between to atoms in the following) by QTAIM means, a BCP is located as the minimum on the connecting line possessing maximal electron density between the two NCPs called bond path. All bond paths within a molecule with the BCPs represent the molecular graph. Another important property of the topology of the electron density is the natural partitioning of the molecule into separate mononuclear regions, the atoms in molecules. The basin of atom A is determined by zero flux surfaces, where the gradient $\nabla\rho(r)$ is orientated perpendicular to the normal of the surface. The BCP's exhibit specific properties, enabling classification of a bond between two atoms:

- $\rho(r_c)$ accounting to high values for covalent, polar and donor-acceptor bonds and low values for closed shell interactions.
- $\nabla^2\rho(r_c) < 0$: accumulation of electron density present along the bond path, which is the case in a shared interaction.
- $\nabla^2\rho(r_c) > 0$: the electron density is mainly separated in the atomic basins representing an ionic, hydrogen-bonded, van der Waals or repulsive interaction.
- The total electron density $H(r_c)$, represented by the sum of potential energy density $V(r_c)$ and the kinetic energy density $G(r_c)$. $H(r_c)$ is negative for bonds exhibiting significant electron sharing, with its magnitude as a measure of covalence interaction[302]
- Bond ellipticity ε defined as $[\lambda_1/\lambda_2 - 1]$ with $\lambda_1 > \lambda_2$ and $\lambda_{1/2}$ representing the two negative eigenvalues of the Hessian matrix. ε is high if ρ is preferentially accumulated in a plane along the bond path, thus representing a measure of π-bonding character present in a bond (as it is the case for double bonds), and vice versa if the electron density bears a cylindrical symmetry along the bond path the ellipticity is low (as occurring for single as well as triple bonds).
- The delocalisation index $\delta_{A,B}$, representing the number of electron pairs delocalised between atoms A and B, as another different definition for the bond order.
- The atomic charge q_A is defined by the nuclear charge and the integral of the electron density residing within the basin of atom A according to:

$$q_A = Z_A - \int_{\Omega_A} \rho(r)dr \quad (35)$$

All these listed properties can be used to classify a particular bond of interest. However, strong polar bonds need special attention. For these bonds, which generally possess (i) a shift of the BCP to the electropositive element, (ii) a high electron density at the BCP and (iii) and $\nabla^2\rho(r_c) > 0$, the BCP can be located close to a nodal surface of the Laplacian $\nabla^2\rho(r)$. If this is the case, the sign of $\nabla^2\rho(r_c)$ is no more indicative and thus additional analysis is necessary for bond classification. The one-dimensional profile of $\nabla^2\rho(r)$ along the bond path can be used to distinguish covalent and dative bonds, based on the location of valence shell charge concentrations (VSCC), represented by maxima within $\nabla^2\rho(r)$ (due to superposition, the appearance of less pronounced shoulders is also possible). For a covalent bond, the VSCC of both atoms reside within their respective atomic basin, which are separated by the BCP. In contrast, dative bonds are indicative of both VSCCs residing in the basin of the donor atom. This has been shown by the Holthausen group in the case of the central Si–Si bond in a amine-stabilised disilene **L44** as well as a NHC-stabilised disilene **L45** (Figure 15).[70,181] Within this thesis, QTAIM analysis was performed using the programs AIMALL[303-304] or Multiwfn.[305-307]

5. Motivation and Objective

Main group chemistry has undergone a renaissance, from synthetic curiosity to a broad range of applications, which has even aroused attention from industry. As highlighted in the prior chapters, low-valent silicon and aluminium compounds bear similar frontier orbitals to transition-metals, and as such, their transition-metal like properties have recently emerged. Since silicon and aluminium are highly abundant (Figure 2a), their use in catalytic applications could be a further measure to tackle the problem of limited resources linked with transition metals. However, at the start of this thesis only one example of a low-valent silicon centre acting as a catalyst was reported (Scheme **3**A). Furthermore, the supplementary application of theoretical methods, to gain insight into the electronic structure of new isolated structural motives, rose steeply. Thus, this thesis aims to combine experimental and theoretical studies of low-valent silicon and aluminium compounds, namely acyclic silylenes, disilenes, silyliumylidene ions and dialumenes. The scope here is examination of the range of attached ligands and how they influence the stability and reactivity of the aforementioned complexes. Of particular focus is the activation of small molecules, as this is considered challenging even for transition metals due to the strong bonds in compounds such as H_2, CO_2, CO etc. The gained knowledge of how these low-valent centres bind and activate such molecules can then be further applied towards catalysis (Scheme 7).

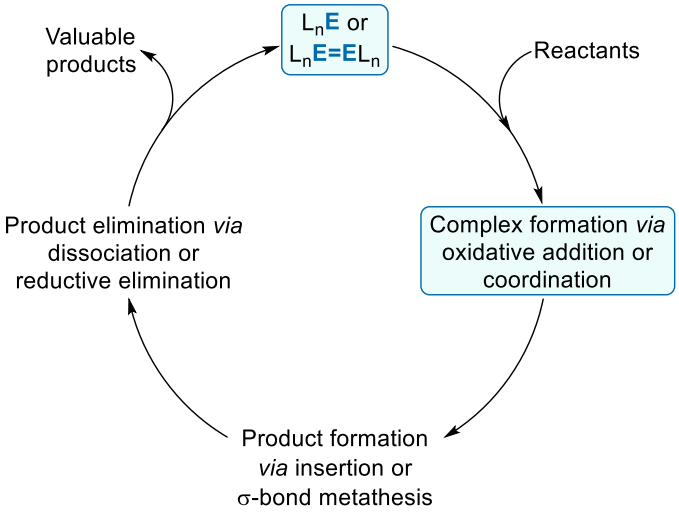

Scheme 7: Overview of the important steps of a generalized catalytic cycle for low-valent monomeric or dimeric main group compounds. The low-valent main group compounds as well as the complex formation are highlighted, as they are the focus of this thesis.

In this way, theoretical methods are used to concept relations between structural motifs, being connected to their bonding situation, and the observed reactivity of acyclic silylenes and their reaction products in chapters 6.1-6.4. The work on acyclic silylenes starts with the combination of NHI and hypersilyl ligands together with initial reactivity tests, see chapter 6.1. In the second study, this approach is further extended to the supersilyl-substituent in combination with their unique reactivity towards N_2O. Furthermore, dependent on the substituents different rearrangement reactions are identified, which yield valuable insight into their bonding situation (chapter 6.2). Inspired by the differences in reactivity upon exchange of hypersilyl and supersilyl group, incorporation of both silyl groups in one molecule is attempted in chapter 6.3. Combined reactivity tests and computational analysis illustrate the underlying mechanistic picture. In the last silylene chapter (6.4), the reactivity of the accessible bis(silyl)silylene is studied towards carbon monoxide and isocyanides and its ability to act as a transition-metal mimic. Furthermore, the decisive role of the two silyl-substituents on the stability of the silicon carbonyl complex is studied theoretically.

The aluminium part of this thesis focuses on hitherto non-isolable dialumenes. The combination of silyl-substitution and NHC-stabilisation has allowed for isolation of the first dialumene, discussed together with initial reactivity studies in chapter 6.6. Furthermore, the structure of dialumenes is shown to be highly influenced by the ligand used. Hence, a comparative study between silyl- and aryl-substitution is performed and discussed in chapter 6.6.

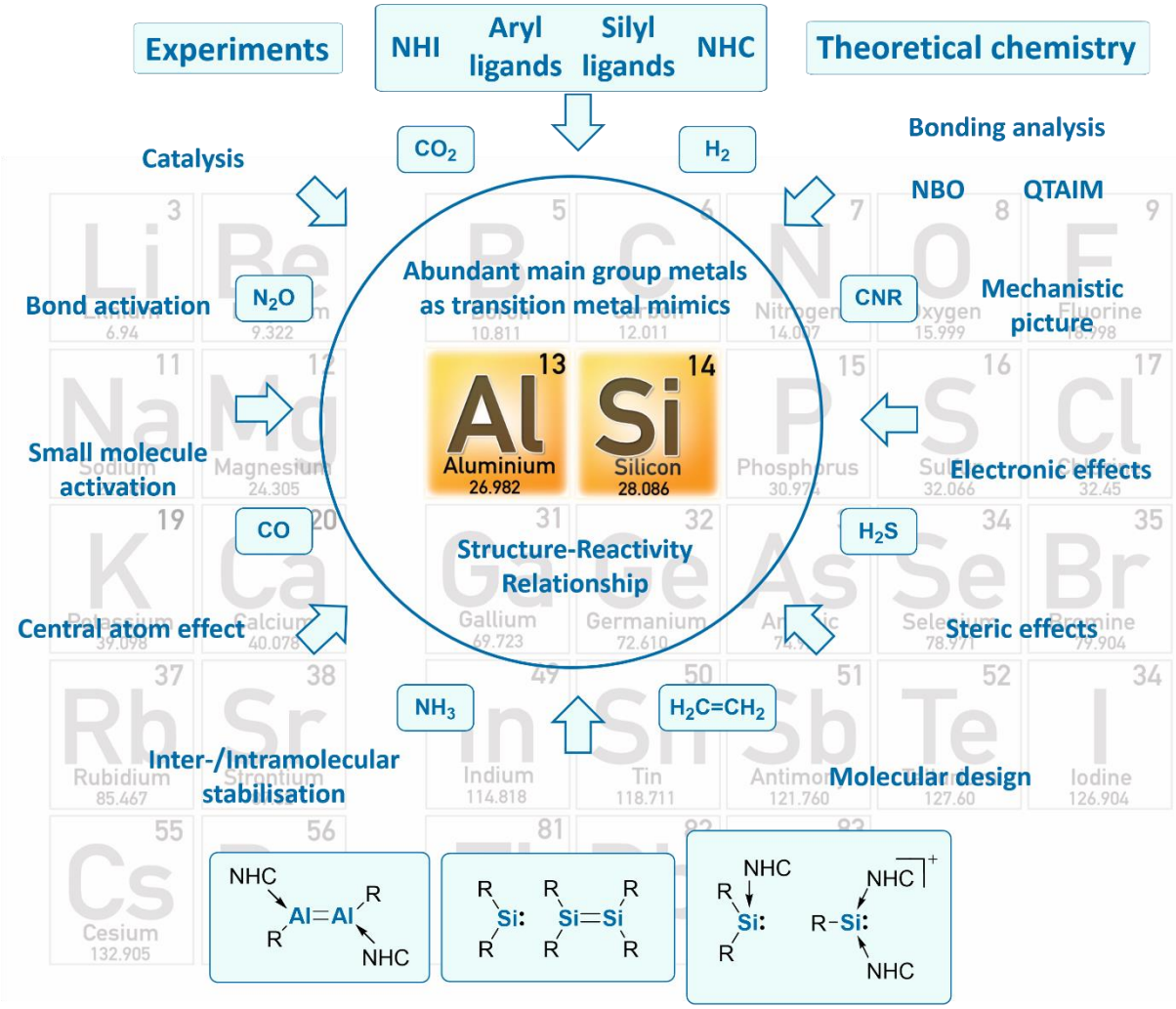

Scheme 8: Overview of the studies conducted within this thesis on silyl-/aryl-/NHI-substituted and/or NHC-stabilised low-valent silicon and aluminium compounds.

As a last part, the reactivity of silyliumylidene ions is studied in a combined experimental and theoretical approach. In chapter 6.7 the reactivity towards hydrogen sulphide is reported, together with mechanistic insights and bonding analysis of the obtained compound. Further reactivity tests were hampered by their low-solubility and the interfering chloride anion. To circumvent this, the anion is exchanged, which is discussed jointly with the determination of its donor properties in chapter 6.8.

6. Results – Publication Summaries

6.1. From Si(II) to Si(IV) and Back: Reversible Intramolecular Carbon–Carbon Bond Activation by an Acyclic Iminosilylene

Title:	From Si(II) to Si(IV) and Back: Reversible Intramolecular Carbon–Carbon Bond Activation by an Acyclic Iminosilylene
Status:	Communication, published online June 6, 2017
Journal:	Journal of the American Chemical Society, 2017, 139 (24), 8134-8137.
Publisher:	American Chemical Society
DOI:	10.1021/jacs.7b05136
Authors:	Daniel Wendel, Amelie Porzelt, Fabian A. D. Herz, Debotra Sarkar, Christian Jandl, Shigeyoshi Inoue, Bernhard Rieger

Content: Prior to this publication, only four examples of isolable, acyclic silylene were reported, which bear structural differences and reactivity. We thus used the combination of NHI and silyl ligands to broaden the scope of these species with expected reactivity differences. Indeed, treatment of NHI-tri(bromo)-silane IDippNSiBr$_3$ with two equivalents of KSiTMS$_3$ at –78 °C resulted in a green solution which decolourized upon warming to rt. The formation of silepin **2**, built *via* intramolecular insertion of the silylene into the C=C bond of the IDippN group, was verified by SC-XRD analysis. Hence, a slightly reduced system (Dipp replaced with Ph) was used to elucidate the interconversion of **1** and **2**, which revealed them to be close in energy. The interconversion starts from **1** with an approach of the silicon centre to the aromatic C=C bond in the Dipp ligand followed by cleavage of this bond as the rate-determining step. Furthermore, the calculated model of silylene **1** exhibits a low singlet-triplet gap of 25 kcal/mol, in line with other acyclic silylenes. In the following i*n-situ* analysis of the non-isolable silylene **1** in combination with DFT calculations were performed. ^{29}Si NMR measurement of the reaction mixture at –78 °C revealed a signal at 300.0 ppm in line with reported acyclic silylenes**,** although conversion to **2** was already detectable. *In-situ* variable-temperature UV/vis measurements revealed an equilibrium of the silepin with the silicon centre in oxidation state +IV and the accessible silylene (Si +II). TD-DFT calculations verified the experimental UV/vis band at 612 nm as the HOMO (lone pair at the silicon centre) to LUMO (empty p-orbital) transition, which is responsible for the green colour. Treatment of **2** with BCF gave the *Lewis* acid adduct **3**. Further experiments focused on the use of silepin **2** as a masked silylene in the activation of small molecules. Treatment of **2** with CO_2 gave selective formation of the first monomeric silicon carbonate complex **4**. Moreover, activation of ethylene and H_2 by **2** yielded the oxidative addition products **5** and **6**, although the latter required a temperature increase to 50 °C. In summary, this report represents the first example of a reversible oxidative addition and reductive elimination being possible at a low-valent silicon centre.

Contributions to the publication:

- DFT calculations on the structure of the non-isolable silylene intermediate **1** in singlet/triplet state
- TD-DFT calculations to support the experimentally observed UV/vis shifts of **1**
- Quantum chemical investigations on the experimentally accessible silepin-silylene equilibrium
- Interpretation and discussion of the results

JACS
JOURNAL OF THE AMERICAN CHEMICAL SOCIETY
Communication
pubs.acs.org/JACS

From Si(II) to Si(IV) and Back: Reversible Intramolecular Carbon–Carbon Bond Activation by an Acyclic Iminosilylene

Daniel Wendel,[†] Amelie Porzelt,[‖] Fabian A. D. Herz,[†] Debotra Sarkar,[‖] Christian Jandl,[‡] Shigeyoshi Inoue,*[,‖] and Bernhard Rieger*[,†]

[†]WACKER-Chair of Macromolecular Chemistry, [‖]WACKER-Institute of Silicon Chemistry, [‡]Catalysis Research Center, Technische Universität München, Lichtenbergstraße 4, 85748 Garching bei München, Germany

Supporting Information

ABSTRACT: Reversibility is fundamental for transition metal catalysis, but equally for main group chemistry and especially low-valent silicon compounds, the interplay between oxidative addition and reductive elimination is key for a potential catalytic cycle. Herein, we report a highly reactive acyclic iminosilylsilylene **1**, which readily performs an intramolecular insertion into a C=C bond of its aromatic ligand framework to give silacycloheptatriene (silepin) **2**. UV–vis studies of this Si(IV) compound indicated a facile transformation back to Si(II) at elevated temperatures, further supported by density functional theory calculations and experimentally demonstrated by isolation of a silylene–borane adduct **3** following addition of $B(C_6F_5)_3$. This tendency to undergo reductive elimination was exploited in the investigation of silepin **2** as a synthetic equivalent of silylene in the activation of small molecules. In fact, the first monomeric, four-coordinate silicon carbonate complex **4** was isolated and fully characterized in the reaction with carbon dioxide under mild conditions. Additionally, the exposure of **2** to ethylene or molecular hydrogen gave silirane **5** and Si(IV) dihydride **6**, respectively.

Ever since discovery of decamethylsilicocene $Cp^*_2Si(II)$ in 1986,[1] considerable attention has been paid to explore and elucidate the nature of monomeric low-valent silicon compounds.[2] To date, a plethora of stable silylenes have been isolated and studied. Progress in experimental techniques has even granted synthetic access to acyclic silylenes (Chart 1).[3] These compounds are ideal for selective small molecule activation, due to their coordinative flexibility and reduced HOMO–LUMO gap (~2–4 eV).[2b,4] Both attributes are key to facilitate oxidative addition of targets like NH_3, H_2 or ethylene. Although traditionally these types of activation are associated with *d-block*-metal complexes, acyclic silylenes have proven their potential as transition metal mimics. For instance, oxidative cleavage of the strong σ-bond of dihydrogen was accomplished with silylenes **I**[3c] and **II**.[3d] Further studies show easy splitting of ammonia under mild conditions by **I**[5] and **IV**.[3a] In terms of a potential silylene-based catalytic cycle, this oxidative step is only considered as one substep; far more complex is the regeneration of the Si(II) species via reductive elimination. First approaches toward this goal were accomplished for heavier germanium[6] and tin[5] analogs, but for subvalent silicon compounds this reverse reaction remains challenging. Silylene **III**[7] shows behavior toward ethylene by reversibly binding the olefin in a dissociation equilibrium with the corresponding silirane ring under ambient conditions. The same reversible [2+1]-cycloaddition with ethylene was reported by Baceiredo et al. for a cyclic phosphine-stabilized silylene.[8] In addition, this structure stands out by unprecedented reversible insertions into Si–X (X = H, Cl) and P–H bonds.[9]

Chart 1. Selected Examples of Room Temperature Stable Acyclic Silylenes with Small HOMO–LUMO Gaps (~2–4 eV)

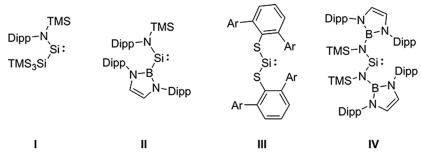

Dipp = C_6H_3-2,6-*i*-Pr_2, Mes = C_6H_2-2,4,6-Me_3, Tripp = C_6H_2-2,4,6-*i*-Pr_3, Ar = Mes, Dipp, Tripp

Recently, we utilized *N*-heterocyclic imino (NHI) ligands for stabilization of low-valent compounds based on group 13 and 14 elements.[10] Herein, we report synthesis of acyclic iminosilylsilylene **1**, which undergoes an intermolecular C=C insertion into its aromatic ligand framework to form room temperature stable silacycloheptatriene (silepin) **2**. Reactivity studies of **2** show this formal Si(IV) compound is easily converted back to Si(II) as a silylene–borane adduct and even acts as "masked" silylene in small molecule activation of carbon dioxide, ethylene and hydrogen.

In analogy to the one-pot method by Jones and Aldridge et al. for the preparation of **I**[3c] and **II**,[3d] we determined Rivard's bis(2,6-diisopropylphenyl)imidazolin-2-iminotribromosilane (IPrNSiBr$_3$)[11] ideal for our synthetic route. Treatment of 1 equiv of IPrNSiBr$_3$ in toluene with 2 equiv of $KSiTMS_3$ at −78 °C gave a light green solution with precipitation of KBr (Scheme 1). An instant color change to yellow was observed upon warming the solution to room temperature. The ^{1}H NMR spectrum of the crude reaction mixture showed a complicated series of Dipp resonances (Figure S8), similar to those observed for the ligand activation by Rivard et al.,[11] but here the quantitative formation of TMS_3SiBr as side product and distinct signals in the ^{29}Si NMR spectrum (central Si at 16.1 ppm) pointed to a defined product. Yellow crystals of this compound were obtained by crystallization

Received: May 18, 2017
Published: June 6, 2017

DOI: 10.1021/jacs.7b05136
J. Am. Chem. Soc. 2017, 139, 8134–8137

Scheme 1. Reaction Sequence of the Preparation of Silepin 2 via *in Situ* Generated Iminosilylsilylene 1

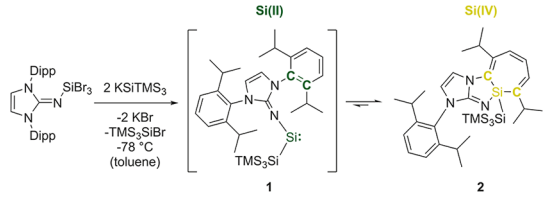

in *n*-hexane (−35 °C, 3 months), but due to its similar solubility to TMS_3SiBr only in low yields (6%).

Subsequently, X-ray analysis revealed the structure of silepin **2**, formed by intramolecular insertion of the *in situ* generated iminosilylsilylene **1** into a C═C bond of one of the Dipp groups (Figure 1). To verify this mechanism, we performed ^{29}Si NMR

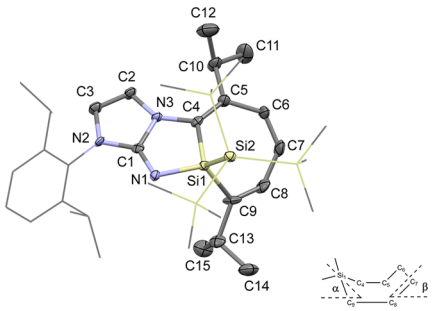

Figure 1. Molecular structure of **2** in the solid state with ellipsoids set at the 50% probability level (one out of two molecules in the asymmetric unit). For clarity, hydrogen atoms and cocrystallized solvent molecules are omitted and TMS as well as Dipp groups are simplified as wireframes. Selected bond lengths (Å) and angles (deg): Si1−C4 1.891(6), Si1−C9 1.876(6), C8−C9 1.333(9), C7−C8 1.433(9), C6−C7 1.354(9), C5−C6 1.452(8), C4−C5 1.352(7), Si1−N1 1.748(5), Si1−Si2 2.342(4), N1−C1 1.279(6), N1−Si1−Si2 109.37(17), C4−Si1−C9 105.3(3), α (C4−Si1−C9 and C4−C5−C8−C9) 41.06, β (C5−C6−C7−C8 and C4−C5−C8−C9) 31.70.

experiments in toluene-d_8 at −78 °C. The initial light green solution gave a characteristic signal at 300.0 ppm for the central silicon atom of **1**, which rapidly vanished upon warming the solution (Figure S2). Even at −78 °C, a further reaction to **2** was detectable. As expected, the shift of **1** lies between the chemical shift of **IV** (204.6 ppm)[3a] or West's $[(SiMe_3)_2N]_2Si(II)$ (223.9 ppm)[12] and **II** (439.7 ppm).[3d] The high-field shift of **1** compared to structural analog **I** (438.2/467.5 ppm)[3c] illustrates the stronger donor qualities of the NHI ligand. For further characterization, we performed variable temperature (VT) UV−vis measurements from −70 to +20 °C with a concentrated reaction solution. A characteristic low intensity band at 612 nm was observed at −70 °C, which, analogously to the NMR study, disappeared upon warming up the solution (Figure S3). Similarly, monitoring a reaction mixture of **2**/TMS_3SiBr from room temperature to 100 °C displayed reversible formation of the same characteristic signal of **1** (617 nm) at elevated temperatures (100 °C), pointing to an equilibrium between silepin and silylene at higher temperatures (Figure S4). To support this and elucidate the mechanism of silepin formation, we performed density functional theory (DFT) calculations (B3LYP/6-311+G(d,p)) with a reduced iminosilylsilylene **1′** (replacement of Dipp substituents with phenyl groups). We determined in fact silylene **1′** is 17.7 kJ/mol lower in energy than silepin **2′** (Figure S26), further suggesting a thermally accessible interconversion. The calculated singlet−triplet energy of **1′** (103.9 kJ/mol) is small, in the range of **I** (103.7 kJ/mol),[3c] and may explain its reactivity. There are two reported examples of insertion of silylenes into aromatic C═C bonds.[13] Here, either a transient silylene is generated at elevated temperatures (>70 °C)[13e] or the Si(II) center is photochemically elevated to an excited state.[13c] Both silylenes react intermolecularly with aromatic compounds, extending the reaction or irradiation times to several hours.[13a−e] As expected due to the close proximity, the first intramolecular ring closure to **2** is much faster and proceeds even at low temperatures. The seven-membered ring system of **2** (Figure 1) is in a typical folded boat conformation with a C4−Si1−C9 angle of 105.3(3)° and angles between the planes of 41.06° (α) and 31.70° (β), which are in the range of reported silepins.[14] However, the silicon−carbon lengths (Si1−C4 = 1.891(6) Å and Si−C9 = 1.876(6) Å) are slightly elongated (cf. 1.82−1.88 Å in literature),[14] presumably a result of the sterically encumbered ligands. This structural feature and the obtained theoretical data aroused our interest in whether a facilitated bond breakage under regeneration of a Si(II) species might be feasible. Recently, Müller et al. introduced a new synthetic approach to NHC-stabilized silylenes by using NHCs to cleave selectively elongated Si−C bonds of 7-silanorbornadienes.[15] We pursued the idea a strong Lewis acid such as $B(C_6F_5)$ (BCF) may break the Si−C bonds of the silepin ring and form the corresponding silylene−borane adduct.[16]

Addition of 1 equiv of BCF to a mixture of **2**/TMS_3SiBr led to rearomatization and full conversion into the respective iminosilylene−BCF adduct **3** within 20 min (Scheme 2). The

Scheme 2. Reaction of 2 with $B(C_6F_5)_3$ To Form Iminosilylene−BCF Adduct 3

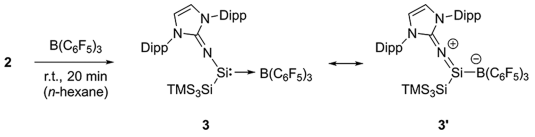

solubility in hexane decreased, presumably a result of the polarized bond between both partners, and adduct **3** could be separated from TMS_3SiBr as yellow crystals in moderate yield (45%). Although compound **3** is only stable in solution at room temperature for a maximum of 1 day, it was fully characterized by NMR, MS and X-ray analysis. The ^{29}Si NMR spectrum of **3** showed a quartet at 160.7 ppm ($^1J_{SiB}$ = 53.9 Hz) arising from the coordination of the central silicon atom to boron.

Compared to related room temperature stable IPrNCp*Si(II)−BCF adduct (114.5 ppm, $^1J_{SiB}$ = 70 Hz),[16d] the downfield shift of around 45 ppm emphasizes decreased electron density at the silicon atom. The crystallographic data of **3** (Figure 2) confirm a trigonal planar Si(II) center (bonding angles at Si1 add up to 360° within their standard deviations) with a Si1−B1 bond of 2.117(2) Å, longer than that of IPrNCp*Si(II)−BCF (2.080(5) Å)[16d] and similar to that of donor−acceptor adduct NHC → $SiCl_2$ → BCF (2.106(6) Å).[16b] Moreover, although the Si1−N1 bond (1.6354(16) Å) is shortened, the N1−C1 bond (1.306(2) Å) is elongated compared to precursor **2** (corresponding distances of 1.748(5) and 1.279(6) Å, respectively). This points to an increase of π-donation to the silicon atom, suggesting a linear 1-sila-2-azaallene resonance form **3′**. However, in comparison to IPrNCp*Si(II)-BCF (Si1−N1 = 1.605(3) Å and N1−C1 = 1.302(4) Å), this structure should be less pronounced (C1−N1−Si1 of **3** 151.10(14)° vs 158.7(3)°).[16d]

DOI: 10.1021/jacs.7b05136
J. Am. Chem. Soc. 2017, 139, 8134−8137

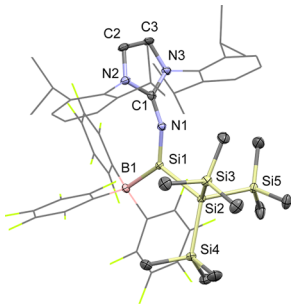

Figure 2. Molecular structure of **3** in the solid state with ellipsoids set at the 50% probability level. For clarity, hydrogen atoms and cocrystallized solvent molecules are omitted and Dipp- as well as C_6F_5-groups are simplified as wireframes. Selected bond lengths (Å) and angles (deg): Si1−B1 2.117(2), Si1−N1 1.6354(16), Si1−Si2 2.3827(6), N1−C1 1.306(2), C1−N2 1.387(2), C1−N3 1.381(2), N1−Si1−Si2 112.26(6), Si2−Si1−B1 118.28(6), B1−Si1−N1 129.45(8), C1−N1−Si1 151.10(14).

After this convincing proof of extrusion of a Si(II) species from silepin **2**, we targeted its direct use as "masked" silylene in small molecule activation (Scheme 3B).

Scheme 3. (A) Selected Examples of Known Silicon Carbonate Complexes (B); Small Molecule Activation of 2 with CO_2, Ethylene and H_2

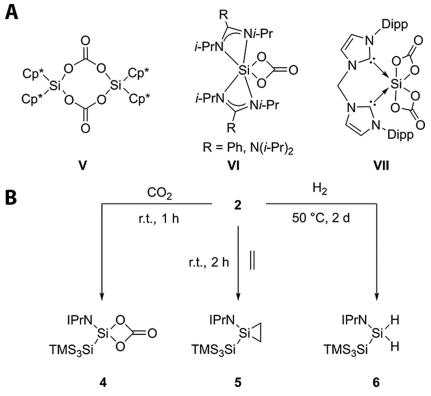

Over the last 3 decades, the metal-free binding of carbon dioxide by low-valent silicon compounds has drawn attention.[17] Jutzi et al. demonstrated the first reduction of carbon dioxide to carbon monoxide via stoichiometric formation of Si(IV) biscarbonato complex **V** (Scheme 3A).[18] Since then, a few other low-valent silicon compounds have been shown to activate successfully CO_2.[17] To the best of our knowledge, all but two of these reaction products are dimeric. Tacke et al. reported formation of six-coordinate, monomeric bis(amidinato/guadinato) silicon carbonate **VI** from the reaction of CO_2 with the respective silylene,[17b,d] and a silicon dicarbonate complex **VII** was isolated by Driess et al. from the activation of CO_2 by a silylone.[17a] The reaction of **2** with CO_2 proceeded rapidly (within 1 h) under mild conditions (1 bar, r.t.). Silepin **2** behaves as dormant form of iminosilylene **1**, which then follows the mechanism described in literature to give the corresponding silicon carbonate **4** (Scheme 3B).[17e,18] As mentioned, these products are usually prone to dimerization, but in our case the first four-coordinate, monomeric carbonato chelated silicon(IV) compound **4** was isolated in 60% yield. The ^{29}Si NMR shift of the central silicon atom of **4** (−35.0 ppm) is in the range of typical four-coordinate silicon compounds and is comparable to that of the biscarbonato dimer **V** (−28.3 ppm).[18] The characteristic C═O stretch of the carbonato unit of **4** was found at 1789 cm^{-1} (cf. **V**[18] $\nu_{C=O}$ = 1760 cm^{-1}, **VII**[17a] $\nu_{C=O}$ = 1746 cm^{-1}). The single crystal X-ray diffraction analysis of **4** (Figure 3) revealed its monomeric structure and exposed the position of the carbonato group in a pocket between the two bulky ligands.

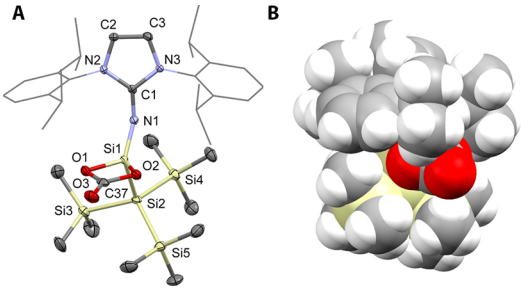

Figure 3. (A) Molecular structure of **4** in the solid state with ellipsoids set at the 50% probability level. For clarity, hydrogen atoms are omitted and Dipp groups are simplified as wireframes. Selected bond lengths (Å) and angles (deg): Si1−O1 1.7413(17), Si1−O2 1.7395(17), Si1−N1 1.6275(19), Si1−Si2 2.3161(10), N1−C1 1.297(3), O1−C37 1.360(3), O2−C37 1.348(3), O3−C37 1.194(3), N1−Si1−Si2 117.94(8), O1−Si1−O2 76.18(8), O1−C37−O2 104.93(18). (B) Space filling representation of **4**.

Because of this protection, no dimerization was observed in solution (C_6D_6) even after several weeks. The bond lengths related to the carbonato group are similar to those of published structures.[17b,d,18] The widening of the N1−Si1−Si2 angle (117.94(8)°) is noticeable in comparison to **3** (112.26(6)°) as a consequence of the lower space requirement of the carbonato moiety compared to the borane group. Acyclic silylenes have shown some reactivity toward ethylene[7,19] and molecular hydrogen.[3c,d] Therefore, we were interested whether silepin **2** was capable of activating such challenging targets. According to NMR studies, exposure of a freshly prepared solution of **2** to ethylene at room temperature gave the corresponding silirane ring **5** within 2 h (Scheme 3B). Despite several isolation attempts, this product could not be purified by crystallization due to its similar solubility properties to TMS_3SiBr, but is characterized sufficiently via ^{1}H, ^{13}C, ^{29}Si and 2D NMR spectroscopy. The ^{29}Si NMR spectrum gave a signal for the central silicon atom at −100.9 ppm, which is slightly high-field shifted compared to the analogous product from using **I** (−80.8 ppm),[19] illustrating once again the donor strength of the imino ligand. In addition, coupling of this central silicon to the ring-bound protons in the ^{1}H-^{29}Si HMBC spectrum confirmed the silirane structure. According to literature, exclusively acyclic silylenes with small HOMO−LUMO gaps (~2 eV) have been able to split the strong and nonpolar bond of dihydrogen.[3c,d] For silepin **2**, NMR studies revealed a slow reaction with hydrogen at room temperature; however, heating to 50 °C led to full conversion within 2 days (Scheme 3B). Here too, isolation of the product was problematic, but the obtained ^{29}Si NMR showed clear evidence for the assumed compound **6** with a triplet for the central silicon atom at −60.7 ppm ($^1J_{SiH}$ = 189 Hz), in accordance with the data of H_2 activation product of **I** (−35.2 ppm, $^1J_{SiH}$ = 195 Hz).[3c]

In summary, we provided proof of the first example of an acyclic iminosilylsilylene **1** via low temperature NMR and UV−vis experiments, which undergoes an intramolecular insertion into an aromatic C═C bond to form silepin **2**. As confirmed by X-ray

DOI: 10.1021/jacs.7b05136
J. Am. Chem. Soc. 2017, 139, 8134−8137

analysis, the newly formed Si—C bonds of **2** are elongated and facilitate the reductive elimination to Si(II) in combination with the driving force of rearomatization. This idea was verified by (HT) UV−vis experiments, DFT calculations and isolation of the silylene−borane adduct **3** upon addition of BCF. Compound **3** belongs to the small list of isolable silylene−BCF adducts and shows a minor contribution of the resonance structure 1-sila-2-azaallene **3′**. The concept of reversibility was further probed by directly using silepin **2** as a "masked" silylene in the activation of small molecules. For CO_2, the first example of a monomeric, four-coordinate silicon carbonate complex **4** was isolated. In addition, the activation of ethylene and molecular hydrogen with **2** was achieved under mild conditions. Beside the established oxidative addition of a silylene species, our work demonstrates the key concept of a reductive elimination from Si(IV) to Si(II), opening the door to the ultimate goal of silylene-based metal-free catalysis.

■ ASSOCIATED CONTENT

Supporting Information

The Supporting Information is available free of charge on the ACS Publications website at DOI: 10.1021/jacs.7b05136.

Experimental details (PDF)
Crystallographic data (CIF)

■ AUTHOR INFORMATION

Corresponding Authors

*rieger@tum.de
*s.inoue@tum.de

ORCID

Shigeyoshi Inoue: 0000-0001-6685-6352
Bernhard Rieger: 0000-0002-0023-884X

Notes

The authors declare no competing financial interest.

■ ACKNOWLEDGMENTS

We are grateful to the WACKER Chemie AG for continued financial support. We thank Dominik Reiter, Martin Machat and Philipp Pahl for revising the paper. We thank Dr. Alexander Pöthig for crystallographic advice, Fabian Linsenmann and Manuel Kaspar for IR and (VT) UV−vis measurements. We also express appreciation to the Leibniz Supercomputing Center of the Bavarian Academy of Science and Humanities for the provision of computing time.

■ REFERENCES

(1) Jutzi, P.; Kanne, D.; Kruger, C. *Angew. Chem., Int. Ed. Engl.* **1986**, *25*, 164−165.

(2) For recent reviews on silylenes, see: (a) Rivard, E. *Chem. Soc. Rev.* **2016**, *45*, 989−1003. (b) Blom, B.; Driess, M. *Struct. Bonding (Berlin, Ger.)* **2013**, *156*, 85−123. (c) Yao, S.-L.; Xiong, Y.; Driess, M. *Organometallics* **2011**, *30*, 1748−1767. (d) Asay, M.; Jones, C.; Driess, M. *Chem. Rev. (Washington, DC, U. S.)* **2011**, *111*, 354−396. (e) Mizuhata, Y.; Sasamori, T.; Tokitoh, N. *Chem. Rev. (Washington, DC, U. S.)* **2009**, *109*, 3479−3511.

(3) (a) Hadlington, T. J.; Abdalla, J. A. B.; Tirfoin, R.; Aldridge, S.; Jones, C. *Chem. Commun.* **2016**, *52*, 1717−1720. (b) Rekken, B. D.; Brown, T. M.; Fettinger, J. C.; Lips, F.; Tuononen, H. M.; Herber, R. H.; Power, P. P. *J. Am. Chem. Soc.* **2013**, *135*, 10134−10148. (c) Protchenko, A. V.; Schwarz, A. D.; Blake, M. P.; Jones, C.; Kaltsoyannis, N.; Mountford, P.; Aldridge, S. *Angew. Chem., Int. Ed.* **2013**, *52*, 568−571. (d) Protchenko, A. V.; Birjkumar, K. H.; Dange, D.; Schwarz, A. D.; Vidovic, D.; Jones, C.; Kaltsoyannis, N.; Mountford, P.; Aldridge, S. *J. Am. Chem. Soc.* **2012**, *134*, 6500−6503. (e) Rekken, B. D.; Brown, T. M.; Fettinger, J. C.; Tuononen, H. M.; Power, P. P. *J. Am. Chem. Soc.* **2012**, *134*, 6504−6507.

(4) Driess, M. *Nat. Chem.* **2012**, *4*, 525−526.

(5) Protchenko, A. V.; Bates, J. I.; Saleh, L. M. A.; Blake, M. P.; Schwarz, A. D.; Kolychev, E. L.; Thompson, A. L.; Jones, C.; Mountford, P.; Aldridge, S. *J. Am. Chem. Soc.* **2016**, *138*, 4555−4564.

(6) Inomata, K.; Watanabe, T.; Miyazaki, Y.; Tobita, H. *J. Am. Chem. Soc.* **2015**, *137*, 11935−11937.

(7) Lips, F.; Fettinger, J. C.; Mansikkamaki, A.; Tuononen, H. M.; Power, P. P. *J. Am. Chem. Soc.* **2014**, *136*, 634−7.

(8) (a) Rodriguez, R.; Gau, D.; Kato, T.; Saffon-Merceron, N.; De Cozar, A.; Cossio, F. P.; Baceiredo, A. *Angew. Chem., Int. Ed.* **2011**, *50*, 10414−10416. (b) Rodriguez, R.; Gau, D.; Contie, Y.; Kato, T.; Saffon-Merceron, N.; Baceiredo, A. *Angew. Chem., Int. Ed.* **2011**, *50*, 11492−5.

(9) (a) Rodriguez, R.; Contie, Y.; Nougué, R.; Baceiredo, A.; Saffon-Merceron, N.; Sotiropoulos, J.-M.; Kato, T. *Angew. Chem.* **2016**, *128*, 14567−14570. (b) Rodriguez, R.; Contie, Y.; Mao, Y.; Saffon-Merceron, N.; Baceiredo, A.; Branchadell, V.; Kato, T. *Angew. Chem., Int. Ed.* **2015**, *54*, 15276−15279.

(10) (a) Ochiai, T.; Inoue, S. *RSC Adv.* **2017**, *7*, 801−804. (b) Bag, P.; Ahmad, S. U.; Inoue, S. *Bull. Chem. Soc. Jpn.* **2017**, *90*, 255−271. (c) Ochiai, T.; Szilvási, T.; Inoue, S. *Molecules* **2016**, *21*, 1155−1167. (d) Ochiai, T.; Szilvási, T.; Franz, D.; Irran, E.; Inoue, S. *Angew. Chem., Int. Ed.* **2016**, *55*, 11619−11624. (e) Ochiai, T.; Franz, D.; Inoue, S. *Chem. Soc. Rev.* **2016**, *45*, 6327−6344.

(11) Lui, M. W.; Merten, C.; Ferguson, M. J.; McDonald, R.; Xu, Y.; Rivard, E. *Inorg. Chem.* **2015**, *54*, 2040−2049.

(12) Lee, G.-H.; West, R.; Müller, T. *J. Am. Chem. Soc.* **2003**, *125*, 8114−8115.

(13) (a) Kosai, T.; Ishida, S.; Iwamoto, T. *Chem. Commun.* **2015**, *51*, 10707−10709. (b) Kira, M.; Ishida, S.; Iwamoto, T.; de Meijere, A.; Fujitsuka, M.; Ito, O. *Angew. Chem., Int. Ed.* **2004**, *43*, 4510−4512. (c) Kira, M.; Ishida, S.; Iwamoto, T.; Kabuto, C. *J. Am. Chem. Soc.* **2002**, *124*, 3830−3831. (d) Suzuki, H.; Tokitoh, N.; Okazaki, R. *Bull. Chem. Soc. Jpn.* **1995**, *68*, 2471−81. (e) Suzuki, H.; Tokitoh, N.; Okazaki, R. *J. Am. Chem. Soc.* **1994**, *116*, 11572−3. Example of a silicon-mediated aryl group activation: (f) Mondal, K. C.; Samuel, P. P.; Roesky, H. W.; Aysin, R. R.; Leites, L. A.; Neudeck, S.; Lübben, J.; Dittrich, B.; Holzmann, N.; Hermann, M.; Frenking, G. *J. Am. Chem. Soc.* **2014**, *136*, 8919−8922.

(14) (a) Sohn, H.; Merritt, J.; Powell, D. R.; West, R. *Organometallics* **1997**, *16*, 5133−5134. (b) Nishinaga, T.; Izukawa, Y.; Komatsu, K. *Tetrahedron* **2001**, *57*, 3645−3656. (c) Nishinaga, T.; Izukawa, Y.; Komatsu, K. *Chem. Lett.* **1998**, *27*, 269−270. (d) Nishinaga, T.; Komatsu, K.; Sugita, N. *J. Org. Chem.* **1995**, *60*, 1309−1314.

(15) Lutters, D.; Severin, C.; Schmidtmann, M.; Müller, T. *J. Am. Chem. Soc.* **2016**, *138*, 6061−6067.

(16) Reported silylene−BCF adducts: (a) Jana, A.; Azhakar, R.; Sarish, S. P.; Samuel, P. P.; Roesky, H. W.; Schulzke, C.; Koley, D. *Eur. J. Inorg. Chem.* **2011**, *2011*, 5006−5013. (b) Ghadwal, R. S.; Roesky, H. W.; Merkel, S.; Stalke, D. *Chem. - Eur. J.* **2010**, *16*, 85−88. (c) Metzler, N.; Denk, M. *Chem. Commun.* **1996**, 2657−2658. (d) Inoue, S.; Leszczynska, K. *Angew. Chem., Int. Ed.* **2012**, *51*, 8589−8593.

(17) Recent examples of activation of CO_2 by low-valent silicon compounds: (a) Burchert, A.; Yao, S.; Müller, R.; Schattenberg, C.; Xiong, Y.; Kaupp, M.; Driess, M. *Angew. Chem., Int. Ed.* **2017**, *56*, 1894−1897. (b) Mück, F. M.; Baus, J. A.; Nutz, M.; Burschka, C.; Poater, J.; Bickelhaupt, F. M.; Tacke, R. *Chem. - Eur. J.* **2015**, *21*, 16665−16672. (c) Wang, Y.; Chen, M.; Xie, Y.; Wei, P.; Schaefer, H. F.; Robinson, G. H. *J. Am. Chem. Soc.* **2015**, *137*, 8396−8399. (d) Junold, K.; Nutz, M.; Baus, J. A.; Burschka, C.; Fonseca Guerra, C.; Bickelhaupt, F. M.; Tacke, R. *Chem. - Eur. J.* **2014**, *20*, 9319−9329. (e) Liu, X.; Xiao, X.-Q.; Xu, Z.; Yang, X.; Li, Z.; Dong, Z.; Yan, C.; Lai, G.; Kira, M. *Organometallics* **2014**, *33*, 5434−5439. (f) Gau, D.; Rodriguez, R.; Kato, T.; Saffon-Merceron, N.; de Cózar, A.; Cossío, F. P.; Baceiredo, A. *Angew. Chem., Int. Ed.* **2011**, *50*, 1092−1096.

(18) Jutzi, P.; Eikenberg, D.; Moehrke, A.; Neumann, B.; Stammler, H.-G. *Organometallics* **1996**, *15*, 753−9.

(19) Wendel, D.; Eisenreich, W.; Jandl, C.; Pöthig, A.; Rieger, B. *Organometallics* **2016**, *35*, 1−4.

DOI: 10.1021/jacs.7b05136
J. Am. Chem. Soc. 2017, 139, 8134−8137

6.2. Silicon and Oxygen's Bond of Affection: An Acyclic Three-Coordinate Silanone and Its Transformation to an Iminosiloxysilylene

Title: Silicon and Oxygen's Bond of Affection: An Acyclic Three-Coordinate Silanone and Its Transformation to an Iminosiloxysilylene

Status: Article, published online November 3, 2017

Journal: Journal of the American Chemical Society, 2017, 139 (47), 17193-17198.

Publisher: American Chemical Society

DOI: 10.1021/jacs.7b10634

Authors: Daniel Wendel, Dominik Reiter, Amelie Porzelt, Philipp J. Altmann, Shigeyoshi Inoue, Bernhard Rieger

Content: This report is an extension of the silepin project (see chapter 6.1) and addresses the isolation of a three coordinate, acyclic silanone - the heavier congener of a ketone - and its different isomerisation pathways depending on the silyl group used. Silanones have been sought after by many generations of silicon chemists since the pioneering work of F.S. Kipping in 1901, which gave access to the nowadays important field of poly(siloxanes). Silanones **2a** and **2b** were obtained *via* treatment of the silepins **1a** and **1b** with N_2O. They are stable in the solid state but show different rearrangements within lifetimes of 14 h (**2a**) and 48 h (**2b**) in solution. The bonding situation of **2b** is discussed, which revealed that the silyl-substituent effectively reduces the polarisation at the silicon centre. Additionally, mixing of the π(Si–O) bond with the lone pair of the exocyclic nitrogen atom adds to stabilisation of this compound. Initial reactivity investigations yielded silicon carbonate complexes **3a** and **3b** (already reported in chapter 6.1) *via* a different route. Treatment with methanol provides access to the silanols **4a**/**4b**, which are the heavier congeners of hemiketals. Hypersilyl-substituted silanone **2a** shows 1,3-TMS group migration in solution, yielding disilene **INT**, which can be trapped *via* NHC coordination in **6** as well as being able to activate ethylene to give **5**. Bonding analysis of **6** revealed the zwitterionic formulation as the most appropriate. Supersilyl-substitution at the silanone enables rearrangement to imino-siloxy-silylene **7**, thus again representing a reductive elimination at the silicon centre with a change in oxidation state (from +IV in **2b** to +II in **7**). Imino-siloxy-silylene **7** bears an increased HOMO-LUMO gap compared to **1b** but is still able to activate ethylene at rt within 20 min. This report presents the first example of an isolable, three coordinate silanone, showing different interesting isomerisation pathways depending on the silyl-substituents, wherefrom new disilenes and silylenes could be achieved.

Contributions to the publication:

- Initial test calculations for silanone **2a**
- DFT calculations on silanone **2b**, intermediate disilene **INT**, the reaction product of the disilene and ethylene **5**, the NHC-stabilised disilene **6** and rearranged acyclic imino-siloxy-silylene **7**
- Bonding analysis of silanone **2b** including comparison to smaller model systems with varying substituents to deduce the effect of the imino- and silyl-substitution at the silicon centre
- Bonding analysis of NHC-stabilised disilene **6**
- Interpretation of the data, composition of the theoretical parts in the manuscript
- Co-writing of the manuscript

JACS
JOURNAL OF THE AMERICAN CHEMICAL SOCIETY
Article
Cite This: J. Am. Chem. Soc. 2017, 139, 17193-17198
pubs.acs.org/JACS

Silicon and Oxygen's Bond of Affection: An Acyclic Three-Coordinate Silanone and Its Transformation to an Iminosiloxysilylene

Daniel Wendel,[†,‡] Dominik Reiter,[†,§] Amelie Porzelt,[§] Philipp J. Altmann,[⊥] Shigeyoshi Inoue,*[,§] and Bernhard Rieger*[,‡]

[‡]WACKER-Chair of Macromolecular Chemistry, [§]WACKER-Institute of Silicon Chemistry, [⊥]Catalysis Research Center, Technische Universität München, Lichtenbergstraße 4, 85748 Garching bei München, Germany

Supporting Information

ABSTRACT: A long-term dream comes true: An acyclic, neutrally charged silanone at last! Here, we report on the first examples of isolable acyclic, neutral, three-coordinate silanones **2** with indefinite stability as solids and lifetimes in solution of up to 2 days. The electronic properties of the Si═O bond were investigated via DFT calculations and revealed the π-donating *N*-heterocyclic imino (NHI) and σ-donating silyl groups as key factors for their enhanced stability. Besides initial reactivity studies of **2** toward CO_2 and methanol, different isomerization pathways depending on the silyl substitution pattern were found. For **2a** (R = TMS), a 1,3-silyl shift gave an intermediary disilene, which was trapped as unique NHC-disilene adduct **6**. For the more stable silanone **2b** (R = *t*-Bu), a selective transformation to the first reported room temperature stable, acyclic, two-coordinate *N*,*O*-silylene **7** exhibiting a fascinating siloxy ligand was observed. Both compounds were fully characterized experimentally and their bonding features were analyzed by theoretical calculations.

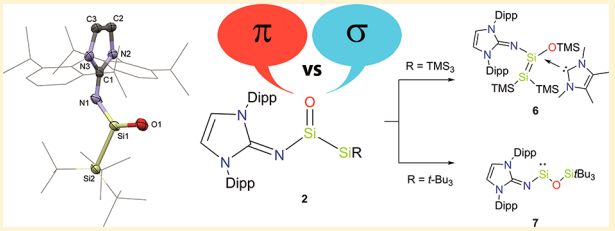

INTRODUCTION

Poly(siloxanes) are some of the most important and widely used inorganic polymers with a broad spectrum of applications ranging from industrial purposes to custom-designed materials of our daily life.[1] Considering today's widespread success, it is quite peculiar that poly(siloxanes) $(R_2SiO)_n$ were discovered by mere accident, when about one century ago organosilicon pioneer Frederic S. Kipping had actually been seeking silicon analogs of ketones ($R_2Si{=}O$).[2] Since then, the truly monomeric $R_2Si{=}O$ unit, generally referred to as silanone, has been one of the most sought-after compounds in modern main group chemistry ("Kipping's dream").[3] Unlike their lighter congeners, silanones possess a highly reactive Si═O double bond, which tends to undergo rapid head-to-tail polymerization to form stable Si−O σ-bonds.[4] This extreme reactivity is mainly attributed to the strong $Si^{\delta+}{-}O^{\delta-}$ polarization as a result of the large difference in electronegativity between both elements and an unfavorable overlap of the interacting silicon and oxygen p_π-orbitals.[5] Therefore, until a few years ago, silanones have been observed only in the gas phase or in argon matrices at low temperatures.[6] However, the recent decade has witnessed several attempts to tame the polarized Si═O double bond by additional coordination to Lewis acids or bases,[7] giving rise to a variety of isolable donor−acceptor[8] or donor-stabilized[9] complexes. A more recent approach abstains from this external perturbation and relies on the basic idea of kinetic and thermodynamic stabilization of the Si═O moiety by only two adjacent ligands (Chart 1).[10] The first impressive breakthrough toward three-coordinate silanones was achieved by Filippou et al., who isolated stable cationic metallosilanone **I**, which may partly be considered as an NHC-adduct of silicon monoxide.[11] Iwamoto and co-workers followed shortly after by reporting transient dialkylsilanone **II** stable at −80 °C.[12] Even more spectacular is the recent success of the group of Kato, who took advantage of two strong π-donors and isolated the first crystalline cyclic silanone **III** with half-life times in solution of up to 5 h at room temperature.[13]

Chart 1. Literature Known Examples of Three-Coordinate Silanones I−III

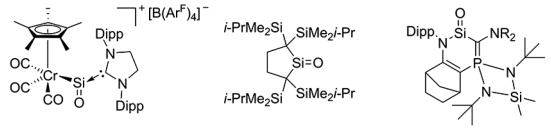

Dipp = C_6H_3-2,6-*i*-Pr_2
Ar^F = C_6H_3-3,5-$(CF_3)_2$
R = *i*-Pr / *c*Hex

We have previously reported an acyclic iminosilylsilylene, which reversibly inserts into a C═C double bond of its aromatic ligand framework to form silepin **1a** (Scheme 1).[14] This tendency to undergo reductive elimination has been exploited to use **1a** as direct synthetic equivalent of silylene in the activation of small molecules. Continuing this study, we were interested to see whether the *N*-heterocyclic imino (NHI) ligand[15] as single π-donor of the silepin-silylene system may sufficiently stabilize a highly polarized Si═O moiety.

Received: October 6, 2017
Published: November 3, 2017

DOI: 10.1021/jacs.7b10634
J. Am. Chem. Soc. 2017, 139, 17193−17198

Scheme 1. Preparation and Reactivity of Acyclic Three-Coordinate Silanones 2

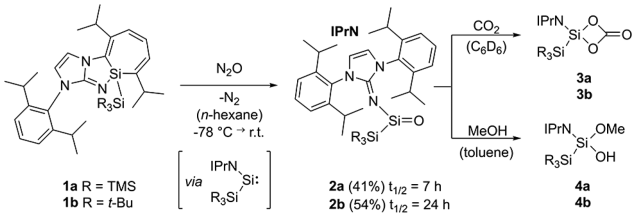

Herein, we present the first examples of acyclic and neutrally charged silanones **2** with a planar three-coordinate Si atom. Furthermore, chemical lifetimes, isomerization pathways, and initial reactivity studies of **2** are discussed in detail.

RESULTS AND DISCUSSIONS

Exposure of an *n*-hexane solution of silepin **1** at −78 °C to an atmosphere of N_2O followed by warming to room temperature instantly gave a white precipitate, which was separated by filtration, washed with *n*-hexane and dried in vacuo to give pure silanone **2** in moderate yield (**2a** 41%, **2b** 54%) (Scheme 1). The ^{29}Si NMR spectra of both compounds displayed signals for the central silicon atom at 33.7 ppm for **2a** and 28.8 ppm for **2b** (calc. 33.3 ppm at SMD-B3LYP/6-311+G(2d,2p) level of theory), respectively. Both NMR shifts are in the typical region for three-coordinate silicon compounds, but are considerably high-field shifted in comparison to **I** (169.6 ppm)[11] and **II** (128.4 ppm).[12] They even fall in the same range as cyclic silanone **III** (38.4 ppm)[13] with two π-donating substituents, illustrating the strong donor qualities of a single NHI ligand. The characteristic Si═O stretching vibration was found at 1144 cm^{-1} for both compounds, which is in good agreement with the calculated value ($\nu_{Si=O}$ = 1155 cm^{-1}) and comparable to other Si═O containing structures.[12,16] The UV−vis spectrum of **2b** in toluene revealed an broad absorption peak at 282 nm in the same region as related acyclic three-coordinate germanone (297 nm).[10] Colorless crystals of **2b** were obtained by slow diffusion of Et_2O into a saturated THF solution at −35 °C over several days. Single-crystal X-ray analysis confirmed the monomeric structure of **2b** and exposed the position of the Si═O moiety in a well-protected steric pocket between the two bulky ligands (Figure 1).

The crystal structure revealed a trigonal planar silicon center (sum of bonding angles: 360°) and a Si1−O1 bond length of **2b** (1.537(3) Å), which is slightly longer than that of metallosilanone **I** (1.526 Å)[11] and cyclic silanone **III** (1.533 Å),[13] but generally shorter than those of tetra-coordinate base-stabilized silanones.[8,9] The potent electron donation from the exocyclic nitrogen atom of the NHI ligand to the electron deficient silicon atom is clearly evidenced by a short Si1−N1 bond (1.646(3) Å), for which reason resonance form **2b′** should be denoted (Chart 2). Further, the N1−C1 bond (1.319(4)Å) is elongated and the endocyclic C−N bonds (C1−N2 1.364(5) Å/ C1−N3 1.368(5) Å) are slightly shortened.[17] Combined with a small Si1−N1−C1 angle of merely 131.7(3)° one can assume that the positive charge may be delocalized over the iminato ring as illustrated in structure **2b″**. However, according to the X-ray data, the almost perpendicular assembly of the planar NHC fragment to the N1Si1O1 plane (dihedral angle 89.9(4)°) seems to limit this conjugative effect. To obtain further insights into the bonding properties of **2b**, we performed density functional theory (DFT) calculations at

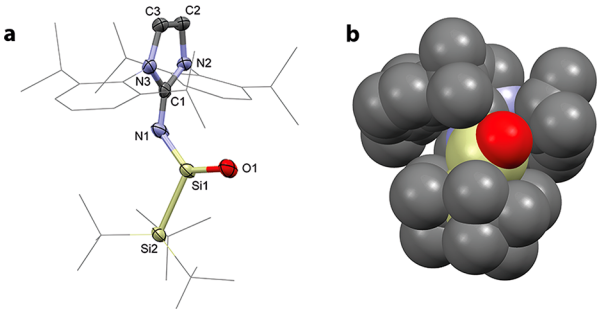

Figure 1. (a) Molecular structure and (b) space filling representation of silanone **2b** in the solid state with ellipsoids set at the 50% probability level (one out of two independent molecules in the asymmetric unit). For clarity, hydrogen atoms are omitted and *t*-Bu as well as Dipp groups are simplified as wireframes. Selected bond lengths (Å) and angles (deg): Si1−O1 1.537(3), Si1−N1 1.646(3), N1−C1 1.319(4), C1−N2 1.364(5), C1−N3 1.368(5), Si1−Si2 2.358(2), N1−Si1−Si2 112.6(1), C1−N1−Si1 131.7(3).

Chart 2. (a) DFT-Calculated HOMO−10 *E* = −7.78 eV and LUMO+4 *E* = −0.41 eV of 2b, (b) Plausible Resonance Forms of 2b and Calculated Smaller Silanones A, B, C, and D Including NPA Charges and Bond Orders (in bold and italics)

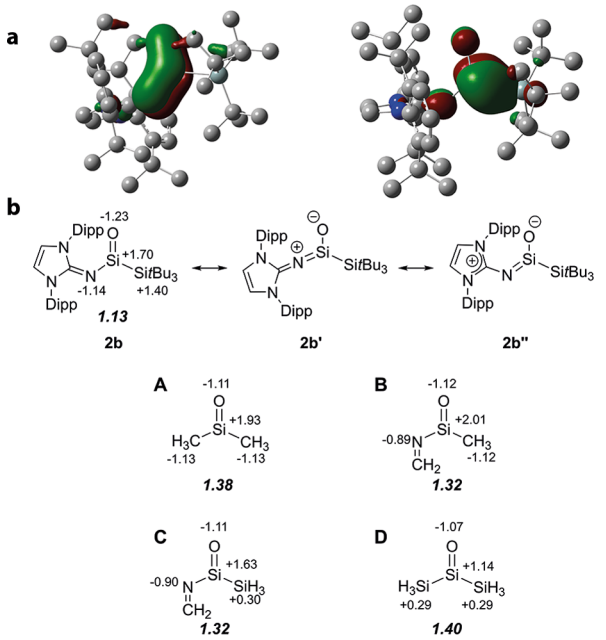

the B3LYP/6-311+G(d) level of theory. The analysis of the Kohn−Sham orbitals (Chart 2a) showed that HOMO−10 represents the Si═O π-bond, which obviously mixes with the nonbonding orbital of the exocyclic nitrogen atom, explaining the observed short Si1−N1 distance. As already extracted from the X-ray data, an expansion of the conjugation to the NHC ring fragment could not be found. Interestingly, the LUMO+4 reveals significant hyperconjugation from the Si−C σ-bond of the silyl group to the π^*-bonding orbital of Si═O moiety. Moreover, from NBO analysis (Chart 2b) a decreased Si═O bond order (1.13) and an increased negative charge on the oxygen center (−1.23) compared to those of dimethylsilanone **A** (1.38 and −1.11) were found, illustrating the strong polarization of the Si═O double bond. However, the positive character at Si1 decreases. To explain this effect, we calculated

DOI: 10.1021/jacs.7b10634
J. Am. Chem. Soc. 2017, 139, 17193−17198

the smaller iminoalkyl- **B**, iminosilyl- **C** and disilylsilanone **D** analogs. Here too the trend is visible, that the positive charge at the silicon center is effectively reduced by presumable σ-donation and hyperconjugation of the silyl group.[4b] In compound **2b** this effect fully sets in and Si1 has only a slightly higher positive charge (1.70) than Si2 attached to *t*-Bu groups (1.40). Our analysis proves that besides the kinetical stabilization due to steric encumbrance, especially the π-donor qualities of NHI ligand but as well σ-donor properties of silyl group are key to stabilize acyclic silanone **2b**.

In terms of reactivity, both silanones **2** were directly and quantitatively converted by CO_2 to the respective silicon carbonate complexes **3**, similarly to the reaction of silepin **1a** with carbon dioxide (Scheme 1).[14] Moreover, the reaction of silanones **2** toward methanol was tested. As in carbonyl chemistry, where ketones form hemiketals with alcohols, the corresponding silanol **4** was isolated in good yield (**4a** 71%, **4b** 69%). The ^{29}Si NMR shift of the silicon center of **4a** at −38.6 ppm and **4b** at −46.6 ppm, respectively, clearly displayed the change in coordination number from three to four. The X-ray diffraction analysis of **4a** (Figure 2) verified the presence of a

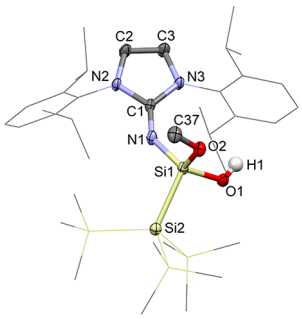

Figure 2. Molecular structure of silanol **4a** in the solid state with ellipsoids set at the 50% probability level. For clarity, hydrogen atoms and cocrystallized solvent molecules are omitted and TMS as well as Dipp groups are simplified as wireframes. Selected bond lengths (Å) and angles (deg): Si1−O1 1.642(2), Si1−O2 1.660(2), Si1−N1 1.680(2), N1−C1 1.278(3), C1−N2 1.394(3), C1−N3 1.396(3), N1−Si1−O1 118.7(1), C1−N1−Si1 142.4(2).

tetra-coordinate silicon center attached to one methoxy and one hydroxyl group. The Si1−O1 bond length of **4a** (1.642(2) Å) is unambiguously distinguishable from the original Si═O bond of **2b**. Interestingly, in this structure, the Si1−N1 bond (1.680(2) Å) is elongated and the N1−C1 bond (1.278(3) Å) slightly shortened in comparison to **2b**, which underlines the disappearance of the former Si═N double-bond character.

A key criterion for storage, handling and reaction design of silanones is their lifetime. Monitoring a C_6D_6 solution of silanone **2a** via ^{1}H NMR spectroscopy showed the full decomposition to an unspecific product mixture within 14 h ($t_{1/2}$ = 7 h). ^{1}H, ^{29}Si and ^{1}H/^{29}Si HMBC NMR data pointed to one major asymmetric product, presumably formed by TMS migration from the hypersilyl group to the Si═O center and subsequent activation of the NHI ligand (see the Supporting Information). Further experiments revealed that its half-life can be extended considerably by using **2a** in CD_3CN solutions ($t_{1/2}$ = 4 days). Consistent with additional Lewis base coordination, the ^{29}Si NMR signal of the Si═O center is shifted from +33.7 ppm to −48.3 ppm. Crystals of tetra-coordinate acetonitrile-silanone adduct **2a** × CD_3CN were isolated and verified the additional solvent coordination (see SI). Still, we were interested to pin down the reactive intermediate in the decomposition process of **2a**. According to literature, a 1,3-silyl migration has been reported for transient cyclic dialkylsilanone **II** to form an intermediary silene.[12] Indeed, we figured out that the same TMS migration can be instantly induced by addition of THF-d_8 to solid **2a**, resulting in a strongly yellow colored solution (Scheme 2). Subsequent NMR

Scheme 2. Isomerization Pathway of Silanone 2a and Trapping of Intermediary Disilene INT

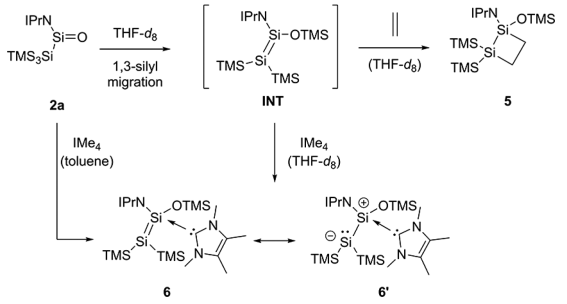

analysis indicated the quantitative formation of the proposed transient disilene **INT**. Strikingly, the different electronic environment at both silicon centers of **INT** due to the asymmetric substitution pattern is already noticeable in the ^{29}Si NMR shifts (−8.0 ppm (*Si*OTMS), − 196.6 ppm (*Si*TMS$_2$)), which suggest a polarized Si═Si double bond with high zwitterionic character. Because of the short lifetime of this species, isolation and full characterization was not possible and so trapping experiments were performed. Exposure of a THF-d_8 solution of **2a**, in situ forming **INT**, to ethylene immediately gave the colorless [2 + 2]-cycloaddition product **5**. 1,2-Disiletane **5** was sufficiently characterized via 2D NMR experiments and matching theoretical NMR shifts. Further, we tried to stabilize **INT** with a strong NHC donor. Reaction of **INT** in THF-d_8 or alternatively directly silanone **2a** in toluene with IMe_4 exclusively gave room-temperature-stable NHC-stabilized disilene adduct **6**. The ^{29}Si NMR shifts of **6** (−35.2 ppm (*Si*OTMS), − 174.6 ppm (*Si*TMS$_2$)) are similar to those of intermediary disilene **INT**, especially the latter, illustrating the presence of a highly negatively charged silicon atom, consistent with typical silyl anions.[18]

Orange-red crystals of **6** were isolated from an *n*-hexane solution at −35 °C. Subsequent X-ray analysis confirmed the coordination of the NHC donor to the distorted tetrahedral Si1 center (Figure 3a). The Si1−C28 bond length (1.958(2) Å) is in the range of typical dative NHC-Si bonds,[19] the assumed Si1−Si2 double bond is extremely elongated (2.3297(9) Å), slightly shorter than Si2−Si3 (2.3397(9) Å) and Si2−Si4 (2.3445(9) Å) bond, but beyond the range of classical Si═Si double bonds (2.13−2.31 Å).[20]

Still, compound **6** possesses a typical trans-bent geometry and shows significant pyramidalization, especially at the Si2 center (bent angles θ(Si1) = 42.7° and θ(Si2) = 57.8°). This strong bending underpins the assumption of zwitterionic resonance structure **6′** with a lone pair at Si2, but is distinguishable from a potential Si1−Si2 dative bond as recently discovered for base-stabilized disilene adduct $Me_2EtN \rightarrow SiCl_2 \rightarrow Si(SiCl_3)_2$ with an even larger bent angle ($\theta(Si(SiCl_3)_2$ = 79.1°).[21] Because NHC adducts of multiply bonded silicon compounds are rarely found in literature,[22] we were further interested in the electronic

DOI: 10.1021/jacs.7b10634
J. Am. Chem. Soc. 2017, 139, 17193−17198

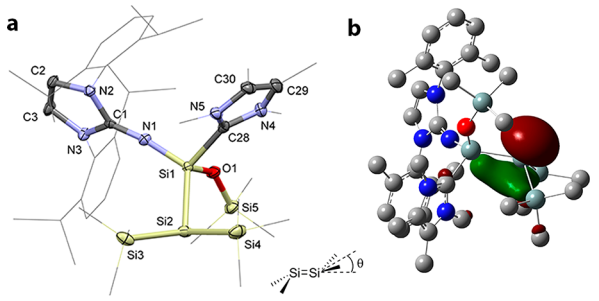

Figure 3. (a) Molecular structure of IMe_4 stabilized disilene adduct **6** in the solid state with ellipsoids set at the 50% probability level (one out of two independent molecules in the asymmetric unit). For clarity, hydrogen atoms and TMS as well as Dipp groups are simplified as wireframes. Selected bond lengths (Å) and angles (deg): Si1−Si2 2.3297(7), Si2−Si3 2.3397(9), Si2−Si4 2.3445(9), Si1−C28 1.958(2), Si1−O1 1.656(2), Si1−N1 1.659(2), N1−C1 1.263(3), C1−N2 1.407(3), C1−N3 1.400(3), C1−N1−Si1 168.9(2). b) DFT-calculated HOMO (−3.54 eV) of **6**.

properties of **6**. DFT calculations indicated that the HOMO (Figure 3b) mainly represents the lone pair at the Si2 atom with only short extensions not only to Si1 but to all surrounding silicon centers. The bond indices (see the Supporting Information) follow the same trend, with a WBI of Si1−Si2 (1.04) only slightly insinuating double bond character compared to Si2−Si3 (0.99) and Si2−Si4 (0.98). Regarding NPA charges, the polarization of Si1 (1.61) and Si2 (−0.60) in comparison to Si3 and Si4 (1.18) come to the same conclusion that the proposed zwitterionic canonical form **6′** is the most fitting representation to describe the electronic nature of this compound.

In strong contrast to the 1,3-silyl migration of **2a**, silanone **2b** shows almost no variations in the ^{29}Si NMR shifts during the solvent change from C_6D_6 to THF-d_8, indicating no observable donor−acceptor interaction between solvent and silanone. Because of replacement of TMS by *t*-Bu groups, silanone **2b** is indefinitely stable as a solid at room temperature, but remarkably forms mixed *N,O*-silylene **7** in C_6D_6 or THF-d_8 solution at ambient conditions within 48 h ($t_{1/2}$ = 24 h) in quantitative yield. This transformation can be accelerated by heating the solution to 60 °C, where full conversion was detected by NMR spectroscopy in less than 1 h (Scheme 3).

Scheme 3. Selective Transformation of Silanone 2b to Acyclic *N,O*-Silylene 7 and Formation of Silirane 8

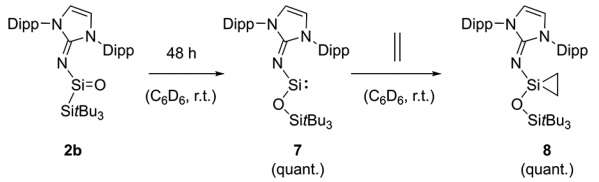

The facile thermal rearrangement is supported by theoretical calculations, which determined that *N,O*-silylene **7** is in fact 28.8 kJ/mol more stable than silanone **2b**. We believe that most likely the oxophilicity of silicon, promoting formation of stable Si−O single bonds, is the driving force of this reaction, which even overcomes the counteracting change of oxidation state from Si(IV) back to less stable Si(II). The ^{29}Si NMR signal of the central silicon atom of silylene **7** at 58.9 ppm (C_6D_6) is high-field shifted compared to other room-temperature-stable two-coordinate diamino (204.6 ppm)[23] and dithiolato silylenes (285.5 ppm).[24]

In particular, the upfield shift in comparison to strongly related in situ generated iminosilylsilylene IPrNSi(II)$SiTMS_3$ (300.0 ppm)[14] suggests additional π-donation by the siloxy ligand. A band for the characteristic $Si_n \rightarrow Si_{3p}$ transition of **7** was observed at 328 nm, which is very close to the theoretically predicted data (HOMO → LUMO 341 nm). X-ray analysis of colorless crystals of **7** revealed a two-coordinate silicon center exhibiting an N1−Si1−O1 angle of 103.56(8)° (Figure 4a).

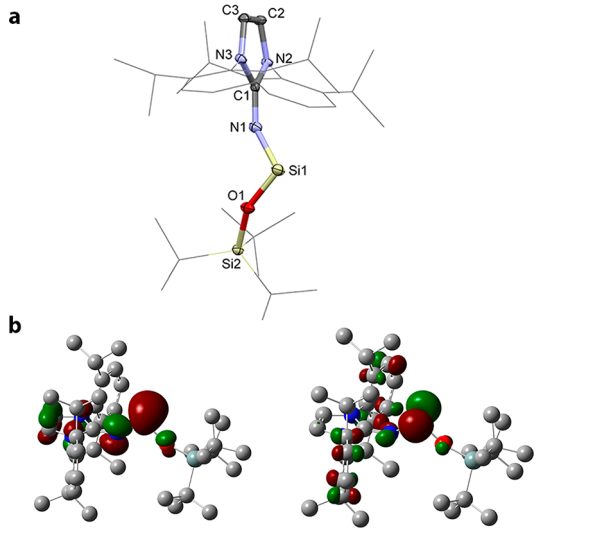

Figure 4. (a) Molecular structure of *N,O*-silylene **7** in the solid state with ellipsoids set at the 50% probability level (one out of two independent molecules in the asymmetric unit). For clarity, hydrogen atoms and *t*-Bu as well as Dipp groups are simplified as wireframes. Selected bond lengths (Å) and angles (deg): Si1−O1 1.643(1), O1−Si2 1.637(1), Si1−N1 1.661(2), N1−C1 1.281(2), C1−N2 1.380(3), C1−N3 1.386(2), N1−Si1−O1 103.56(8), C1−N1−Si1 147.7(2), Si1−O1−Si2 153.2(1). b) DFT-calculated HOMO (left, −5.04 eV) and LUMO (right, −0.71 eV) of **7**.

This angle is clearly wider than for cyclic NHSis (e.g., $(CH(t\text{-}Bu)N)_2Si(II)$ 88.6°),[25] but considerably more compressed than for acyclic DippNTMSSi(II)$SiTMS_3$ (116.91°).[26] The Si1−N1 bond length (1.661(2) Å) is marginally longer than in the parent silanone structure **2b**, illustrating again a partial Si═N double bond character. Surprisingly, regarding potential π-donation by the siloxy group, both Si−O bonds have nearly the same length (Si1−O1 1.643(1) Å, O1−Si2 1.637(1) Å). Therefore, only a minor Si═O double bond character may be suggested. DFT calculations are in line with these findings, the HOMO of *N,O*-silylene **7** exhibits mainly lone pair character (Si_n), the LUMO resembles the empty Si_{3p} orbital with a HOMO−LUMO gap of 4.33 eV (Figure 4b). Both orbitals show only minor contributions from donating N or O atoms. For orbitals lower in energy, some interactions of silicon with nitrogen (HOMO−6), and even lower, minor interactions with oxygen can be found (see SI). The HOMO−LUMO gap is close to that of the acyclic dithiolato silylene by Power et al. (4.23 eV),[24] indicating a similar level of reactivity toward small molecules. Indeed, both silylenes show no sign of reactivity with molecular hydrogen, even if a reaction solution of **7** in H_2 atmosphere (1 bar) is heated to 60 °C for several days.[24] Regarding the activation of ethylene, it is reported that dithiolato silylene reversibly binds the olefin in a dissociation

DOI: 10.1021/jacs.7b10634
J. Am. Chem. Soc. 2017, 139, 17193−17198

equilibrium.[27] In contrast, *N,O*-silylene **7** quantitatively forms the corresponding silirane **8** within 20 min at room temperature with no observable reverse reaction. We believe that this disparity in reactivity is likely caused by reduced steric shielding at the Si(II) center of **7**.[28]

CONCLUSIONS

In summary, we have successfully isolated and fully characterized the first examples of acyclic, neutral, three-coordinate silanones **2** with indefinite stability as solids and lifetimes in solution up to 2 days. DFT calculations provided insight into the Si=O bonding and verified π-donating NHI and σ-donating silyl groups as important factors for their enhanced stability. First reactivity of silanones **2** toward CO_2 and methanol was tested and potential isomerization pathways were discovered. Here, a 1,3-silyl migration of **2a**, gave an intermediary disilene **INT**, which was trapped as 1,2-disiletane **5** in a [2 + 2]-cycloaddition with ethylene. Further, the NHC-disilene adduct **6** was isolated and analyzed by quantum chemical methods. Interestingly, for **2b**, the selective transformation to the first acyclic, two-coordinate *N,O*-silylene **7** was observed. Here, the enormous potential of acyclic silylene **7** to act as transition-metal mimic was demonstrated by successful activation of ethylene under ambient conditions. In total, our work not only continues the fulfillment of Kipping's dream of isolable silanones, but gives first insights into similarities and differences between this novel compound class and well-known carbonyl compounds.

ASSOCIATED CONTENT

Supporting Information

The Supporting Information is available free of charge on the ACS Publications website at DOI: 10.1021/jacs.7b10634.

Experimental details (PDF)

Crystallographic data (CCDC 1577580−1577584) (CIF)

AUTHOR INFORMATION

Corresponding Authors

*E-mail.: rieger@tum.de (B.R.).
*E-mail: s.inoue@tum.de (S.I.).

ORCID

Shigeyoshi Inoue: 0000-0001-6685-6352
Bernhard Rieger: 0000-0002-0023-884X

Author Contributions

†D.W. and D.R. contributed equally.

Notes

The authors declare no competing financial interest.

ACKNOWLEDGMENTS

We are exceptionally grateful to the WACKER Chemie AG and European Research Council (SILION 63794) for financial support. We thank Dr. Samuel Powley, Philipp Pahl, and Martin Machat for revising the manuscript and Dr. Alexander Pöthig for crystallographic advice. We also express our appreciation to the Leibniz Supercomputing Center of the Bavarian Academy of Science and Humanities for provision of computing time.

REFERENCES

(1) Jones, R. G.; Ando, W.; Chojnowski, J. *Silicon-Containing Polymers*; Springer: Dordrecht, The Netherlands, 2000.

(2) Kipping, F. S.; Lloyd, L. L. *J. Chem. Soc., Trans.* **1901**, *79*, 449−459.

(3) Sen, S. S. *Angew. Chem., Int. Ed.* **2014**, *53*, 8820−8822.

(4) (a) Kudo, T.; Nagase, S. *J. Am. Chem. Soc.* **1985**, *107*, 2589−2595. (b) Kimura, M.; Nagase, S. *Chem. Lett.* **2001**, *30*, 1098−1099.

(5) Avakyan, V. G.; Sidorkin, V. F.; Belogolova, E. F.; Guselnikov, S. L.; Gusel'nikov, L. E. *Organometallics* **2006**, *25*, 6007−6013.

(6) Examples of gas-phase and matrix-isolation experiments: (a) Glinski, R. J.; Gole, J. L.; Dixon, D. A. *J. Am. Chem. Soc.* **1985**, *107*, 5891−5894. (b) Withnall, R.; Andrews, L. *J. Am. Chem. Soc.* **1985**, *107*, 2567−2568. (c) Maier, G.; Meudt, A.; Jung, J.; Pacl, H., Matrix Isolation Studies of Silicon Compounds. In *The Chemistry of Organic Silicon Compounds*; John Wiley & Sons: Chichester, U.K., 1998; pp 1143−1185.

(7) Review on silanones and their heavier homologues: Xiong, Y.; Yao, S.; Driess, M. *Angew. Chem., Int. Ed.* **2013**, *52*, 4302−4311.

(8) (a) Yao, S.; Brym, M.; van Wuellen, C.; Driess, M. *Angew. Chem., Int. Ed.* **2007**, *46*, 4159−4162. (b) Xiong, Y.; Yao, S.; Driess, M. *Angew. Chem., Int. Ed.* **2010**, *49*, 6642−6645. (c) Xiong, Y.; Yao, S.; Driess, M. *Dalton Trans.* **2010**, *39*, 9282−9287. (d) Xiong, Y.; Yao, S.; Müller, R.; Kaupp, M.; Driess, M. *J. Am. Chem. Soc.* **2010**, *132*, 6912−6913. (e) Ghadwal, R. S.; Azhakar, R.; Roesky, H. W.; Pröpper, K.; Dittrich, B.; Klein, S.; Frenking, G. *J. Am. Chem. Soc.* **2011**, *133*, 17552−17555. (f) Muraoka, T.; Abe, K.; Haga, Y.; Nakamura, T.; Ueno, K. *J. Am. Chem. Soc.* **2011**, *133*, 15365−15367. (g) Ghadwal, R. S.; Azhakar, R.; Roesky, H. W.; Propper, K.; Dittrich, B.; Goedecke, C.; Frenking, G. *Chem. Commun.* **2012**, *48*, 8186−8188. (h) Rodriguez, R.; Gau, D.; Troadec, T.; Saffon-Merceron, N.; Branchadell, V.; Baceiredo, A.; Kato, T. *Angew. Chem., Int. Ed.* **2013**, *52*, 8980−8983. (i) Muraoka, T.; Abe, K.; Kimura, H.; Haga, Y.; Ueno, K.; Sunada, Y. *Dalton Trans.* **2014**, *43*, 16610−16613. (j) Reyes, M. L.; Troadec, T.; Rodriguez, R.; Baceiredo, A.; Saffon-Merceron, N.; Branchadell, V.; Kato, T. *Chem. - Eur. J.* **2016**, *22*, 10247−10253. (k) Rodriguez, R.; Gau, D.; Saouli, J.; Baceiredo, A.; Saffon-Merceron, N.; Branchadell, V.; Kato, T. *Angew. Chem., Int. Ed.* **2017**, *56*, 3935−3939.

(9) (a) Yao, S.; Xiong, Y.; Brym, M.; Driess, M. *J. Am. Chem. Soc.* **2007**, *129*, 7268−7269. (b) Xiong, Y.; Yao, S.; Driess, M. *J. Am. Chem. Soc.* **2009**, *131*, 7562−7563. (c) Yao, S.; Xiong, Y.; Driess, M. *Chem. - Eur. J.* **2010**, *16*, 1281−1288. (d) Xiong, Y.; Yao, S.; Müller, R.; Kaupp, M.; Driess, M. *Nat. Chem.* **2010**, *2*, 577−580. (e) Epping, J. D.; Yao, S.; Karni, M.; Apeloig, Y.; Driess, M. *J. Am. Chem. Soc.* **2010**, *132*, 5443−5455. (f) Rodriguez, R.; Troadec, T.; Gau, D.; Saffon-Merceron, N.; Hashizume, D.; Miqueu, K.; Sotiropoulos, J.-M.; Baceiredo, A.; Kato, T. *Angew. Chem., Int. Ed.* **2013**, *52*, 4426−4430. (g) Hansen, K.; Szilvási, T.; Blom, B.; Irran, E.; Driess, M. *Chem. - Eur. J.* **2015**, *21*, 18930−18933. (h) Troadec, T.; Lopez Reyes, M.; Rodriguez, R.; Baceiredo, A.; Saffon-Merceron, N.; Branchadell, V.; Kato, T. *J. Am. Chem. Soc.* **2016**, *138*, 2965−2968.

(10) Analog strategy for isolation of acyclic three-coordinate germanone: Li, L.; Fukawa, T.; Matsuo, T.; Hashizume, D.; Fueno, H.; Tanaka, K.; Tamao, K. *Nat. Chem.* **2012**, *4*, 361−365.

(11) Filippou, A. C.; Baars, B.; Chernov, O.; Lebedev, Y. N.; Schnakenburg, G. *Angew. Chem., Int. Ed.* **2014**, *53*, 565−570.

(12) Ishida, S.; Abe, T.; Hirakawa, F.; Kosai, T.; Sato, K.; Kira, M.; Iwamoto, T. *Chem. - Eur. J.* **2015**, *21*, 15100−15103.

(13) Alvarado-Beltran, I.; Rosas-Sánchez, A.; Baceiredo, A.; Saffon-Merceron, N.; Branchadell, V.; Kato, T. *Angew. Chem., Int. Ed.* **2017**, *56*, 10481−10485.

(14) Wendel, D.; Porzelt, A.; Herz, F. A. D.; Sarkar, D.; Jandl, C.; Inoue, S.; Rieger, B. *J. Am. Chem. Soc.* **2017**, *139*, 8134−8137.

(15) Ochiai, T.; Franz, D.; Inoue, S. *Chem. Soc. Rev.* **2016**, *45*, 6327−6344.

(16) Linden, M. M.; Reisenauer, H. P.; Gerbig, D.; Karni, M.; Schäfer, A.; Müller, T.; Apeloig, Y.; Schreiner, P. R. *Angew. Chem., Int. Ed.* **2015**, *54*, 12404−12409.

DOI: 10.1021/jacs.7b10634
J. Am. Chem. Soc. 2017, 139, 17193−17198

(17) Inoue, S.; Leszczynska, K. *Angew. Chem., Int. Ed.* **2012**, *51*, 8589−8593.
(18) Marschner, C. *Eur. J. Inorg. Chem.* **1998**, *1998*, 221−226.
(19) Ahmad, S. U.; Szilvasi, T.; Irran, E.; Inoue, S. *J. Am. Chem. Soc.* **2015**, *137*, 5828−5836.
(20) (a) Weidenbruch, M., In *The Chemistry of Organic Silicon Compounds*, Rappoport, Z., Apeloig, Y., Eds.; John Wiley & Sons: Chichester, U.K., 2001; Vol. 3, pp 391−428. (b) Wendel, D.; Szilvási, T.; Jandl, C.; Inoue, S.; Rieger, B. *J. Am. Chem. Soc.* **2017**, *139*, 9156−9159.
(21) Schweizer, J. I.; Scheibel, M. G.; Diefenbach, M.; Neumeyer, F.; Würtele, C.; Kulminskaya, N.; Linser, R.; Auner, N.; Schneider, S.; Holthausen, M. C. *Angew. Chem., Int. Ed.* **2016**, *55*, 1782−1786.
(22) (a) Yamaguchi, T.; Sekiguchi, A.; Driess, M. *J. Am. Chem. Soc.* **2010**, *132*, 14061−14063. (b) Leszczynska, K.; Abersfelder, K.; Mix, A.; Neumann, B.; Stammler, H.-G.; Cowley, M. J.; Jutzi, P.; Scheschkewitz, D. *Angew. Chem., Int. Ed.* **2012**, *51*, 6785−6788. (c) Yamaguchi, T.; Asay, M.; Sekiguchi, A. *J. Am. Chem. Soc.* **2012**, *134*, 886−889. (d) Cowley, M. J.; Huch, V.; Rzepa, H. S.; Scheschkewitz, D. *Nat. Chem.* **2013**, *5*, 876−879.
(23) Hadlington, T. J.; Abdalla, J. A. B.; Tirfoin, R.; Aldridge, S.; Jones, C. *Chem. Commun.* **2016**, *52*, 1717−1720.
(24) Rekken, B. D.; Brown, T. M.; Fettinger, J. C.; Tuononen, H. M.; Power, P. P. *J. Am. Chem. Soc.* **2012**, *134*, 6504−6507.
(25) Moser, D. F.; Guzei, I. A.; West, R. *Main Group Met. Chem.* **2001**, *24*, 811−812.
(26) Protchenko, A. V.; Schwarz, A. D.; Blake, M. P.; Jones, C.; Kaltsoyannis, N.; Mountford, P.; Aldridge, S. *Angew. Chem., Int. Ed.* **2013**, *52*, 568−571.
(27) Lips, F.; Fettinger, J. C.; Mansikkamaki, A.; Tuononen, H. M.; Power, P. P. *J. Am. Chem. Soc.* **2014**, *136*, 634−637.
(28) Kato, T.; Rosas-Sánchez, A.; Alvarado-Beltran, I.; Baceiredo, A.; Saffon-Merceron, N.; Massou, S.; Hashizume, D.; Branchadell, V. *Angew. Chem.* **2017**, DOI: 10.1002/ange.201710358.

DOI: 10.1021/jacs.7b10634
J. Am. Chem. Soc. 2017, 139, 17193−17198

6.3. Disilene-Silylene Interconversion: A Synthetically Accessible Acyclic Bis(silyl)silylene

Title: Disilene-Silylene Interconversion: A Synthetically Accessible Acyclic Bis(silyl)silylene

Status: Article, published online July 28, 2019

Journal: Journal of the American Chemical Society, 2019, 141 (34), 13536-13546.

Publisher: American Chemical Society

DOI: 10.1021/jacs.9b05318

Authors: Dominik Reiter, [†] Richard Holzner, [†] Amelie Porzelt, [†] Philipp J. Altmann, Philipp Frisch, Shigeyoshi Inoue

[†]authors contributed equally

Content: This report approaches the disilene-silylene interconversion enabled by combination of hypersilyl and supersilyl ligands attached to a low-valent silicon centre. Isolable two-coordinate, acyclic bis(silyl)silylenes have not been isolated previously, this is now possible in our case due to TMS group migration between tetrasilyl-disilene **3'** and bis(silyl)silylene **3**. Disilene **3'**, which was verified by extended DFT calculations, is stable in solution below –35 °C for more than one year but slowly and selectively forms disiletane **4** *via* C–H bond activation at one ^{t}Bu group of the supersilyl ligand in solution at rt. DFT calculations revealed a possible triplet ground state for bis(silyl)silylene **3/3''** (**3''**: the second accessible bis(silyl)silylene), which however could not be proven experimentally. Neither EPR measurements nor [2+1] or [2+2] cycloaddition reactions provided evidence for a triplet ground state of bis(silyl)silylene **3**, which is accessible from **3'**. In terms of reactivity testing, the fastest reaction of an acyclic silylene with H_2 was observed by treatment of **3'** with H_2 at –40 °C. With the singlet state of **3** bearing a high HOMO-LUMO gap of 4.18 eV, the low activation barrier for the bimolecular reaction of **3** and H_2 of 4.2 kcal/mol highly contrasts the general assumption that a low HOMO-LUMO gap is required for H_2 activation. High level calculations revealed the triplet state to be located 4.6 kcal/mol higher in energy than the singlet state, thus further supporting the assumed reactivity towards H_2, as well as the singlet bis(silyl)silylene being experimentally attainable. Furthermore, treatment of the equilibrium mixture **3/3'** at -80 ° with NH_3 yielded the hydro-amination product of disilene **3'**, which was verified by combined experimental and theoretical methods. DFT calculations verified **3'** as the kinetic product, which is in equilibrium with **3** and **3''**, and the decomposition *via* C–H activation connected with a substantial higher barrier. Further insight into the disilene-silylene interconversion was provided by isolation of *Lewis* base adducts of the two bis(silyl)silylenes **3** and **3''**, which are obtainable *via* reduction of the di(bromo)-silane in the presence of the corresponding *Lewis* base. Use of I^{i}Pr$_2$Me$_2$ yielded the adduct of **3''** (compound **13**), whereas use of DMAP results in the adduct of **3** (compound **14**). Compound **13** was converted into **15** - the I^{i}Pr$_2$Me$_2$ adduct of **3** - *via* thermal dissociation, rearrangement and re-association. Moreover, *Lewis* base exchange in the order DMAP → I^{i}Pr$_2$Me$_2$ → IMe$_4$ was accessible, in line with increasing bond dissociation energies and donor strength. Treatment of **13** with NO_2 at –80 °C yields the NHC-stabilised silanoic-ester **17**, most probably *via* initial generation of a silanone, followed by silyl migration and further oxidation. Compound **17** decomposes in solution above –30 °C, which is attributed to both Si–O bonds being highly polarized. NBO analysis revealed a zwitterionic formulation as the leading resonance structure with an enhanced Si–O interaction based on negative hyperconjugation of the oxygen lone pairs into the antibonding Si–C^{NHC} and the second Si–O bond. In summary, this report provides access to a bis(silyl)silylene **3**, which is in equilibrium with tetra(silyl)-disilene **3'** and represents the resting state at low-temperature. The equilibrium mixture can directly be used for activation of small molecules like H_2 and ammonia under very mild conditions, demonstrating their potential as transition-metal mimics. Upon warming to rt, disilene **3'**

slowly but irreversibly undergoes C-H activation, which is line with the achieved mechanistic picture. Whereas trapping reactions with DMAP give the corresponding Lewis base adduct of **3**, the use of $I^iPr_2Me_2$ yields the adduct of a second bis(silyl)silylene **3''** instead. **3''** is in equilibrium with **3**/**3',** which was verified by thermal rearrangement and *Lewis* base exchange reactions. In addition, the first NHC-stabilised silanoic-ester was obtained from the reaction of NHC adduct of **3** with N_2O and characterized thoroughly.

Contributions to the publication:

- Initial test calculations concerning disilene **3'** with complete relaxed potential energy scans of the dihedral angle of the silyl groups including the effect on the calculated ^{29}Si NMR shifts, verifying the presence of a disilene as corresponding XRD data were not obtainable for **3'**
- DFT calculations of bis(silyl)silylene **3** and **3''** in singlet and triplet state including systematic search of the conformational space using the AM1 method to obtain the global minimum followed by geometry optimisation at the DFT level of theory
- DFT calculations of the mechanism for the interconversion of the bis(silyl)silylene and disilene **3**/**3'**/**3''** including the deactivation to disiletane **4**
- DFT calculations of DMAP and NHC-stabilised silylenes **13**, **14**, **15**, **16** and their related isomers to verify experimental ^{29}Si NMR shifts and bond dissociation energies
- Bonding analysis of NHC-stabilised silanoic ester **17** including model systems deducing the effects of complete silyl-substitution onto the two different Si–O bonds
- Interpretation of the data
- Writing of the manuscript

JACS
JOURNAL OF THE AMERICAN CHEMICAL SOCIETY
Article
Cite This: J. Am. Chem. Soc. 2019, 141, 13536−13546
pubs.acs.org/JACS

Disilene−Silylene Interconversion: A Synthetically Accessible Acyclic Bis(silyl)silylene

Dominik Reiter,[†] Richard Holzner,[†] Amelie Porzelt,[†] Philipp J. Altmann, Philipp Frisch, and Shigeyoshi Inoue*

Department of Chemistry, WACKER-Institute of Silicon Chemistry and Catalysis Research Center, Technische Universität München, Lichtenbergstraße 4, 85748 Garching bei München, Germany

Supporting Information

ABSTRACT: Silylenes have recently shown fascinating reactivity patterns, which are normally observed almost exclusively for transition-metal complexes. In particular, very reactive representatives are considered to be promising candidates, which may become powerful and economical alternatives for catalytic applications in the future. Here, we present the isolation of an equilibrium mixture consisting of a tetrasilyldisilene and its isomeric bis(silyl)silylene, the first isolable silylene of this type. Preliminary investigations demonstrate the extreme inherent reactivity via facile small-molecule activation even under very mild conditions. Thus, the oxidative addition of challenging targets such as H_2 and NH_3 was achieved. In addition, by synthesizing donor-stabilized bis(silyl)silylenes we gained further insights into the disilene−silylene rearrangement by 1,2-silyl migrations. Thorough theoretical calculations support the observed experimental results.

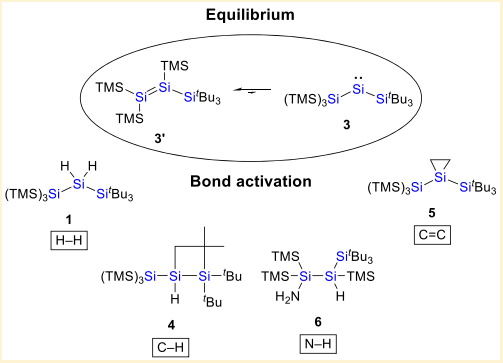

INTRODUCTION

Low-valent silicon compounds have attracted considerable attention and nowadays make an important contribution to modern main group chemistry.[1] In particular, two-coordinate silylenes (RR′Si:), the silicon analogues of carbenes (RR′C:), play an important role because of their ambiphilic nature, which is reflected in a wide variety of reactivity patterns. Silylenes have a free $3p_z$ orbital and a lone pair of electrons and, in contrast to carbenes, are almost exclusively in the singlet ground state.[2] To ensure the isolation of silylenes, sufficient kinetic and/or thermodynamic stabilization by adjacent, tailormade substituents is essential. Therefore, a vast majority of stable silylenes are embedded in cyclic frameworks, including the well-established group of *N*-heterocyclic silylenes (NHSis), the silicon version of *N*-heterocyclic carbenes (NHCs).[3]

In contrast to their diverse counterparts, there are only scarce examples of stable acyclic silylenes reported.[4] Their true potential is revealed by silylenes bearing nucleophilic boryl and/or electropositive silyl substituents, leading to wide RSiR′ angles and small HOMO−LUMO gaps. Thus, these highly reactive compounds are to a certain extent capable of mimicking transition-metal complexes in the activation of small molecules. Remarkably, acyclic silylenes can even undergo the oxidative addition of enthalpically strong molecules such as H_2.[4a,d,g] Very recently, the reductive coupling of CO by an isolable aminoborylsilylene was also reported.[5] Bis(silyl)silylenes with sterically demanding substituents are considered to be even more reactive species because of their wider RSiR′ angles, smaller HOMO−LUMO gaps, and potential triplet ground state.[2a−d,6] Lately, the intrinsic nature of triplet ground state silylenes was experimentally proven by in situ generated silylenes analyzed by low-temperature glass matrix EPR studies;[7] however, typical triplet silylene reactivity is still unexplored.[2f] Nevertheless, no isolable two-coordinate acyclic bis(silyl)silylene has been reported so far. In situ generated, extremely reactive $(R_3Si)_2Si$: species are verifiable only as stable tetravalent silicon compounds, formed as products of subsequent intra- and intermolecular reactions. The general decomposition pathways include dimerization to disilenes (heavier alkene congeners), 1,2-silyl migration, and/or intramolecular C−H/Si−Si bond activation affording disilenes or cyclic silanes (Scheme 1).

Klinkhammer, for example, observed the formation of hexakis(trimethylsilyl)cyclotrisilane **I** as the formal decomposition product of bis(hypersilyl)silylene $(((TMS)_3Si)_2Si$:) by treating $HSiCl_3$ with alkali metal hypersilanides (silyl anions).[8] The experimentally evidenced triplet ground state bis(supersilyl)silylene $(({}^tBu_3Si)_2Si$:) undergoes an intramolecular C−H activation reaction (occurring from the singlet state[2f]) even at very low temperatures, providing disiletane **II**.[7a] Sekiguchi et al. pursued the isolation of the sterically crowded bis(silyl)silylene $(({}^tBu_2MeSi)_2MeSi)_2Si$:, but irreversible formation of disilene **III** occurred via a 1,2-silyl migration.[9] To

Received: May 17, 2019
Published: July 28, 2019

DOI: 10.1021/jacs.9b05318
J. Am. Chem. Soc. 2019, 141, 13536−13546

Scheme 1. Isomerization Reactions of Transient Bis(silyl)silylenes I–III and Reported Examples of Bis(silyl)silylene NHC Adducts IV–VI

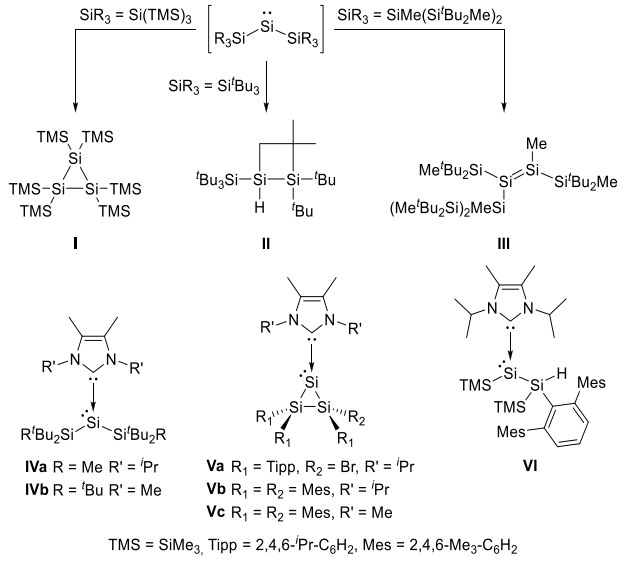

date, isolable bis(silyl)silylenes are accessible only with the aid of additional σ-donor molecules such as NHCs.[10] The first examples of acyclic bis(silyl)silylene NHC adducts **IV** were obtained by reductive debromination of the corresponding dibromosilanes with KC_8 in the presence of NHCs.[11] Scheschkewitz et al. and the Lips group reported cyclic derivatives **V** with a Si_3 scaffold via the reaction of NHC·$SiBr_4$ with a disilenyllithium reagent and the coreduction of NHC·$SiCl_4$ and Mes_2SiCl_2 (Mes = 2,4,6-Me_3-C_6H_2), respectively.[12] Very recently, Cowley and colleagues experimentally demonstrated the disilene–silylsilylene equilibrium[13] for the first time by synthesizing and isolating NHC-stabilized bis(silyl)silylene **VI** from the corresponding donor-supported disilene.[14] Thus, the quest for isolable, acyclic two-coordinate bis(silyl)silylenes is ongoing.

Sterically demanding silyl groups are ideal candidates for the stabilization of otherwise elusive species because they are strong σ-donors and provide kinetic stabilization; however, they sometimes tend to migrate.[1] On the basis of the previous results achieved with the hypersilyl- and supersilyl groups, we envisioned a combination of both substituents as a promising approach to gaining access to unprecedented low-coordinate silicon compounds through controlled 1,2-silyl shifts. Herein, we present the isolation of a novel tetrasilyldisilene displaying bis(silyl)silylene reactivity.

RESULTS AND DISCUSSION

Bis(silyl)silylene–Tetrasilyldisilene Interconversion. The entry into this chemistry provided the isolation of the silane $((TMS)_3Si)(^tBu_3Si)SiH_2$ (**1**).[15] Bromination of **1** in *n*-pentane furnished the corresponding dibromosilane **2**, which was isolated as colorless crystals in high yield and fully characterized (Scheme 2).

Subsequent reductive debromination of **2** with 2 equiv of KC_8 at low temperatures resulted in a color change from colorless to blood red with the concomitant formation of black graphite. Multinuclear and 2D NMR analyses of the isolated product suggested the formation of tetrasilyldisilene **3′**, the isomer of (hypersilyl)(supersilyl)silylene **3**. The three-coordinate silicon nuclei of **3′** resonate at δ = 161.9 ppm ($SiTMS_2$) and δ = 132.4 ppm ($Si(TMS)Si^tBu_3$) in the ^{29}Si NMR spectrum, which is in line with the signals for disilene **III** (δ = 158.9 and 103.8 ppm).[9] However, all attempts to crystallize the reaction product have been unsuccessful so far. Calculations performed at the M06-2X/6-31+g(d,p) level of density functional theory revealed a bent and twisted structure for tetrasilyldisilene **3′** (Figure 2)[16] comparable to that for disilene **III**.[9] The calculated ^{29}Si NMR resonances at δ = 162.5 and 140.5 ppm (gauge-independent atomic orbital (GIAO)/M06-L/6-311++(2d,2p); solvent model based on density (SMD): benzene)) are in good agreement with the experimental values. (For details see the Supporting Information[16]).

Variable-temperature (VT) UV–vis spectroscopy revealed only two characteristic absorption bands at λ_{max} = 352 and 469 nm. The calculated transitions, by means of time-dependent density functional theory (TD-DFT), at 335 and 467 nm are assigned to the HOMO−1 → LUMO and HOMO → LUMO transitions of disilene **3′**, respectively.

Keeping a product solution at room temperature results in a rather slow decomposition and the selective formation of disiletane **4**. Nevertheless, full conversion was not observed

Scheme 2. Synthesis and Reactivity of Bis(silyl)silylene 3 and Its More Stable Isomer Tetrasilyldisilene 3′

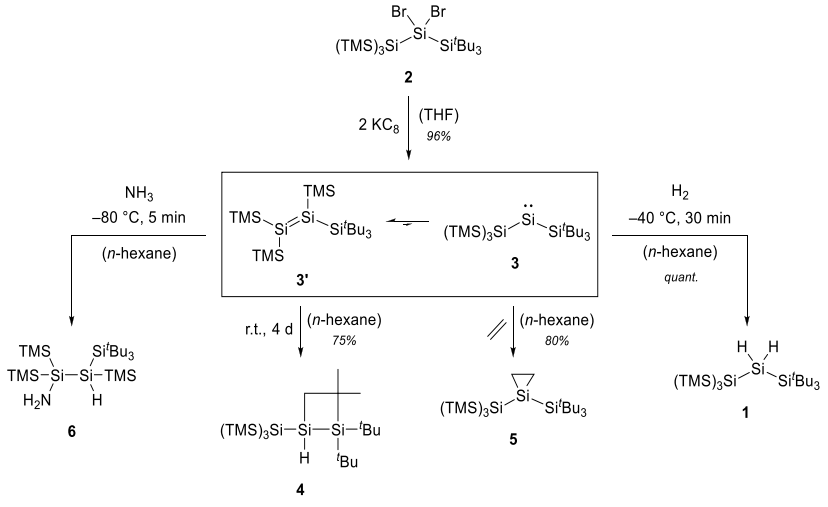

DOI: 10.1021/jacs.9b05318
J. Am. Chem. Soc. 2019, 141, 13536–13546

until after 4 days. Monitoring the decomposition reaction by NMR spectroscopy revealed no signals other than those assigned to **3′** and **4**. In addition, no signs of decomposition were observed when a product solution was stored at −35 °C in a glovebox for at least 1 year. Disiletane **4** was fully characterized, and its molecular structure was unambiguously confirmed by single-crystal X-ray diffraction (SC-XRD) (Figure 1). As already shown in the case of **II**,[7a] the formation

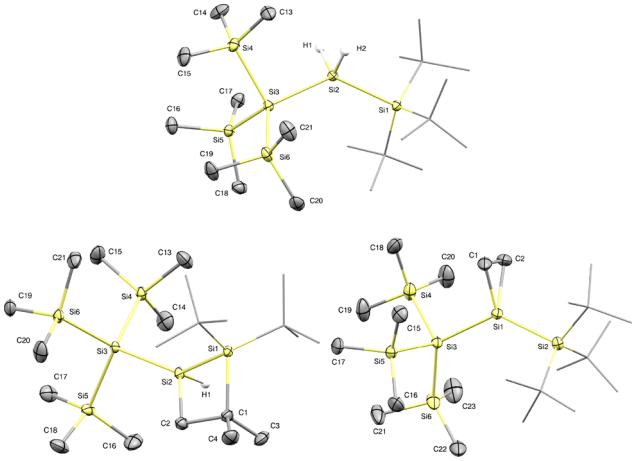

Figure 1. Molecular structures of **1** (top), **4** (bottom left), and **5** (bottom right). Ellipsoids are set at 50% probability. Hydrogen atoms are omitted for clarity, except for the respective Si−H nuclei of silane **1** and disiletane **4**. Selected bond lengths (Å) and angles (°): **1**: Si1−Si2 2.369(1), Si2−Si3 2.350(1); Si1−Si2−Si3 132.1(1). **4**: Si1−Si2 2.345(1), Si1−C1 1.957(2), C1−C2 1.572(2), Si2−C2 1.916(2), Si2−Si3 2.346(1); C1−Si1−Si2 76.3(1), Si1−Si2−C2 76.6(1), Si1−C1−C2 97.3(1), C1−C2−Si2 99.7(1). **5**: Si1−C1 1.885(2), Si1−C2 1.890(2), C1−C2 1.542(3), Si1−Si2 2.372(1), Si1−Si3 2.371(1); Si1−C1−C2 66.1(1), C1−C2−Si1 65.7(1), C2−Si1−C1 48.2(1), Si2−Si1−Si3 131.7(1).

of **4** quite likely originates from C−H bond activation of a *tert*-butyl group of bis(silyl)silylene **3**. Thus, the slow conversion of **3′** to **4** already indicates the existence of an equilibrium between bis(silyl)silylene **3** and disilene **3′** in solution. DFT calculations concerning **3** revealed the silylene located 5.7 kcal/mol in energy above its disilene isomer **3′** as well as its triplet state 2.5 kcal/mol lower in energy (Si−Si:−Si bond angles: 140.7° (triplet) and 116.2° (singlet)) (Figure 2).[16] Several theoretical studies concerning possible triplet ground state silylenes have been published in the last few decades. For different bis(silyl)silylenes, however, deviating values for the respective singlet−triplet energy gaps were found, depending on the methods and basis sets used.[2b,f,6a] Clearly, the singlet triplet gap of **3** with a value of 2.5 kcal/mol is not high enough to readily take it for granted and judge the ground state multiplicity of **3** at the moment.

Therefore, we intended to experimentally elucidate the ground state multiplicity of bis(silyl)silylene isomer **3**. Because NMR spectroscopy provided no further insights (possible resonances for the singlet silylene of **3** were not observed), we used EPR spectroscopy (X-band: 9.267 GHz), the method of choice for potential triplet ground state detection. However, all EPR spectra obtained from a solution containing the equilibrium mixture of **3**/**3′**, measured in the temperature range of 133−286 K, exhibited only a strong EPR signal at around 331 mT (g = 2.0067), corresponding to a typical silyl radical of still unknown structure. Sekiguchi et al. observed similar species (at around 340 mT, g = 2.0055) when measuring the in situ generated triplet silylenes.[7] Nonetheless, under our measurement conditions, no analogous weak, broad signal at around 800 mT, assignable to the triplet silylene of **3**, was observed. Thus, the combined results suggest the position of the equilibrium being either almost entirely shifted to disilene **3′** or the decomposition to disiletane **4** being too rapid and beyond the detection limit for both the singlet and triplet ground state bis(silyl)silylene **3**.

As further evidence for the equilibrium, we intended [2 + 1] or [2 + 2] cycloaddition reactions with unsaturated organic substrates under the formation of defined trapping products. Whereas the reaction of **3**/**3′** with phenylacetylene, diphenylacetylene, and anthracene led to complicated mixtures of products, exposure to ethylene resulted in the clean formation of silirane **5** as the sole product, clearly indicating silylene reactivity (Scheme 2). Interestingly, no [2 + 2] cycloaddition reaction of tetrasilyldisilene **3′** with ethylene was observed. Silirane **5** was fully characterized, including its solid-state structure (Figure 1). The ring silicon nucleus resonates at δ = −164.3 ppm in the ^{29}Si NMR spectrum and exhibits a large Si−Si−Si bond angle of 131.7(1)° due to the sterically congested electropositive silyl groups.

According to the ethylene addition selectivity, we pursued [2 + 1] cycloaddition reactions of (*E*)/(*Z*) alkenes with respect to the Skell rule to further investigate the ground state multiplicity of bis(silyl)silylene **3**.[17] The Skell rule originates

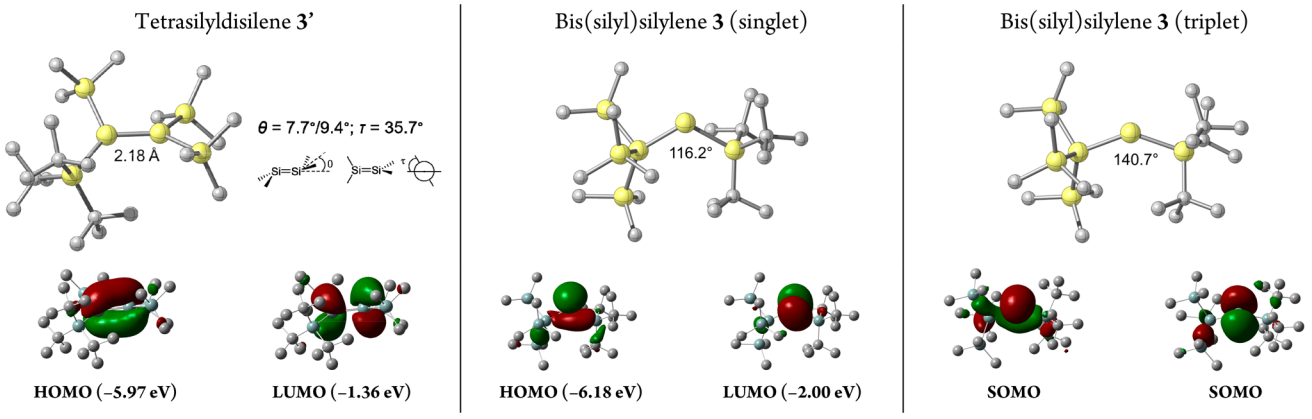

Figure 2. Calculated structures of tetrasilyldisilene **3′** and bis(silyl)silylene **3** (singlet/triplet state) with their corresponding frontier orbitals.

DOI: 10.1021/jacs.9b05318
J. Am. Chem. Soc. 2019, 141, 13536−13546

from carbene chemistry and predicts the stereospecific olefin addition of singlet carbenes. Triplet carbenes undergo a nonstereospecific cycloaddition via a diradical intermediate, allowing for facile rotation and a loss of initial stereochemistry. In the case of silylenes, however, the situation might be more complicated, and a failure of the Skell rule cannot be ruled out.[2c,f,6a] Nonetheless, investigated singlet silylenes react according to the rule, and intended cycloaddition reactions of the transient triplet silylene $(^tBu_3Si)_2Si$: did not furnish any corresponding silirane.[6a,7a,18] This prompted us to investigate the stereochemistry of olefin cycloaddition with the equilibrium mixture of **3**/**3′**. Because of the different silyl groups, not only two silirane isomers (cis and trans) but four different stereoisomers can be formed (Scheme 3). Therefore, we

Scheme 3. Plausible Silirane Stereoisomers Formed Upon [2 + 1] Cycloaddition Reaction of (Hypersilyl)(supersilyl)silylene 3 with (*E*)- and (*Z*)-Alkenes

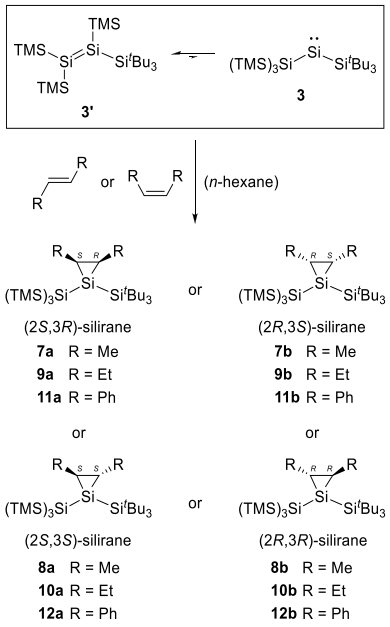

initially used the simplest isomers, (*E*)- and (*Z*)-2-butenes. The exposure of **3**/**3′** to (*Z*)-2-butene selectively afforded *cis*-silirane **7**. Compound **7** was sufficiently characterized by multinuclear and 2D NMR spectroscopy, albeit not being able to resolve its stereochemistry ((2*S*,3*R*)-silirane **7a** or (2*R*,3*S*)-silirane **7b**). The observed ^{29}Si NMR resonance at $\delta = -131.7$ ppm for the silirane silicon nucleus is shifted to slightly lower field compared to those observed for reported *cis*-bis(trialkylsilyl)siliranes ($\delta = -154.5$ to -159.1 ppm) and silirane **5**.[6a,18c] On the other hand, the reaction of **3**/**3′** with (*E*)-2-butene furnished approximately a 50:50 mixture of *cis*-silirane **7** and *trans*-silirane **8**. Again, the absolute configuration of **8** remains unclear, but the silirane silicon atom exhibits a similar downfield shift in the ^{29}Si NMR spectrum ($\delta = -123.3$ ppm) in comparison to reported bis(trialkylsilyl)siliranes ($\delta = -144.1$ to -149.6 ppm) and **5**.[6a,18c] The observed nonstereospecificity most likely originates from (*Z*)-2-butene contamination (~1.3%) because the purity of the utilized alkenes is crucial to the silirane product ratio. This was already recognized in the initially observed nonstereospecific cycloadditions of 2-butenes to dimesitylsilylene, in which gas contamination of the respective other isomer led to misinterpretations.[18b,19] Accordingly, the reaction of **3**/**3′** with an approximately 50:50 mixture of both stereogenic alkenes provided *cis*-silirane **7** as the sole product because of the higher reactivity of the (*Z*)-isomer.

To gain deeper insight, we turned to sterically more demanding alkenes with higher isomeric purity. However, the utilization of 3-hexenes and stilbenes (1,2-diphenylethylenes) led to significantly slower or even no (stilbene) cycloaddition reactions with the concomitant formation of disiletane **4**, especially with the respective (*E*)-isomer. The most satisfying result was obtained with (*Z*)-3-hexene, with ^{29}Si NMR analysis ($\delta = -133.2$ ppm) indicating the selective formation of *cis*-silirane **9**. The reaction of **3**/**3′** with (*E*)-3-hexene, on the contrary, led to the formation of a mixture of products. However, *trans*-silirane **10** was identified by ^{1}H and ^{29}Si NMR ($\delta = -127.1$ ppm; typical downfield shift compared to the cis isomer) spectroscopy. Interestingly, no resonances for *cis*-silirane **9** were observed. Therefore, we conclude that [2 + 1] cycloaddition reactions of bis(silyl)silylene **3** with stereogenic alkenes are most likely stereospecific.

Overall, the outcome of the cycloaddition reactions with stereogenic alkenes cannot yet reveal with certainty the ground state multiplicity of bis(silyl)silylene **3** because even triplet ground state silylenes could react via their singlet state.[2c,f,6a] Therefore, further examinations are essential and both a reliable method for determining the ground state multiplicity (besides EPR spectroscopy) and typical triplet silylene reactivity have yet to be found.

Surprisingly, the disilene/silylene equilibrium mixture is also capable of activating dihydrogen via oxidative addition. So far, only a few examples of low-coordinate silicon compounds are known to react similarly. This series consists of three acyclic silylenes and one disilene with small HOMO−LUMO gaps (2.0−3.0 eV), which undergo fast reactions under relatively mild conditions (from 2 h at 0 °C to up to 2 days at 50 °C).[4a,d,g,20] Recently, Iwamoto et al. reported hydrogen splitting reactions by boryldisilenes.[21] Although no observable sign of reaction was detectable at −80 °C (3 h), treating an *n*-hexane solution of **3**/**3′** at −40 °C with H_2 (1 bar) resulted in a color change from blood red to pale yellow within 30 min. The quantitative formation of silane **1** was detected by NMR spectroscopy (Scheme 2). Again, no formation of the respective disilene addition product was detected. The molecular structure of **1** revealed a large Si−Si−Si bond angle of 132.1(1)° comparable to that of silirane **5**, indicating a large Si−Si:−Si bond angle for bis(silyl)silylene **3** (Figure 1). Contrary to reported acyclic silylenes, which are able to activate H_2, singlet bis(silyl)silylene **3** exhibits a large HOMO−LUMO gap of 4.18 eV (Figure 2). Because acyclic silylenes with a comparable large HOMO−LUMO gap have shown no reaction toward H_2,[4b] the extreme reactivity of bis(silyl)silylene **3** is rather astonishing. Thus, we performed additional calculations concerning the bimolecular reaction of H_2 and singlet **3** and determined a very low effective barrier of 4.2 kcal/mol. The calculated barrier is significantly lower than that reported for Aldridge's acyclic aminoborylsilylene (23.2 kcal/mol),[4a] which therefore rationalizes the observed fast reaction of bis(silyl)silylene **3**. These results contrast with the generally assumed connectivity of a low HOMO−LUMO gap and the activation of dihydrogen for acyclic silylenes. Thus, this correlation presumably does not account for acyclic bis(silyl)silylenes. Additionally, this observation represents the first example of dihydrogen activation by a bis(silyl)silylene

DOI: 10.1021/jacs.9b05318
J. Am. Chem. Soc. 2019, 141, 13536−13546

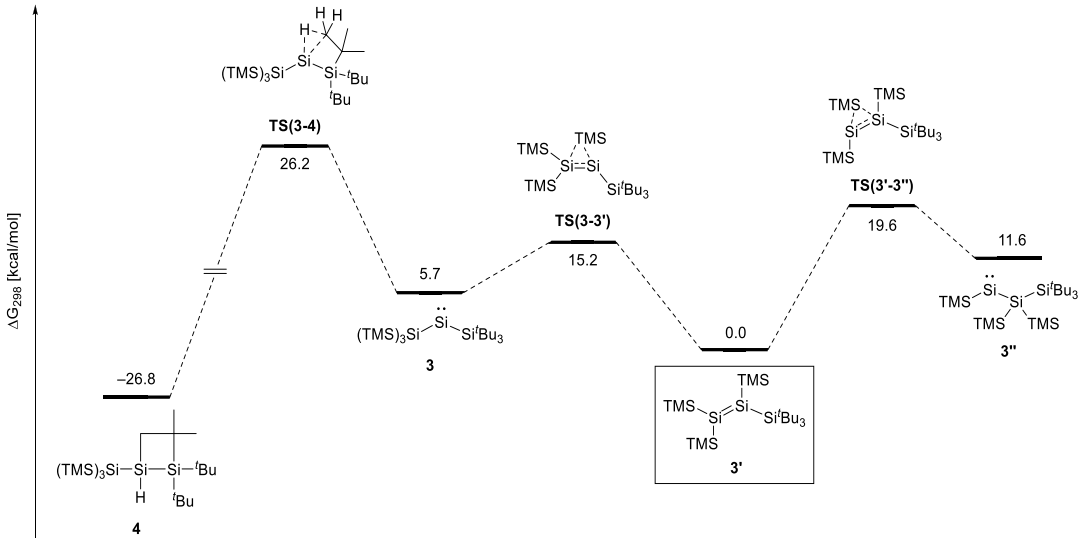

Figure 3. DFT-derived energy profile for the silylene−disilene−silylene equilibrium at the M06-2X/6-311+G(d,p)(SMD = benzene)//M06-2X/6-31+G(d,p) level of theory.

and the fastest reaction of a low-coordinate silicon compound toward H_2 to date.

DLPNO-CCSD(T)/cc-pVQZ single-point calculations based on the PBEh-3c optimized structures of **3** revealed the singlet state of **3** located 4.6 kcal/mol lower in energy than the triplet, thus supporting the assumed reactivity toward H_2.[22]

Besides dihydrogen, the activation of ammonia via oxidative addition is still a challenging target even for transition-metal complexes.[23] However, the rapid growth of main group chemistry in recent decades has revealed various reactive compounds capable of activating ammonia under mild conditions.[24] Among them are only a few silicon compounds, all of which bear low-coordinate centers, represented by their most prominent examples, silylenes[4f,25] and disilenes.[26] On the basis of the results so far, we envisaged the reaction of **3**/**3′** with ammonia as a promising target. Indeed, a facile reaction was observed even at −80 °C by treating an *n*-hexane solution of **3**/**3′** with an equimolar amount of NH_3 (0.4 M solution in 1,4-dioxane). The successful hydroamination reaction was clearly evident by the immediate color change from blood red to pale yellow. Multinuclear and 2D NMR spectroscopy identified the major product formed as aminosilane **6**, the addition product derived from tetrasilyldisilene **3′**. The reaction is completely regiospecific, with the preferred regioisomer bearing the amino group attached to the silicon nucleus with the two TMS groups, presumably for steric reasons. A similar observation was reported by Scheschkewitz and colleagues.[26b] The Si−NH_2 atom resonates at δ = −35.7 ppm in the ^{29}Si NMR spectrum, which agrees well with those observed for similar compounds (δ = −14.7 to −48.6 ppm)[26] and the theoretically calculated value (δ = −36.8 ppm). The Si−H nucleus exhibits a high-field shift in the ^{29}Si NMR spectrum at δ = −119.9 ppm compared to the reported ones (δ = −57.1 to −72.4 ppm) but is in good accordance with the calculated shift (δ = −116.6 ppm). Performing the reaction at elevated temperatures leads to less-selective product formation, presumably also affording the respective regioisomer and the adduct of bis(silyl)silylene **3**. Besides proving the existence of tetrasilyldisilene **3′**, these results further strengthen the assumption of an equilibrium between silylene **3** and disilene **3′**. Further calculations to obtain a conclusive mechanistic picture concerning ammonia activation are under current investigation.

In addition, very fast reactions of **3**/**3′** with small molecules O_2, CO_2, and P_4 were observed, but in all cases, nonselective reactions occurred, leading to product mixtures. However, these observations underline the high reactivity of the equilibrium mixture containing bis(silyl)silylene **3** and tetrasilyldisilene **3′**.

As previously investigated theoretically for $((H_3Si)H_2Si)$-(H)Si: and $(H_3Si)HSi{=}SiH_2$,[13b] further verification of the experimentally observed equilibrium was provided by DFT calculations (Figure 3). Accordingly, disilene **3′** represents the most stable isomer, with an effective barrier of 15.2 kcal/mol for the TMS group migration affording bis(silyl)silylene **3**. Interestingly, another regioisomeric bis(silyl)silylene (TMS)-$((TMS)_2(^tBu_3Si)Si)$Si: **3′′** is accessible via a second 1,2-silyl shift with its formation connected to an effective barrier of 19.6 kcal/mol. Thus, the isomerization reactions between bis(silyl)-silylenes **3**/**3′′** and disilene **3′** via TMS group migrations represent an equilibrium, with disilene **3′** as the kinetic product. The decomposition of disilene **3′**/silylene **3** proceeds via C−H activation, connected to a substantially higher barrier of 26.2 kcal/mol, affording thermodynamic product **4** in an irreversible reaction.

Lewis Base-Stabilized Bis(silyl)silylenes. To gain deeper insight into the disilene−silylene interconversion, we attempted to trap **3** and/or **3′** with additional Lewis bases such as phosphines and NHCs. However, treating the equilibrium mixture of **3**/**3′** with PMe_3 and NHCs with varying steric demand did not furnish a clean donor−acceptor product. The resulting mixtures of products contained several donor-stabilized species, presumably including both bis(silyl)silylene and disilene adducts. Instead, the reductive debromination of **2** with KC_8 in the presence of 1,3-diisopropyl-4,5-dimethyl-imidazolin-2-ylidene ($I^iPr_2Me_2$) selectively furnished NHC-stabilized bis(silyl)silylene **13** in excellent yield (Scheme 4). Interestingly, the formation of initially targeted bis(silyl)-silylene NHC adduct **15** (Scheme 5) was not observed, but two consecutive 1,2-silyl migrations from silylene **3** through disilene **3′** to silylene **3′′** occurred and finally NHC-stabilized regioisomeric silylene **13** was obtained. Presumably, **13** is

DOI: 10.1021/jacs.9b05318
J. Am. Chem. Soc. 2019, 141, 13536−13546

Scheme 4. Synthesis and Interconversion of Novel Donor-Stabilized Bis(silyl)silylenes

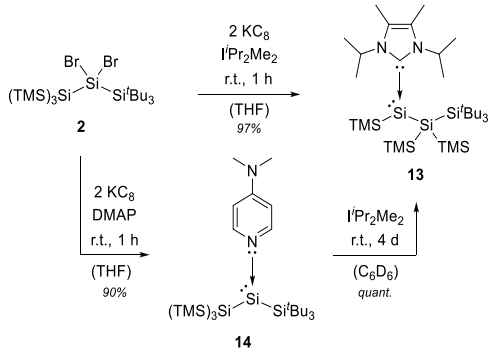

Scheme 5. Reactivity of NHC-Stabilized Bis(silyl)silylene 13

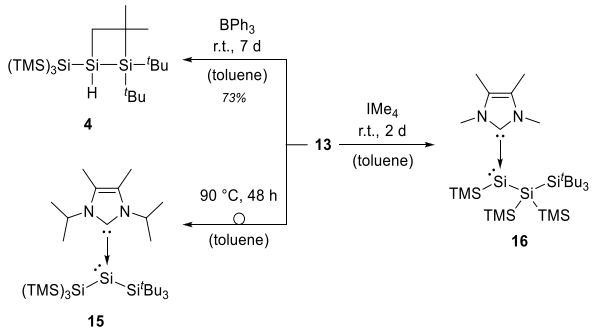

formed as the preferred product as a result of less steric congestion between $I^iPr_2Me_2$ and silylene **3′′** compared to silylene **3**. The divalent silicon nucleus of **13** exhibits a downfield-shifted resonance in the ^{29}Si NMR spectrum (δ = −104.7 ppm) relative to those observed for reported bis(silyl)silylenes **IV**–**VI** (δ = −110.5 to −136.6 ppm). The molecular structure of **13** was unambiguously confirmed by SC-XRD analysis (Figure 4). The $I^iPr_2Me_2$-stabilized divalent silicon center adopts a trigonal pyramidal geometry with the sum of bond angles amounting to 340.9° (**IVb**, 344.3°; **Va**, 302.7°, **Vb**, 293.4°, **Vc**, 255.5°; and **VI**, 317.3°). The low degree of pyramidalization indicates less-pronounced s character of the lone pair of electrons at the three-coordinate

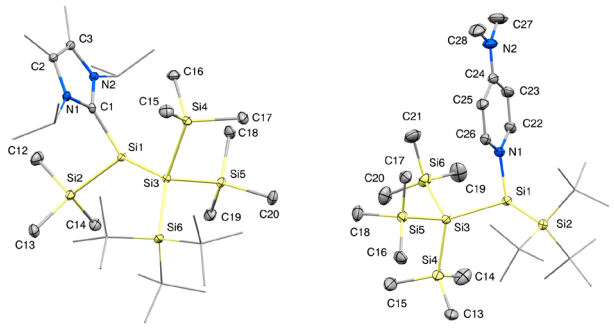

Figure 4. Molecular structures of **13** (left) and **14** (right). Ellipsoids are set at 50% probability. Hydrogen atoms and solvent molecules are omitted for clarity. Selected bond lengths (Å) and angles (°): **13**: Si1–Si2 2.360(1), Si1–Si3 2.437(1), Si1–C1 1.961(2); C1–Si1–Si2 99.3(1), C1–Si1–Si3 115.6(1), Si2–Si1–Si3 126.0(1). **14**: Si1–Si2 2.433(1), Si1–Si3 2.420(1), Si1–N1 1.942(2); N1–Si1–Si2 104.5(1), N1–Si1–Si3 98.1(1), Si2–Si1–Si3 116.1(1).

silicon atom. The C_{NHC}–Si bond length is 1.961(2) Å, which is in the typical range for C_{NHC}–Si bonds[10b] but elongated in comparison to **IV**–**VI** (1.933–1.960 Å) and thus displaying a weaker interaction between the NHC $I^iPr_2Me_2$ and the silylene moiety in complex **13**.

In contrast, the utilization of weaker Lewis base 4-*N*,*N*-dimethylaminopyridine (DMAP) afforded DMAP-coordinated silylene **14** in 90% yield. In this case, regioisomeric (hypersilyl)(supersilyl)silylene **3** was trapped as donor–acceptor complex **14**. The less-shielded three-coordinate silicon atom shows a significant downfield shift in the ^{29}Si NMR spectrum at δ = 68.8 ppm. A similar trend was observed for donor-stabilized β-diketiminato silylenes (δ = −12.0 to 37.4 ppm)[27] reported by Driess et al. However, that case is far less pronounced because the respective donor-free silylene resonates only at δ = 88.4 ppm.[28] The solid-state structure (Figure 4) revealed a higher degree of pyramidalization around the divalent silicon nucleus (sum of bond angles: 318.7°) and therefore illustrates the increased s character of base-stabilized silylene **14**. The N_{DMAP}–Si bond length of 1.942(2) Å agrees well with those observed for previously reported DMAP-stabilized low-valent silicon complexes ($d_{(N-Si)}$ = 1.85–2.01 Å).[27b,29] Surprisingly, the treatment of silylene **14** with an equimolar amount of $I^iPr_2Me_2$ does not afford corresponding NHC-stabilized silylene **15** but, selectively again, provides rearranged silylene NHC adduct **13**. This observation for the Lewis base exchange further indicates the presence of the silylene–disilene–silylene equilibrium discussed above. In addition, our results are an extension of the recent findings regarding the disilene–silylene rearrangement, reported by Cowley, Holthausen, and colleagues.[14]

To gain more profound knowledge concerning the accessibility of all isomers in equilibrium, we investigated the reactivity of silylene **13** with respect to Lewis base abstraction and exchange. The reaction of **13** with 1 equiv of Lewis acid BPh_3 provided disiletane **4** through NHC abstraction and the concomitant formation of the NHC–borane adduct $I^iPr_2Me_2$·BPh_3 (Scheme 5). Full conversion, however, was observed only after a reaction time of 1 week at ambient temperature. Monitoring the reaction with ^1H and ^{29}Si NMR spectroscopy revealed the intermediary formation of tetrasilyldisilene **3′**. Therefore, NHC abstraction initially affords respective donor-free silylene **3′′** being in equilibrium with disilene **3′** and silylene **3**. As already mentioned, the irreversible decomposition of the equilibrium mixture is kinetically limited but thermodynamically preferred, thus accounting for the long reaction times.

Silylene **13** is completely stable as a solid and in solution at room temperature. However, heating a solution of **13** to 90 °C results again in a double TMS migration and the formation of initially targeted NHC-supported silylene **15** (Scheme 5) in 58% yield (NMR). Additional DFT calculations revealed that **15** is slightly more stable than **13** with an effective activation barrier of 30.0 kcal/mol for the interconversion, thus being in line with the required elevated temperature and prolonged reaction time for the isomerization. Nevertheless, silylene **15** could not be isolated in its pure form because of incomplete conversion and concomitant decomposition via the formation of disiletane **4** and free $I^iPr_2Me_2$. Neither prolonged heating (at different temperatures) nor solvent change to benzene, *n*-hexane, or THF affected the outcome of the reaction in favor of silylene **15**, thus further confirming the existence of the equilibrium. Nonetheless, **15** was unambiguously characterized

DOI: 10.1021/jacs.9b05318
J. Am. Chem. Soc. 2019, 141, 13536–13546

by a combination of multinuclear and 2D NMR studies, supported by the results obtained from DFT calculations. The ^{29}Si resonance of the three-coordinate Si nucleus is shifted to higher field (δ = −120.6 ppm) compared to that for donor-stabilized silylenes **13** and **14** and agrees well with its GIAO-predicted chemical shift (δ = −127.2 ppm). In particular, the huge difference from that observed for analogous DMAP-stabilized silylene **14** emphasizes the stronger interaction between bis(silyl)silylene **3** and the better σ-donor molecule.

Furthermore, an even stronger donor−acceptor interaction was shown by the successful exchange of I^{i}Pr$_2$Me$_2$ with the stronger σ-donating NHC, 1,3,4,5-tetramethylimidazolin-2-ylidene (IMe$_4$). IMe$_4$-stabilized bis(silyl)silylene **16** was sufficiently characterized by multinuclear NMR spectroscopy (Scheme 5). The low-valent silicon nucleus exhibits a signal observed at δ = −117.1 ppm in the ^{29}Si NMR spectrum. The high-field-shifted resonance compared to that observed for **13** indicates a stronger interaction between NHC and bis(silyl)-silylene **3**. The theoretically determined resonance at δ = −115.2 ppm supports the formation of NHC adduct **16**. However, it was neither possible to remove free I^{i}Pr$_2$Me$_2$, nor to observe a rearrangement to the corresponding IMe$_4$-stabilized bis(silyl)silylene adduct of **3** because of an even more facile decomposition reaction.

Additional DFT calculations also reflect the trend observed for the σ-donor−silylene interactions by ^{29}Si NMR spectroscopy (details in Tables S9 and S11 in the Supporting Information), and thus the gas-phase Gibbs free bond-dissociation energy increases from 15.3 kcal/mol (**14**) to 16.3 kcal/mol (**15**) to 22.0 kcal/mol (**13**) and finally to 27.6 kcal/mol (**16**). These observations correlate well with the increasing donor strength of the Lewis base used and also confirm the inability to access ((TMS)$_3$Si)(^{t}Bu$_3$Si)Si:(IMe$_4$), the regioisomeric product of **16**. In addition to the higher gas-phase Gibbs free bond-dissociation energy, the reduced steric demand of IMe$_4$ makes **16** more susceptible for subsequent reactions. This is evidenced by the slow decomposition of 16 in solution. In the case of NHC-stabilized silylene **13**, rearrangement to **15** is still the preferred pathway, although decomposition and disiletane **4** formation occur during heating. For DMAP-stabilized silylene **14**, the isomerization equilibrium finally providing **13** appears to be the only accessible pathway subsequent to Lewis base dissociation.

NHC-Stabilized Silanoic Ester. Even though the oxygenation of **3**/**3′** led only to complicated mixtures with no isolable products, we investigated the reaction of **13** toward various oxidizing agents because the last decades have witnessed significant attention in the synthesis of heavier analogues of carbonyl compounds. However, in particular, the isolation of organosilicon compounds bearing a Si=O moiety is a rather demanding task because of their extreme reactivity. The origin of this reactivity lies in the kinetic and thermodynamic instability of the weak Si=O π-bond attributed to the unfavorable p$_\pi$-orbital overlap of silicon and oxygen.[30] In addition, the Pauling electronegativity difference between silicon and oxygen ($\Delta\chi_{(Si-O)}$ = 1.54) is much larger than that between carbon and oxygen ($\Delta\chi_{(C-O)}$ = 0.89).[31] Thus, the zwitterionic, ylide-like Si$^{\delta+}$−O$^{\delta-}$ resonance form makes a large contribution to the nature of the strongly polarized Si=O double bond.[32] As a consequence, the Si=O double bond is prone to barrierless, rapid head-to-tail oligomerization affording oligosiloxanes via Si−O σ-bond formation.[33] Despite this challenge, the Si=O moiety could be tamed[10b,34] and a series of donor-[27a,c,35] and donor−acceptor-stabilized[27b,36] heavier carbonyl compounds have been reported. Even a few examples of donor-free, three-coordinate silanones (silicon analogues of ketones) have been isolated.[4h,37] Nevertheless, silanoic esters, the heavier congeners of carboxylate esters, remain rather elusive compounds with scarcely any reported example species.[38]

Because we recently reported the isolation of a stable silyl-substituted silanone,[4h] we assumed that **13**, with two silyl groups, was a promising precursor for gaining access to silanone derivatives. However, the reaction of NHC-stabilized silylene **13** toward Me$_3$NO, CO$_2$, and O$_2$ resulted in either no reaction or the formation of a complicated mixture of products. Interestingly, the exposure of an *n*-hexane solution of **13** to N$_2$O results in a color change from purple-red to pale red with the concomitant formation of a white precipitate. After workup, unique NHC-supported silanoic ester **17** was isolated in 18% yield (Scheme 6). The exact mechanism of the

Scheme 6. Oxygenation of Silylene 13 Furnishing NHC-Stabilized Silanoic Ester 17

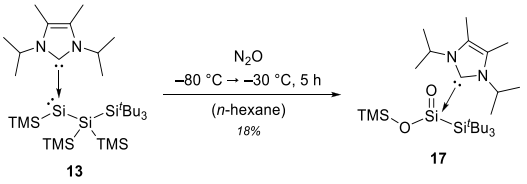

formation of **17** is unclear but presumably includes the initial generation of a silanone. Subsequent silyl migration, further oxidation, and rearrangement might eventually lead to **17**. In ^{29}Si NMR, the Si=O silicon nucleus exhibits a resonance at δ = −50.8 ppm, which exactly matches the GIAO-DFT value and agrees with those reported for related species (δ = −49.1 to −91.5 ppm).[38] The ^{1}H NMR spectrum provided the most intriguing spectroscopic feature of **17**, an unusual broad splitting of the NHC wingtip methine protons ($\Delta\delta$ = 2.68 ppm). The reason for this observation is presumably hydrogen bonding of one isopropyl C−H proton to the oxygen atom of the Si=O bond. The solid-state structure of **17** (Figure 5) revealed a close O···H distance of 2.143 Å, being much shorter than the sum of the van der Waals radii of hydrogen and oxygen (2.72 Å) and thus supporting this assumption.[39] The

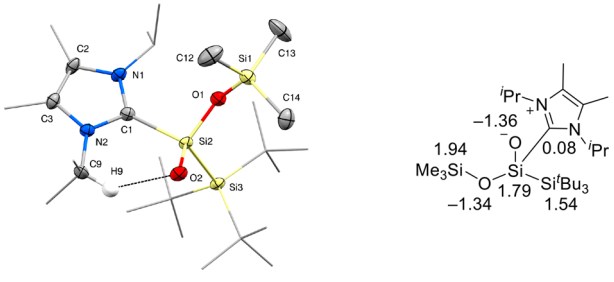

Figure 5. Molecular structure of **17** with ellipsoids set at 50% probability (left) and the results of NBO analysis of **17** (right). Hydrogen atoms, except for H9 involved in hydrogen bonding (visualized by the dashed line), are omitted for clarity. Selected bond lengths (Å) and angles (°): Si1−O1 1.641(2), Si2−O2 1.556(2), Si2−O1 1.655(3); Si2−Si3 2.415(1), Si2−C1 1.984(3); O2−Si2−O1 115.5(1), O2−Si2−C1 106.9(1), O1−Si2−C1 101.2(1), O2−Si2−Si3 111.7(1), O1−Si2−Si3 107.0(1), C1−Si2−Si3 114.3(1).

DOI: 10.1021/jacs.9b05318
J. Am. Chem. Soc. 2019, 141, 13536−13546

experimentally determined Si═O bond length of 1.556(2) Å is in the range observed for similar compounds ($d_{Si=O}$ = 1.52−1.59 Å) and much shorter than the measured Si−O single bonds (d_{Si-O} = 1.641(2) and 1.655(3) Å).[38] Interestingly, the TMS−O σ-bond is shorter than the Si2−O1 bond and the C_{NHC}−Si bond is elongated compared to that observed for the precursor, silylene NHC adduct **13** (d_{C-Si} = 1.961(2) Å).

Characteristic Si═O and Si−O−Si stretching vibrations at $\tilde{\nu}$ = 1069 and 971 cm^{-1}, respectively, were found in the IR spectrum of **17**. NHC-stabilized silanoic ester **17** is not a particularly stable compound because decomposition to an unidentified mixture of products was observed in solution at temperatures higher than −30 °C. Possible multiple bonding in four-coordinate silanoic esters and related thioesters has already been investigated in detail by Driess, Apeloig, and co-workers.[35a] Nevertheless, our entirely silyl-substituted silanoic ester is the first example of its kind. Natural bond orbital (NBO) analysis revealed strong polarization for both central silicon oxygen bonds (details in the Supporting Information). The Wiberg bond indices (WBIs) of the Si2−O1 (0.47) and Si2−O2 (0.91) bonds are relatively low, contradictory to the short Si2−O2 bond observed in the solid state. Natural resonance theory (NRT) revealed the zwitterionic formulation as the major resonance structure (Table S15). However, NBO analysis further features negative hyperconjugation of the lone pairs of O2 into the σ^* orbitals of Si2−C1 and Si2−O1, thus rationalizing the observed short Si2−O2 bond as well as the elongated O1−Si2 and Si2−C1 bonds (Figure S81). Moreover, both highly polarized Si−O bonds and the reduced C_{NHC}−Si interaction account for the limited thermal stability of **17**.

CONCLUSIONS

We used the novel dibromosilane $((TMS)_3Si)(^tBu_3Si)SiBr_2$ (**2**) to gain access to the equilibrium mixture of tetrasilyldisilene **3′** and the first example of an isolable bis(silyl)silylene **3**. The highly reactive nature of **3**/**3′** was demonstrated by the facile activation of small molecules under very mild conditions. In particular, the fastest reactions discovered for a low-valent silicon compound toward dihydrogen and ammonia via oxidative addition were observed. These results further demonstrate the potential of main group compounds as transition-metal mimics and possible catalysts for the future. In the course of our study, we further isolated unprecedented donor-stabilized bis(silyl)silylenes **13** and **14** and revealed deeper insights into the disilene−silylene rearrangement. In addition, the first acyclic NHC-stabilized silanoic ester, **17**, was isolated. Currently, the synthesis of bis(silyl)silylene transition-metal complexes to examine the inherent σ-donor strength and further studies regarding the ground state multiplicity of **3** are under active investigation in our laboratories.

ASSOCIATED CONTENT

Supporting Information

The Supporting Information is available free of charge on the ACS Publications website at DOI: 10.1021/jacs.9b05318.

Experimental details, including synthesis, spectroscopic, crystallographic, and computational data (PDF)

Crystallographic data (CCDC 1915625−1915631) (CIF)

AUTHOR INFORMATION

Corresponding Author

*s.inoue@tum.de

ORCID

Shigeyoshi Inoue: 0000-0001-6685-6352

Author Contributions

†D.R., R.H., and A.P. contributed equally to this work.

Notes

The authors declare no competing financial interest.

ACKNOWLEDGMENTS

We are exceptionally grateful to the WACKER Chemie AG and the European Research Council (SILION 637394) for continued financial support. We thank Dr. Daniel Wendel for revising the manuscript, Maria Matthews for the low-temperature NMR studies, and Dr. Oksana Storcheva for the EPR measurements. We also thank Prof. Dr. M. C. Holthausen (Goethe-Universität Frankfurt am Main) and J. I. Schweizer for fruitful discussions, computational resources, and advice. Quantum chemical calculations were performed in parts at the Leibniz Supercomputing Center of the Bavarian Academy of Science and Humanities.

REFERENCES

(1) Lee, V. Y. *Organosilicon Compounds: Theory and Experiment (Synthesis)*; Academic Press: New York, 2017.

(2) (a) Grev, R. S.; Schaefer, H. F., III; Gaspar, P. P. In search of triplet silylenes. *J. Am. Chem. Soc.* **1991**, *113*, 5638−5643. (b) Holthausen, M. C.; Koch, W.; Apeloig, Y. Theory Predicts Triplet Ground-State Organic Silylenes. *J. Am. Chem. Soc.* **1999**, *121*, 2623−2624. (c) Gaspar, P. P.; Xiao, M.; Pae, D. H.; Berger, D. J.; Haile, T.; Chen, T.; Lei, D.; Winchester, W. R.; Jiang, P. The quest for triplet ground state silylenes. *J. Organomet. Chem.* **2002**, *646*, 68−79. (d) Yoshida, M.; Tamaoki, N. DFT Study on Triplet Ground State Silylenes Revisited: The Quest for the Triplet Silylene Must Go On. *Organometallics* **2002**, *21*, 2587−2589. (e) Apeloig, Y.; Pauncz, R.; Karni, M.; West, R.; Steiner, W.; Chapman, D. Why Is Methylene a Ground State Triplet while Silylene Is a Ground State Singlet? *Organometallics* **2003**, *22*, 3250−3256. (f) Kosa, M.; Karni, M.; Apeloig, Y. Were Reactions of Triplet Silylenes Observed? *J. Am. Chem. Soc.* **2013**, *135*, 9032−9040.

(3) For recent reviews on silylenes, see (a) Haaf, M.; Schmedake, T. A.; West, R. Stable Silylenes. *Acc. Chem. Res.* **2000**, *33*, 704−714. (b) Gehrhus, B.; Lappert, M. F. Chemistry of thermally stable bis(amino)silylenes. *J. Organomet. Chem.* **2001**, *617*−*618*, 209−223. (c) Nagendran, S.; Roesky, H. W. The Chemistry of Aluminum(I), Silicon(II), and Germanium(II). *Organometallics* **2008**, *27*, 457−492. (d) Mizuhata, Y.; Sasamori, T.; Tokitoh, N. Stable Heavier Carbene Analogues. *Chem. Rev.* **2009**, *109*, 3479−3511. (e) Kira, M. An isolable dialkylsilylene and its derivatives. A step toward comprehension of heavy unsaturated bonds. *Chem. Commun.* **2010**, *46*, 2893−2903. (f) Asay, M.; Jones, C.; Driess, M. *N*-Heterocyclic Carbene Analogues with Low-Valent Group 13 and Group 14 Elements: Syntheses, Structures, and Reactivities of a New Generation of Multitalented Ligands. *Chem. Rev.* **2011**, *111*, 354−396. (g) Yao, S.; Xiong, Y.; Driess, M. Zwitterionic and Donor-Stabilized *N*-Heterocyclic Silylenes (NHSis) for Metal-Free Activation of Small Molecules. *Organometallics* **2011**, *30*, 1748−1767. (h) Sen, S. S.; Khan, S.; Samuel, P. P.; Roesky, H. W. Chemistry of functionalized silylenes. *Chem. Sci.* **2012**, *3*, 659−682. (i) Sen, S. S.; Khan, S.; Nagendran, S.; Roesky, H. W. Interconnected Bis-Silylenes: A New Dimension in Organosilicon Chemistry. *Acc. Chem. Res.* **2012**, *45*, 578−587.

(4) (a) Protchenko, A. V.; Birjkumar, K. H.; Dange, D.; Schwarz, A. D.; Vidovic, D.; Jones, C.; Kaltsoyannis, N.; Mountford, P.; Aldridge,

DOI: 10.1021/jacs.9b05318
J. Am. Chem. Soc. 2019, 141, 13536−13546

S. A Stable Two-Coordinate Acyclic Silylene. *J. Am. Chem. Soc.* **2012**, *134*, 6500−6503. (b) Rekken, B. D.; Brown, T. M.; Fettinger, J. C.; Tuononen, H. M.; Power, P. P. Isolation of a Stable, Acyclic, Two-Coordinate Silylene. *J. Am. Chem. Soc.* **2012**, *134*, 6504−6507. (c) Inoue, S.; Leszczyńska, K. An Acyclic Imino-Substituted Silylene: Synthesis, Isolation, and its Facile Conversion into a Zwitterionic Silaimine. *Angew. Chem., Int. Ed.* **2012**, *51*, 8589−8593. (d) Protchenko, A. V.; Schwarz, A. D.; Blake, M. P.; Jones, C.; Kaltsoyannis, N.; Mountford, P.; Aldridge, S. A Generic One-Pot Route to Acyclic Two-Coordinate Silylenes from Silicon(IV) Precursors: Synthesis and Structural Characterization of a Silylsilylene. *Angew. Chem., Int. Ed.* **2013**, *52*, 568−571. (e) Rekken, B. D.; Brown, T. M.; Fettinger, J. C.; Lips, F.; Tuononen, H. M.; Herber, R. H.; Power, P. P. Dispersion Forces and Counterintuitive Steric Effects in Main Group Molecules: Heavier Group 14 (Si−Pb) Dichalcogenolate Carbene Analogues with Sub-90° Interligand Bond Angles. *J. Am. Chem. Soc.* **2013**, *135*, 10134−10148. (f) Hadlington, T. J.; Abdalla, J. A. B.; Tirfoin, R.; Aldridge, S.; Jones, C. Stabilization of a two-coordinate, acyclic diaminosilylene (ADASi): completion of the series of isolable diaminotetrylenes,:$E(NR_2)_2$ (E = group 14 element). *Chem. Commun.* **2016**, *52*, 1717−1720. (g) Wendel, D.; Porzelt, A.; Herz, F. A. D.; Sarkar, D.; Jandl, C.; Inoue, S.; Rieger, B. From Si(II) to Si(IV) and Back: Reversible Intramolecular Carbon−Carbon Bond Activation by an Acyclic Iminosilylene. *J. Am. Chem. Soc.* **2017**, *139*, 8134−8137. (h) Wendel, D.; Reiter, D.; Porzelt, A.; Altmann, P. J.; Inoue, S.; Rieger, B. Silicon and Oxygen's Bond of Affection: An Acyclic Three-Coordinate Silanone and Its Transformation to an Iminosiloxysilylene. *J. Am. Chem. Soc.* **2017**, *139*, 17193−17198. (i) Loh, Y. K.; Ying, L.; Ángeles Fuentes, M.; Do, D. C. H.; Aldridge, S. An *N*-Heterocyclic Boryloxy Ligand Isoelectronic with *N*-Heterocyclic Imines: Access to an Acyclic Dioxysilylene and its Heavier Congeners. *Angew. Chem., Int. Ed.* **2019**, *58*, 4847−4851.

(5) Protchenko, A. V.; Vasko, P.; Do, D. C. H.; Hicks, J.; Ángeles Fuentes, M.; Jones, C.; Aldridge, S. Reduction of carbon oxides by an acyclic silylene: reductive coupling of CO. *Angew. Chem., Int. Ed.* **2019**, *58*, 1808−1812.

(6) (a) Gaspar, P. P.; Beatty, A. M.; Chen, T.; Haile, T.; Lei, D.; Winchester, W. R.; Braddock-Wilking, J.; Rath, N. P.; Klooster, W. T.; Koetzle, T. F.; Mason, S. A.; Albinati, A. Tris(triisopropylsilyl)silane and the Generation of Bis(triisopropylsilyl)silylene. *Organometallics* **1999**, *18*, 3921−3932. (b) Jiang, P.; Gaspar, P. P. Tri-*tert*-butylsilyl(triisopropylsilyl)silylene $(^tBu)_3Si{-}Si{-}Si(^iPr)_3$ and Chemical Evidence for Its Reactions from a Triplet Electronic State. *J. Am. Chem. Soc.* **2001**, *123*, 8622−8623.

(7) (a) Sekiguchi, A.; Tanaka, T.; Ichinohe, M.; Akiyama, K.; Tero-Kubota, S. Bis(tri-*tert*-butylsilyl)silylene: Triplet Ground State Silylene. *J. Am. Chem. Soc.* **2003**, *125*, 4962−4963. (b) Sekiguchi, A.; Tanaka, T.; Ichinohe, M.; Akiyama, K.; Gaspar, P. P. Tri-*tert*-butylsilylsilylenes with Alkali Metal Substituents $(^tBu_3Si)SiM$ (M = Li, K): Electronically and Sterically Accessible Triplet Ground States. *J. Am. Chem. Soc.* **2008**, *130*, 426−427.

(8) (a) Klinkhammer, K. W. Tris(trimethylsilyl)silanides of the Heavier Alkali Metals—A Structural Study. *Chem. - Eur. J.* **1997**, *3*, 1418−1431. (b) Klinkhammer, K. W. In *Organosilicon Chemistry III: From Molecules to Materials*; Auner, N., Weis, J., Eds.; Wiley-VCH: Weinheim, 1998.

(9) Ichinohe, M.; Kinjo, R.; Sekiguchi, A. The First Stable Methyl-Substituted Disilene: Synthesis, Crystal Structure, and Regiospecific MeLi Addition. *Organometallics* **2003**, *22*, 4621−4623.

(10) (a) Marschner, C. Silylated Group 14 Ylenes: An Emerging Class of Reactive Compounds. *Eur. J. Inorg. Chem.* **2015**, *2015*, 3805−3820. (b) Nesterov, V.; Reiter, D.; Bag, P.; Frisch, P.; Holzner, R.; Porzelt, A.; Inoue, S. NHCs in Main Group Chemistry. *Chem. Rev.* **2018**, *118*, 9678−9842.

(11) Tanaka, H.; Ichinohe, M.; Sekiguchi, A. An Isolable NHC-Stabilized Silylene Radical Cation: Synthesis and Structural Characterization. *J. Am. Chem. Soc.* **2012**, *134*, 5540−5543.

(12) (a) Jana, A.; Omlor, I.; Huch, V.; Rzepa, H. S.; Scheschkewitz, D. *N*-Heterocyclic Carbene Coordinated Neutral and Cationic Heavier Cyclopropylidenes. *Angew. Chem., Int. Ed.* **2014**, *53*, 9953−9956. (b) Guddorf, B. J.; Hepp, A.; Lips, F. Efficient Synthesis of a NHC-Coordinated Trisilacyclopropylidene and Its Coordination Behavior. *Chem. - Eur. J.* **2018**, *24*, 10334−10338.

(13) (a) Sakurai, H.; Nakadaira, Y.; Sakaba, H. Chemistry of organosilicon compounds. 181. Silylene-to-disilene and disilene-to-silylene rearrangements. *Organometallics* **1983**, *2*, 1484−1486. (b) Nagase, S.; Kudo, T. Silylene-disilene isomerizations. A theoretical study. *Organometallics* **1984**, *3*, 1320−1322.

(14) Stanford, M. W.; Schweizer, J. I.; Menche, M.; Nichol, G. S.; Holthausen, M. C.; Cowley, M. J. Intercepting the Disilene-Silylsilylene Equilibrium. *Angew. Chem., Int. Ed.* **2019**, *58*, 1329−1333.

(15) Detailed experimental and analytical data for the preparation of **1** and its precursors can be found in the Supporting Information.

(16) Geometry optimizations and harmonic frequency calculations were performed at the M06-2X/6-31+G(d,p) level of density functional theory. NMR chemical shift values were calculated using the gauge-independent atomic orbital (GIAO) method implemented in *Gaussian 09* and the M06-L functional along with the 6-311G(2,p) basis set and the SMD solvent model for the structures obtained at the M06-2X/6-31+G(d,p) level of theory. For detailed information, see the Supporting Information.

(17) Skell, P. S.; Woodworth, R. C. Structure of Carbene, CH_2. *J. Am. Chem. Soc.* **1956**, *78*, 4496−4497.

(18) (a) Pae, D. H.; Xiao, M.; Chiang, M. Y.; Gaspar, P. P. Diadamantylsilylene and its stereochemistry of addition. *J. Am. Chem. Soc.* **1991**, *113*, 1281−1288. (b) Zhang, S.; Wagenseller, P. E.; Conlin, R. T. Addition of dimesitylsilylene to olefins. A reinvestigation. *J. Am. Chem. Soc.* **1991**, *113*, 4278−4281. (c) Kira, M.; Iwamoto, T.; Maruyama, T.; Kuzuguchi, T.; Yin, D.; Kabuto, C.; Sakurai, H. Hexakis(trialkylsilyl)cyclotrisilanes and photochemical generation of bis(trialkylsilyl)silylenes. *J. Chem. Soc., Dalton Trans.* **2002**, 1539−1544.

(19) Ando, W.; Fujita, M.; Yoshida, H.; Sekiguchi, A. Stereochemistry of the addition of diarylsilylenes to *cis*- and *trans*-2-butenes. *J. Am. Chem. Soc.* **1988**, *110*, 3310−3311.

(20) Wendel, D.; Szilvási, T.; Jandl, C.; Inoue, S.; Rieger, B. Twist of a Silicon−Silicon Double Bond: Selective Anti-Addition of Hydrogen to an Iminodisilene. *J. Am. Chem. Soc.* **2017**, *139*, 9156−9159.

(21) (a) Kosai, T.; Iwamoto, T. Stable Push−Pull Disilene: Substantial Donor−Acceptor Interactions through the Si = Si Double Bond. *J. Am. Chem. Soc.* **2017**, *139*, 18146−18149. (b) Kosai, T.; Iwamoto, T. Cleavage of Two Hydrogen Molecules by Boryldisilenes. *Chem. - Eur. J.* **2018**, *24*, 7774−7780.

(22) Personal communication: Prof. M. C. Holthausen (Goethe-Universität Frankfurt am Main); References for the additional calculations: (a) Riplinger, C.; Neese, F. An efficient and near linear scaling pair natural orbital based local coupled cluster method. *J. Chem. Phys.* **2013**, *138*, 034106. (b) Riplinger, C.; Sandhoefer, B.; Hansen, A.; Neese, F. Natural triple excitations in local coupled cluster calculations with pair natural orbitals. *J. Chem. Phys.* **2013**, *139*, 134101. (c) Kendall, R. A.; Dunning, T. H., Jr. Electron affinities of the first-row atoms revisited. Systematic basis sets and wave functions. *J. Chem. Phys.* **1992**, *96*, 6796−6806. (d) Woon, D. E.; Dunning, T. H., Jr. Gaussian basis sets for use in correlated molecular calculations. III. The atoms aluminum through argon. *J. Chem. Phys.* **1993**, *98*, 1358−1371. (e) Grimme, S.; Brandenburg, J. G.; Bannwarth, C.; Hansen, A. Consistent structures and interactions by density functional theory with small atomic orbital basis sets. *J. Chem. Phys.* **2015**, *143*, 054107.

(23) Hoover, J. Ammonia activation at a metal. *Science* **2016**, *354*, 707−708.

(24) (a) Power, P. P. Interaction of Multiple Bonded and Unsaturated Heavier Main Group Compounds with Hydrogen, Ammonia, Olefins, and Related Molecules. *Acc. Chem. Res.* **2011**, *44*, 627−637. (b) Yadav, S.; Saha, S.; Sen, S. S. Compounds with Low-Valent p-Block Elements for Small Molecule Activation and Catalysis. *ChemCatChem* **2016**, *8*, 486−501.

DOI: 10.1021/jacs.9b05318
J. Am. Chem. Soc. 2019, 141, 13536−13546

(25) (a) Jana, A.; Schulzke, C.; Roesky, H. W. Oxidative Addition of Ammonia at a Silicon(II) Center and an Unprecedented Hydrogenation Reaction of Compounds with Low-Valent Group 14 Elements Using Ammonia Borane. *J. Am. Chem. Soc.* **2009**, *131*, 4600−4601. (b) Protchenko, A. V.; Bates, J. I.; Saleh, L. M. A.; Blake, M. P.; Schwarz, A. D.; Kolychev, E. L.; Thompson, A. L.; Jones, C.; Mountford, P.; Aldridge, S. Enabling and Probing Oxidative Addition and Reductive Elimination at a Group 14 Metal Center: Cleavage and Functionalization of E−H Bonds by a Bis(boryl)stannylene. *J. Am. Chem. Soc.* **2016**, *138*, 4555−4564.

(26) (a) Boomgaarden, S.; Saak, W.; Weidenbruch, M.; Marsmann, H. Ammonia and Chlorine Additions to a Tetrasilabuta-1,3-diene: Conglomerate versus Racemate Crystallization. *Z. Anorg. Allg. Chem.* **2001**, *627*, 349−352. (b) Meltzer, A.; Majumdar, M.; White, A. J. P.; Huch, V.; Scheschkewitz, D. Potential Protecting Group Strategy for Disila Analogues of Vinyllithiums: Synthesis and Reactivity of a 2,4,6-Trimethoxyphenyl-Substituted Disilene. *Organometallics* **2013**, *32*, 6844−6850. (c) Wendel, D.; Szilvási, T.; Henschel, D.; Altmann, P. J.; Jandl, C.; Inoue, S.; Rieger, B. Precise Activation of Ammonia and Carbon Dioxide by an Iminodisilene. *Angew. Chem., Int. Ed.* **2018**, *57*, 14575−14579.

(27) (a) Xiong, Y.; Yao, S.; Driess, M. An Isolable NHC-Supported Silanone. *J. Am. Chem. Soc.* **2009**, *131*, 7562−7563. (b) Xiong, Y.; Yao, S.; Müller, R.; Kaupp, M.; Driess, M. Activation of Ammonia by a Si = O Double Bond and Formation of a Unique Pair of Sila-Hemiaminal and Silanoic Amide Tautomers. *J. Am. Chem. Soc.* **2010**, *132*, 6912−6913. (c) Yao, S.; Xiong, Y.; Driess, M. *N*-Heterocyclic Carbene (NHC)-Stabilized Silanechalcogenones: NHC-Si(R_2)=E (E = O, S, Se, Te). *Chem. - Eur. J.* **2010**, *16*, 1281−1288.

(28) Driess, M.; Yao, S.; Brym, M.; Van Wüllen, C.; Lentz, D. A New Type of *N*-Heterocyclic Silylene with Ambivalent Reactivity. *J. Am. Chem. Soc.* **2006**, *128*, 9628−9629.

(29) Yeong, H.-X.; Xi, H.-W.; Li, Y.; Lim, K. H.; So, C.-W. A Silyliumylidene Cation Stabilized by an Amidinate Ligand and 4-Dimethylaminopyridine. *Chem. - Eur. J.* **2013**, *19*, 11786−11790.

(30) Avakyan, V. G.; Sidorkin, V. F.; Belogolova, E. F.; Guselnikov, S. L.; Gusel'nikov, L. E. AIM and ELF Electronic Structure/G2 and G3 π-Bond Energy Relationship for Doubly Bonded Silicon Species, H_2Si = X (X = $E^{14}H_2$, $E^{15}H$, E^{16}). *Organometallics* **2006**, *25*, 6007−6013.

(31) Allred, A. L. Electronegativity values from thermochemical data. *J. Inorg. Nucl. Chem.* **1961**, *17*, 215−221.

(32) Kapp, J.; Remko, M.; Schleyer, P. v. R. H_2XO and $(CH_3)_2XO$ Compounds (X = C, Si, Ge, Sn, Pb): Double Bonds vs Carbene-Like Structures−Can the Metal Compounds Exist at All? *J. Am. Chem. Soc.* **1996**, *118*, 5745−5751.

(33) (a) Kudo, T.; Nagase, S. Theoretical study on the dimerization of silanone and the properties of the polymeric products $(H_2SiO)_n$ (n = 2, 3, and 4). Comparison with dimers $(H_2SiS)_2$ and $(H_2CO)_2$. *J. Am. Chem. Soc.* **1985**, *107*, 2589−2595. (b) Kimura, M.; Nagase, S. The Quest of Stable Silanones: Substituent Effects. *Chem. Lett.* **2001**, *30*, 1098−1099.

(34) Xiong, Y.; Yao, S.; Driess, M. Chemical Tricks To Stabilize Silanones and Their Heavier Homologues with E = O Bonds (E = Si−Pb): From Elusive Species to Isolable Building Blocks. *Angew. Chem., Int. Ed.* **2013**, *52*, 4302−4311.

(35) (a) Epping, J. D.; Yao, S.; Karni, M.; Apeloig, Y.; Driess, M. Si = X Multiple Bonding with Four-Coordinate Silicon? Insights into the Nature of the Si = O and Si = S Double Bonds in Stable Silanoic Esters and Related Thioesters: A Combined NMR Spectroscopic and Computational Study. *J. Am. Chem. Soc.* **2010**, *132*, 5443−5455. (b) Xiong, Y.; Yao, S.; Müller, R.; Kaupp, M.; Driess, M. From silicon(II)-based dioxygen activation to adducts of elusive dioxasiliranes and sila-ureas stable at room temperature. *Nat. Chem.* **2010**, *2*, 577−580. (c) Ahmad, S. U.; Szilvási, T.; Irran, E.; Inoue, S. An NHC-Stabilized Silicon Analogue of Acylium Ion: Synthesis, Structure, Reactivity, and Theoretical Studies. *J. Am. Chem. Soc.* **2015**, *137*, 5828−5836. (d) Hansen, K.; Szilvási, T.; Blom, B.; Irran, E.; Driess, M. From an Isolable Acyclic Phosphinosilylene Adduct to Donor-Stabilized Si = E Compounds (E = O, S, Se). *Chem. - Eur. J.* **2015**, *21*, 18930−18933. (e) Troadec, T.; Lopez Reyes, M.; Rodriguez, R.; Baceiredo, A.; Saffon-Merceron, N.; Kato, T. Donor-Stabilized Silacyclobutanone: A Precursor of 1-Silaketene via Retro-[2 + 2]-Cycloaddition Reaction at Room Temperature. *J. Am. Chem. Soc.* **2016**, *138*, 2965−2968.

(36) (a) Yao, S.; Brym, M.; van Wüllen, C.; Driess, M. From a Stable Silylene to a Mixed-Valent Disiloxane and an Isolable Silaformamide−Borane Complex with Considerable Silicon−Oxygen Double-Bond Character. *Angew. Chem., Int. Ed.* **2007**, *46*, 4159−4162. (b) Xiong, Y.; Yao, S.; Driess, M. Silicon Analogues of Carboxylic Acids: Synthesis of Isolable Silanoic Acids by Donor−Acceptor Stabilization. *Angew. Chem., Int. Ed.* **2010**, *49*, 6642−6645. (c) Xiong, Y.; Yao, S.; Driess, M. Coordination of a Si = O subunit to metals: complexes of donor-stabilized silanone featuring a terminal Si = O→M coordination (M = Zn, Al). *Dalton Trans* **2010**, *39*, 9282−9287. (d) Gao, Y.; Hu, H.; Cui, C. The Reactivity of a Silacyclopentadienylidene towards Aldehydes: Silole Ring Expansion and the Formation of Base-Stabilized Silacyclohexadienones. *Chem. - Eur. J.* **2011**, *17*, 8803−8806. (e) Muraoka, T.; Abe, K.; Haga, Y.; Nakamura, T.; Ueno, K. Synthesis of a Base-Stabilized Silanone-Coordinated Complex by Oxygenation of a (Silyl)(silylene)tungsten Complex. *J. Am. Chem. Soc.* **2011**, *133*, 15365−15367. (f) Ghadwal, R. S.; Azhakar, R.; Roesky, H. W.; Pröpper, K.; Dittrich, B.; Goedecke, C.; Frenking, G. Donor−acceptor stabilized silaformyl chloride. *Chem. Commun.* **2012**, *48*, 8186−8188. (g) Muraoka, T.; Abe, K.; Kimura, H.; Haga, Y.; Ueno, K.; Sunada, Y. Synthesis, structures, and reactivity of the base-stabilized silanone molybdenum complexes. *Dalton Trans* **2014**, *43*, 16610−16613. (h) Fukuda, T.; Hashimoto, H.; Sakaki, S.; Tobita, H. Stabilization of a Silaaldehyde by its η_2 Coordination to Tungsten. *Angew. Chem., Int. Ed.* **2016**, *55*, 188−192. (i) Lopez Reyes, M.; Troadec, T.; Rodriguez, R.; Baceiredo, A.; Saffon-Merceron, N.; Branchadell, V.; Kato, T. Donor/Acceptor-Stabilized 1-Silaketene: Reversible [2 + 2] Cycloaddition with Pyridine and Evolution by an Olefin Metathesis Reaction. *Chem. - Eur. J.* **2016**, *22*, 10247−10253. (j) Muraoka, T.; Kimura, H.; Trigagema, G.; Nakagaki, M.; Sakaki, S.; Ueno, K. Reactions of Silanone(silyl)tungsten and -molybdenum Complexes with MesCNO, $(Me_2SiO)_3$, MeOH, and H_2O: Experimental and Theoretical Studies. *Organometallics* **2017**, *36*, 1009−1018.

(37) (a) Filippou, A. C.; Baars, B.; Chernov, O.; Lebedev, Y. N.; Schnakenburg, G. Silicon−Oxygen Double Bonds: A Stable Silanone with a Trigonal-Planar Coordinated Silicon Center. *Angew. Chem., Int. Ed.* **2014**, *53*, 565−570. (b) Ishida, S.; Abe, T.; Hirakawa, F.; Kosai, T.; Sato, K.; Kira, M.; Iwamoto, T. Persistent Dialkylsilanone Generated by Dehydrobromination of Dialkylbromosilanol. *Chem. - Eur. J.* **2015**, *21*, 15100−15103. (c) Alvarado-Beltran, I.; Rosas-Sánchez, A.; Baceiredo, A.; Saffon-Merceron, N.; Branchadell, V.; Kato, T. A Fairly Stable Crystalline Silanone. *Angew. Chem., Int. Ed.* **2017**, *56*, 10481−10485. (d) Rosas-Sánchez, A.; Alvarado-Beltran, I.; Baceiredo, A.; Saffon-Merceron, N.; Massou, S.; Hashizume, D.; Branchadell, V.; Kato, T. Cyclic (Amino)(Phosphonium-Bora-Ylide)-Silanone: A Remarkably Room Temperature Persistent Silanone. *Angew. Chem., Int. Ed.* **2017**, *56*, 15916−15920.

(38) (a) Yao, S.; Xiong, Y.; Brym, M.; Driess, M. An Isolable Silanoic Ester by Oxygenation of a Stable Silylene. *J. Am. Chem. Soc.* **2007**, *129*, 7268−7269. (b) Ghadwal, R. S.; Azhakar, R.; Roesky, H. W.; Pröpper, K.; Dittrich, B.; Klein, S.; Frenking, G. Donor—Acceptor-Stabilized Silicon Analogue of an Acid Anhydride. *J. Am. Chem. Soc.* **2011**, *133*, 17552−17555. (c) Rodriguez, R.; Gau, D.; Troadec, T.; Saffon-Merceron, N.; Branchadell, V.; Baceiredo, A.; Kato, T. A Base-Stabilized Sila-β-Lactone and a Donor/Acceptor-Stabilized Silanoic Acid. *Angew. Chem., Int. Ed.* **2013**, *52*, 8980−8983. (d) Rodriguez, R.; Troadec, T.; Gau, D.; Saffon-Merceron, N.; Hashizume, D.; Miqueu, K.; Sotiropoulos, J.-M.; Baceiredo, A.; Kato, T. Synthesis of a Donor-Stabilized Silacyclopropan-1-one. *Angew. Chem., Int. Ed.* **2013**, *52*, 4426−4430. (e) Wang, Y.; Chen, M.; Xie, Y.; Wei, P.; Schaefer, H. F., III; Robinson, G. H. Stabilization of Silicon−Carbon Mixed Oxides. *J. Am. Chem. Soc.* **2015**, *137*, 8396−8399. (f) Wang, Y.; Chen, M.; Xie,

DOI: 10.1021/jacs.9b05318
J. Am. Chem. Soc. 2019, 141, 13536−13546

Y.; Wei, P.; Schaefer, H. F., III; Schleyer, P. v. R.; Robinson, G. H. Stabilization of elusive silicon oxides. *Nat. Chem.* **2015**, *7*, 509−513. (g) Rodriguez, R.; Gau, D.; Saouli, J.; Baceiredo, A.; Saffon-Merceron, N.; Branchadell, V.; Kato, T. A Stable Monomeric SiO_2 Complex with Donor−Acceptor Ligands. *Angew. Chem., Int. Ed.* **2017**, *56*, 3935−3939. (h) Do, D. C. H.; Protchenko, A. V.; Ángeles Fuentes, M.; Hicks, J.; Kolychev, E. L.; Vasko, P.; Aldridge, S. A β-diketiminate stabilized sila-acyl chloride: systematic access to base-stabilised silicon analogues of classical carbonyl compounds. *Angew. Chem., Int. Ed.* **2018**, *57*, 13907−13911. (i) Rodriguez, R.; Alvarado-Beltran, I.; Saouli, J.; Saffon-Merceron, N.; Baceiredo, A.; Branchadell, V.; Kato, T. Reversible CO_2 Addition to a Si = O Bond and Synthesis of a Persistent SiO_2−CO_2 Cycloadduct Stabilized by a Lewis Donor−Acceptor Ligand. *Angew. Chem., Int. Ed.* **2018**, *57*, 2635−2638.
(39) Bondi, A. van der Waals Volumes and Radii. *J. Phys. Chem.* **1964**, *68*, 441−451.

DOI: 10.1021/jacs.9b05318
J. Am. Chem. Soc. 2019, 141, 13536−13546

6.4. Silylated silicon-carbonyl complexes as mimics of ubiquitous transition-metal carbonyls

Title:	Silylated silicon-carbonyl complexes as mimics of ubiquitous transition-metal carbonyls
Status:	Article, published online October 19, 2020
Journal:	Nature Chemistry, 2020, 12, 1131-1135.
Publisher:	Springer Nature
DOI:	10.1038/s41557-020-00555-4
Authors:	Dominik Reiter, Richard Holzner, Amelie Porzelt, Philipp Frisch, Shigeyoshi Inoue

Content: This publication is an extension of the bis(silyl)silylene project (see chapter 6.3). Until recently, the chemistry of silicon carbonyl complexes was limited to matrix isolation studies with their instability precluding isolation and thus remained rather unexplored. In this paper, we report the synthesis of a silicon carbonyl complex **3** obtainable *via* treatment of the equilibrium mixture of **1'**/**1** or DMAP-stabilised bis(silyl)silylene **2** with CO. The strongly bent structural motif of **3** obtained from SC-XRD data revealed a short S–C bond length and an elongated C–O bond which is accompanied by the remarkable stability of this compound in solution. DFT calculations including NBO and QTAIM analysis were performed to provide insight into the nature of the Si–C bond. It can be described as a Si–C double-bonded species with CO→Si σ-donation and Si→CO π-back-donation although substantial electron donation from the oxygen lone pair into the π*(Si–C_{CO}) orbital is present. Further studies incorporated the effects of different substituents on the silicon carbonyl complexes, where silyl-substituted model systems were found to highly differ from all others in terms of charge distribution, bonding energies and increased double bonding character. This was also tested experimentally, with the bis(supersilyl)-substituted silicon carbonyl complex **8** being accessible. Ligand exchange reactions with an isocyanide yielded a rare example of an isocyanide silicon complex, possessing structural features and bonding analysis comparable to **3**. As a last step functionalisation of the carbonyl moiety was addressed, however compound **3** showed only limited further reactivity attributed to its high stability. However, successful conversion of **3** with TMS-azide gave the silyl-cyanide complex **7**, which was verified by combined experimental and theoretical methods. This reaction pathway is quite different to transition-metal analogues, which is attributed to the high oxophilicity of silicon. In summary, this study succeeded in the synthesis of the isolable silicon carbonyl complex **3**, which bears a structure and reactivity reminiscent of transition-metal carbonyls. Its bonding motif was shown to be highly dependent on the two silyl groups attached to the central silicon centre. Moreover, the CO moiety at the silicon centre was successfully converted into a CN group with silicon carbonyl granting access to novel reactivity profiles.

Contributions to the publication:

- Bonding analysis of **3** and **5** by NBO and QTAIM analysis
- Calculation of numerous small model systems to deduce the effect of the two silyl ligands onto the bonding situation in **3**
- Calculations concerning the product of the reaction of **3** and TMS-N_3, including calculated $^{13}C/^{29}Si$ NMR shifts for multiple possible products and **7**, as corresponding XRD data were not obtainable for **7**
- Writing of the manuscript

nature chemistry

ARTICLES

https://doi.org/10.1038/s41557-020-00555-4

Silylated silicon–carbonyl complexes as mimics of ubiquitous transition-metal carbonyls

Dominik Reiter, Richard Holzner, Amelie Porzelt, Philipp Frisch and Shigeyoshi Inoue ✉

Transition-metal–carbonyl complexes are common organometallic reagents that feature metal–CO bonds. These complexes have proven to be powerful catalysts for various applications. By contrast, silicon–carbonyl complexes, organosilicon reagents poised to be eco-friendly alternatives for transition-metal carbonyls, have remained largely elusive. They have mostly been explored theoretically and/or through low-temperature matrix isolation studies, but their instability had typically precluded isolation under ambient conditions. Here we present the synthesis, isolation and full characterization of stable silyl-substituted silicon–carbonyl complexes, along with bonding analysis. Initial reactivity investigations showed examples of CO liberation, which could be induced either thermally or photochemically, as well as substitution and functionalization of the CO moiety. Importantly, the complexes exhibit strong Si–CO bonding, with CO→Si σ-donation and Si→CO π-backbonding, which is reminiscent of transition-metal carbonyls. This similarity between the abundant semi-metal silicon and rare transition metals may provide new opportunities for the development of silicon-based catalysis.

Since the discovery of $PtCl_2(CO)_2$ by Schützenberger in 1868, transition-metal–carbonyl complexes have gained huge attention both in academia and industry[1–3]. In the following years, Hieber, in particular, played a pivotal role in the extensive development of transition-metal carbonyls[4]. Today, these organometallic compounds are key reagents in numerous applications, including the Cativa process, hydroformylation and the Pauson–Khand reaction[5]. Although these versatile processes are highly efficient, they still have considerable disadvantages. They often require expensive and rare transition metals, which raises questions of sustainability and frequently use rather toxic metals that have a negative impact on the environment. There has been a concerted effort in current chemical research to develop environmentally benign and sustainable processes that replace transition metals with ecologically and economically more advantageous main group elements[6–8]. However, despite intensive investigations, carbonyl complexes with elements other than transition metals remain rare.

Aside from several remarkable boron–mono-carbonyl complexes[9], Braunschweig et al. have isolated borylene–dicarbonyl complex **A**, a unique example of a multicarbonyl main group element adduct (Fig. 1)[10]. Apart from boron, phosphorus–carbonyl compounds (including phosphaketene **B**)[11,12] have been obtained and recently alkaline earth metal carbonyls[13] were observed in low-temperature matrix isolation studies. In addition, reports on carbonyl complexes with group 14 elements (carbon group) are also very rare. Thus, carbonylation of specific carbenes (R_2C:) led to the formation of ketenes ($R_2C{=}C{=}O$) instead of Lewis adducts ($R_2C{\leftarrow}CO$)[14,15].

Silicon, the heavier homologue of carbon and the second most abundant element in the Earth's crust, has been demonstrated to participate in bonding situations, structures and reactivity patterns at the interface of transition metals and main group elements. Thus, not only the isolation of carbon analogous compounds, but also transition-metal-like reactivity, such as the activation of small molecules, has already been demonstrated[16]. Together with its high availability and low toxicity, silicon therefore represents a very promising element for metal-free catalysis. Nevertheless, reports on silicon–carbonyl complexes have so far been limited mainly to computational and matrix isolation studies[17–23]. It was found that linear silaketenes ($R_2Si{=}C{=}O$) are not even a minimum on the potential energy surface, but are merely the transition state for inversion of the Lewis adducts ($R_2Si{\leftarrow}CO$). Recently, the reactivity of isolable silylenes (heavier carbenes; R_2Si:) towards CO has been investigated, but no silicon–carbonyl complexes were obtained[24–26]. Thus, the structural motif of these elusive compounds and their chemical behaviour remained unclear. Ganesamoorthy et al. have recently reported the first ambient temperature stable silicon–carbonyl complex **C**, bearing a gallium-based ligand framework, when this manuscript was under review.[27]

Herein, we present the synthesis, isolation and initial reactivity investigations of structurally characterized metal-free silicon–carbonyl complexes, which resemble classical transition-metal carbonyls.

Results and discussion

Synthesis, characterization and reactivity. Exposure of an *n*-hexane solution of the recently reported equilibrium mixture containing bis(silyl)silylene **1** and its tetrasilyldisilene isomer **1′** (ref. [28]) to CO (1 bar) at −30 °C resulted in a colour change from blood-red to purple. Silicon–carbonyl complex **3** was isolated as purple crystals in 90% yield after work-up and crystallization from *n*-hexane (Fig. 2). Alternatively, **3** can also be obtained by the reaction of 4-*N*,*N*-dimethylaminopyridine (DMAP)-stabilized bis(silyl)silylene **2** (ref. [28]) with CO (1 bar) in quantitative yield. Bis(silyl)silylene–carbonyl complex **3** exhibits a downfield-shifted signal in the ^{13}C NMR spectrum at $\delta = 226.1$ ppm compared to the resonance observed for 'free' carbon monoxide ($\delta = 184.5$ ppm) and compound **C** ($\delta = 206.5$ ppm)[27]. The silicon nucleus of the SiCO moiety resonates at $\delta = -228.5$ ppm in the ^{29}Si NMR spectrum, the typical region for silyl anions[16], but at lower field than that of complex **C** ($\delta = -256.5$ ppm). In addition, the observed signal is strongly upfield-shifted compared to Lewis adduct **2** ($\delta = 68.8$ ppm) and thus indicates a significantly stronger donor–acceptor interaction. Infrared spectroscopy

Department of Chemistry, WACKER-Institute of Silicon Chemistry and Catalysis Research Center, Technische Universität München, Garching bei München, Germany. ✉e-mail: s.inoue@tum.de

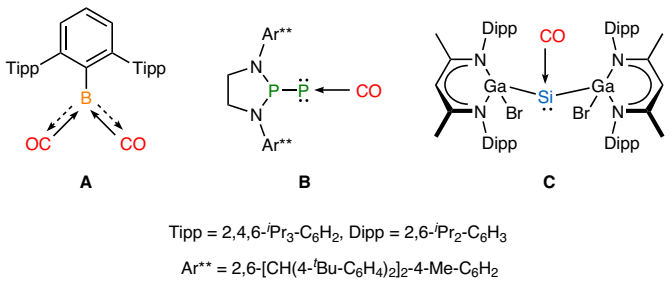

Fig. 1 | Selected examples of isolable main group carbonyl complexes. Borylene–dicarbonyl complex **A** is the only representative of a main group element multicarbonyl complex stable at ambient temperature. Phosphaketene **B** and silicon–carbonyl complex **C** were obtained via direct carbonylation of the respective phosphinidene and silylene species.

showed a substantial bathochromic shift (red shift) for the CO stretching mode at $\tilde{\nu}$ = 1,908 cm^{-1} with respect to that of free CO ($\tilde{\nu}$ = 2,143 cm^{-1})[29]. The absorption band is observed at even lower wavenumbers than those of the transient silicon–carbonyl complexes studied by argon matrix isolation methods, the borylene–dicarbonyl complex **A** and isolable silicon–carbonyl complex **C** ($\tilde{\nu}$ = 2,065–1,942 cm^{-1})[10,18,20,21,23,27]. This remarkable red shift for the CO band is closely related to classical transition-metal–carbonyl complexes bearing π-backbonding from the metal to the carbonyl moiety (terminal M–CO: $\tilde{\nu}$ = 2,120–1,850 cm^{-1})[3].

The molecular structure of **3** was unambiguously confirmed by single-crystal X-ray diffraction (SC-XRD) analysis (Fig. 3), which showed a strongly bent (trigonal pyramidal) structure with an angle between the Si2–Si1–Si3 plane and the Si1–C1 bond vector of θ = 103.7(1)° and an almost linear Si1–C1–O1 moiety (bond angle of 171.3(1)°). Furthermore, the C1–O1 distance (1.153(2) Å) is considerably elongated compared to those of gaseous CO (1.128 Å)[3] and complex **C** (1.136(7) Å)[27] and is essentially the same as that observed for typical transition-metal carbonyls[3]. The short Si1–C1 bond length (1.794(2) Å) is significantly shorter than that of silicon–carbonyl complex **C** (1.865(6) Å) and lies between the commonly observed Si=C double (1.70–1.76 Å) and Si–C single (1.87–1.93 Å) bonds[30].

Compound **3** is indefinitely stable at ambient temperature in the solid state and in solution under an argon atmosphere. Silicon–carbonyl complex **3** shows a higher thermal stability than DMAP-stabilized bis(silyl)silylene **2** and only decomposes completely after 2 hours at 130 °C to disiletane **4** under liberation of CO. The formation of **4** originates from C–H bond activation of a *tert*-butyl group of bis(silyl)silylene **1** as reported previously[28].

Analogous to transition-metal–carbonyl complexes, photolysis of **3** (λ_{max} = 340 nm) resulted in the immediate liberation of CO with simultaneous colour change from purple to blood-red and formation of **1**/**1′**. The photodissociation is partially reversible until disiletane **4** is irreversibly formed after 4 days of continuous irradiation. Since these results indicate a preserved silylene reactivity of **3**, we investigated the activation of the small molecules dihydrogen and ethylene. Although no reaction was observed at ambient temperature, silane [(TMS)$_3$Si](^{t}Bu$_3$Si)SiH$_2$ and silirane (silacyclopropane) [(TMS)$_3$Si](^{t}Bu$_3$Si)Si(CH$_2$CH$_2$) are formed selectively and rapidly upon irradiation[28]. These oxidative addition products can also be obtained via the thermally induced dissociation of **3**, but only with prolonged reaction times.

The combined analytical data suggest a bent donor–acceptor bonding motif [(TMS)$_3$Si](^{t}Bu$_3$Si)Si⇆CO, where the double arrows represent a CO→Si σ-donation with π-backdonation from the silylene moiety to the carbonyl group (strong Si1–C1 and weakened C1–O1 bond) for silicon–carbonyl complex **3**.

Theoretical calculations. To provide insight into the electronic structure of **3**, we performed calculations at the M06-2X/6-311+G(d,p)//M06-2X/6-31+G(d,p) level of density functional theory (DFT) including a variety of simplified model compounds (for details, see Supplementary Information). This analysis showed the bis(silyl)-substituted derivatives **3** and (TMS)$_2$SiCO (**I**) exhibiting the highest Si–C$_{CO}$ bond dissociation energies, as the energetically most preferred complexes with respect to complex formation (from the free silylenes), which is also reflected in the structural data of the complexes. Natural population analysis (NPA) charges of the complexes clearly depict the silyl effect. The electropositive silyl groups with their strong σ-donating nature increase the electron density at the central Si atom and thus change the polarization of the SiCO moiety (Fig. 4a) (compare with NPA charges of the central Si nuclei in (R)(R′)SiCO: **3**: −0.07; **I**: −0.02; **II** (R=CH$_3$ / R′=Ph):

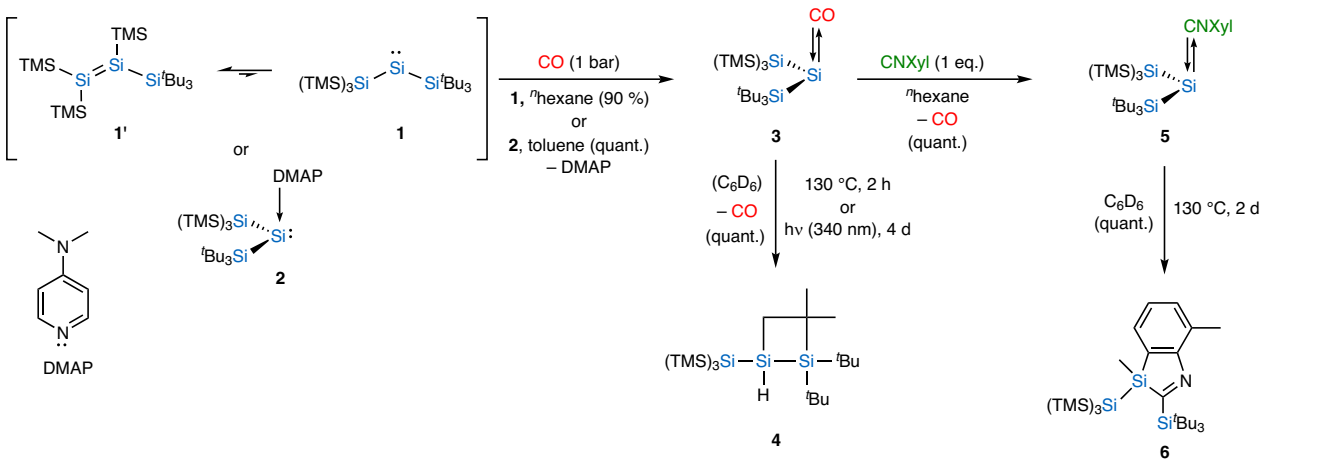

Fig. 2 | Synthesis and transition-metal mimic chemistry of silicon–carbonyl complex [(TMS)$_3$Si](^{t}Bu$_3$Si)Si⇆CO (3) (TMS = trimethylsilyl). Carbonylation of donor-free bis(silyl)silylene **1** and DMAP-stabilized bis(silyl)silylene **2** provided silicon–carbonyl complex [(TMS)$_3$Si](^{t}Bu$_3$Si)Si⇆CO (**3**). A thermally or photochemically induced liberation of CO led to formation of disiletane **4** via intramolecular C–H bond activation of silylene **1**. Substitution of CO with 2,6-dimethylphenyl isocyanide afforded silicon isocyanide complex [(TMS)$_3$Si](^{t}Bu$_3$Si)Si⇆CNXyl (**5**). By contrast to compound **3**, heating of **5** did not lead to formation of **4**, but resulted in an intramolecular isomerization reaction and formation of 1,3-azasilole **6**. DMAP, 4-*N*, *N*-dimethylaminopyridine; CNXyl, 2,6-dimethylphenyl isocyanide). The double arrows represent CO→Si σ-donation and Si→CO π-backbonding.

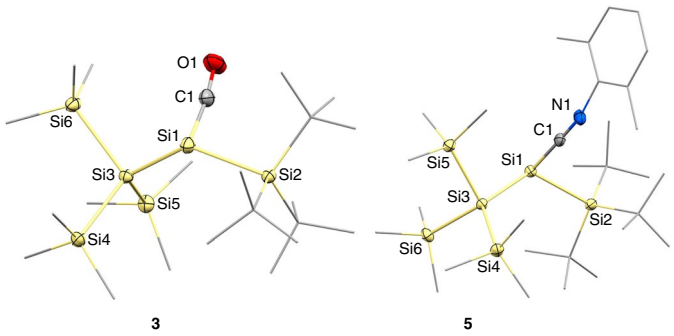

Fig. 3 | Molecular structures of compounds 3 and 5 with thermal ellipsoids set at 50% probability as derived from SC-XRD analysis. Hydrogen atoms are omitted for clarity. Compound **3** adopts a trigonal pyramidal structure; complex **5** is a silylene isocyanide.

0.78; **III** (R=R′=H): 0.23). In sharp contrast to **II** and **III**, both the central silicon atoms and the CO units in **I** and **3** have negative NPA charges, further highlighting π-backdonation from the silylene centres to the carbonyl ligands being present. The calculated Wiberg bond indices (WBIs), which give an indication of the bond orders, decrease going from **3** (1.31) to **I** (1.23), as an effect of the reduced steric demand of the silyl groups and further upon exchange of the silyl groups in **II** (1.00) and **III** (0.97). Natural bond orbital (NBO) analysis of **3** showed two bonds between the silylene and the CO moiety, bearing different polarization for the σ bond (27% Si1 $sp^{5.23}$/73% C1 $sp^{0.54}$) and the π bond (68% Si1 $sp^{7.02}$/32% C1 $sp^{17.11}$). Natural resonance theory (NRT) analysis unveiled a preference for the doubly bonded Si–C_{CO} moiety even though second-order perturbation theory showed substantial electron donation from the oxygen lone pair into the π^*(Si–C_{CO}) orbital. This is apparent in the natural localized molecular orbitals (NLMOs, Fig. 4b) with the oxygen lone pair bearing a contribution of the CO carbon atom (14%). By contrast, NBO and NRT analyses of the simplified model compound $(TMS)_2SiCO$ (**I**) showed only a singly bonded Si–C_{CO} unit in line with the reduced WBI. While in the case of **II** electron donation from the silylene moiety to the CO solely occurs from the silylene lone pair, model compound **I** bears additional electron donation from the Si–Si bonds into the π^*(CO) orbitals justifying the increased interaction.

Additional insights into the bonding situation of **3** were obtained using Bader's quantum theory of atoms in molecules[31]. Accordingly, a strongly polar covalent interaction was found for the Si–C_{CO} bond of **3** (ref. [32,33]) (Supplementary Fig. 33 and Supplementary Table 12) with the delocalization indices δ_{AB} (number of electron pairs shared between two atoms A and B) reflecting the elongated C–O bond and strong Si–C_{CO} interaction with a decreased δ_{CO} (1.56; compare with free CO: δ_{CO}=1.78) and a high δ_{SiC} (1.03), respectively. The 1D Laplacian profile along the Si–C_{CO} bond path is rather indicative of a dative bonding situation[32,34,35]. The inherent π-backbonding is consistent with a significant Si···O_{CO} interaction present in **3** ($\delta_{Si\cdots O(CO)}$=0.17; model compounds **I**: $\delta_{Si\cdots O(CO)}$=0.17; **II**: $\delta_{Si\cdots O(CO)}$=0.13; **III**: $\delta_{Si\cdots O(CO)}$=0.12), reminiscent of the bonding situation in transition-metal–carbonyl complexes[32,36].

To further investigate the decisive silyl effect experimentally, we exposed the recently reported acyclic iminosilyl- and iminosiloxy-silylenes[37,38] to CO and observed no reaction. However, reductive debromination of $(^tBu_3Si)_2SiBr_2$ with potassium graphite (KC_8) in the presence of CO successfully provided the corresponding silicon–carbonyl complex $(^tBu_3Si)_2Si{\leftrightarrows}CO$ (**8**) (Supplementary Figs. 25–28).

CO substitution and functionalization reactions. To study the relationship of **3** to transition-metal carbonyls in more detail, we turned to ligand exchange reactions. Upon treatment of **3** with 2,6-dimethylphenyl isocyanide (CNXyl) in *n*-hexane, an immediate colour change from purple to dark blue was observable. Complex **5**, a rare example of silylene isocyanide, was obtained in quantitative yield after solvent removal (Figs. 2 and 3). The exchange reaction of these valence isoelectronic ligands is prototypical for transition-metal–carbonyl complexes and therefore another feature of silicon–carbonyl complex **3** as a transition-metal mimic[3,39]. The driving force of the reaction is the stronger σ-donating nature of the isocyanide ligand compared to CO. ^{29}Si NMR spectroscopy showed a downfield-shifted resonance for the SiCNXyl moiety at δ=–177.0 ppm compared to **3**, but a strong highfield shift with respect to other reported silicon isocyanide complexes (δ=26 to –55.0 ppm)[40,41]. Infrared spectroscopy unveiled a substantial red shift for the CN stretching mode at $\tilde{\nu}$=1,966 cm^{-1} compared to that observed for free CNXyl ($\tilde{\nu}$=2,119 cm^{-1}). SC-XRD analysis exposed a strongly bent molecular structure (θ=107.3(1)°) with an almost linear Si1–C1–N1 bond angle (174.0(1)°) and a short Si1–C1 bond (1.819(2) Å).

Complex **5** is thermally more stable than compound **3** and isomerizes selectively and quantitatively to 1,3-azasilole **6** only after

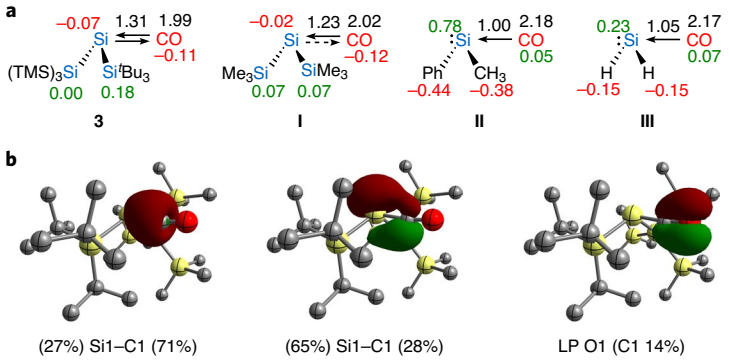

Fig. 4 | Bonding analysis of $[(TMS)_3Si](^tBu_3Si)SiCO$ (3). a, Results from NBO analysis of **3** and the related simplified model compounds **I**, **II** and **III**. NPA charges are shown in green and red, respectively and WBIs for the Si⇆C and C=O bonds are shown in black. The π-backdonation from the silylene moiety to the CO ligand in silicon-carbonyl complex **3** is reflected in the higher Si-C and the lower C-O WBIs (1.31 and 1.99) compared to the model compounds. Additionally, the higher electron density at the central Si nucleus (NPA: -0.07) highlights the importance of the sterically demanding silyl groups for the stabilization and isolation of silicon-carbonyl complex **3**. **b**, NLMOs representing the Si1-C1 bonds and the electron pair at O1 in complex **3**.

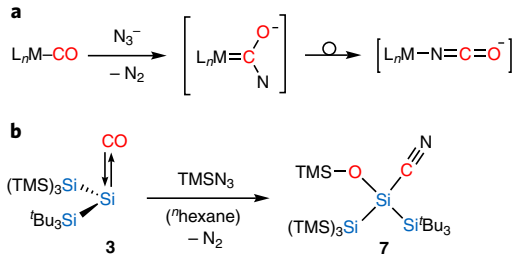

Fig. 5 | Reactivity of carbonyl complexes with azides. a, Transition-metal carbonyls typically react with azides under liberation of gaseous nitrogen and formation of isocyanato complexes via isomerization of transient carbene species. **b**, Conversion of **3** with $TMSN_3$ led to the formation of silyl cyanide **7** instead of a related silyl isocyanide. A possible explanation for the deviating reactivity is the high oxophilicity of silicon, thus different reaction pathways are conceivable.

2 days at 130 °C, analogous to an observation by Takeda et al. with a related complex[40]. Interestingly, intramolecular C–C bond activation and subsequent 1,2-silyl migration occurred, instead of Si–C_{CNXyl} bond cleavage and formation of **4**, which is consistent with an increased bond dissociation energy of 40.8 kcal mol^{-1} for compound **5** compared to 29.8 kcal mol^{-1} for complex **3**. The combined experimental and theoretical data for complex **5** showed a structural motif analogous to [(TMS)$_3$Si](^{t}Bu$_3$Si)Si⇆CO (**3**) (Supplementary Figs. 37–39 and Supplementary Tables 22–25). Thus, **5** should be considered as a silicon–isocyanide complex with π-backbonding {[(TMS)$_3$Si](^{t}Bu$_3$Si)Si⇆CNXyl}, reflecting the results of a recent theoretical study on metallylene–isocyanide complexes[42].

Finally, we were interested in functionalizing the carbon monoxide moiety. Thus, we investigated the reactivity of silicon–carbonyl complex **3** towards nucleophiles. Surprisingly, even at elevated temperatures, **3** does not react with water but is sensitive to oxygen with the formation of an unidentified product mixture. Additionally, no reaction with MeOH, EtOH, MeLi or ^{t}BuLi was observed. Since transition-metal carbonyls are known to react with azides to form isocyanato complexes (Fig. 5a)[43], we envisaged a similar reaction with **3**. Whereas no reaction of **3** with NaN_3 in THF was observed (even at elevated temperatures), treatment of **3** with trimethylsilyl azide ($TMSN_3$) resulted in a colour change from purple to colourless with simultaneous conversion into a novel product. Multinuclear and 2D NMR studies, elemental analysis and mass spectrometry in combination with supportive DFT calculations identified the obtained compound as a silyl cyanide [(TMS)$_3$Si](^{t}Bu$_3$Si)Si(OTMS)(CN) (**7**) (Fig. 5b) (Supplementary Figs. 18–24 and Supplementary Table 26). The experimentally observed NMR resonances are in good agreement with the calculated values ($\delta_{exp/cal}(^{13}C_{CN})$ = 131.4/133.2 ppm and $\delta_{exp/cal}(^{29}Si_{SiCN})$ = –27.6/–29.3 ppm). Despite the revealed similarity of **3** to transition-metal carbonyls, silyl ether **7** is formed, not the silyl isocyanate analogous to the case of transition metals. However, this can be easily understood by considering the high oxophilicity of silicon, which provides alternative reaction pathways to favour Si–O bond formation.

Summary. In conclusion, we have succeeded in synthesizing and fully characterizing isolable and room temperature stable silylated silicon–carbonyl complexes, which are reminiscent of traditional transition-metal complexes in structure, bonding motif and reactivity. Besides photodissociation and exchange of the CO ligand by a stronger donor molecule, the CO moiety was successfully converted into a CN group. In addition to the close analogy to transition-metal carbonyls, silicon–carbonyl complexes showed novel reactivity profiles, which overall may enable the development of new catalytic processes in the future.

Online content

Any methods, additional references, Nature Research reporting summaries, source data, extended data, supplementary information, acknowledgements, peer review information; details of author contributions and competing interests; and statements of data and code availability are available at https://doi.org/10.1038/s41557-020-00555-4.

Received: 13 March 2020; Accepted: 20 August 2020;
Published online: 19 October 2020

References

1. Herrmann, W. A. 100 years of metal carbonyls: a serendipitous chemical discovery of major scientific and industrial impact. *J. Organomet. Chem.* **383**, 21–44 (1990).
2. Werner, H. Complexes of carbon monoxide and its relatives: An organometallic family celebrates its birthday. *Angew. Chem. Int. Ed.* **29**, 1077–1089 (1990).
3. Holleman, A. F., Wiberg, E. & Wiberg, N. *Lehrbuch der Anorganischen Chemie* Vol. 102 (de Gruyter, 2007).
4. Behrens, H. The chemistry of metal carbonyls: 'the life work of Walter Hieber'. *J. Organomet. Chem.* **94**, 139–159 (1975).
5. Beller, M. in *Topics in Organometallic Chemistry* Vol. 18 (Springer-Verlag, 2006).
6. Power, P. P. Main-group elements as transition metals. *Nature* **463**, 171–177 (2010).
7. Martin, D., Soleilhavoup, M. & Bertrand, G. Stable singlet carbenes as mimics for transition metal centers. *Chem. Sci.* **2**, 389–399 (2011).
8. Weetman, C. & Inoue, S. The road travelled: after main-group elements as transition metals. *ChemCatChem* **10**, 4213–4228 (2018).
9. Légaré, M.-A., Pranckevicius, C. & Braunschweig, H. Metallomimetic chemistry of boron. *Chem. Rev.* **119**, 8231–8261 (2019).
10. Braunschweig, H. et al. Multiple complexation of CO and related ligands to a main-group element. *Nature* **522**, 327–330 (2015).
11. Puschmann, F. F. et al. Phosphination of carbon monoxide: A simple synthesis of sodium phosphaethynolate (NaOCP). *Angew. Chem. Int. Ed.* **50**, 8420–8423 (2011).
12. Hansmann, M. M. & Bertrand, G. Transition-metal-like behavior of main group elements: ligand exchange at a phosphinidene. *J. Am. Chem. Soc.* **138**, 15885–15888 (2016).
13. Wu, X. et al. Observation of alkaline earth complexes $M(CO)_8$ (M = Ca, Sr, or Ba) that mimic transition metals. *Science* **361**, 912–916 (2018).
14. Lavallo, V., Canac, Y., Donnadieu, B., Schoeller, W. W. & Bertrand, G. CO fixation to stable acyclic and cyclic alkyl amino carbenes: Stable amino ketenes with a small HOMO–LUMO gap. *Angew. Chem. Int. Ed.* **45**, 3488–3491 (2006).
15. Hudnall, T. W. & Bielawski, C. W. An N,N′-diamidocarbene: studies in C–H insertion, reversible carbonylation, and transition-metal coordination chemistry. *J. Am. Chem. Soc.* **131**, 16039–16041 (2009).
16. Lee, V. Y. *Organosilicon Compounds: Theory and Experiment (Synthesis)* Vol. 1 (Academic Press, 2017).
17. Pearsall, M. A. & West, R. The reactions of diorganosilylenes with carbon monoxide. *J. Am. Chem. Soc.* **110**, 7228–7229 (1988).
18. Arrington, C. A., Petty, J. T., Payne, S. E. & Haskins, W. C. K. The reaction of dimethylsilylene with carbon monoxide in low-temperature matrices. *J. Am. Chem. Soc.* **110**, 6240–6241 (1988).
19. Hamilton, T. P. & Schaefer, H. F. III Silaketene: A product of the reaction between silylene and carbon monoxide? *J. Chem. Phys.* **90**, 1031–1035 (1989).
20. Tacke, M. et al. Complexes of decamethylsilicocene: $Cp_2^*Si(CO)$ and $Cp_2^*Si(N_2)$. *Z. Anorg. Allg. Chem.* **619**, 865–868 (1993).
21. Maier, G., Reisenauer, H. P. & Egenolf, H. Quest for silaketene: A matrix-spectroscopic and theoretical study. *Organometallics* **18**, 2155–2161 (1999).
22. Becerra, R., Cannady, J. P. & Walsh, R. Silylene does react with carbon monoxide: some gas-phase kinetic and theoretical studies. *J. Phys. Chem. A* **105**, 1897–1903 (2001).
23. Bornemann, H. & Sander, W. Reactions of methyl(phenyl)silylene with CO and PH_3—the formation of acid–base complexes. *J. Organomet. Chem.* **641**, 156–164 (2002).
24. Protchenko, A. V. et al. Reduction of carbon oxides by an acyclic silylene: reductive coupling of CO. *Angew. Chem. Int. Ed.* **58**, 1808–1812 (2019).
25. Wang, Y. et al. Silicon-mediated selective homo- and heterocoupling of carbon monoxide. *J. Am. Chem. Soc.* **141**, 626–634 (2019).
26. Xiong, Y., Yao, S., Szilvási, T., Ruzicka, A. & Driess, M. Homocoupling of CO and isocyanide mediated by a C,C′-bis(silylenyl)-substituted *ortho*-carborane. *Chem. Commun.* **56**, 747–750 (2020).

27. Ganesamoorthy, C. et al. A silicon–carbonyl complex stable at room temperature. *Nat. Chem.* **12**, 608–614 (2020).
28. Reiter, D. et al. Disilene-silylene interconversion: A synthetically accessible acyclic bis(silyl)silylene. *J. Am. Chem. Soc.* **141**, 13536–13546 (2019).
29. Huber, K. P. & Herzberg, G. *Molecular Spectra and Molecular Structure IV. Constants of Diatomic Molecules* Vol. 4 (Van Nostrand Reinhold Company, 1979).
30. Fischer, R. C. & Power, P. P. π-Bonding and the lone pair effect in multiple bonds involving heavier main group elements: developments in the new millennium. *Chem. Rev.* **110**, 3877–3923 (2010).
31. Bader, R. F. W. *Atoms in Molecules: A Quantum Theory* (Oxford Univ. Press, 1990).
32. Macchi, P. & Sironi, A. Chemical bonding in transition metal carbonyl clusters: complementary analysis of theoretical and experimental electron densities. *Coord. Chem. Rev.* **238–239**, 383–412 (2003).
33. Macchi, P. & Sironi, A. in *The Quantum Theory of Atoms in Molecules: From Solid State to DNA and Drug Design* (eds Matta, C. F. & Boyd, R. J.) Ch. 13 (Wiley-VCH, Weinheim, 2007).
34. Schweizer, J. I. et al. A disilene base adduct with a dative Si–Si single bond. *Angew. Chem. Int. Ed.* **55**, 1782–1786 (2016).
35. Stanford, M. W. et al. Intercepting the disilene-silylsilylene equilibrium. *Angew. Chem. Int. Ed.* **58**, 1329–1333 (2019).
36. Cabeza, J. A., Van der Maelen, J. F. & García-Granda, S. Topological analysis of the electron density in the N-heterocyclic carbene triruthenium cluster $[Ru_3(\mu\text{-}H)_2(\mu_3\text{-}MeImCH)(CO)_9]$ (Me_2Im = 1,3-dimethylimidazol-2-ylidene). *Organometallics* **28**, 3666–3672 (2009).
37. Wendel, D. et al. From Si(II) to Si(IV) and back: Reversible intramolecular carbon–carbon bond activation by an acyclic iminosilylene. *J. Am. Chem. Soc.* **139**, 8134–8137 (2017).
38. Wendel, D. et al. Silicon and oxygen's bond of affection: an acyclic three-coordinate silanone and its transformation to an iminosiloxysilylene. *J. Am. Chem. Soc.* **139**, 17193–17198 (2017).
39. Boyarskiy, V. P., Bokach, N. A., Luzyanin, K. V. & Kukushkin, V. Y. Metal-mediated and metal-catalyzed reactions of isocyanides. *Chem. Rev.* **115**, 2698–2779 (2015).
40. Takeda, N., Kajiwara, T., Suzuki, H., Okazaki, R. & Tokitoh, N. Synthesis and properties of the first stable silylene–isocyanide complexes. *Chem. Eur. J.* **9**, 3530–3543 (2003).
41. Abe, T., Iwamoto, T., Kabuto, C. & Kira, M. Synthesis, structure, and bonding of stable dialkylsilaketenimines. *J. Am. Chem. Soc.* **128**, 4228–4229 (2006).
42. Mansikkamäki, A., Power, P. P. & Tuononen, H. M. Computational analysis of $n\rightarrow\pi^*$ back-bonding in metallylene–isocyanide complexes R_2MCNR' (M = Si, Ge, Sn; R = ^{t}Bu, Ph; R′ = Me, ^{t}Bu, Ph). *Organometallics* **32**, 6690–6700 (2013).
43. Beck, W. & Fehlhammer, W. P. Reactions of metal carbonyls with the azide ion and—vice versa—reactions of azido complexes with carbon monoxide: isocyanato complexes. analogous reactions in NO^+/N_3^- transition metal chemistry. *Z. Anorg. Allg. Chem.* **636**, 157–162 (2010).

Methods

General methods and instrumentation. All manipulations were carried out under exclusion of H_2O and O_2 under an atmosphere of argon 4.6 (≥99.996%; Westfalen AG) using standard Schlenk techniques or in a LABstar glovebox from MBraun Inertgas-Systeme GmbH with H_2O and O_2 levels below 0.5 ppm. The glassware used was heat-dried under fine vacuum prior to use with Triboflon III grease (mixture of polytetrafluoroethylene (PTFE) and perfluoropolyether) from Freudenberg & Co. KG as sealant. All solvents were refluxed over sodium/benzophenone, freshly distilled under argon and deoxygenated before use. Deuterated benzene was obtained from Sigma-Aldrich Chemie GmbH, dried over Na/K alloy, flask-to-flask condensed, deoxygenated by 3 freeze-pump-thaw cycles and stored over 3 Å molecular sieves in the glovebox. All NMR samples were prepared under argon in J. Young PTFE valve NMR tubes. The NMR spectra were recorded on Bruker Avance Neo 400 (^{1}H: 400.23 MHz, ^{13}C: 100.65 MHz), or AV500C (^{1}H: 500.36 MHz, ^{13}C: 125.83 MHz, ^{29}Si: 99.41 MHz) spectrometers at ambient temperature (300 K). The ^{1}H, ^{13}C{^{1}H} and ^{29}Si{^{1}H} NMR spectroscopic chemical shifts δ are reported in ppm relative to tetramethylsilane. ^{1}H and ^{13}C{^{1}H} NMR spectra are calibrated against the residual proton and natural abundance carbon resonances of the deuterated solvent as internal standard (C_6D_6: $\delta(^1H) = 7.16$ ppm and $\delta(^{13}C) = 128.1$ ppm). The following abbreviations are used to describe signal multiplicities: s = singlet, d = doublet, t = triplet, m = multiplet and combinations thereof (for example dd = doublet of doublets). Quantitative elemental analyses were carried out using a EURO EA (HEKAtech) instrument equipped with a CHNS combustion analyser at the Laboratory for Microanalysis at the TUM Catalysis Research Center. Elemental analyses provided partially and reproducibly low carbon percentages (~1% deviation), presumably due to the formation of incombustible SiC compounds. Infrared spectra were recorded on a Perkin Elmer FT-IR spectrometer (diamond ATR, Spectrum Two) in the range 400–4,000 cm^{-1} at room temperature inside an argon-filled glovebox. The intensities of the infrared bands are abbreviated as follows: s = strong, m = medium, w = weak. The UV-vis spectra were taken on a Varian, Inc. Cary 50 spectrophotometer with a Schlenk quartz cuvette. Melting points (m.p.) were determined in sealed glass capillaries under inert gas using a Büchi M-565 melting point apparatus. Liquid injection field desorption ionization mass spectra (LIFDI-MS) were recorded on a Waters Micromass LCT TOF mass spectrometer equipped with a LIFDI-ion source (LIFDI-700) from Linden CMS GmbH. The samples were provided as filtered solutions in toluene. Electrospray ionization mass spectra (ESI-MS) were acquired using an LTQ FT Ultra mass spectrometer from Thermo Fisher. Photochemical experiments were carried out using an Asahi Spectra Co., Ltd. MAX-302 xenon light source at $\lambda_{max} = 340$ nm. Unless otherwise stated, all commercially available reagents were purchased from abcr GmbH or Sigma-Aldrich Chemie GmbH and were used without further purification. Carbon monoxide (CO) 4.7 (≥99.997%), ethylene 3.5 (≥99.95%) and hydrogen 5.0 (≥99.999%) were purchased from Air Liquide S.A. or Westfalen AG and used as received. ^{13}C-labelled CO was obtained from Sigma-Aldrich Chemie GmbH.

Synthesis of [(TMS)$_3$Si](*t*Bu$_3$Si)Si⇆CO (3). Silicon–carbonyl complex **3** was obtained by two different methods, either by direct carbonylation of **1**/**1′** (Method A) or more conveniently by exposure of **2** to CO via a Lewis base exchange reaction (Method B):

Method A. A solution of **1**/**1′** (100 mg, 210 µmol) in *n*-hexane (3 ml) was cooled to −30 °C, degassed and exposed to CO (1 bar). Subsequently, the reaction mixture was warmed to ambient temperature, whereby a colour change from blood-red to purple was observed. After stirring for 1 h, all volatiles were removed under reduced pressure. Purple crystals of **3** (95.0 mg, 189 µmol, 90%), which were suitable for SC-XRD analysis, were obtained by cooling a concentrated *n*-hexane solution of **3** to −35 °C for several days.

Method B. A solution of **2** (600 mg, 1.00 mmol) in toluene (15 ml) was degassed and subsequently exposed to CO (1 bar) at room temperature. The reaction mixture was stirred for 5 h, whereby a colour change from red-brown to purple was observed. After removal of all volatiles under reduced pressure, the residue was extracted with cold *n*-hexane (3 × 5 ml, −35 °C). DMAP was separated from the mixture by filtration. Removal of the solvent under reduced pressure provided **3** as a purple solid (505 mg, 1.00 mmol, quantitative yield).

Note. Removal of free DMAP is also possible by addition of an equimolar amount of silicon tetrabromide ($SiBr_4$) to the reaction mixture and subsequent filtration (DMAP forms an unidentified Lewis acid/base adduct with $SiBr_4$, which is insoluble in common organic solvents; no reaction of **3** with $SiBr_4$ in solution was detected at least within 1 day).

Silicon–carbonyl complex **3** is indefinitely stable as a solid and in solution under an argon atmosphere at ambient temperature, but slowly decomposes in solution at elevated temperatures (≥90 °C) to free, gaseous CO and disiletane **4**; m.p. 76–77 °C (decomposition; colour change from purple to black); ^{1}H NMR (500 MHz, C_6D_6, 300 K): $\delta = 1.23$ (s, 27H, C(CH_3)$_3$), 0.39 (s, 27H, *TMS*) ppm; ^{13}C{^{1}H} NMR (126 MHz, C_6D_6, 300 K): $\delta = 226.1$ (*C*O), 32.0 (C(*C*H$_3$)$_3$), 25.5 (*C*(CH$_3$)$_3$), 3.0 (*TMS*) ppm; ^{29}Si{^{1}H} NMR (99 MHz, C_6D_6, 300 K): $\delta = 42.8$ (*Si*^{t}Bu$_3$), −6.9 (*TMS*), −119.0 (*Si*(TMS)$_3$), −228.5 (*Si*CO) ppm; IR (solid): $\tilde{\nu}$ [cm^{-1}] = 2,950 (w), 2,857 (m), 1,908 (s) ($\tilde{\nu}_{CO}$), 1,477 (w), 1,388 (w), 1,244 (m), 1,011 (w), 826 (s), 684 (m), 622 (m), 468 (m); Analysis calculated for $C_{22}H_{54}OSi_6$: C, 52.51; H, 10.82; found: C, 52.76; H, 10.54%; UV-vis (*n*-hexane, 298 K): $\lambda_{max} = 373$ (theoretical: 351; HOMO→LUMO+1) nm; LIFDI-MS calculated for **3** ($C_{22}H_{54}OSi_6$): 502.2790; observed: 502.3820.

Synthesis of disiletane (4). Disiletane **4** was obtained by two distinct methods, either by thermal decomposition of silicon–carbonyl complex [(TMS)$_3$Si](*t*Bu$_3$Si)Si⇆CO (**3**) (Method A) or upon irradiation of **3** (Method B). In both cases a C–H bond activation of a *tert*-butyl group by the silylene moiety takes place after the dissociation of CO.

Method A (thermally). A solution of silicon–carbonyl complex **3** (30.0 mg, 59.6 µmol) in C_6D_6 (0.5 ml) was heated to 130 °C for 2 h. A colour change from purple to colourless indicated quantitative conversion, which was verified by ^{1}H NMR spectroscopy. Removal of all volatiles under reduced pressure provided disiletane **4** as a colourless solid (28.3 mg, 59.6 µmol, quantitative yield).

Method B (photochemically). A J. Young PTFE valve NMR tube was charged with a solution of **3** (30.0 mg, 59.6 µmol) in C_6D_6 (0.5 ml). Photolysis of **3** ($\lambda_{max} = 340$ nm) resulted in an immediate colour change from purple to blood-red with concomitant gas evolution (CO) and formation of bis(silyl)silylene [(TMS)$_3$Si](*t*Bu$_3$Si)Si:) (**1**) and its tetrasilyldisilene isomer (TMS)$_2$Si=Si(TMS)(Si*t*Bu$_3$) (**1′**). The photodissociation is partially reversible (observable colour change from blood-red to purple after interruption of irradiation) until after irradiation at room temperature for 4 days, quantitative conversion to 1,2-disilacyclobutane **4** was detected by ^{1}H NMR spectroscopy. Removal of all volatiles under reduced pressure afforded **4** as a colourless solid (28.3 mg, 59.6 µmol, quantitative yield); ^{1}H NMR (500 MHz, C_6D_6, 300 K): $\delta = 4.37$ (dd, $^3J = 7.8$ Hz, $^3J = 5.9$ Hz, 1H, Si*H*), 1.45 (s, 3H, C(CH_3)$_2$), 1.36 (s, 3H, C(CH_3)$_2$), 1.33–1.30 (m, 2H, CH_2), 1.29 (s, 9H, C(CH_3)$_3$), 1.23 (s, 9H, C(CH_3)$_3$), 0.34 (s, 27H, *TMS*) ppm; ^{13}C{^{1}H} NMR (126 MHz, C_6D_6, 300 K): $\delta = 37.4$ (*C*(CH$_3$)$_2$), 31.9 (C(*C*H$_3$)$_2$), 31.9 (C(*C*H$_3$)$_2$), 31.5 (C(*C*H$_3$)$_3$), 31.0 (C(*C*H$_3$)$_3$), 29.5 (*C*H$_2$), 23.6 (*C*(CH$_3$)$_3$), 22.9 (*C*(CH$_3$)$_3$), 2.8 (*TMS*) ppm; ^{29}Si{^{1}H} NMR (99 MHz, C_6D_6, 300 K): $\delta = 35.6$ (*Si*^{t}Bu$_2$), −9.2 (*TMS*), −60.4 (Si*H*), −133.8 (*Si*(TMS)$_3$) ppm. The spectroscopic data match those recently reported[28].

Synthesis of [(TMS)$_3$Si](*t*Bu$_3$Si)Si⇆CNXyl (5). To a mixture of silicon–carbonyl complex **3** (100 mg, 199 µmol, 1.0 equiv.) and 2,6-dimethylphenyl isocyanide (CNXyl) (26.1 mg, 199 µmol, 1.0 equiv.) was added *n*-hexane (3 ml). An immediate colour change from purple to deep blue with concomitant gas evolution (CO) was observed. The reaction mixture was stirred for an additional hour. Subsequent removal of the solvent under reduced pressure afforded silicon isocyanide complex **5** as a deep blue solid (121 mg, 199 µmol, quantitative yield). Crystals suitable for SC-XRD analysis were obtained by cooling a saturated *n*-hexane solution to −35 °C for several days. Silicon isocyanide complex **5** is indefinitely stable as a solid and in solution at ambient temperature, but very slowly isomerizes in solution at elevated temperatures (≥130 °C) to 1,3-azasilole **6**. Characterization for compound **5**: m.p. 79–80 °C (decomposition; colour change from deep blue to black); ^{1}H NMR (500 MHz, C_6D_6, 300 K): $\delta = 6.78$–6.75 (m, 1H, *p*-C$_{ar}$*H*), 6.70–6.69 (m, 2H, *m*-C$_{ar}$*H*), 2.49 (s, 6H, *o*-C$_{ar}$CH_3), 1.36 (s, 27H, C(CH_3)$_3$), 0.44 (s, 27H, *TMS*) ppm; ^{13}C{^{1}H} NMR (126 MHz, C_6D_6, 300 K): δ = 192.1 (*C*N), 138.2 (*o*-*C*$_{ar}$), 130.1 (*ipso*-*C*$_{ar}$), 129.3 (*p*-*C*$_{ar}$H), 128.9 (*m*-*C*$_{ar}$H), 32.4 (C(*C*H$_3$)$_3$), 25.5 (*C*(CH$_3$)$_3$), 19.3 (*o*-C$_{ar}$*C*H$_3$), 3.6 (*TMS*) ppm; ^{29}Si{^{1}H} NMR (99 MHz, C_6D_6, 300 K): $\delta = 37.6$ (*Si*^{t}Bu$_3$), −8.1 (*TMS*), −119.1 (*Si*(TMS)$_3$), −177.0 (*Si*CN) ppm; IR (solid): $\tilde{\nu}$ [cm^{-1}] = 2,950 (w), 2,856 (m), 1,966 (w) ($\tilde{\nu}_{CN}$), 1,471 (w), 1,387 (w), 1,244 (m), 1,012 (m), 826 (s), 683 (m), 622 (m), 465 (m); Analysis calculated for $C_{30}H_{63}NSi_6$: C, 59.43; H, 10.47; N, 2.31; found: C, 58.17; H, 10.54; N, 2.34%; UV-vis (*n*-hexane, 298 K): $\lambda_{max} = 389$ (theoretical: 366; HOMO→LUMO+1) nm.

Synthesis of 1,3-azasilole (6). A solution of silicon isocyanide complex **5** (50.0 mg, 82.5 µmol) in C_6D_6 (0.5 ml) was heated to 130 °C for 2 days. A colour change from deep blue to deep green and finally to yellow was observed during the reaction. ^{1}H NMR spectroscopy indicated quantitative conversion into 1,3-azasilole **6**. Removal of the solvent under reduced pressure provided **6** as yellow solid (50.0 mg, 82.5 µmol, quantitative yield); m.p. 163–164 °C (decomposition; colour change from yellow to orange); ^{1}H NMR (500 MHz, C_6D_6, 300 K): $\delta = 7.71$ (d, $^3J = 7.0$ Hz, 1H, SiCC*H*), 7.15 (d, $^3J = 7.0$ Hz, 1H, NCCCH$_3$C*H*, overlapping with solvent signal), 7.09 (pseudo t, $^3J = 7.0$ Hz, 1H, SiCCHC*H*), 2.76 (s, 3H, C$_{ar}$CH_3), 1.36 (s, 27H, C(CH_3)$_3$), 0.68 (s, 3H, SiCH_3), 0.24 (s, 27H, *TMS*) ppm; ^{13}C{^{1}H} NMR (126 MHz, C_6D_6, 300 K): $\delta = 212.8$ (Si*C*=N), 158.4 (N*C*CCH$_3$), 134.4 (NC*C*CH$_3$), 132.9 (NCCCH$_3$*C*H), 131.4 (Si*C*CH), 130.6 (SiC*C*H), 127.4 (SiCCH*C*H), 32.1 (C(*C*H$_3$)$_3$), 23.1 (*C*(CH$_3$)$_3$), 19.2 (NCC*C*H$_3$), 4.0 (*TMS*), −0.3 (SiCH$_3$) ppm; ^{29}Si{^{1}H} NMR (99 MHz, C_6D_6, 300 K): $\delta = 2.4$ (*Si*CH$_3$), 0.8 (*Si*^{t}Bu$_3$), −8.8 (*TMS*), −126.7 (*Si*(TMS)$_3$) ppm; Analysis calculated for $C_{30}H_{63}NSi_6$: C, 59.43; H, 10.47; N, 2.31; found : C, 58.11; H, 10.59; N, 2.28%.

Synthesis of [(TMS)$_3$Si](*t*Bu$_3$Si)Si(OTMS)(CN) (7). To a solution of silicon–carbonyl complex **3** (100 mg, 199 µmol, 1.0 equiv.) in *n*-hexane (3 ml) was added

$TMSN_3$ (26.4 µl, 22.9 mg, 199 µmol, 1.0 equiv.). Subsequently, the reaction mixture was stirred for 1 h, whereby a colour change from purple to colourless was observed. Removal of all volatiles under reduced pressure provided crude silyl cyanide **7** as a colourless waxy solid. Compound **7** is highly thermally (no sign of decomposition was observed upon heating **7** to 130 °C in C_6D_6) and photochemically stable and resistant to air and moisture. Silyl cyanide **7** is soluble in *n*-hexane, benzene, toluene, THF, Et_2O and CH_2Cl_2, but sparingly soluble in acetonitrile, ethanol, methanol and water.

Note. Compound **7** contains a minor by-product, most likely the isomeric silyl isocyanide [$(TMS)_3Si$](^{t}Bu_3Si)Si(OTMS)(NC) (identified by infrared, ^{13}C NMR and DFT calculations). However, all further purification attempts by crystallization, distillation/sublimation, washing or flash chromatography have been unsuccessful so far. In addition, the molecular structure of **7** could not be obtained by SC-XRD analysis because all grown 'crystals' from a saturated acetonitrile solution did not diffract sufficiently; m.p. 132–133 °C; ^1H NMR (500 MHz, C_6D_6, 300 K): $\delta = 1.29$ (s, 27H, C(CH_3)$_3$), 0.45 (s, 27H, *TMS*), 0.31 (s, 9H, O*TMS*) ppm; $^{13}C\{^1H\}$ NMR (126 MHz, C_6D_6, 300 K): $\delta = 131.4$ (Si*C*N), 32.4 (C(*C*H_3)$_3$), 24.8 (*C*(CH_3)$_3$), 5.0 (*TMS*), 4.2 (O*TMS*) ppm; $^{29}Si\{^1H\}$ NMR (99 MHz, C_6D_6, 300 K): $\delta = 14.4$ (*Si*^{t}Bu_3), 11.9 (O*TMS*), −8.2 (*TMS*), −27.6 (*Si*CN), −111.6 (*Si*(TMS)$_3$) ppm; IR (solid): $\tilde{\nu}$ [cm^{-1}] = 2,952 (m), 2,856 (m), 2,129 (w) ($\tilde{\nu}_{NC}$), 1,659 (w), 1,477 (w), 1,389 (w), 1,245 (m), 1,023 (m), 829 (s). The observed NC stretching mode at $\tilde{\nu} = 2{,}129\ cm^{-1}$ most likely originates from the presence of a minor amount of the corresponding silyl isocyanide isomer [$(TMS)_3Si$](^{t}Bu_3Si)Si(OTMS)(NC). The respective CN stretching mode of silyl cyanide **7** is not observable (estimated low intensity). These observations are in good agreement with those for other silyl cyanides and the results of our DFT calculations: Analysis calculated for $C_{25}H_{63}NOSi_7$: C, 50.86; H, 10.76; N, 2.37; found: C, 50.72; H, 10.63; N, 2.68%; ESI-MS: calculated for $[7–CN]^+$ ($C_{24}H_{63}OSi_7$): 563.33; observed: 563.33.

The full experimental details and characterization of the new compounds can be found in the Supplementary Information.

Data availability

X-ray crystallographic data are available free of charge from the Cambridge Crystallographic Data Centre under the reference numbers CCDC 1976834 (**3**) and CCDC 1976835 (**5**) via https://www.ccdc.cam.ac.uk/structures/. All other data supporting the findings are contained in the main text or the Supplementary Information.

Acknowledgements

We thank M. C. Holthausen and J. I. Schweizer for fruitful discussions, computational resources and advice. Quantum chemical calculations were performed in part at the Leibniz Supercomputing Center of the Bavarian Academy of Science and Humanities. We acknowledge M. Muhr (R. A. Fischer) for the LIFDI-MS measurement. We thank the WACKER Chemie AG and the European Research Council (SILION 637394) for continued financial support.

Author contributions

D.R. and R.H. planned and carried out all experiments and analysed the data. A.P. designed and conducted the computational investigations. P.F. performed the SC-XRD measurements. S.I. designed and conceived the project. D.R. and S.I. wrote the manuscript with input and critical revision from all authors.

Competing interests

The authors declare no competing interest.

Additional information

Supplementary information is available for this paper at https://doi.org/10.1038/s41557-020-00555-4.

Correspondence and requests for materials should be addressed to S.I.

Reprints and permissions information is available at www.nature.com/reprints.

6.5. A Stable Neutral Compound with an Aluminum-Aluminum Double Bond

Title:	A Stable Neutral Compound with an Aluminum-Aluminum Double Bond
Status:	Communication, published online September 12, 2017
Journal:	Journal of the American Chemical Society, 2017, 139 (41), 14384-14387.
Publisher:	American Chemical Society
DOI:	10.1021/jacs.7b08890
Authors:	Prasenjit Bag, Amelie Porzelt, Philipp J. Altmann, Shigeyoshi Inoue

Content: Homonuclear multiple-bonded neutral aluminium compounds have been a challenging target with only masked species, radical species or di-anionic species with a bond order > 1 isolated prior to this report. In this paper, we targeted the synthesis of a neutral Al–Al double bond by using a combination of two strong σ-donating groups directly attached to the aluminium centres: a NHC, namely I^{i}Pr$_2$Me$_2$, and the electropositive silyl group SitBu$_2$Me. Key to isolation of a dialumene was the access to suitable precursors, I^{i}Pr$_2$Me$_2$-AlX$_2$Si^{t}Bu$_2$Me **2/3** (X = Br/I), which enabled the conversion to the first dialumene **4** in good to moderate yields on treatment with the reducing agent KC$_8$. SC-XRD analysis revealed a *trans*-planar structure for **4**, with the shortest Al–Al distance reported to date. The results of DFT calculations clearly confirmed a double bond being present in **4**, with the HOMO representing the π(AlAl) bond and HOMO-1 the σ(AlAl) bond. Initial reactivity studies focused on conversion with the C-C multiple bonds in ethylene and phenylacetylene, which both react with **4** at rt or below to give **5**,**6** and **7**. NBO analysis revealed a high WBI for **4**, which is almost halved in the reaction products **5**,**6** and **7**. Dialumene **4** exhibits a dark purple colour, assigned to π-π* transitions by TD-DFT calculations. In summary, this publication reports the first example of a neutral double bonded Al–Al compound, called dialumene, which bears a *trans*-planar structure. DFT calculations clearly demonstrate the presence of a double bond in this compound. Experimentally this was proven by initial reactivity studies focusing on C-C multiple bonds to yield the [2+2] cycloaddition products, though C-H activation was observed as well.

Contributions to the publication:

- Quantum chemical calculations on NHC-stabilised dialumene **4** including TD-DFT calculations
- Bonding analysis of the novel dialumene **4** *via* NBO analysis including internal referencing to the phenyl-acetylene and ethylene reaction products (**5**, **6** and **7**)
- Interpretation of the data, composition of the theoretical parts in the manuscript
- Co-writing of the manuscript

JACS
JOURNAL OF THE AMERICAN CHEMICAL SOCIETY
Communication
Cite This: J. Am. Chem. Soc. 2017, 139, 14384-14387
pubs.acs.org/JACS

A Stable Neutral Compound with an Aluminum−Aluminum Double Bond

Prasenjit Bag, Amelie Porzelt, Philipp J. Altmann, and Shigeyoshi Inoue*

Department of Chemistry, Catalysis Research Center and Institute of Silicon Chemistry, Technische Universität München, Lichtenbergstraße 4, 85748 Garching bei München, Germany

Supporting Information

ABSTRACT: Homodinuclear multiple-bonded neutral Al compounds, aluminum analogues of alkenes, have been a notoriously difficult synthetic target over the past several decades. Herein, we report the isolation of a stable neutral compound featuring an Al═Al double bond stabilized by N-heterocyclic carbenes. X-ray crystallographic and spectroscopic analyses demonstrate that the dialuminum entity possesses *trans*-planar geometry and an Al−Al bond length of 2.3943(16) Å, which is the shortest distance reported for a molecular dialuminum species. This new species reacts with ethylene and phenyl acetylene to give the [2+2] cycloaddition products. The structure and bonding were also investigated by detailed density functional theory calculations. These results clearly demonstrate the presence of an Al═Al double bond in this molecule.

Aluminum is the most abundant metal in the Earth's crust, and its many chemical derivatives have a diverse range of applications in organic and organometallic synthesis.[1] Most of those compounds find Al in the +III oxidation state. Particularly, the discoveries of the pivotal role of trialkyl aluminum compounds in Ziegler−Natta olefin polymerization processes[2] and Al(III) halide salts as potent Lewis acid in Friedel−Crafts reactions[3] provided a tremendous boost to organometallic Al chemistry. In sharp contrast, the chemistry of low-valent Al compounds remains in its infancy. A major discovery in Al(I) chemistry was the isolation of neutral organometallic compounds, namely $[(Cp^*Al)_4]$ (Cp^* = pentamethylcyclopentadienyl),[4] which has a tetrahedral arrangement of Al centers in the solid state but is believed to dissociate in solution to the monomeric form Cp^*Al at elevated temperatures. Later, a stable monomeric Al(I) compound with a β-diketiminato ligand was isolated,[5] and its reactivity toward a broad range of small molecules has been extensively investigated.[6,7] However, neutral Al(I) compounds containing an Al═Al double bond, namely dialumenes, have yet to be reported. It is worth mentioning that even compounds with an Al—Al single bond are highly reactive and can only be isolated with the help of bulky substituents; otherwise they easily undergo disproportionation to elemental Al and trivalent Al(III) species.[8] In general, group 13 multiple bonds are extremely reactive for a variety of reasons, such as their inherent Lewis acidity and the difficulty of supplying steric bulk with a single substituent. These double bonds also have significant singlet diradical character, which further increases their potential reactivity and reduces stability.[9] Despite these challenges, there have been reports of homodinuclear multiple bonds comprising exclusively group 13 elements, with the exception of Al. For example, in the case of boron, a handful of compounds containing boron−boron double[10] and triple bonds[11] have been reported since the landmark discovery of the first N-heterocyclic carbene (NHC)-stabilized neutral parent diborenes by Robinson and co-workers.[12] The latter was achieved through reductive dehalogenation of the corresponding NHC-coordinated BBr_3 in the presence of excess potassium graphite (KC_8) at room temperature in diethyl ether. In fact, all of these examples employ a strategy of Lewis base stabilization. Employing sterically bulky terphenyl ligand systems, other heavier group 13 neutral double-bonded compounds—having a general formula ArMMAr (M = Ga, In, Tl; Ar = 2,6-$Dipp_2C_6H_3$, Dipp = 2,6-iPr$_2$C$_6$H$_3$)—have been isolated and characterized.[13] However, all these compounds show considerable *trans*-bending and dissociate into their corresponding monomers (ArM:) in hydrocarbon solvents, providing evidence for the weak nature of the metal−metal bond. These unsaturated multiple-bonded compounds exhibit a diverse range of fascinating chemistry, including some unique bond-activating reactions that were traditionally dominated by transition metal compounds.[10,14]

Chart 1. Examples of Dialuminum Compounds Having a Formal Bond Order >1 (A−C) and Masked Dialumene Compounds (D, E)

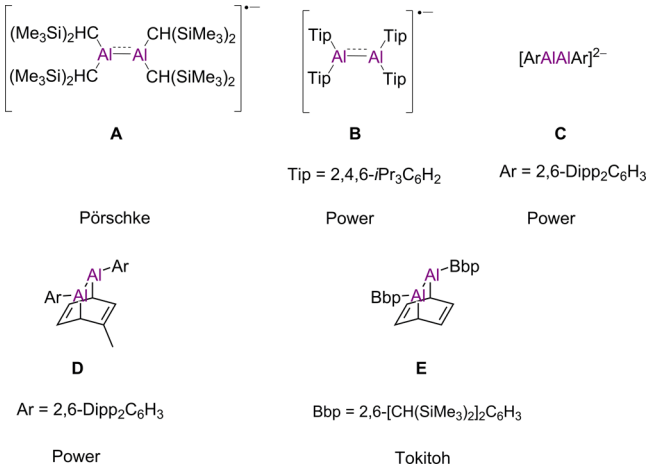

Received: August 24, 2017
Published: September 12, 2017

DOI: 10.1021/jacs.7b08890
J. Am. Chem. Soc. 2017, 139, 14384−14387

Therefore, considering the ever-increasing popularity of unsaturated boron and other heavier group 13 compounds, neutral multiple-bonded Al compounds are highly desirable to understand its true bonding nature as well as to explore their reactivity.

In this regard, a few scattered efforts were made to isolate multiple-bonded Al compounds. Among them, in the early 1990s, three examples of structurally authenticated dialuminum compounds having formal bond orders >1 were documented through the synthesis of the radical monoanionic complexes **A** and **B** (Chart 1)[15] and the dianionic compound (Na_2[Ar′AlAlAr′]) (**C**, Ar′ = C_6H_3-2,6-(C_6H_2-2,4,6-iPr$_3$)$_2$).[16] Later, the groups of Power and Tokitoh independently reported the synthesis of bicyclo masked dialumenes **D**[17] and **E**[18] (Chart 1) and interpreted their formation by a classical [4+2] cycloaddition of the intermediate dialumene with toluene or benzene. Recently, the possible formation of dianionic dialumene as a reactive intermediate during the reaction of α-diimine-stabilized dialumane [L(thf)Al−Al(thf)L] (L = [{(2,6-iPr$_2$C$_6$H$_3$)NC(Me)}$_2$]$^{2-}$) with a substituted butadiene under reductive condition was proposed.[19] However, none of these studies has been successful in isolating the proposed intermediate dialumene species. The extremely reactive nature presumably arises from the highly electrophilic character of the incipient dialumene, caused by the presence of a vacant p orbital on each Al center leading to intrinsic thermodynamic instability.

Nonetheless, an earlier extensive quantum chemical calculation revealed that the neutral dialumene (Al_2H_2) could exist within the constraints of *trans*-bent structural motif (HAlAlH); however, it lies relatively higher in energy than the corresponding planar two times H-bridged global minimum isomer (AlHHAl).[20] This clearly reflects the reduced π-bond strength in the *trans*-bent form. Moreover, the existence of both isomers has been studied by IR spectroscopy in a low-temperature argon matrix.[21] Recent theoretical calculations by Frenking et al. revealed that coordination of external bases, like NHCs, can alter the potential energy landscape to the extent where dialumenes (Al_2H_2 and Al_2Cl_2) could be realized.[22] The calculations further highlight the profound influence of the substituents on the Al−Al bond length as well as geometry around each Al center. Al_2H_2(NHC)$_2$ has completely *trans*-planar structure with relatively short Al−Al bond length (2.444 Å) compared to more electronegative chloride-substituted Al_2Cl_2(NHC)$_2$ (2.494 Å), which shows considerable pyramidalization around each Al atom. In fact, NHCs have been extensively employed for the thermodynamic and kinetic stabilization of highly reactive molecules through their tunable steric demand[23] and effective σ-electron-donating properties. Moreover, silyl groups,[24] in particular di-*tert*-butyl(methyl)silyl groups, have been used extensively as substituents for a variety of unsaturated main-group compounds because of their desirable steric shielding and significant electron-donating capabilities.[25] Also in light of the theoretical calculations by Frenking,[22] the di-*tert*-butyl(methyl)-silyl, being more σ-donating and sterically bulky than hydrogen, could possibly isolate dialumene with better thermodynamic and kinetic stability. With these factors in mind, we sought to synthesize di-*tert*-butyl(methyl)silyl-subsituted aluminum(III) dihalide precursors with coordinated NHCs, which could be reductively coupled to form the desired dialumene. The readily available NHC 1,3-diisopropyl-4,5-dimethyl-imidazolin-2-ylidene (I*i*Pr) was selected as Lewis base because of its easy accessibility, excellent donor properties, and moderate steric bulk.

Scheme 1. Synthetic Route to Dihalide Precursors 2, 3 and Their Subsequent Reduction to the NHC-Stabilized, Di-*tert*-butyl(methyl)silyl-Substituted Dialumene 4

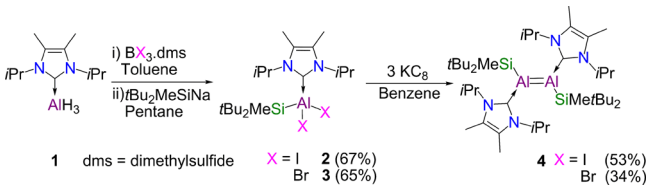

Until now, there has been no reliable route known for the clean and high-yield synthesis of NHC-coordinated organoaluminum(III) alkyl, aryl, or silyl dihalides. Therefore, we have devised an elegant two-step synthetic approach starting with the clean conversion of NHC-stabilized aluminum trihydride (I*i*Pr-AlH$_3$) (**1**) to the corresponding trihalide, I*i*Pr-AlX$_3$ (X = Br, I), by reaction with a slight excess of BX$_3$·dms adduct (X = Br, I; dms = dimethylsulfide) as a halogen-transfer agent.[26] The resultant NHC-stabilized aluminum trihalides have limited thermal stability and were therefore reacted *in situ* with di-*tert*-butyl(methyl)silyl sodium [*t*Bu$_2$MeSiNa] at −78 °C to obtain the Al(III) precursors **2** and **3** as colorless crystalline solids in good yields (∼65%) (Scheme 1). Upon treatment of both Al(III) dihalide precusors **2** and **3** with 3 equiv of KC$_8$ in benzene at room temperature, we were able to isolate the dialumene **4** as a dark purple crystalline compound in good yield (53%) from **2**, and in lower yield from **3** (34%) (Scheme 1).

Compound **4** is stable at room temperature under an inert atmosphere for weeks and has moderate solubility and high thermal stability in solutions of benzene or toluene, although it undergoes slow decomposition over several hours to an unidentified mixture of products in ethereal solvents (tetrahydrofuran or diethyl ether). The ^{1}H NMR spectrum of compound **4** in C$_6$D$_6$ shows a septet at 6.42 ppm (see Supporting Information (SI)) assigned to the isopropyl CH proton of the NHC, considerably shifted downfield compared to starting materials **2** and **3** (5.82 and 5.75 ppm, see SI).

Single-crystal X-ray analysis revealed that compound **4** possesses a completely *trans*-planar geometry in the solid state (see Figure 1), similar to the NHC-stabilized diborene compounds.[10] Each Al atom adopts an almost trigonal planar coordination environment (sum of the angles at Al: 359.99°), and the dihedral angles between the ligands are 180° (C1a−Al−Al−C1 and Si1a−Al−Al−Si1) (SI Table S9). The Al−Al bond length in **4** is 2.3943(16) Å and thus shorter than those

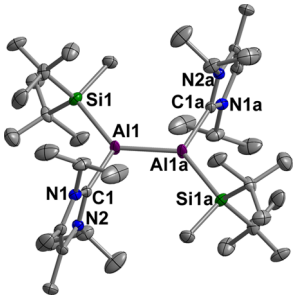

Figure 1. Molecular structure of dialumene **4** in the solid state (thermal ellipsoids drawn at the 50% probability level; H-atoms omitted for clarity). Selected bond lengths [Å] and angles [°] of **4**: Al1−Al1a 2.3943(16), Al1−Si1 2.4939(13), Al1−C1 2.073(3), C1−Al1−Al1a 114.85(8), Al1a−Al1−Si1 146.49(10), C1−Al1−Si1 98.65(11).

DOI: 10.1021/jacs.7b08890
J. Am. Chem. Soc. 2017, 139, 14384−14387

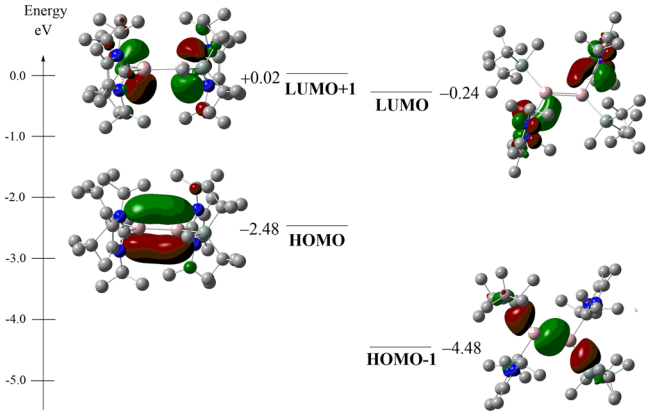

Figure 2. DFT-calculated molecular orbitals of compound **4** (H-atoms omitted for clarity).

theoretically calculated for the NHC-stabilized parent dihydro- and dichloro-dialumenes (2.444 and 2.494 Å, respectively)[22] due to the more σ-electron-donating effect of the silyl groups. It is also notably shorter than the bonds in the theoretically predicted parent dialumene Al_2H_2 (2.613 Å)[20] and the structurally characterized one-electron π-bonded monoanionic dialuminum compounds **A** and **B** (Chart 1, 2.470(2) and 2.53(1) Å, respectively),[15] and even shorter than in the dianionic compound (Na_2[Ar′AlAlAr′]) (**C**) (Chart 1, 2.428(1) Å).[16] Therefore, compound **4** represents the shortest Al−Al bond reported to date.

To get further insight into the bonding motif of compound **4**, we performed density functional theory (DFT) calculations at the B3LYP/6-311G(d) level of theory. The HOMO of compound **4** clearly shows the out-of-plane π-bond, whereas the HOMO−1 represents the Al−Al σ-bond and also has a contribution from the Al−SiMe*t*Bu$_2$ bonds (Figure 2). Natural bond orbital (NBO) analysis (see SI Table S8) reveals electron occupancies of the Al−Al σ bond of 1.91 and 1.78 for the π bond. The Al−Al σ-bond is formed by overlap of the natural hybrid orbitals of Al, bearing high sp-character ($sp^{1.28}$), while the π-bond is formed by almost pure Al p-orbitals (99.9%). The Wiberg bond index (WBI) of **4** is 1.70, clearly indicating the significant double bond character of the Al−Al bond (SI Table S8). Further, the intense purple color encouraged us to check the photophysical behavior of compound **4** through combined experimental and time-dependent TD-DFT calculations (B3LYP/6-311G(d) level of theory, SI Figure S16). The UV−vis spectrum of compound **4** in toluene shows an intense absorption band at 573 nm (ε = 26 750 L mol^{-1} cm^{-1}), mainly attributed to the HOMO to LUMO+1 (π−π*) transition coupled with a small contribution from the HOMO to LUMO+3 and LUMO+5 transitions, which is responsible for the dark purple color (SI Table S7).

In order to demonstrate its double-bonding nature and inherent potential as a synthon, compound **4** was reacted with ethylene and phenyl acetylene. Upon exposure of a toluene solution of **4** to ethylene gas at room temperature, the dark purple color of the solution vanished gradually and was replaced by a bright yellow color within 2 h. The ^{1}H NMR spectrum reveals almost quantitative conversion to the dialumina-cyclobutane compound **5** through a formal [2+2] cycloaddition reaction, which was observed for a variety of unsaturated main-group compounds.[27] Compound **5** was isolated in 64% yield as bright yellow crystals from toluene at −25 °C overnight (Scheme 2). The signal for the −CH proton of the isopropyl group of I*i*Pr-NHC in **5** is split into two septets (δ = 5.26, 5.55 ppm), compared to one of dialumene **4** (δ = 6.42 ppm), caused by steric factors restricting the rotation of the NHC in the former case. Similarly, the reaction of phenyl acetylene with **4** in toluene proceeds smoothly even at −40 °C and undergoes both [2+2] cycloaddition and terminal C−H insertion (Scheme 2) to produce **6** and **7**. Compounds **6** and **7** were isolated by fractional crystallization from pentane as orange and yellow crystals, respectively. Solid-state structure analyses of **5**, **6**, and **7** (Figure 3) revealed considerable elongation of the Al−Al bond lengths (2.6503(10), 2.6363(11), and 2.6411(9) Å) compared to the dialumene **4** (2.3943(16) Å). All these bond lengths lie in the typical range of Al−Al single bonds (2.55−2.70 Å).[28] To classify this value, the WBIs of compounds **5**, **6**, and **7** were also calculated (see SI Table S8), possessing values of 0.83, 0.85, and 0.89, respectively, which are almost half of that of compound **4**, demonstrating the considerable decrease in the bond order upon reaction with ethylene and phenyl acetylene.

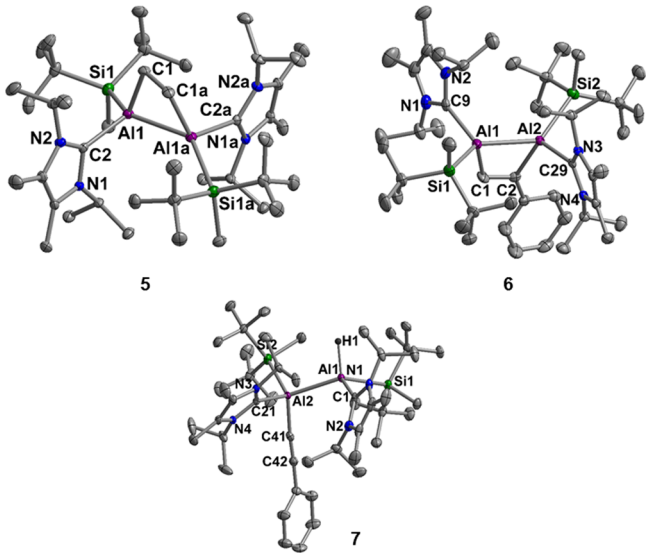

Figure 3. Molecular structures of dialuminacyclobutane **5**, dialumina-cyclobutene **6**, and C−H insertion product **7** (thermal ellipsoids drawn at the 50% probability level; H-atoms except that attached to aluminium and co-crystallized solvent molecules omitted for clarity). Selected bond lengths [Å]: for **5**, Al1−Al1a 2.6503(10), Al1−C1 2.0221(17), Al1−C2 2.0825(18), Si1−Al1 2.5233(7), C1−C1a 1.544(4); for **6**, Al1−Al2 2.6363(11), Si1−Al1 2.5285(11), Si2−Al2 2.5339(11), C1−C2 1.346(4), Al1−C9 2.082(3), Al2−C29 2.086(2); for **7**, Al1−Al2 2.6411(9), Al1−C1 2.088(2), Al2−C21 2.121(2), Al1−H1 1.73(3), Al2−C41 1.982(3), C41−C42 1.208(4).

Scheme 2. Reaction of Dialumene 4 with Ethylene and Phenyl Acetylene

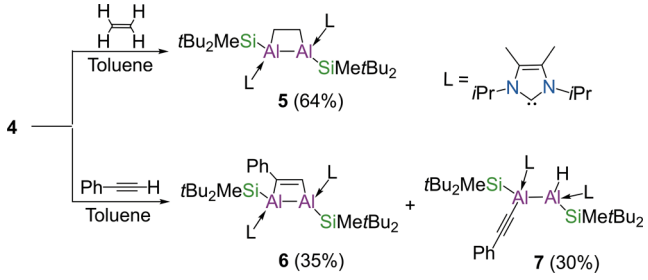

DOI: 10.1021/jacs.7b08890
J. Am. Chem. Soc. 2017, 139, 14384−14387

The presence of a terminal Al−H bond in **7** was confirmed by the appearance of a broad signal at δ = 4.48 ppm in the ^{1}H NMR spectrum (SI Figure S11) as well as by a peak at 1666 cm^{-1} in the IR spectrum (SI Figure S13). This value appears at slightly lower wavenumbers than the reported terminal Al−H stretching frequency of the Dipp-NHC-stabilized tetrahydrodialumane (1682 cm^{-1}).[29]

Thus, we have presented the isolation of the first example of a neutral dialumene **4** with an Al═Al double bond employing the steric bulk and σ-electron-donating capabilities of the di-*tert*-butyl(methyl)silyl group in conjunction with strong donor properties of I*i*Pr-NHC. Dialumene **4** has a significantly low HOMO−LUMO gap (2.24 eV) (Figure 2), also reflected by the low-energy absorption band in UV−vis spectroscopy (573 nm) and facile reaction with unsaturated organic molecules such as ethylene and phenyl acetylene. Therefore, the dialumene **4** has considerable potential to react with a wide range of molecules to access a wide array of novel Al-based functional material as well as organoaluminum compounds, and these are under investigation in our laboratory. Therefore, this new unsaturated Al species sets up a new dimension in Al chemistry.

■ ASSOCIATED CONTENT

Supporting Information

The Supporting Information is available free of charge on the ACS Publications website at DOI: 10.1021/jacs.7b08890.

Crystallographic data for **2**−**7**, experimental procedures, full spectroscopic analysis, and DFT calculations (PDF)

X-ray crystallographic data for **2**, **3**, **4**, **5**, **6**, and **7** (CIF)

■ AUTHOR INFORMATION

Corresponding Author

*s.inoue@tum.de

ORCID

Shigeyoshi Inoue: 0000-0001-6685-6352

Notes

The authors declare no competing financial interest.

■ ACKNOWLEDGMENTS

Financial support from WACKER Chemie AG, as well as the European Research Council (SILION 637394), is gratefully acknowledged. We thank Dr. Daniel Franz, Technische Universität München, for helpful discussion and proofreading the manuscript and Dr. Alexander Pöthig for his advice pertaining to crystallography. We also express appreciation to the Leibniz Supercomputing Center of the Bavarian Academy of Science and Humanities for the provision of computing time.

■ REFERENCES

(1) Blümke, T.; Chen, Y. -H.; Dagorne, S.; Diéguez, M.; D'yakonov, V. A.; Dzhemilev, U. M.; Fliedel, C.; Groll, K.; Knochel, P.; Kolb, A.; Lewiński, J.; Maruoka; Naganawa, Y.; Pàmies, O.; Schulz, S.; von Zezschwitz, P.; Wehmschulte, R. J.; Wheatley, A. E. H. *Modern Organoaluminum Reagents: Preparation, structure, Reactivity and Use*; Woodward, S., Dalgarno, S., Eds.; Springer-Verlag: Berlin/Heidelberg, 2013.

(2) Boor, J., Jr. *Zeigler-Natta catalysts and polymerizations*; Academic Press Inc.: New York, 1979.

(3) Olah, G. A. *Friedel-Crafts and Related Reactions*; Wiley: New York, 1963.

(4) Dohmeier, C.; Robl, C.; Tacke, M.; Schnöckel, H. *Angew. Chem., Int. Ed. Engl.* **1991**, *30*, 564.

(5) Cui, C.; Roesky, H. W.; Schmidt, H.-G.; Noltemeyer, M.; Hao, H.; Cimpoesu, F. *Angew. Chem., Int. Ed.* **2000**, *39*, 4274.

(6) Nagendran, S.; Roesky, H. W. *Organometallics* **2008**, *27*, 457.

(7) Chu, T.; Korobkov, I.; Nikonov, G. I. *J. Am. Chem. Soc.* **2014**, *136*, 9195.

(8) (a) Uhl, W. *Adv. Organomet. Chem.* **2004**, *51*, 53. (b) Uhl, W. *Z. Naturforsch.* **1988**, *43b*, 1113. (c) Uhl, W. *Angew. Chem., Int. Ed. Engl.* **1993**, *32*, 1386.

(9) Moilanen, J.; Power, P. P.; Tuononen, H. M. *Inorg. Chem.* **2010**, *49*, 10992.

(10) Arrowsmith, M.; Braunschweig, H.; Stennett, T. E. *Angew. Chem., Int. Ed.* **2017**, *56*, 96.

(11) Braunschweig, H.; Dewhurst, R. D.; Hammond, K.; Mies, J.; Radacki, K.; Vargas, A. *Science* **2012**, *336*, 1420.

(12) (a) Wang, Y.; Quillian, B.; Wei, P.; Wannere, C. S.; Xie, Y.; King, R. B.; Schaefer, H. F., III; Schleyer, P. v. R.; Robinson, G. H. *J. Am. Chem. Soc.* **2007**, *129*, 12412. (b) Wang, Y.; Quillian, B.; Wei, P.; Xie, Y.; Wannere, C. S.; King, R. B.; Schaefer, H. F., III; Schleyer, P. v. R.; Robinson, G. H. *J. Am. Chem. Soc.* **2008**, *130*, 3298.

(13) (a) Hardman, N. J.; Wright, R. J.; Phillips, A. D.; Power, P. P. *Angew. Chem., Int. Ed.* **2002**, *41*, 2842. (b) Wright, R. J.; Phillips, A. D.; Hardman, N. J.; Power, P. P. *J. Am. Chem. Soc.* **2002**, *124*, 8538. (c) Wright, R. J.; Phillips, A. D.; Hino, S.; Power, P. P. *J. Am. Chem. Soc.* **2005**, *127*, 4794.

(14) (a) Power, P. P. *Chem. Rec.* **2012**, *12*, 238. (b) Caputo, C. A.; Guo, J.- D.; Nagase, S.; Fettinger, J. C.; Power, P. P. *J. Am. Chem. Soc.* **2012**, *134*, 7155.

(15) (a) Uhl, W.; Vester, A.; Kaim, W.; Poppe, J. *J. Organomet. Chem.* **1993**, *454*, 9. (b) Pluta, C.; Pörschke, K.-R.; Kruger, C.; Hildenbrand, K. *Angew. Chem., Int. Ed. Engl.* **1993**, *32*, 388. (c) Wehmschulte, R. J.; Ruhlandt-Senge, K.; Olmstead, M. M.; Hope, H.; Sturgeon, B. E.; Power, P. P. *Inorg. Chem.* **1993**, *32*, 2983.

(16) Wright, R. J.; Brynda, M.; Power, P. P. *Angew. Chem., Int. Ed.* **2006**, *45*, 5953.

(17) Wright, R. J.; Phillips, A. D.; Power, P. P. *J. Am. Chem. Soc.* **2003**, *125*, 10784.

(18) Agou, T.; Nagata, K.; Tokitoh, N. *Angew. Chem., Int. Ed.* **2013**, *52*, 10818.

(19) Zhao, Y.; Lei, Y.; Dong, Q.; Wu, B.; Yang, X. − J. *Chem. - Eur. J.* **2013**, *19*, 12059.

(20) Palágyi, Z.; Grev, R. S.; Schaefer, H. F., III *J. Am. Chem. Soc.* **1993**, *115*, 1936.

(21) Chertihin, G. V.; Andrews, L. *J. Phys. Chem.* **1993**, *97*, 10295.

(22) Holzmann, N.; Stasch, A.; Jones, C.; Frenking, G. *Chem. - Eur. J.* **2011**, *17*, 13517.

(23) Hudnall, T. W.; Ugarte, R. A.; Perera, T. A. *N-Heterocyclic Carbenes: From Laboratory Curiosities to Efficient Synthetic Tools*, 2nd ed.; Díez-González, S., Ed.; The Royal Society of Chemistry: London, 2017; Chapter 5, pp 178−237.

(24) Lee, V. Y.; Sekiguchi, A. *Organometallic Compounds of Low-Coordinate Si, Ge, Sn and Pb: From Phantom Species to Stable Compounds*; Wiley: Chichester, 2010.

(25) (a) Sekiguchi, A.; Inoue, S.; Ichinohe, M.; Arai, Y. *J. Am. Chem. Soc.* **2004**, *126*, 9626. (b) Nakata, N.; Sekiguchi, A. *J. Am. Chem. Soc.* **2006**, *128*, 422.

(26) Franz, D.; Irran, E.; Inoue, S. *Dalton Trans.* **2014**, *43*, 4451.

(27) (a) Power, P. P. *Acc. Chem. Res.* **2011**, *44*, 627. (b) Caputo, C. A.; Zhu, Z.; Brown, Z. D.; Fettinger, J. C.; Power, P. P. *Chem. Commun.* **2011**, *47*, 7506. (c) Caputo, C. A.; Koivistoinen, J.; Moilanen, J.; Boynton, J. N.; Tuononen, H. M.; Power, P. P. *J. Am. Chem. Soc.* **2013**, *135*, 1952. (d) Sasamori, T.; Sugahara, T.; Agou, T.; Sugamata, K.; Guo, J. − D.; Nagase, S.; Tokitoh, N. *Chem. Sci.* **2015**, *6*, 5526.

(28) The search was carried out through the WebCSD: online portal to Cambridge Structural Database, search conducted July 2017.

(29) Bonyhady, S. J.; Collis, D.; Frenking, G.; Holzmann, N.; Jones, C.; Stasch, A. *Nat. Chem.* **2010**, *2*, 865.

DOI: 10.1021/jacs.7b08890
J. Am. Chem. Soc. 2017, 139, 14384−14387

6.6. Dialumenes – Aryl vs. Silyl Stabilisation for Small Molecule Activation and Catalysis

Title: Dialumenes – Aryl vs. Silyl Stabilisation for Small Molecule Activation and Catalysis

Status: Article, published online April 21, 2020

Journal: Chemical Science, 2020, 11, 4817-4827.

Publisher: Royal Society of Chemistry

DOI: 10.1039/D0SC01561J

Authors: Catherine Weetman, Amelie Porzelt, Prasenjit Bag, Franziska Hanusch, Shigeyoshi Inoue

Content: This report is an extension of the dialumene project (chapter 6.5). The report targets the differences in structure and reactivity between the already published silyl-substituted dialumene **3^{Si}** and Tipp-substituted dialumene **3**, introduced in this report. Again synthesis of its precursor, namely I^{i}Pr$_2$Me$_2$AlI$_2$Tipp (**2**), was key to access the new dialumene **3**, which is obtained upon reduction of **2** with KC_8. Different to *trans*-planar **3^{Si}**, SC-XRD analysis of dialumene **3** revealed a *trans*-bent and twisted structure. In depth DFT calculations on different model systems revealed the steric demand of the ligand being responsible for the observed structural differences, which enabled the possibility of delocalisation of the π(AlAl) bond onto the NHC moiety in **3**. Moreover, also the electronic properties are affected, with a decreased HOMO-LUMO gap and changed polarisation of the Al_2 core in **3** due to increased polarisation of the Al–Tipp bonds. Thus, an enhanced reactivity as well as increased accessibility of the Al_2 core in reaction with strong bonds was anticipated. Experimental investigations on the reactivity of **3** started with C–C multiple bonded reagents. In comparison to **3^{Si}**, conversion with phenylacetylene solely yielded the [2+2] cycloaddition product, which underwent intramolecular C–H activation to yield styrene. Compound **3** was also able to react with the sterically more demanding di(phenyl)acetylene, which was not possible in **3^{Si}**. Additionally, the reactivity of **3** towards C≡N triple bonds was tested, which yielded butterfly compound **7** as the first of its kind for aluminium. Activation of small molecules like CO_2, O_2 and NO_2 revealed results similar to the silyl-version, albeit the inorganic epoxide **11** was obtainable for the Tipp-substituted dialumene. Additionally, the aryl-substituted compound **3** was further shown to enable the activation of H_2, supported by DFT calculations. In addition to these results, the comparison of the two dialumenes in the catalytic application in hydroboration of CO_2 and amine borane dehydrogenation was conducted. In both cases, product distributions were highly dependent on the used ligand, thus giving rise to different accessible pathways for those reactions solely by change of the ligand. In summary, we report the second example of a NHC-stabilised dialumene with its fundamental structure and reactivity highly differing depending on the ligand, which was revealed in a combined experimental and theoretical approach.

Contributions to the publication:

- DFT calculations to determine the differences between the dialumenes **3** and **3^{Si}**, including sterically reduced systems and corresponding monomers for both cases
- NBO analysis of compounds **3**/**3^{Si}**, the smaller model systems, their monomers and **7**
- Calculations on the structure of **11** and **12**, as (discussable) SC-XRD data were missing
- Interpretation of the data
- Writing of the manuscript

Chemical Science

ROYAL SOCIETY OF CHEMISTRY

EDGE ARTICLE

View Article Online
View Journal | View Issue

Cite this: *Chem. Sci.*, 2020, **11**, 4817

All publication charges for this article have been paid for by the Royal Society of Chemistry

Dialumenes – aryl *vs.* silyl stabilisation for small molecule activation and catalysis†

Catherine Weetman, Amelie Porzelt, Prasenjit Bag, Franziska Hanusch and Shigeyoshi Inoue *

Received 16th March 2020
Accepted 17th April 2020

DOI: 10.1039/d0sc01561j

rsc.li/chemical-science

Main group multiple bonds have proven their ability to act as transition metal mimics in the last few decades. However, catalytic application of these species is still in its infancy. Herein we report the second neutral NHC-stabilised dialumene species by use of a supporting aryl ligand (**3**). Different to the *trans*-planar silyl-substituted dialumene (**3^{Si}**), compound **3** features a *trans*-bent and twisted geometry. The differences between the two dialumenes are explored computationally (using B3LYP-D3/6-311G(d)) as well as experimentally. A high influence of the ligand's steric demand on the structural motif is revealed, giving rise to enhanced reactivity of **3** enabled by a higher flexibility in addition to different polarisation of the aluminium centres. As such, facile activation of dihydrogen is now achievable. The influence of ligand choice is further implicated in two different catalytic reactions; not only is the aryl-stabilised dialumene more catalytically active but the resulting product distributions also differ, thus indicating the likelihood of alternate mechanisms simply through a change of supporting ligand.

Introduction

The ability to isolate and stabilise complexes containing metal–metal bonds is of fundamental interest, providing both experimental and theoretical insights into the intrinsic nature of the metal centre.[1] Since the discovery that the so-called 'double bond rule' could be broken in the beginning of the last quarter of the 20th century,[2–5] efforts within main group chemistry have strived towards isolating a plethora of both homo- and hetero-main group element multiply bonded compounds, which have been the subject of numerous reviews.[6,7] Aside from curiosity, one of the driving forces behind this research area is the ability to use main group multiple bonds as transition metal mimics.[8–10] This is possible due to similarly energetically accessible frontier molecular orbitals. Thus, reduction of small molecules, such as dihydrogen, under ambient conditions by sustainable main group metal centres is achievable.[11]

Whilst the ability to mimic transition metals is now possible in regard to oxidative addition reactions, main group elements still fall short in terms of catalytic activity due to the resulting stability of the higher oxidation state complexes, *i.e.* the first step in a redox based catalytic cycle. In order to truly compete with transition metals that are currently employed in industry, the ability to influence the stability, and thus reactivity, of main group metal centres is paramount. One method of influencing stability is through choice of stabilising ligand. If you consider disilenes, the choice of silyl, aryl and nitrogen-based ligands has been shown to influence the structural parameters around the double bond,[12,13] with silyl groups tending towards *trans*-planar geometries[13] and aryl groups promoting *trans*-bent character. It was not until the use of an N-heterocyclic imine (NHI) based ligand, which results in a highly *trans*-bent and twisted geometry, that dihydrogen activation was achieved.[14]

An electropositive silyl supporting ligand was used to stabilise the first neutral aluminium–aluminium double bond, namely dialumene.[15] DFT calculations found the HOMO to consist of a π-bond formed from almost pure Al p-orbitals and as such a planar geometry was observed. As predicted, the dialumene behaved as a transition metal mimic towards a variety of small molecules, as well as enabling catalytic reduction of CO_2.[16] Prior to the isolation of the first neutral dialumene, several compounds with Al–Al bond orders greater than 1 were isolated.[17] These can be classed as radical mono-anionic species, one electron π-bonded compounds, a dianionic complex and masked dialumenes. The stick with latter, reported independently by Power[18] and Tokitoh,[19] proposed the intermediacy of aryl-stabilised dialumenes, with the masked species being a result of [2 + 4]-cycloaddition reaction due to the use of aromatic solvent. This was additionally accounted for through a series of [2 + 2]-cycloaddition reactions with internal alkynes. Tokitoh further showed that the benzene derived masked species was capable of activating dihydrogen;[20] however, upon switching to an anthracene derived masked species no reactivity towards dihydrogen was observed.

Department of Chemistry, Catalysis Research Center and Institute of Silicon Chemistry, Technische Universität München, Lichtenbergstra ße 4, 85748, Garching bei München, Germany. E-mail: s.inoue@tum.de

† Electronic supplementary information (ESI) available. CCDC 1989167–1989172. For ESI and crystallographic data in CIF or other electronic format see DOI: 10.1039/d0sc01561j

On descending group 13, heavier digallenes and dithallenes have been isolated which show notable *trans*-bent character and have been known to dissociate to their corresponding monomers in hydrocarbon solutions.[21–25] However, digallanes have been shown to react as the double bonded species, rather than the monomer with regards to cycloadditions of unsaturated C–C bonds and even dihydrogen activation.[26–28]

Motivated by our group's previous efforts in dialumene chemistry, we targeted the isolation of a neutral aryl-stabilised dialumene to compare the intrinsic nature of the aluminium–aluminium double bond through the influence of ligand stabilisation. Whilst silyl and aryl groups have been routinely used in main group multiple bond chemistry, no direct comparisons of their influence on multiple bonds as reactive species have been drawn. As such, we proposed a systematic study of both dialumenes towards activation of a range of small molecules and their use in catalysis, with the aim of providing experimental and theoretical insight into the influence of these ligand classes on main group multiple bond reactivity.

Results and discussion

Synthesis of aryl-stabilised dialumene

Following on from the successful isolation of the first neutral dialumene, we focused our attention on expanding the scope of this class of compounds towards aryl stabilised systems. As such, we targeted the use of the Tipp ligand (Tipp = 2,4,6-tri-*iso*-propylphenyl) for the stabilisation of a new dialumene. In keeping with the previous dialumene, the choice of N-heterocyclic carbene (NHC) remained the same, $I^iPr_2Me_2$ ($I^iPr_2Me_2$ = 1,3-di-*iso*-propyl-4,5-dimethyl-imidazolin-2-ylidene). Direct reaction of $I^iPr_2Me_2AlH_3$ and LiTipp at −78 °C resulted in formation of the monosubstituted aluminium dihydride complex $I^iPr_2Me_2Al(Tipp)H_2$ (**1**) (Scheme 1) in good yield (66%, ^{27}Al: δ 112.9 ppm).[29] The identity of compound **1** was confirmed upon inspection of the ^{1}H NMR spectrum wherein three resonances for the *iso*-propyl groups were identified in a 2 : 2 : 1 ratio (NHC : *o*-Tipp : *p*-Tipp *iso*-propyl signals) as well as a characteristic broad signal for the Al–H_2 protons (^{1}H: δ 5.11 ppm). Additionally, a sharp IR stretching band at 1711 cm^{-1} (Al–H) was observed in the IR spectrum.

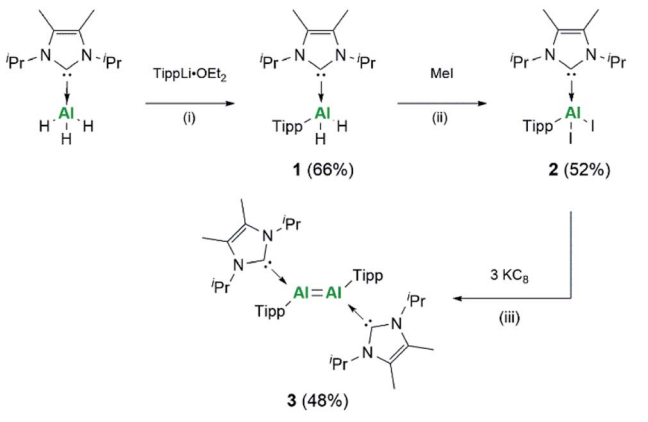

Scheme 1 Synthesis of aryl substituted Al compounds, Tipp = 2,4,6-tri-*iso*-propylphenyl. Reaction conditions: (i) TippLi·OEt_2, Et_2O −78 °C to RT 48 h; (ii) MeI, toluene 0 °C to RT 24 h; (iii) 3 eq. of KC_8, C_6H_6, RT 72 h.

Conversion of **1** towards formation of $I^iPr_2Me_2Al(Tipp)I_2$ (**2**) could be achieved through reaction with BI_3·dms (dms = dimethyl sulfide) or with a small excess of methyl iodide, with the latter resulting in higher and cleaner conversion; moreover, the concomitant formation of methane allows for facile reaction monitoring. Loss of signals relating to Al–H were observed in both the ^{1}H NMR and IR spectra, and further characterisation by single crystal XRD confirmed the identity of **2** (Fig. S54†). Compound **2** is structurally analogous to the corresponding silyl supported complex ($\mathbf{2^{Si}}$) with Al–C^{NHC} bond lengths essentially the same (**2**: 2.0645(18) Å; $\mathbf{2^{Si}}$: 2.0673(17) Å), indicating the dative nature of the NHC ligand. This is additionally confirmed on comparison with the Al–C^{Tipp} bond length (1.9887(19) Å), which is smaller than the sum of the covalent radii (R_{Al-C} = 2.01 Å).[30]

Following the analogous synthetic protocol to the silyl dialumene, compound **2** was stirred vigorously with KC_8 at room temperature (Scheme 1). Through monitoring the reaction by ^{1}H NMR, it was found that this reaction requires 72 hours rather than the 24 hours required for the previous case. Compound **3** was isolated as a black solid, and in contrast to the silyl stabilised dialumene ($\mathbf{3^{Si}}$), **3** is highly soluble in a broad range of aromatic, alkyl and ethereal solvents. Both dialumenes are stable in the solid state in an inert atmosphere for prolonged periods; however, they decompose in solution after 24 hours. The ^{1}H NMR spectrum of **3** shows a large broad signal at room temperature (~7.0–5.5 ppm) which resolves into distinct signals at 228 K for the *iso*-propyl groups, indicating a degree of rotational fluxionality in this system (Fig. S11†).

Single crystals were grown from a concentrated *n*-hexane solution at 5 °C and revealed a *trans*-bent and twisted geometry of the aryl stabilised dialumene (compound **3**, Fig. 1) (θ = 17.25°, 23.70°, τ = 12.06°), which contrasts with the *trans*-planar geometry observed previously. Furthermore, in $\mathbf{3^{Si}}$ the NHC groups were found to be parallel to each other, whilst in **3** they are found to be almost perpendicular (85°). The change from a planar to a *trans*-bent and twisted geometry has also been observed in disilene chemistry on switching between aryl and silyl-based ligands.[12,13] The Al–Al bond length is 2.4039(8) Å which is fractionally longer than that in the previous dialumene ($\mathbf{3^{Si}}$: 2.3943(16) Å). Another notable difference between the two systems lies in the Al–C_{NHC} bond length (**3**: 2.0596(16), 2.0422(17); $\mathbf{3^{Si}}$: 2.073(3) Å). The shorter bond length in the case of aryl stabilisation likely indicates a decrease in dative character and thus an increase in the covalent nature of the Al–C_{NHC} bond (which is also supported by the calculated bond dissociation energy, see below).

Computational discussion of aryl-stabilised dialumene

To gain a deeper insight into the differences between these two classes of dialumenes, we performed density functional theory (DFT) calculations at the B3LYP-D3/6-311G(d) level of theory (for detailed information see the ESI†). The optimised

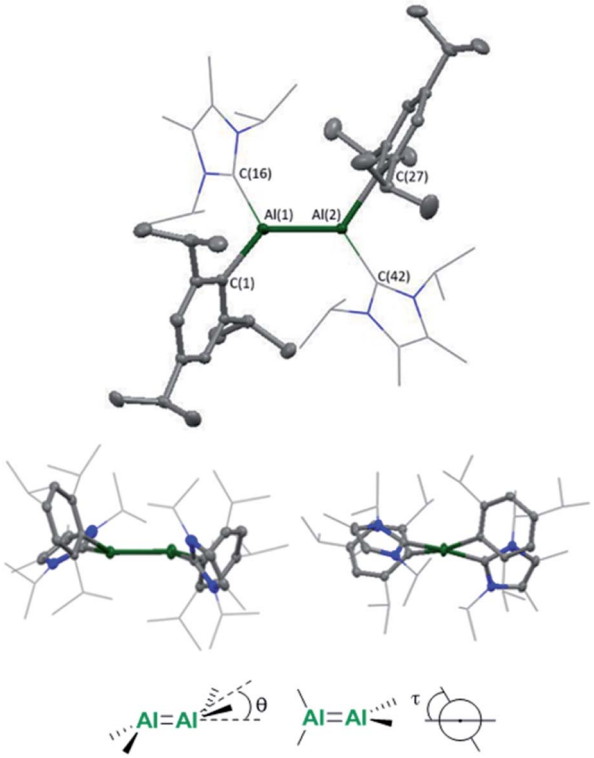

Fig. 1 Molecular structure of compound **3** in the solid state. Ellipsoids are set at the 50% probability level; hydrogen atoms and co-crystallised solvent molecules are omitted for clarity and NHC ligands are depicted in wireframe for simplicity. Selected bond lengths (Å) and angles (°): Al(1)–Al(2) 2.4039(8), Al(1)–C(16) 2.0596(16), Al(2)–C(42) 2.0422(17), Al(1)–C(1) 2.0292(16), Al(2)–C(27) 2.0180(16), C(16)–Al(1)–Al(2) 119.55(5), C(42)–Al(2)–Al(1) 114.13(5), C(1)–Al(1)–Al(2) 123.56(5), C(27)–Al(2)–Al(1) 129.55(5), C(1)–Al(1)–C(16) 110.28(6), C(27)–Al(2)–C(42) 112.84(7), $\theta = 17.25, 23.70$, $\tau = 12.06$.

geometry of **3** is in good agreement with experimental values, with the addition of the dispersion required to account for the *trans*-bent and twisted geometry. For comparison, all calculated values for $\mathbf{3^{Si}}$ including dispersion are given in the ESI.† Analysis of the frontier orbitals of **3** revealed similar features to $\mathbf{3^{Si}}$, in which the HOMO−1 and HOMO contain the Al–Al σ- and π-bonds, respectively, as well as the LUMO representing the Al–C^{NHC} π bond (Fig. 2). The main difference to $\mathbf{3^{Si}}$ (see Fig. S57† for the corresponding orbitals) is the loss of uniform arrangement of the HOMO on the two aluminium centres as well as additional π-incorporation of the NHC present in **3**. We attribute this to the different orientation of the NHCs in **3**, enabling overlap with the p-orbital of the carbene carbon atom, which is experimentally observed as a shortened Al–C^{NHC} bond in the SC-XRD structure and further evidenced by an increased Gibbs free energy of bond dissociation of 26.0 kcal mol^{-1} (*cf.* $\mathbf{3^{Si}}$ = 16.9 kcal mol^{-1}). The conjugation towards the Al–C^{NHC} π-bond in **3** is also observed on inspection of the monomers (for further details see ESI Fig. S62†), which also gives rise to the decreased HOMO–LUMO gap in **3** compared to $\mathbf{3^{Si}}$ (**3** = 1.86 eV, $\mathbf{3^{Si}}$ = 2.24 eV) based on decreased overlap of the monomers being possible.

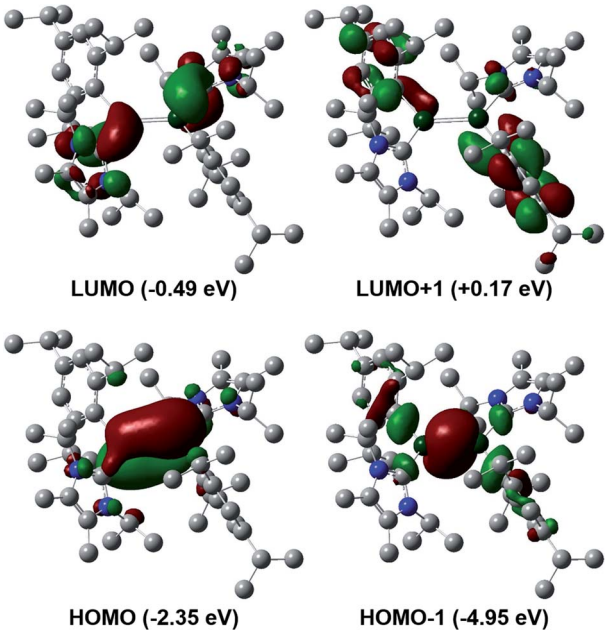

Fig. 2 Frontier orbitals of aryl substituted dialumene **3**.

TD-DFT calculations corroborated the experimental UV/vis spectrum of **3**. This showed an intense absorption band at 833 nm ($\varepsilon = 6273$ L mol^{-1} cm^{-1}) (calc. value 794 nm), which can be assigned to the HOMO to LUMO transition and is responsible for the highly coloured compound.[31] Natural bond orbital (NBO) analysis provided electronic insight into the nature of the Al–Al double bond. The Al–Al π-bond of **3** bears reduced *p*-character compared to $\mathbf{3^{Si}}$. Moreover, this NBO orbital has a lower occupancy based on partial population of the π*-orbitals of the C–N bonds of the NHC, rationalising the increased interaction of the NHC for **3**. This is based on its different orientation, which we mainly attribute to the reduced steric demand of the ligand. Furthermore, this is reflected in the decreased Wiberg bond index (WBI) of the Al–Al bond of 1.67 to 1.53 going from silyl to aryl (Fig. 3), yet still indicating a high degree of multiple bonding character in both systems.

Analysis of NPA charges clearly reflects the silyl effect (Fig. 3): the aluminium centres in $\mathbf{3^{Si}}$ bear a nearly neutral charge of +0.08, while in **3** they account for +0.48/+0.49. We attribute this to the silyl substituents, with their strong σ-donating properties, possessing a more effective orbital overlap with the aluminium centres in the σ(Al–Si) bonds. This also becomes evident upon examination of the results of NBO analysis for the

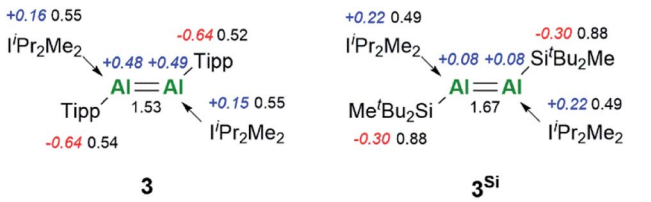

Fig. 3 Results of the NBO analysis of **3** and $\mathbf{3^{Si}}$. NPA charges (blue and red) and WBIs (black).

Al–C^{Tipp}/Al–Si bonds: the Al–C^{Tipp} bonds are highly polarised (17% Al, 83% C^{Tipp}) compared to Al–Si bonds in $\mathbf{3^{Si}}$ (36% Al, 64% Si). This difference is also rationalised upon comparison of Al–C and Al–Si Pauling electronegativities ($\Delta\chi$ Al–C 0.94; $\Delta\chi$ Al–Si 0.29), thus resulting in less polarised Al–Si bonds.

To elucidate the effect of sterics around the aluminium centre, we initially compared the steric demand of the Tipp and Si^{t}Bu$_2$Me ligands, which revealed similar percentages of buried volume (% V_{bur}) of 29.9% (**3**) and 30.7% ($\mathbf{3^{Si}}$) (Fig. S58 and S59†). However, the shape and thus distribution of kinetic stabilisation vary. Further calculation and comparison of reduced model systems were performed with the I^{i}Pr$_2$Me$_2$ carbene replaced by IMe$_4$ ($^{IMe4}\mathbf{3}$ and $^{IMe4}\mathbf{3^{Si}}$, Fig. S60†).[32]

For $^{IMe4}\mathbf{3^{Si}}$ the most stable isomer exhibits a strongly *trans*-bent and twisted geometry ($\theta = 42.1°$, 30.4°, $\tau = 11.7°$) with the NHC planes orientated almost parallel and a substantially elongated Al–Al bond length of 2.43 Å. In the Tipp-substituted $^{IMe4}\mathbf{3}$ the *trans*-bent character is decreased compared to **3**, accompanied by a small increase of the Al–Al bond length due to further rotation of the NHC planes towards the Al–Al plane, enabling more effective π-interaction of NHC and the AlAl moiety. This also becomes more apparent upon examination of the corresponding frontier orbitals with $^{IMe4}\mathbf{3}$. This features enhanced delocalisation of the HOMO onto the NHC moiety, as a consequence of further rotation of the NHC planes towards the Al–Al bond (angle between NHC planes: 49°). In contrast, the HOMO in $^{IMe4}\mathbf{3^{Si}}$ exhibits contributions from the silyl groups, as conjugation towards the NHC π-system is not possible due to the different orientation. Moreover, the HOMO–LUMO gap decreases for aryl and increases for the silyl case, attributed to the decreased/increased *trans*-bent geometry.

The smallest possible model systems, by reducing I^{i}Pr$_2$Me$_2$ to IH$_4$ as well as Tipp/Si^{t}Bu$_2$Me to phenyl/TMS, were calculated and yield comparable results: $^{S}\mathbf{3}$ and $^{S}\mathbf{3^{Si}}$ both possess *trans*-bent but no twisted configuration. In $^{S}\mathbf{3^{Si}}$ a slightly shorter Al–Al bond length and a decreased *trans*-bent angle (21.2° *vs.* 31.8° for $^{S}\mathbf{3}$) are observed; however, in each case the NHC planes are rotated towards the Al=Al bond (see Fig. S61†). Hence, *trans*-bent structures are obtained for the aryl and the silyl substituted dialumenes bearing minimal steric effects. Thus, it is clearly demonstrated that the steric effects of both NHC and the ligands govern the binding motif of dialumenes. The shape of the ligand influences the interaction with the NHC: either only a weak and purely σ-donating type of interaction, as observed in planar $\mathbf{3^{Si}}$, or more flexible coordination of the NHC, with the p-orbital of the $C^{carbene}$ able to form a slipped π-bond with the AlAl core, as observed in **3**. The *trans*-bent and twisted structure obtained for **3** is therefore a result of the difference in steric demand of the Tipp ligand compared to Si^{t}Bu$_2$Me.

From the different aspects, steric as well as electronic, discussed above we thus conclude that the structural difference between **3** and $\mathbf{3^{Si}}$ is caused by the different steric demand of the ligands. From the electronic point of view the change of silyl to Tipp ligand in the dialumene changes the orbital situation at the central AlAl core, which is accompanied by a reduced HOMO–LUMO gap. Moreover, the polarisation of the aluminium centres is different, based on differences in electronegativity between C and Si. We thus anticipate differences in reactivity with respect to activation of strong bonds, such as those in small molecules, as well as an increased accessibility towards a bigger range of reagent molecules of **3**, based on the increased flexibility of this system.

Reactivity of dialumenes

Further differences between these two systems were sought experimentally. Firstly, reactivity towards a series of C–C multiple bonds was examined (Scheme 2). In the case of ethylene, compound **3** underwent formal [2 + 2]-cycloaddition to yield the dialuminacyclobutane compound **4**, akin to the reactivity observed with $\mathbf{3^{Si}}$.[15] Upon reaction with 1 equivalent of phenylacetylene, clean formation of a single species by NMR spectroscopy was noted to occur to form compound **5**. This is in contrast to the reactivity of $\mathbf{3^{Si}}$ where both [2 + 2]-cycloaddition ($\mathbf{5^{Si}}$) and C–H activation were observed. Varying the number of equivalents of phenyl acetylene (2 : 1 and 3 : 1 with respect to **3**) did not result in further incorporation of phenyl acetylene into the complex even at elevated temperatures. However, compound **5** was found to decompose in solution to yield styrene (see ESI Fig. S37 and S38†). Monitoring a C_6D_6 solution of **5** showed that this occurs intramolecularly, with the additional protons required to make styrene likely the result of C–H activation. In further support of an intramolecular C–H activation, addition of a hydrogen source, *e.g.* dihydrogen, phenyl silane, pinacol borane or amine borane, failed to provide any notable increase in the rate of styrene formation. Unfortunately, attempts to identify the fate of the resulting aluminium containing species were unsuccessful. It is proposed that initially [2 + 2]-cycloaddition occurs to form compound **5**, followed by C–H activation of the *iso*-propyl groups of the Tipp ligand, as this was not observed with the analogous silyl complex. Intramolecular C–H activation of the Mes* ligand (Mes* = 2,4,6-tri-*tert*-butylphenyl) has been previously observed by thermolysis of (Mes*)$_2$AlH,[33] whilst 1-germapropadiene, which contains a Ge=C double bond supported by Tipp ligands, also undergoes C–H activation of the Tipp ligand.[34]

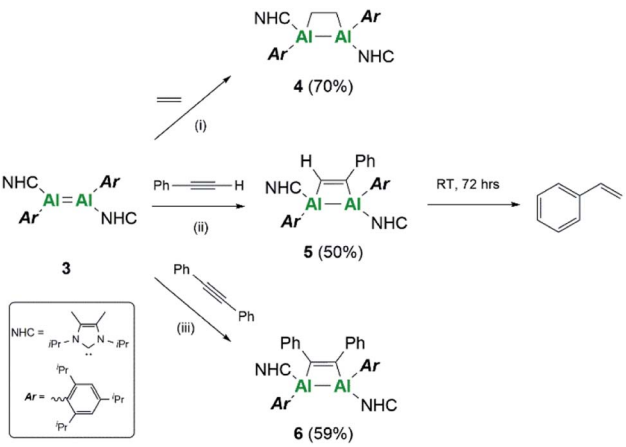

Scheme 2 Reactivity of dialumene (**3**) towards C–C multiple bonds. (i–iii) Toluene, RT, 4 h.

Further reactivity towards C–C multiple bonds was trialed with diphenylacetylene (PhCCPh). Addition of 1 eq. of PhCCPh to $\mathbf{3^{Si}}$ failed to cause a reaction, and after prolonged heating only decomposition of $\mathbf{3^{Si}}$ was observed. In contrast, PhCCPh was observed to react readily with **3**, notably through the instant colour change from the dark black solution of **3** to a yellow solution of compound **6**. This difference in reactivity was surprising, considering that both **3** and $\mathbf{3^{Si}}$ reacted cleanly with both non-polar (ethylene to form **4** and $\mathbf{4^{Si}}$) and polar (phenylacetylene to form **5** and $\mathbf{5^{Si}}$) C–C multiple bonds. This difference in reactivity is thought to be a direct result of the choice of stabilising ligand. The flexibility of the Tipp ligand, due to the rotational *iso*-propyl groups, makes the central AlAl core more accessible for reactant molecules, thus enabling reactivity with more sterically demanding reagents. Moreover, the positive NPA charges of **3** make it more electrophilic in comparison to $\mathbf{3^{Si}}$, thus implying higher reactivity towards nucleophilic C–C multiple bonds.

Compounds **4** and **6** were crystallised from concentrated pentane solutions at −30 °C. The XRD structures revealed addition of the C–C multiple bonds to the dialumene, resulting in the formation of 4-membered rings (Fig. 4). Loss of double bond character from the dialumene was confirmed due to elongation of the Al–Al bond (**4** 2.6035(13), **6** 2.5918(6) *vs.* **3** 2.4039(8) Å). Also noted to occur is the elongation of the Al–C^{NHC} bond lengths (**4** 2.079(3), 2.093(3), **6** 2.1097(15) *vs.* **3** 2.0596(16), 2.0422(17) Å). The 4-membered ring in **6** is almost planar (6.37° between Al–Al–C(27) planes), whilst **4** is puckered due to the presence of the sp^3 carbons.

Extension of this work towards C–N triple bonds focused on the use of 2,6-dimethylphenylisocyanide (XylNC). Previously, Tokitoh and co-workers had shown that reaction of their masked dialumene species resulted in homocoupling of isocyanides.[35] Reactions of varying equivalents of XylNC to $\mathbf{3^{Si}}$ all resulted in an ill-defined mixture of species; unfortunately, attempts to separate species through fractional crystallisation failed. In contrast, reaction of 2 eq. of XylNC with **3** resulted in a clear colour change from black to red and produced a well-defined but complex ^{1}H NMR spectrum of compound **7** (Scheme 3). This complex contains bridging CNXyl units due to the observed downfield signal in the ^{13}C NMR spectrum at δ 303.4 ppm. This was similar to the previously observed bridging carbonyl fragment observed with $\mathbf{3^{Si}}$, in the rearrangement of CO_2 (δ 276.0 ppm)[16] and the bridging isocyanide intermediate reported by Tokitoh (δ 294.7 ppm).[35] Single crystals of **7** were grown from a 2 : 1 (toluene : hexane) mixture at 5 °C, revealing a butterfly configuration with two μ-CNXyl units (Fig. 5).

The central Al–C^{Xyl}–Al–C^{Xyl} core in compound **7** is puckered (34.3° between the two C^{Xyl}–Al–C^{Xyl} planes), with the supporting NHC and Tipp ligands now *cis* to the ring. This change from *trans* to *cis*-conformation has been observed previously for the C–H activated phenylacetylene product on reaction with $\mathbf{3^{Si}}$. However, the reasons for such a change in conformation are unclear. Again, elongation of the Al–C^{NHC} bond lengths are observed (Al–C^{NHC} 2.109(3) Å), with the change in Al–C^{Tipp} negligible (**7** 2.042(7) *vs.* **3** (2.0292(16) Å). Reduction of the C–N triple bond to a double bond is confirmed on inspection of the bond length (C(27)–N(3) 1.292(4) Å), which is in line with average C=N bond lengths.[36–39] Additionally, the change in angle around the nitrogen in XylNC from linear to bent (126.3 (2) °) confirms reduction of the C–N triple bond. This butterfly configuration has been previously observed with transition metal complexes;[40–47] however, they all contain a M–M bond, and those without M–M bonds contain a planar central ring.[48–52]

To confirm the nature of the bonding within compound **7** DFT studies were performed again, at the B3LYP-D3/6-311G(d) level of theory. The optimised structure is in good agreement with the one obtained experimentally by SC-XRD, including the calculated C=N IR stretching frequencies (experimental: 1545 cm^{-1} *vs.* calculated: 1568 cm^{-1}). Orbital analysis (Fig. 6)

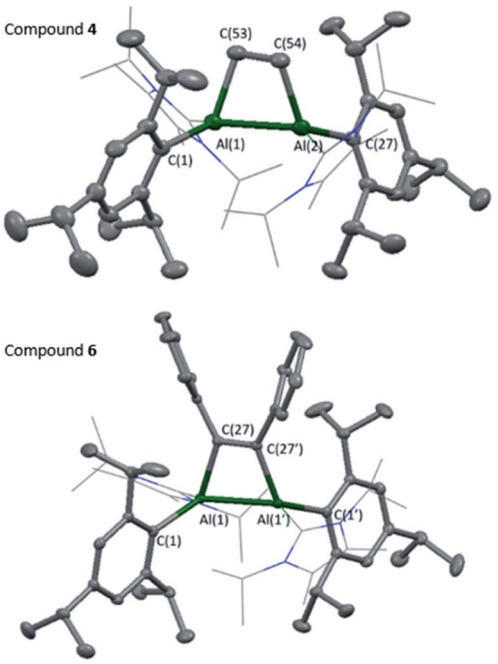

Fig. 4 Molecular structures of compounds **4** and **6** in the solid state. Ellipsoids are set at the 50% probability level; hydrogen atoms and co-crystallised solvent molecules are omitted for clarity and NHC ligands are depicted in wireframe for simplicity. Selected bond lengths (Å) and angles (°): **4**: Al(1)–Al(2) 2.6035(13), Al(1)–C(1) 2.053(3), Al(1)–C(16) 2.079(3), Al(1)–C(53) 2.052(3), C(53)–C(54) 1.565(5), Al(2)–C(27) 2.048(3), Al(2)–C(42) 2.093(3), Al(2)–C(54) 2.040(3), Al(1)–Al(2)–C(54) 73.50(11), Al(2)–Al(1)–C(53) 72.94(11), C(54)–C(53)–Al(1) 101.33(19), C(53)–C(54)–Al(2) 101.23(19). **6**: Al(1)–Al(1′) 2.5918(6), Al(1)–C(1) 2.0413(14), Al(1)–C(16) 2.1097(15), Al(1)–C(27) 2.0246(14), C(27)–C(27′) 1.3701(19), Al(1′)–Al(1)–C(27) 72.19(4), Al(1)–C(27)–C(27′) 107.09(10).

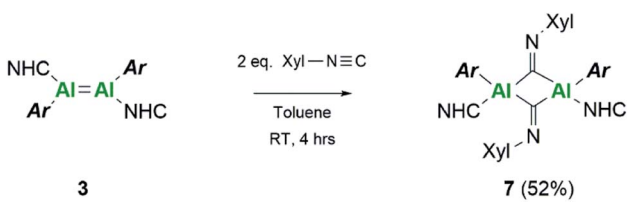

Scheme 3 Reactivity of dialumene (**3**) towards isocyanide.

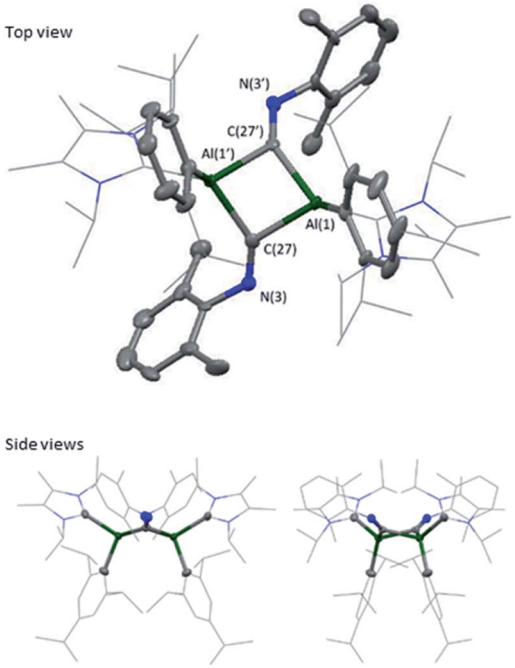

Fig. 5 Molecular structure of compound **7** in the solid state. Ellipsoids are set at the 50% probability level; hydrogen atoms and co-crystallised solvent molecules are omitted for clarity and NHC ligands and iso-propyl groups are depicted in wireframe for simplicity. Selected bond lengths (Å) and angles (°): Al(1)–C(1) 2.042(7), Al(1)–C(16) 2.109(3), Al(1)–C(27) 2.059(3), C(27)–N(3) 1.292(4), Al(1)–C(27)–Al(1′) 91.59(11), C(27)–Al(1)–C(27′) 82.74(11), C(27)–N(3)–C(28) 126.3(2).

revealed the HOMO as an orbital overlap of aluminium and π*(C–N). The LUMO represents the combination perpendicular to the HOMO, including conjugation across the central ring. NBO calculations confirmed that no C–C or Al–Al bond is present in **7** (WBI ($C^{27}C^{27'}$):0.06; WBI ($Al^{1}Al^{1'}$): 0.04).

Small molecule activation

Further reactivity differences were sought through investigation towards small molecules (Scheme 4). Previously, reaction of $\mathbf{3^{Si}}$ towards carbon dioxide (CO_2) resulted in an initial CO_2 fixation complex.[16] This subsequently underwent C–O cleavage reaction, in the absence of additional CO_2 through rearrangement to a bridging carbonyl complex, whilst in the presence of CO_2, formation of a carbonate species with elimination of CO was observed. On reaction of **3** with CO_2 immediate loss of the black

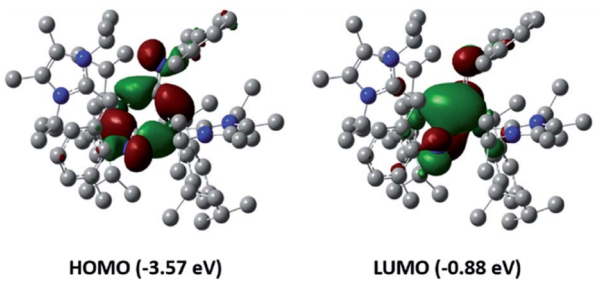

Fig. 6 Frontier orbitals of compound **7**.

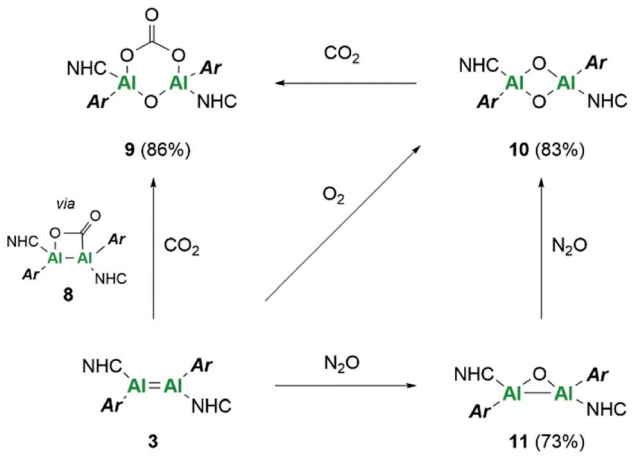

Scheme 4 Reactivity of dialumene (**3**) towards small molecules, CO_2, O_2 and N_2O.

colour and formation of a colourless solution was observed. On inspection of the ^{13}C NMR spectrum, the presence of CO (δ 184.4 ppm) and CO_3 (δ 159.12 ppm) was observed, indicating the formation of the carbonate complex compound **9**. In contrast to $\mathbf{3^{Si}}$, attempts to isolate the CO_2 fixation product were unsuccessful as it rapidly converted to compound **9**. Use of the labile $I^{i}Pr_2Me_2$–CO_2 species allowed for the formal [2 + 2]-cycloaddition product (compound **8**) to be observed due to its characteristic ^{13}C resonance at δ 207.7 ppm ($\mathbf{8^{Si}}$ δ 209.9 ppm). However, this reaction resulted in multiple species as well as compound **9**, owing to the higher reactivity of the Tipp dialumene (compound **3**), thus indicating that formation of **9** proceeds through the CO_2 fixation species in a similar manner to $\mathbf{3^{Si}}$.

Reaction of **3** with O_2 resulted in the expected dioxo product, compound **10**, same as the previously reported reaction of $\mathbf{3^{Si}}$. In a similar manner to $\mathbf{10^{Si}}$, compound **10** can also be reacted with CO_2 resulting in carbonate complex **9**. In a notable difference to the silyl supported reactivity, addition of N_2O to compound **3** resulted in a dark red solution at room temperature ($\mathbf{3^{Si}}$ yielded colourless compound $\mathbf{10^{Si}}$). This red solution was observed to slowly fade to colourless over a few hours and the formation of compound **10** was confirmed by ^{1}H NMR spectroscopy. Use of 1 eq. of an oxygen donor reagent, namely *N*-methylmorpholine-*N*-oxide, with **3** allowed for clean isolation of the red species, compound **11**. Compound **11** is stable in the solid state for up to two months in a glovebox freezer; however, at room temperature and in solution, further oxidation to compound **10** occurs. Whilst ^{1}H NMR showed similar environments for both **10** and **11** (Fig. S39†), compound **11** is intensely coloured (UV/vis = 512 nm, $\varepsilon = 1155$ L mol^{-1} cm^{-1}) whilst **10** is colourless. As such compound **11** was tentatively assigned as a bridging aluminium(II) mono-oxide species, rather than a terminal aluminium(III) mono-oxide complex. Unfortunately, SC-XRD analysis did not provide clear structural parameters for the mono-oxide species due to superposition with compound **10** (Fig. S55†). To provide further insight, calculations were also performed on compounds **10** and **11**. The optimised structure

of **10** is symmetric relating to the Al–O bonds, as previously observed for the analogous silyl compound (**10**^{Si}).[16] TD-DFT calculations revealed the highest transition at 259 nm, in line with the experimental colourless appearance. In contrast, compound **11** bears substantial π-electron density between the two aluminium centres in the HOMO as depicted in Fig. 7, reminiscent of the disilaoxirane reported by our group.[53] The LUMO represents the unoccupied π(Al–C^{NHC}) bond. TD-DFT calculations verified the experimentally observed red colour (UV-vis 512 nm) with good accordance (calc. 519 nm), assigned to the HOMO to LUMO transitions of **11**.

Extension of this small molecule reactivity towards dihydrogen was investigated. Firstly, a J-Young NMR tube containing a purple solution of **3**^{Si} was freeze–pump–thaw degassed and then backfilled with approximately 1 atm of H_2. After 24 hours at room temperature no reaction was noted to have occurred; increasing the temperature to 60 °C and regular monitoring only resulted in the observed decomposition of **3**^{Si}.

Repetition of this reaction with the aryl stabilised dialumene, compound **3**, also resulted in no reaction at room temperature. After 16 h at 50 °C, however, the black colour of **3** had faded to a dark brown/yellow solution (Scheme 5). On inspection of the ^{1}H NMR spectrum, no Al–H signals could be observed owing to the quadrupolar nature of the Al centre. Additionally, three distinct *iso*-propyl signals similar to that observed for compound **1** were identified. These, however, were not identical and therefore complete hydrogenation and cleavage of the Al–Al bond can be ruled out. Thus, it is likely that compound **12** consists of either terminal or bridging hydrides.

IR spectroscopy was utilised to differentiate between the two likely structures; two broad but distinct peaks at 1593 and 1634 cm^{-1} were observed. Compounds containing no Al–Al bond but both terminal and bridging hydrides are found at approximately 1880 cm^{-1} and 1350 cm^{-1}, respectively,[20,54] whilst terminal hydrides within complexes containing Al–Al bonds are found within 1680–1835 cm^{-1},[55] thus pointing more in the direction of a terminal hydride with Al–Al bonds. Additionally, for the previous terminal hydride in the related silyl system, from C–H activation of phenyl acetylene, this Al–H was found at 1666 cm^{-1}.[15] Unfortunately, attempts to grow crystals suitable for SC-XRD were unsuccessful. Therefore, additional insight for this structure was sought computationally. Different possible isomers of product **12** were calculated, including bridging, terminal, and combinations of both as well as different rotational isomers (H: *cis* or *trans*; NHC and Tipp ligands: *cis* or *trans*).

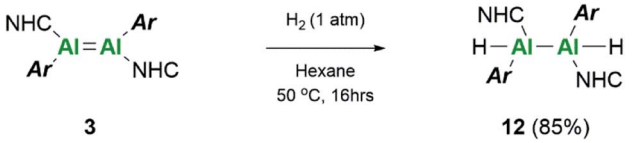

Scheme 5 Reactivity of dialumene (**3**) towards dihydrogen.

The two lowest lying isomers were found to possess terminal hydrides in the *cis* and *trans* configurations (Fig. 8). The Al–H stretching frequencies were calculated to be 1634 and 1676 cm^{-1}, respectively, which is in good agreement with the experimentally obtained values (for detailed information see the ESI†). It is, therefore, suggested that the activation of hydrogen by **3** results in both the *cis* and *trans* isomers of compound **12**.

Catalysis

Further comparisons between the two dialumenes examined their use in catalytic applications. Two archetypal catalytic reactions (hydroboration and dehydrocoupling) were studied due to their prevalence in main group catalysis, as well as the implication of metal-hydrides in facilitating turnover.[56,57] With the ability to form dialuminium-hydrides in the case of **3** and not for **3**^{Si}, differences in activity and mechanistic pathways are anticipated.

CO_2 hydroboration

Previously, **3**^{Si} was found to selectively catalyse the reduction of CO_2 to a formic acid equivalent (product **A**, Scheme 6) with

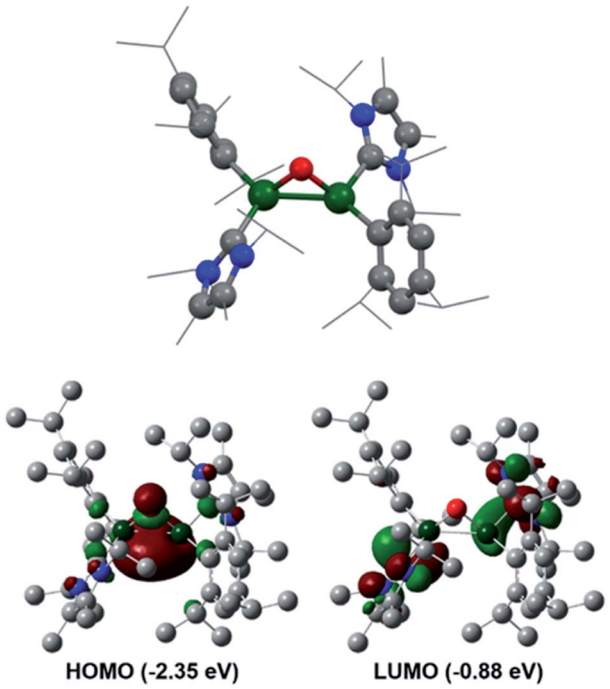

Fig. 7 Calculated molecular structure of compound **11** and its frontier orbitals.

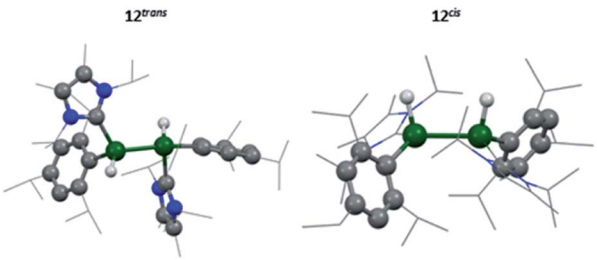

Fig. 8 Calculated molecular structure of **12**^{trans}/**12**^{cis}.

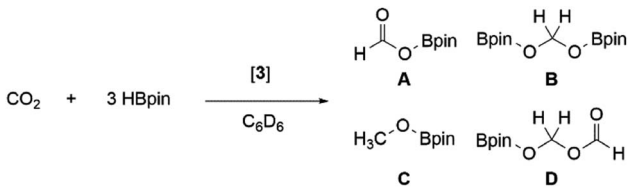

Scheme 6 Catalytic hydroboration of CO_2 mediated by dialumene (**3**).

pinacol borane (HBpin).[16] Whilst this reaction does proceed at room temperature, it required up to 1 week and 10 mol% of $\mathbf{3^{Si}}$ (Table 1, entry 1); use of higher temperatures allowed for reduced catalyst loadings and decreased reaction times (Table 1, entry 2). As **3** has so far shown increased reactivity, a trial reaction with 5 mol% of **3** towards hydroboration of CO_2 at room temperature was carried out (Table 1, entry 3). On regular monitoring through ^{1}H and ^{11}B NMR spectroscopy the consumption of HBpin was noted to occur along with the formation of new B–O containing species. The corresponding ^{1}H NMR spectrum showed the presence of further reduced species (**A–D**, Scheme 6), indicating that **3** is not only more catalytically active, but also proceeds through an alternate mechanism due to the presence of **B–C**.

Again, through use of a higher temperature (60 °C), the catalyst loading could be decreased down to 1 mol% (Table 1, entry 5). This resulted in the same consumption of HBpin after 24 h (at RT) as with 5 mol% (Table 1, entry 4); however, the resulting product distribution differs, with higher temperatures favouring the formation of the triply reduced methanol equivalent (product **C**, Scheme 6).

The formation of more highly reduced species indicates a likely change in the mechanism. Previously, $\mathbf{3^{Si}}$ showed no reactivity towards HBpin and as such a non-hydridic mechanism based on the initial formation of $\mathbf{9^{Si}}$ was proposed. From computational analysis, coordination of HBpin and subsequent reduction of the exocyclic carbonyl of $\mathbf{9^{Si}}$ was found to be rate determining. Turnover was achieved through coordination/insertion of an additional CO_2 on the opposite side of the Al···Al plane resulting in formation of an 8-membered ring which collapses to reform $\mathbf{9^{Si}}$ with release of the formic acid equivalent. This mechanism also further supports the observed selectivity towards product **A**.[16]

In this instance, use of **3** results in the formation of products **B–D** in notable amounts; therefore, an alternative mechanism for the hydroboration of CO_2 is highly likely. As such, **3** was reacted with 1 eq. of HBpin; the ^{11}B NMR spectrum showed complete consumption of HBpin and formation of a new upfield doublet at δ 2.57 ppm (J_{HB} = 112.18 Hz). The same signal and coupling were observed from the reaction of HBpin and $I^iPr_2Me_2$; therefore it is proposed that the stoichiometric reaction of **3** and HBpin results in NHC abstraction. Notably, this does not result in H–B bond cleavage and formation of an Al(H)–Al(Bpin) type species, which was observed with diborene[58] and disilyne[59] chemistry. Addition of CO_2 to this $I^iPr_2Me_2$–HBpin adduct did not result in formation of any reduced CO_2 species, or any reaction after 24 h at room temperature; therefore it is unlikely that this is the catalytically active species. It is of note that NHCs have been shown to catalyse hydroboration (with HBpin) of carbonyl compounds, in acetonitrile.[60]

Whilst these experimental observations preclude definitive mechanistic analysis, it is proposed that the aryl stabilised dialumene (**3**) acts as a pre-catalyst, with CO_2 hydroboration occurring through an initial hydroalumination of CO_2 and subsequent Al–O/B–H σ-bond metathesis, in line with other previously reported main group hydroelementation of CO_2 mechanisms.[61–70]

Amine borane dehydrogenation

Main group catalysts (largely group 1, 2, and 13) have also been shown to be viable dehydrocoupling catalysts.[56,57,71,72] These reactions largely proceed through formation of M–H and M–E

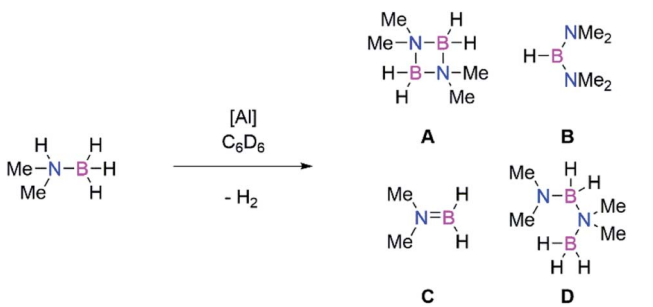

Scheme 7 Catalytic dehydrocoupling of Me_2NHBH_3 mediated by aluminium catalysts.

Table 1 Catalytic hydroboration of CO_2 by dialumenes (**3** and $\mathbf{3^{Si}}$)

						Product distribution[b]/%			
Entry	Catalyst	Loading/mol%	Time/h	Temp/°C	Conversion[a]/%	**A**	**B**	**C**	**D**
1	$\mathbf{3^{Si}}$	10	110	20	86	86	7	7	0
2	$\mathbf{3^{Si}}$	5	4	60	68	94	2	4	0
3	**3**	5	58	20	81	39	27	34	0
4	**3**	5	24	20	66	65	15	17	3
5	**3**	1	24	60	62	49	7	41	3

[a] Conversion of HBpin based on ^{11}B NMR integrals. [b] Ratio of products based on ^{1}H NMR integrals.

Table 2 Catalytic dehydrocoupling of Me_2NHBH_3 by aluminium catalysts

Entry	Catalyst	Loading/mol%	Time/hr	Temp/°C	Conversion[a]/%	Product distribution[b]/%			
						A	**B**	**C**	**D**
1	**3**	5	5	20	72	25	5	—	27
2	**3**	5	44	20	78	35	5	—	23
3	$\mathbf{3^{Si}}$	5	16.5	20	17	5	1	—	11
4	**3**	1	2	20	28	8	1	<1	13
5	**3**	1	16.5	20	60	45	1	<1	14
6	**1**	5	24	20	0	0	0	0	0
7	**1**	5	24	60	31	11	—	—	15

[a] Conversion of Me_2NHBH_3 based on ^{11}B NMR integrals. [b] Ratio of products based on ^{11}B NMR integrals.

bonds, *via* σ-bond metathesis reactions due to the differing protic and hydridic substrates. Therefore, to probe the intermediacy of aluminium hydrides we examined the use of both dialumenes in amine-borane dehydrocoupling catalysis. Use of 5 mol% of **3** and $\mathbf{3^{Si}}$ with Me_2NHBH_3 in C_6D_6 showed rapid evolution of gas at room temperature in the case of the aryl substituted dialumene (**3**). Regular monitoring of both reaction mixtures at room temperature by ^1H and ^{11}B NMR spectroscopy confirmed the formation of H_2 and showed several boron containing species by ^{11}B NMR (Scheme 7, products **A–D**). After 5 h approximately 70% of the Me_2NHBH_3 had been consumed in the case of **3** (Table 2, entry 1); in contrast, the silyl dialumene $\mathbf{3^{Si}}$ after three times as long resulted in 17% consumption of Me_2NHBH_3 (Table 2, entry 3). Notably, prolonged reaction times in the case of the **3** did not lead to significant or complete consumption of Me_2NHBH_3 (Table 2, entry 2), and only a small change in the product distribution was observed with increased reaction times.

It was also possible to use 1 mol% of **3**; again, fast consumption of Me_2NHBH_3 was observed within the first few hours (Table 2, entry 4) with the reaction rate slowing with increased Me_2NHBH_3 consumption (Table 2, entry 5). As aluminium-hydrides have been used in amine borane catalysis previously,[73] and to rule out complete hydrogenation and Al–Al bond cleavage during the reaction, compound **1** was tested for dehydrocoupling activity. After 24 h at room temperature (Table 2, entry 6) no conversion of Me_2NHBH_3 was observed; on increasing the temperature to 60 °C (Table 2, entry 7), some formation of H_2 and products **A–D** was observed. Due to the increased temperature and prolonged reaction times required for compound **1**, it is proposed that the retention of an Al–Al bond accounts for the increased catalytic activity.

Comparable to hydroboration reactions, the aryl stabilised dialumene (**3**) was found to be more catalytically active than the silyl-stabilised counterpart ($\mathbf{3^{Si}}$). Mechanistically speaking, amine-borane dehydrocoupling reactions generally occur through formation of M–H and M–E bonds.[57] As such, it has been shown that formation of Al–H bonds is more accessible from **3** compared to $\mathbf{3^{Si}}$, therefore accounting for the difference in catalytic activity. Both reactions show initial formation of a catalytic equivalent of $HB(NMe_2)_2$ (product **B**, Scheme 7) which then remains constant throughout the catalysis. It has previously been shown by Wright and co-workers that formation of **B** is the result of the formation of the catalytically active Al–H containing species from $Al(NR_3)_3$ (R = Me, iPr).[74] Furthermore, Braunschweig and co-workers recently showed that Me_2NHBH_3 can be used to isolate hydrogenated diborenes; thus, analogous reactivity is anticipated.[75] However, in our hands, stoichiometric reactions of **3** and Me_2NHBH_3 resulted in a mixture of species, whilst reaction with a higher number of equivalents of Me_2NHBH_3 resulted in the dehydrocoupling products. We therefore conclude that the dialumene acts as a pre-catalyst in this reaction and the active catalyst is generated *in situ*.

Conclusions

In conclusion, we have shown the fundamental differences between aryl and silyl supporting ligands for the stabilisation of dialumenes and their subsequent influence on reactivity. The increased flexibility of the *trans*-bent and twisted structure for the aryl dialumene (**3**) enables reactivity with more sterically demanding substrates, and in addition is now able to activate dihydrogen. Further differences are observed in the catalytic ability of the two dialumenes, with the latter exhibiting higher activity. This is likely due to different mechanisms in the catalytic cycle and the ability of the aryl dialumene to stabilise a metal-hydride intermediate in contrast to the silyl ligand.

Conflicts of interest

There are no conflicts to declare.

Acknowledgements

We thank Prof. Dr M. C. Holthausen and Dr J. I. Schweizer (Goethe-Universität Frankfurt am Main) for fruitful discussions, computational resources, and advice. Quantum chemical calculations were performed in parts at the Leibniz Supercomputing Center of the Bavarian Academy of Science and Humanities. We are also grateful to Dr A. Pöthig and Dr C. Jandl for crystallographic advice, and M. Muhr (Prof. R. A. Fischer, TUM) for the LIFDI-MS measurements. This project has received funding from the European Union's Horizon 2020 research and innovation program under the Marie Skłodowska-

Curie grant agreement No 754462 (Fellowship CW), as well as the European Research Council (SILION 637394) and WACKER Chemie AG.

Notes and references

1 F. A. Cotton, C. A. Murillo and R. A. Walton, *Multiple Bonds Between Metal Atoms*, Springer, New York, 3rd edn, 2005.
2 R. West, M. J. Fink and J. Michl, *Science*, 1981, **214**, 1343.
3 P. J. Davidson and M. F. Lappert, *J. Chem. Soc., Chem. Commun.*, 1973, 317a.
4 A. G. Brook, F. Abdesaken, B. Gutekunst, G. Gutekunst and R. K. Kallury, *J. Chem. Soc., Chem. Commun.*, 1981, 191–192.
5 M. Yoshifuji, I. Shima, N. Inamoto, K. Hirotsu and T. J. Higuchi, *J. Am. Chem. Soc.*, 1981, **103**, 4587–4589.
6 P. P. Power, *Chem. Rev.*, 1999, **99**, 3463–3504.
7 R. C. Fischer and P. P. Power, *Chem. Rev.*, 2010, **110**, 3877–3923.
8 P. P. Power, *Nature*, 2010, **463**, 171–177.
9 C. Weetman and S. Inoue, *ChemCatChem*, 2018, **10**, 4213–4228.
10 R. L. Melen, *Science*, 2019, **363**, 479–484.
11 G. H. Spikes, J. C. Fettinger and P. P. Power, *J. Am. Chem. Soc.*, 2005, **127**, 12232–12233.
12 M. Kira, S. Ohya, T. Iwamoto, M. Ichinohe and C. Kabuto, *Organometallics*, 2000, **19**, 1817–1819.
13 M. Kira, *Proc. Jpn. Acad., Ser. B*, 2012, **88**, 167–191.
14 D. Wendel, T. Szilvási, C. Jandl, S. Inoue and B. Rieger, *J. Am. Chem. Soc.*, 2017, **139**, 9156–9159.
15 P. Bag, A. Porzelt, P. J. Altmann and S. Inoue, *J. Am. Chem. Soc.*, 2017, **139**, 14384–14387.
16 C. Weetman, P. Bag, T. Silvási, C. Jandl and S. Inoue, *Angew. Chem., Int. Ed.*, 2019, **58**, 10961–10965.
17 P. Bag, C. Weetman and S. Inoue, *Angew. Chem., Int. Ed.*, 2018, **57**, 14394–14413.
18 R. J. Wright, A. D. Phillips and P. P. Power, *J. Am. Chem. Soc.*, 2003, **125**, 10784–10785.
19 T. Agou, K. Nagata and N. Tokitoh, *Angew. Chem., Int. Ed.*, 2013, **52**, 10818–10821.
20 K. Nagata, T. Murosaki, T. Agou, T. Sasamori, T. Matsuo and N. Tokitoh, *Angew. Chem., Int. Ed.*, 2016, **55**, 12877–12880.
21 N. J. Hardman, R. J. Wright, A. D. Phillips and P. P. Power, *J. Am. Chem. Soc.*, 2003, **125**, 2667–2679.
22 Z. Zhu, R. C. Fischer, B. D. Ellis, E. Rivard, W. A. Merrill, M. M. Olmstead, P. P. Power, J. D. Guo, S. Nagase and L. Pu, *Chem.–Eur. J.*, 2009, **15**, 5263–5272.
23 R. J. Wright, A. D. Phillips, S. Hino and P. P. Power, *J. Am. Chem. Soc.*, 2005, **127**, 4794–4799.
24 E. Rivard and P. P. Power, *Inorg. Chem.*, 2007, **46**, 10047–10064.
25 J. Moilanen, P. P. Power and H. M. Tuononen, *Inorg. Chem.*, 2010, **49**, 10992–11000.
26 C. A. Caputo, J.-D. Guo, S. Nagase, J. C. Fettinger and P. P. Power, *J. Am. Chem. Soc.*, 2012, **134**, 7155–7164.
27 C. A. Caputo, J. Koivistoinen, J. Moilanen, J. N. Boynton, H. M. Tuononen and P. P. Power, *J. Am. Chem. Soc.*, 2013, **135**, 1952–1960.
28 C. A. Caputo and P. P. Power, *Organometallics*, 2013, **32**, 2278–2286.
29 Attempts to follow a similar synthetic strategy to the previous dihalide precursor, *i.e.* halogenation followed by salt metathesis with LiTipp, resulted in a largely unreacted mixture after 36 hrs at room temperature with 10% conversion to a mixture of compounds which could not be separated.
30 P. Pyykkö and M. Atsumi, *Chem.–Eur. J.*, 2009, **15**, 186–197.
31 Compared to $\mathbf{3^{Si}}$, mixing of the π(Al–Al) and π*(C^{NHC}–N) raises the HOMO energy, with the HOMO to LUMO transition shifted to higher wavelength in the UV-vis spectrum. Several smaller absorptions, only observable as a broad band around 600 nm (see Table S4†), are attributed to HOMO to LUMO+1/+3 transitions.
32 Experimental attempts to isolate an IMe_4 stabilised dialumene failed in both silyl and Tipp based systems. This was trialed both through analogous synthetic procedures and ligand exchange reactions on the isolated complexes **3** and $\mathbf{3^{Si}}$.
33 R. J. Wehmschulte and P. P. Power, *Inorg. Chem.*, 1998, **37**, 2106–2109.
34 B. E. Eichler, D. R. Powell and R. West, *Organometallics*, 1999, **18**, 540–545.
35 K. Nagata, T. Agou, T. Sasamori and N. Tokitoh, *Chem. Lett.*, 2015, **44**, 1610–1612.
36 C. Weetman, M. S. Hill and M. F. Mahon, *Chem. Commun.*, 2015, **51**, 14477–14480.
37 W. Uhl and M. Matar, *Z. Naturforsch., B: Chem. Sci.*, 2004, **59**, 1214–1222.
38 R. Lalrempuia, C. E. Kefalidis, S. J. Bonyhady, B. Schwarze, L. Maron, A. Stasch and C. Jones, *J. Am. Chem. Soc.*, 2015, **137**, 8944–8947.
39 J. Spielmann and S. Harder, *Chem.–Eur. J.*, 2007, **13**, 8928–8938.
40 R. C. Pettersen and G. G. Cash, *Acta Crystallogr., Sect. B: Struct. Crystallogr. Cryst. Chem.*, 1977, **33**, 2331–2334.
41 F. A. Cotton and B. A. Frenz, *Inorg. Chem.*, 1974, **13**, 253–256.
42 R. D. Adams, F. A. Cotton and G. A. Rusholme, *J. Coord. Chem.*, 1972, **1**, 275–283.
43 W. E. Carroll, M. Green, A. M. R. Galas, M. Murray, T. W. Turney, A. J. Welch and P. Woodward, *J. Chem. Soc., Dalton Trans.*, 1980, 80–86.
44 T. Takao, N. Obayashi, B. Zhao, K. Akiyoshi, H. Omori and H. Suzuki, *Organometallics*, 2011, **30**, 5057–5067.
45 G. Cox, C. Dowling, A. R. Manning, P. McArdle and D. Cunningham, *J. Organomet. Chem.*, 1992, **438**, 143–158.
46 K. Boss, C. Dowling, A. R. Manning, D. Cunningham and P. McArdle, *J. Organomet. Chem.*, 1999, **579**, 252–268.
47 A. R. Manning, K. Boss, M. G. Cox, A. McCabe, P. Soye, S. C. Wade, P. A. McArdle and D. Cunningham, *J. Organomet. Chem.*, 1995, **487**, 151–162.
48 M. Weidenbruch, B. Brand-Roth, S. Pohl and W. Saak, *Angew. Chem., Int. Ed.*, 1990, **29**, 90–92.
49 M. Weidenbruch, J. Hamann, H. Piel, D. Lentz, K. Peters and H. G. von Schnering, *J. Organomet. Chem.*, 1992, **426**, 35–40.

50 D. Lentz, I. Brüdgam and H. Hartl, *J. Organomet. Chem.*, 1986, **299**, C38–C42.
51 D. Lentz and S. Willemsen, *J. Organomet. Chem.*, 2000, **612**, 96–105.
52 A. K. Adhikari, M. B. Sárosi, T. Grell, P. Lönnecke and E. Hey-Hawkins, *Chem.–Eur. J.*, 2016, **22**, 15664–15668.
53 D. Wendel, T. Szilvási, D. Henschel, P. J. Altmann, C. Jandl, S. Inoue and B. Rieger, *Angew. Chem., Int. Ed.*, 2018, **57**, 14575–14579.
54 R. J. Wehmschulte and P. P. Power, *Inorg. Chem.*, 1994, **33**, 5611–5612.
55 S. J. Bonyhady, D. Collis, G. Frenking, N. Holzmann, C. Jones and A. Stasch, *Nat. Chem.*, 2010, **2**(10), 865–869.
56 M. S. Hill, D. J. Liptrot and C. Weetman, *Chem. Soc. Rev.*, 2016, **45**, 972–988.
57 R. L. Melen, *Chem. Soc. Rev.*, 2016, **45**, 775–788.
58 H. Braunschweig, R. D. Dewhurst, C. Hörl, A. K. Phukan, F. Pinzner and S. Ullrich, *Angew. Chem., Int. Ed.*, 2014, **53**, 3241–3244.
59 K. Takeuchi, M. Ikoshi, M. Ichinohe and A. Sekiguchi, *J. Am. Chem. Soc.*, 2010, **132**, 930–931.
60 T. Li, J. Zhang and C. Cui, *Chin. J. Chem.*, 2019, **37**, 679–683.
61 A. Caise, D. Jones, E. L. Kolychev, J. Hicks, J. M. Goicoechea and S. Aldridge, *Chem.–Eur. J.*, 2018, **24**, 13624–13635.
62 D. Franz, C. Jandl, C. Stark and S. Inoue, *ChemCatChem*, 2019, **11**, 5275–5281.
63 M. D. Anker, M. Arrowsmith, P. Bellham, M. S. Hill, G. Kociok-Köhn, D. J. Liptrot, M. F. Mahon and C. Weetman, *Chem. Sci.*, 2014, **5**, 2826–2830.
64 G. Tan, W. Wang, B. Blom and M. Driess, *Dalton Trans.*, 2014, **43**, 6006–6011.
65 D. Mukherjee, S. Shirase, T. P. Spaniol, K. Mashima and J. Okuda, *Chem. Commun.*, 2016, **52**, 13155–13158.
66 D. Mukherjee, H. Osseili, T. P. Spaniol and J. Okuda, *J. Am. Chem. Soc.*, 2016, **138**, 10790–10793.
67 A. Jana, D. Ghoshal, H. W. Roesky, I. Objartel, G. Schwab and D. Stalke, *J. Am. Chem. Soc.*, 2009, **131**, 1288–1293.
68 T. J. Hadlington, C. E. Kefalidis, L. Maron and C. Jones, *ACS Catal.*, 2017, **7**, 1853–1859.
69 J. A. Abdalla, I. M. Riddlestone, R. Tirfoin and S. Aldridge, *Angew. Chem., Int. Ed.*, 2015, **54**, 5098–5102.
70 A. Jana, G. Tavčar, H. W. Roesky and M. John, *Dalton Trans.*, 2010, **39**, 9487–9489.
71 R. J. Less, R. L. Melen and D. S. Wright, *RSC Adv.*, 2012, **2**, 2191–2199.
72 J. D. Erickson, T. Yi Lai, D. J. Liptrot, M. M. Olmstead and P. P. Power, *Chem. Commun.*, 2016, **52**, 13656–13659.
73 C. Weetman, N. Ito, M. Unno, F. Hanusch and S. Inoue, *Inorganics*, 2019, **7**, 92–103.
74 H. J. Cowley, M. S. Holt, R. L. Melen, J. M. Rawson and D. S. Wright, *Chem. Commun.*, 2011, **47**, 2682–2684.
75 M. Dömling, M. Arrowsmith, U. Schmidt, L. Werner, A. C. Castro, J. O. C. Jiménez-Halla, R. Bertermann, J. Müssig, D. Prieschl and H. Braunschweig, *Angew. Chem., Int. Ed.*, 2019, **58**, 9782–9786.

6.7. S–H Bond Activation in Hydrogen Sulfide by NHC-Stabilized Silyliumylidene Ions

Title: S–H Bond Activation in Hydrogen Sulfide by NHC-Stabilized Silyliumylidene Ions

Status: Article, published online May 24, 2018

Journal: Inorganics, 2018, 6, 54.

Publisher: MDPI

DOI: 10.3390/inorganics6020054

Authors: Amelie Porzelt, Julia I. Schweizer, Ramona Baierl, Philipp J. Altmann, Max C. Holthausen, Shigeyoshi Inoue

Content: Reactivity studies of isolable silyliumylidene ions towards small molecules are limited to only a few. In this publication, we investigated the reactivity of NHC-stabilised silyliumylidene ion **A**/**A'** with hydrogen sulphide in a combined experimental approach. Addition of a H_2S solution to **A** yields NHC-stabilised thiosilaaldehyde, possessing an Si–S bond length closer to the sum of double bond radii than single bond radii. From the analogue reaction, applying the less sterically demanding Tipp group in **A'**, isolation of **B'** was not possible due to lack of kinetic stability. In-depth DFT calculations using NBO and QTAIM analysis revealed a zwitterionic representation of **B** as the most appropriate with an enhanced interaction between silicon and sulphur based on negative hyperconjugation of the lone pairs of sulphur into the antibonding Si–H, Si–C^{NHC} and Si–$C^{m Ter}$ orbitals. Experimental mechanistic studies were precluded by fast conversion of **A** even at sub-zero temperatures. Thus, insight was provided computationally with several possible pathways examined. The energetically preferred route starts with stepwise addition of H_2S to the nucleophilic silicon centre, due to mitigated electrophilicity by coordination of the two NHC moieties. Subsequent barrierless NHC dissociation followed by proton abstraction of the released NHC from the S–H group represents the lowest energy pathway. A concerted NHC dissociation and proton abstraction as well as proton abstraction of the Si–H proton can be ruled out. Intermediacy of the NHC-stabilised chloro-silylene **C** is kinetically precluded based on an activation barrier of 28.8 kcal/mol for the interconversion, which was experimentally verified by heating to 40 °C necessary for several hours to convert **C** to **A** upon addition of one equivalent of NHC. The obtained mechanistic picture with an overall activation barrier of only 15 kcal/mol is fully in line with the experimental observations. Furthermore, an improved and up-scaled synthesis of **A** was included in this report.

Contributions to the publication:

- Planning and execution of all experiments (in parts together with Ramona Baierl during her internship)
- Initiation of the cooperation with the Holthausen group
- Investigation of the reaction mechanism (with guidance of Dr. Julia I. Schweizer)
- Bonding analysis of NHC-stabilised thiosilaaldehyde (with guidance of Dr. Julia I. Schweizer)
- Writing of the manuscript

inorganics

MDPI

Article

S–H Bond Activation in Hydrogen Sulfide by NHC-Stabilized Silyliumylidene Ions

Amelie Porzelt [1], Julia I. Schweizer [2], Ramona Baierl [1], Philipp J. Altmann [1], Max C. Holthausen [2] and Shigeyoshi Inoue [1,*]

1 WACKER-Institute of Silicon Chemistry and Catalysis Research Center, Technische Universität München, Lichtenbergstraße 4, 85748 Garching bei München, Germany; amelie.porzelt@tum.de (A.P.); ga67liz@mytum.de (R.B.); philipp.altmann@mytum.de (P.J.A.)

2 Institut für Anorganische Chemie, Goethe-Universität, Max-von-Laue-Straße 7, 60438 Frankfurt/Main, Germany; schweizer@chemie.uni-frankfurt.de (J.I.S.); Max.Holthausen@chemie.uni-frankfurt.de (M.C.H.)

* Correspondence: s.inoue@tum.de; Tel.: +49-89-289-13596

Received: 24 April 2018; Accepted: 17 May 2018; Published: 24 May 2018

Abstract: Reactivity studies of silyliumylidenes remain scarce with only a handful of publications to date. Herein we report the activation of S–H bonds in hydrogen sulfide by *m*Ter-silyliumylidene ion **A** (*m*Ter = 2,6-Mes_2-C_6H_3, Mes = 2,4,6-Me_3-C_6H_2) to yield an NHC-stabilized thiosilaaldehyde **B**. The results of NBO and QTAIM analyses suggest a zwitterionic formulation of the product **B** as the most appropriate. Detailed mechanistic investigations are performed at the M06-L/6-311+G(d,p)(SMD: acetonitrile/benzene)//M06-L/6-311+G(d,p) level of density functional theory. Several pathways for the formation of thiosilaaldehyde **B** are examined. The energetically preferred route commences with a stepwise addition of H_2S to the nucleophilic silicon center. Subsequent NHC dissociation and proton abstraction yields the thiosilaaldehyde in a strongly exergonic reaction. Intermediacy of a chlorosilylene or a thiosilylene is kinetically precluded. With an overall activation barrier of 15 kcal/mol, the resulting mechanistic picture is fully in line with the experimental observation of an instantaneous reaction at sub-zero temperatures.

Keywords: silicon; *N*-heterocyclic carbenes; silyliumylidenes; small molecule activation; mechanistic insights

1. Introduction

Low-valent main group chemistry is a rapidly developing field and the wealth of new structural motifs, which have been isolated in the past two decades, have increasingly gained interest in using these species for the activation of small molecules and, potentially, for catalysis (for representative reviews see [1–7]). Key to these developments have been the usage of suitable synthetic methodologies in combination with thermodynamic and kinetic stabilization by appropriately chosen ligands. In particular, for the heavier carbon analogue silicon, a plethora of studies reported new low-valent compounds in recent years [8–25] and the chemistry of silylene base adducts has already been carefully developed [14,26–36]. Before these findings, silyliumylidene ions, cationic Si(II) species were found to be promising as similar versatile Lewis amphiphiles [37,38].

In 2004, Jutzi initiated the chemistry of silyliumylidene ions taking advantage of the stabilizing effects of the η^5-coordinated pentamethyl-cyclopentadienyl ligand to prepare hypercoordinate silyliumylidene ion **I** (Figure 1) [39]. Driess and coworkers isolated the two coordinated silyliumylidene ion **II**, stabilized by aromatic 6π-electron delocalization as well as by intramolecular donation of the sterically encumbered β-diketiminate ligand [40]. *N*-heterocyclic carbenes (NHCs) represent another ligand class, widely used in modern main group chemistry. As NHCs are strong σ donors,

their application in main group chemistry enabled the isolation of a large variety of low coordinate and low-valent main group compounds [41,42]. The first NHC-stabilized silyliumylidenes, **III** and **IV** were synthesized by Filippou and coworkers via a three-step protocol from SiI_4 [28], and by Driess and coworkers through the reaction of Roesky's NHC-stabilized dichlorosilylene with their bridged bis-carbene ligand [23].

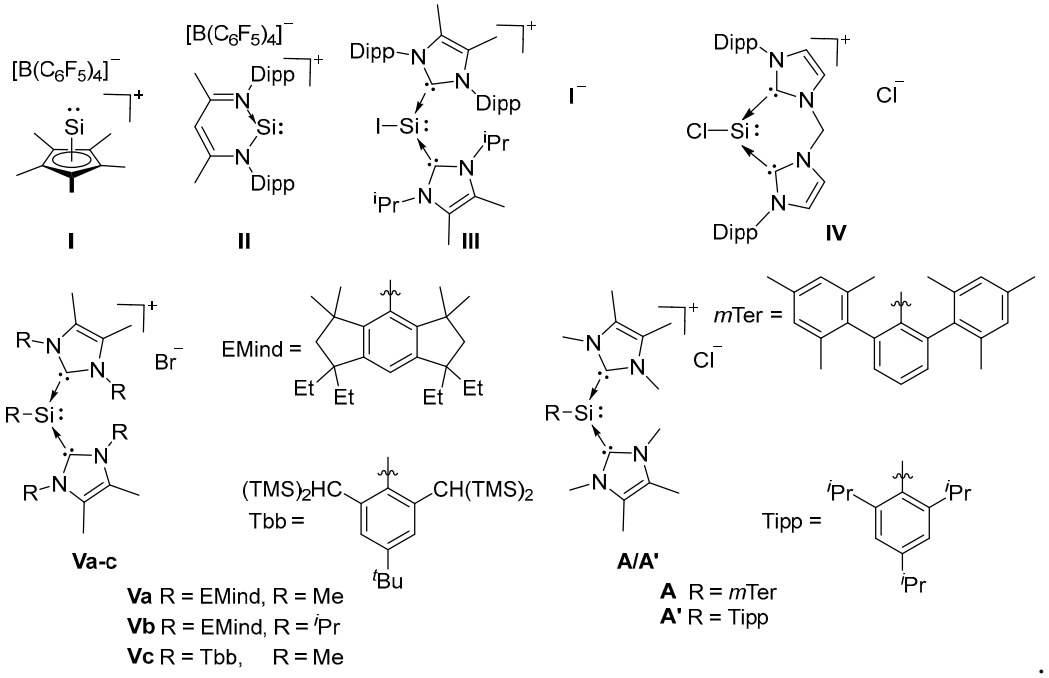

Figure 1. Selected examples of isolated silyiumylidenes.

Sasamori, Matsuo, Tokitoh and coworkers obtained the bulky aryl-substituted silyliumylidenes **Va-c** by treatment of the corresponding diaryldibromodisilene with the carbenes $ImMe_4$ (1,3,4,5-Me_4-imidazol-2-ylidene) or $Im^iPr_2Me_2$ (1,3-$^i Pr_2$-4,5-Me_2-imidazol-2-ylidene) [43]. Around the same time our group reported the *m*Ter- and Tipp-substituted silyliumylidenes **A** and **A'** (*m*Ter = 2,6-Mes_2-C_6H_3, Mes = 2,4,6-Me_3-C_6H_2, Tipp = 2,4,6-$^i Pr_3$-C_6H_2) [44]. Different to all other known silyliumylidenes, **A** and **A'** are accessible via an easy one-step synthesis: the addition of 3 equivalents of $ImMe_4$ to the corresponding Si(IV) aryldichlorosilanes to give the silyliumylidenes via HCl removal by $ImMe_4$ and nucleophilic substitution of chloride. The same approach was recently used by the group of Matsuo, obtaining **Va** via addition of $ImMe_4$ to a solution of (EMind)dichlorosilane (EMind = 1,1,7,7-tetraethyl-3,3,5,5-tetramethyl-s-hydrindacen-4-yl) [45]. It should be noted that the corresponding iodosilyliumylidene stabilized by one NHC and one cAAC (cyclic (alkyl)aminocarbene) moiety have been reported by So and coworkers [46], as well as the parent silyliumylidene [HSi^+] stabilized by two $ImMe_4$ moieties [47].

Although a handful of silyliumylidenes have been reported in the last few years, reactivity studies are limited to the activation of elemental sulfur [24,48], the synthesis of a stable silylone from **IV** [23], and the catalytic application of **I** in the degradation of ethers [49]. For comparison, the neutral silylene derivative of silyliumylidene **II** (Figure 1) has been applied in the activation of several small molecules such as NH_3, H_2S, H_2O, AsH_3 and PH_3 [50–52]. A theoretical assessment of the observed divergent reactivity was provided by Szilvási and coworkers, revealing a unique insertion step to form the 1,4 adducts, followed by varying pathways towards the products [53]. The NHC-stabilized arylchlorosilylene corresponding to **A** has already been published by Filippou and coworkers in 2010, as well as the chlorosilylene with sterically more demanding $m\text{Ter}^{iPr}$ ligand ($m\text{Ter}^{iPr}$ = 2,6-$Tipp_2C_6H_3$) [54]. Subsequently, the $m\text{Ter}^{iPr}$-chlorosilylene was employed as the precursor

for the preparation of a silylidyne complex $Cp(CO)_2Mo{\equiv}Si(mTer^{iPr})$ [55]. The conversion of those chlorosilylenes with lithium diphenylphosphine and $LiPH_2$ to the corresponding phosphinosilylene and 1,2-dihydrophosphasilene reported by Driess and coworkers in 2015 [56,57] as well as the reaction towards diazoalkanes and azides presented by Filippou and coworkers [58] remain as the only reports regarding the reactivity of this species.

In any case, we consider silyliumylidene ions as promising candidates for small molecule activation as they possess two different reactive sites: an electron lone pair, and two empty p-orbitals at the silicon center. The electrophilicity of **A** and **A'** is moderately mitigated by *N*-heterocyclic carbene coordination to the silicon center (Figure 2). Moreover, the zwitterionic representation of **A**/**A'** (Figure 2) emphasizes the view of a silyl-anion, which appears useful further below.

We have already presented the silylene-like reactivity of **A** in the C–H activation of phenylacetylene to give the 1-alkenyl-1,1dialkynylsilane **VI** as the *Z*-isomer exclusively (Figure 2) [44]. We have also reported the application of **A/A'** for the reduction of CO_2 yielding the first NHC-stabilized silaacylium ions (**VII**/**VII'**) [59]. In addition, we have demonstrated the importance of kinetic stabilization by the steric bulk of the aryl ligands. In contrast to **VII**, the less shielded compound **VII'** is kinetically labile even at sub-zero temperatures and could only be characterized spectroscopically. Very recently, we reported the synthesis of the corresponding heavier silaacylium ions **VIIIa-c** obtained from the reactions with CS_2 or S_8, Se, and Te, respectively [60]. Also, we could demonstrate the recovery of silyliumylidene **A** from **VIIIa-c** by the treatment with AuI as well as chalcogen transfer reactions.

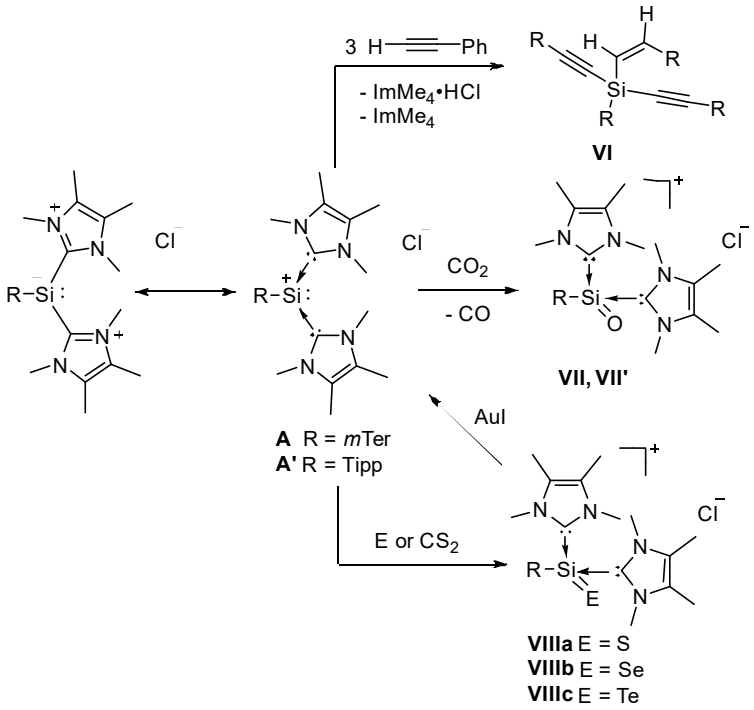

Figure 2. Reactions of silyliumylidenes **A** and **A'**.

For the last 30 years, neutral congeners of **VIIIa-c**, silanechalcogenones $R_2Si{=}E$ with E = S, Se, Te have been studied extensively [61]. In contrast, related compounds of type RHSi=E (E = S, Se, Te) are limited to the studies on intramolecularly stabilized silathioformamide by Driess and coworkers [50] and the NHC-stabilized heavier silaaldehydes by Müller and coworkers [62].

In this article, we further expand our series by the reaction of silyliumylidene **A** with hydrogen sulfide, yielding an NHC-stabilized thiosilaaldehyde, in a combined experimental and theoretical approach.

2. Results and Discussion

*2.1. Reaction of Silyliumylidene **A** with H_2S*

The reaction of NHC-stabilized silyliumylidene **A**, dissolved in acetonitrile, with 1 M H_2S solution in THF proceeded rapidly even at −20 °C, and the orange color of the starting material vanished within seconds. ^{1}H NMR spectroscopy indicated the formation of imidazolium salt, and one remaining $ImMe_4$ coordinated to the silicon center (3.46 ppm, 6H, NCH_3, $ImMe_4$). The splitting of the signals for the ortho-methyl groups and the benzylic protons in the mesityl moieties indicated reduced symmetry in the product. A new signal at 5.35 ppm with ^{29}Si satellites ($^{1}J_{SiH}$ = 209.0 Hz) was assigned to the Si bound hydrogen atom by ^{1}H/^{29}Si-HMBC-NMR spectroscopy. The ^{29}Si NMR signal was shifted down-field from −69.03 ppm in the starting material to −39.59 ppm. Single crystals were obtained after storing the reaction solution at 8 °C overnight. X-ray crystallography confirmed the formation of the NHC-stabilized thiosilaaldehyde **B** (Figure 3). In earlier work by Müller and coworkers, they obtained the analogous species with the bulkier *m*Ter^{iPr} ligand by the reaction of the NHC-stabilized hydridosilylene with elemental sulfur [62]. **B*m*Ter^{iPr}** features the same $^{1}J_{SiH}$ coupling constant (209 Hz), which is smaller compared to the one of silathioformamide (255 Hz) reported by Driess and coworkers. [50]. Compound **B** is stable under the inert atmosphere and shows good solubility in acetonitrile, however, in contrast to thiosilaaldehyde **B*m*Ter^{iPr}**, only a limited solubility in aromatic solvents is observed. Removal of the imidazolium byproduct from **B** was achieved by fractional crystallization from acetonitrile to obtain **B** as an analytically pure crystalline solid in 54% yield. Repetition of the experiments using **A′** featured the same fast decoloring, but the attempts to isolate the corresponding **B′** were not successful, most likely due to the kinetic lability of the formed product.

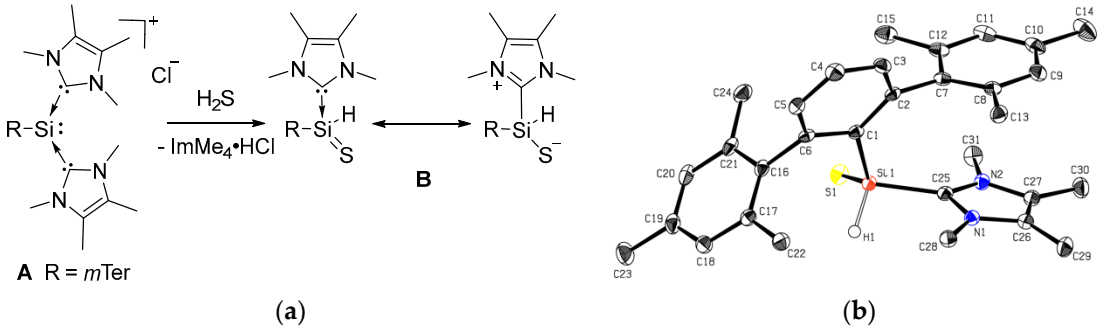

Figure 3. (**a**) Conversion of silyliumylidene **A** to **B** with H_2S and (**b**) the molecular structure of **B**. Thermal ellipsoids are shown at the 50% probability level. Except for the H1 atom, hydrogen atoms are omitted for clarity. Selected bond lengths [Å] and angles [°] of **B**: S1–Si1 2.0227(9), Si1–C1 1.902(2), Si1–C25 1.934(2), Si1–H1 1.41(3), S1–Si1–H1 113.5(11), C1–Si1–S1 121.14(8), C1–Si1–H1 113.3(11).

The tetracoordinate NHC-stabilized thiosilaaldehyde **B** (Figure 3) exhibits a distorted tetrahedral coordination around the silicon atom with a π-stacking of the NHC and a mesityl group of the terphenyl ligand. The Si–S bond length was 2.0227(9) Å, which is slightly longer than in compound **VIIa** (2.013(1) Å and 2.018(1) Å for the two independent molecules) [60], as well as the intramolecular, stabilized thiosilaaldehyde by Driess and coworkers (1.9854(9) Å) [50]. It is closer to the covalent double bond radii of sulphur and silicon (2.01 Å) than to the sum of single bond radii (2.19 Å) [63]. The Si–C^{NHC} bond (1.934(2) Å) and the Si–C^{mTer} bond (1.902(2) Å) are shortened compared to **A** (1.9481(19) Å and 1.9665(19) Å/1.9355(19) Å). The structural parameters are close to those of **B*m*Ter^{iPr}** [62].

Further insight into the nature of the Si–S bond in **B** is provided by density functional theory (DFT) computations at the M06-L/6-311++G(2d,2p)//M06-L/6-31+G(d,p) level. For all bonding analyses, we chose a truncated molecular model replacing the *m*Ter ligand by phenyl and $ImMe_4$ by

$ImMe_2H_2$ (1,3-Me_2-imidazol-2-ylidene). The computed structural parameters of $\mathbf{B}^{\mathbf{Model}}$ agreed well with the experimental molecular structure obtained from X-ray diffraction (see Table S3). Natural bond orbital (NBO) analysis reveal natural localized molecular orbitals (NLMOs, Figure 4b) corresponding to Si–H, Si–C^{NHC}, Si–C^{mTer} and Si–S single bonds as well as three NLMOs representing the electron lone pairs at sulfur. This zwitterionic representation of $\mathbf{B}^{\mathbf{Model}}$ is also the dominant Lewis resonance structure within the natural resonance theory (NRT) formalism (Figure 4a). In line with analysis by Müller and co-workers [62], the short Si–S bond and the Wiberg bond index of 1.38 can be rationalized by negative hyperconjugation [64,65] of the sulphur lone pairs into the σ*(Si–R) orbitals: the occupancy of the LP(S) NBOs is significantly decreased (1.81 e, 1.76 e), while the NBOs for the anti-bonding σ*-orbitals are partly populated (Si–H: 0.11 e, Si–C^{NHC}: 0.14 e, Si–C^{mTer}: 0.12 e). Topological analysis of the computed electron density, by means of Bader's quantum theory of atoms in molecules (QTAIM) [66,67], characterizes the Si–S bond as a strongly polar covalent interaction as indicated by a marked shift of the bond-critical point (bcp) towards the more electropositive Si site, a relatively large electron density ρ_{bcp}, a positive Laplacian $\nabla^2]\rho_{bcp}$ as well as a negative total energy density H_{bcp} at the bcp (Figure 4c) [68,69].

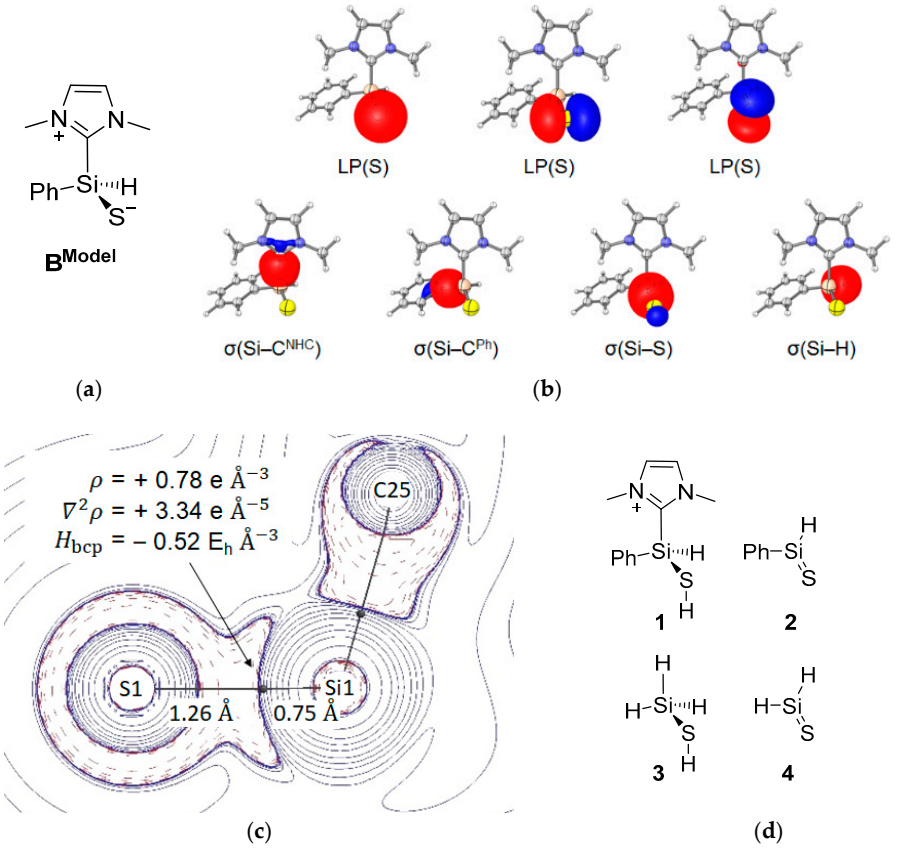

Figure 4. Results of the bonding analysis of $\mathbf{B}^{\mathbf{Model}}$. (**a**) Dominant Lewis resonance structure according to NRT analysis, (**b**) NLMOs representing the electron lone pairs at sulphur and the Si–C^{NHC}, Si–C^{Ph}, Si–S, and Si–H single bonds, (**c**) 2D plot of $\nabla^2\rho$(r) charge concentration (- - -), and depletion (—), bond path (—) and bcps (black dots) with characteristic properties and bond path lengths of the Si–S bond, (**d**) related compounds **1**–**4**.

For a classification of further characteristics at the Si–S bcp, we analyzed related species containing a Si–S single bond (**1** and parent compound **3**) or a Si=S double bond (**2** and parent compound **4**, Figure 4d). The results of the corresponding QTAIM analyses are summarized in Table 1. All molecular graphs display a characteristic shift of the Si–S bcp towards the more electropositive silicon site. In line

with expectation, the values of ρ_{bcp} and $\nabla^2\rho_{bcp}$ are higher for double bonded compounds **2** and **4** compared to single bonded compounds **1** and **3**. The electron density and its Laplacian for the Si–S bond in $\mathbf{B^{Model}}$ are located in between, suggesting the presence of a partial double bond [70,71]. Also, the delocalization gradient $\delta_{Si,S}$, i.e., the number of electron pairs shared between two atoms, lies between the values for the single and double bonded species. However, the bond ellipticity ε_{bcp}, a measure of ρ_{bcp} anisotropy indicating the π character of a bond, is rather small with a value of 0.01. Nevertheless, the Si–S bond shortening, as well as the decrease in ellipticity compared to ε_{bcp} for the Si–S single bonds in **1** and **3**, agree with the presence of negative hyperconjugation in $\mathbf{B^{Model}}$ [72], which was already observed within the NBO framework.

Table 1. Results of QTAIM analyses of $\mathbf{B^{Model}}$ and **1**–**4**. Selected properties of the electron density distribution of the Si–S bond: Bond path lengths $d_{Si–S}$, and distances to bcps $d_{Si–bcp}$ and $d_{bcp–S}$, the electron density ρ_{bcp}, the Laplacian of the electron density $\nabla^2\rho_{bcp}$, the total energy density H_{bcp}, the bond ellipticity $\varepsilon_{bcp} = \lambda_1/\lambda_2 - 1$ (derived from the two negative eigenvalues of the Hessian matrix of the electron density at the bcp with $\lambda_1 \geq \lambda_2$), delocalization index $\delta_{Si,S}$.

Compound	$d_{Si–S}$ [Å]	$d_{Si–bcp}$ [Å]	$d_{bcp–S}$ [Å]	ρ_{bcp} [eÅ^{-3}]	$\nabla^2\rho_{bcp}$ [eÅ^{-5}]	H_{bcp} [E$_h$Å^{-3}]	ε_{bcp}	$\delta_{Si,S}$
$\mathbf{B^{Model}}$	2.00	0.75	1.26	0.78	3.33	−0.52	0.01	0.78
1	2.13	0.77	1.36	0.66	1.36	−0.43	0.12	0.56
2	1.95	0.73	1.22	0.83	5.24	−0.55	0.21	1.15
3	2.14	0.78	1.37	0.64	1.36	−0.40	0.10	0.57
4	1.94	0.73	1.21	0.83	5.39	−0.56	0.23	1.25

These results support a zwitterionic nature of **B** with the partial double bond character of the Si–S bond due to negative hyperconjugation. This enhanced interaction between silicon and sulphur is reflected experimentally by the short bond length found in single crystal XRD analysis.

*2.2. Mechanistic Investigations on the Reaction of Silyliumylidene **A** with H_2S*

The reaction of H_2S and **A** proceeds instantaneously, preventing the NMR detection of intermediates to gain further information on this conversion. To rule out the formation of chlorosilylene **C** as reaction intermediate, we investigated the interconversion of **C** and **A** in a combined experimental and theoretical approach (Figures 5 and 6).

Addition of one further equivalent of $ImMe_4$ to a solution of chlorosilylene **C** in benzene at RT lead to no change in color or ^{1}H-NMR. Heating of the reaction solution to 40 °C resulted in slow darkening of the solution to orange. After several hours the formation of orange crystals in the lower part of the Schlenk tube was observed, yielding silyliumylidene **A** in 58% isolated yield after a prolonged reaction time of 18 h. The reverse reaction could not be demonstrated experimentally due to the limited stability of chlorosilylene **C** and $ImMe_4$ in MeCN, the sole solvent in which **A** is soluble and stable.

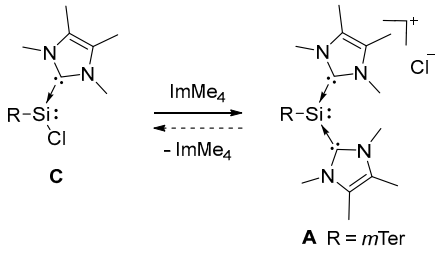

Figure 5. Interconversion of chlorosilylene **C** and silyliumylidene **A** at 40 °C.

DFT calculations on the interconversion of **C** and **A** were performed at the M06-L/6-311+G(d,p) (SMD = benzene)//M06-L/6-31+G(d,p) level of theory with a marginally reduced molecular model

(*m*Ter reduced to 2,6-diphenyl-C_6H_3 and $ImMe_4$ replaced by $ImMe_2H_2$). Silyliumylidene **7** is only slightly lower in energy than chlorosilylene **5** (Figure 6). This is in accordance with a report on the related silyliumylidene ions **Vb** and **Vc**, for which a substituent-dependent shift in relative stabilities was observed [43]. We further investigated the potential energy surface of the interconversion: NHC addition to chlorosilylene **5** via **TS56** ($\Delta^{\ddagger}G$ = 19.6 kcal/mol) leads to tetracoordinate **6**, which is located as an unstable intermediate (18.8 kcal/mol). En route to silyliumylidene ion **7**, a substantial effective barrier of 28.4 kcal/mol for the chloride dissociation in **TS67** is found. This is in line with interconversion of chlorosilylene **C** to silyliumylidene **A** taking place at elevated temperatures but clearly incompatible with the H_2S activation that takes place at −20 °C. Based on our combined experimental and theoretical studies, we thus conclude that formation of thiosilaaldehyde **B** does not involve intermediacy of chlorosilylene **C**.

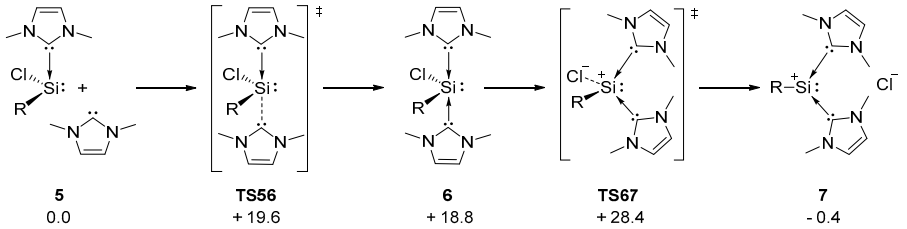

Figure 6. Computed pathway for the interconversion between **5** and **7**, R = 2,6-diphenyl-C_6H_3 and $ImMe_2H_2$; ΔG^{298} in kcal/mol.

The reaction of **8** with hydrogen sulfide commences with a proton transfer via **TS89** to give intermediate **9** as an ion pair in an exergonic step (Figure 7) (M06-L/6-311+G(d,p) (SMD:acetonitrile)//M06-L/6-31+G(d,p) level of theory). Subsequently, the SH moiety adds to the silicon center to yield **10**, a pentacoordinate intermediate, with an effective barrier of 15.1 kcal/mol. The assistance of a second H_2S molecule in **TS²89** is entropically disfavored compared to **TS89**. The NHC-stabilized silyliumylidene **8** acts as a nucleophile in the reaction with hydrogen sulfide, as its electrophilicity is saturated by the presence of two coordinating NHCs. Accordingly, the zwitterionic representation of **8** in the following best emphasizes its nucleophilic character.

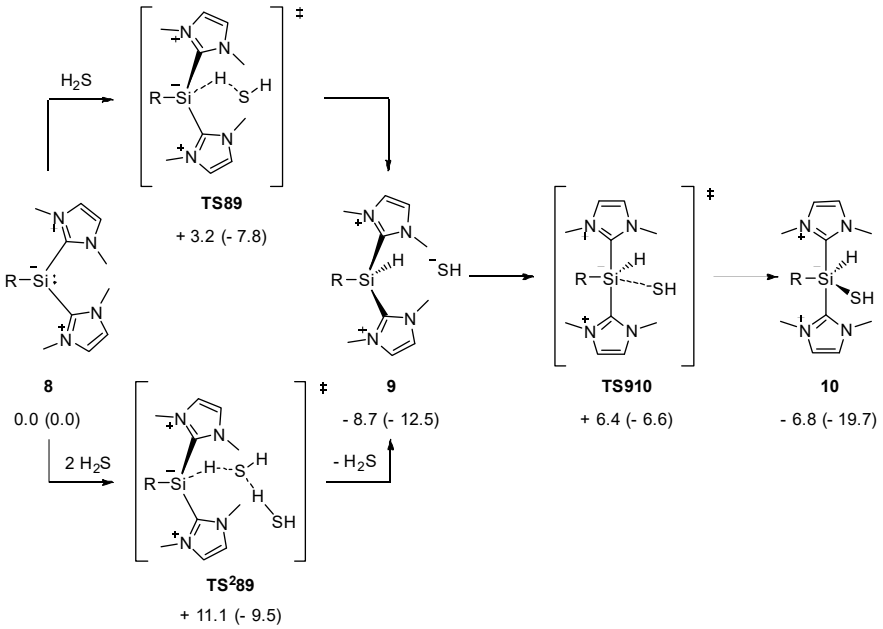

Figure 7. Computed pathway for the reaction from **8** to **10**, R = 2,6-diphenyl-C_6H_3; ΔG^{298} (ΔH^{298}) in kcal/mol.

Starting from **10**, different pathways to NHC-stabilized thiosilaaldehyde **11** were examined (Figure 8). The concerted NHC dissociation and S–H proton abstraction in transition state **TS1011** is connected with a barrier of 6.9 kcal/mol and directly yield **11** in a strongly exergonic reaction. Alternatively, dissociation of one NHC ligand from **10** to **12** was thermodynamically favored and proceeded barrierlessly, as indicated by relaxed potential energy surface scans along the Si–C^{NHC} bonds (see Figures S7 and S8). The NHC liberated subsequently abstracts, with clear kinetic preference, the S–H proton in **12** (**TS1211**: $\Delta^{\ddagger}G$ = 8.7 kcal/mol). The alternative route for Si–H hydride abstraction via **TS1213** is connected with a substantially higher activation barrier ($\Delta^{\ddagger}G$ = 23.5 kcal/mol), which renders this path to **11** kinetically irrelevant. The atomic charges obtained by natural population analysis of **10** (H^{Si}: −0.17 e, H^{S}: 0.18 e) supported the view that the increased activation barrier goes back to the additional charge transfer occuring in the course of the hydride abstraction. Overall, the addition of H_2S to silyliumylidene **8** via **TS910** is rate-limiting with an effective activation barrier of 15 kcal/mol. Subsequent isomerization to thiosilaaldehyde **11** is initiated by barrierless NHC dissociation and accomplished by abstraction of the S–H proton by the free carbene. Concerted proton abstraction and NHC dissociation (**TS1011**) is kinetically disfavored.

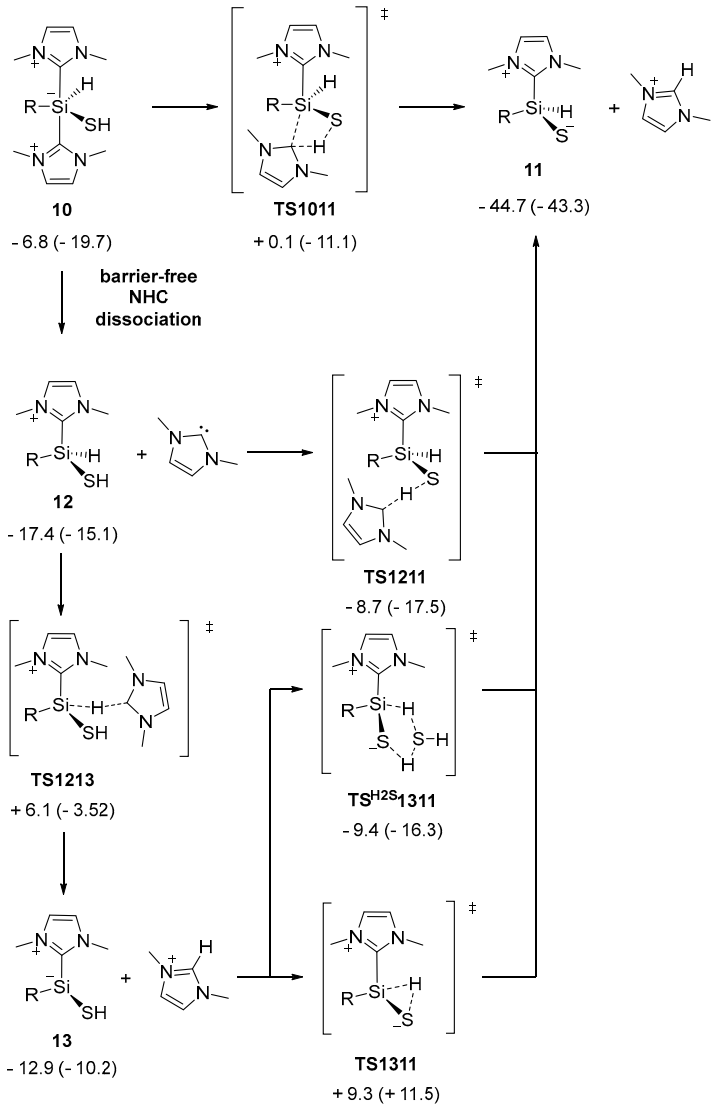

Figure 8. Computed pathway for the reaction from **10** to **11**, R = 2,6-diphenyl-C_6H_3; ΔG^{298} (ΔH^{298}) in kcal/mol.

In conclusion, we have presented the activation of hydrogen sulfide by silyliumylidene ion **A** to give the thiosilaaldehyde **B**. Its nucleophilicity is best rationalized by assuming a zwitterionic character. Combined experimental and theoretical investigations reveal that the thiosilaaldehyde formation does not involve intermediacy of chlorosilylene **C** or thiosilylene **13**. The NHC-stabilized silyliumylidene **A** adds H_2S in a stepwise reaction sequence followed by NHC dissociation. Proton abstraction by the latter yields thiosilaaldehyde in a strongly exergonic reaction. With an overall activation barrier of 15 kcal/mol, the resulting mechanistic picture is fully in line with the experimental observation of an instantaneous reaction at sub-zero temperatures.

3. Materials and Methods

3.1. General Methods and Instruments

All manipulations were carried out under the argon atmosphere using standard Schlenk or glovebox techniques. Glassware was heat-dried under vacuum prior to use. Unless otherwise stated, all chemicals were purchased from Sigma-Aldrich (Steinheim, Germany) and used as received. Benzene, *n*-hexane, and acetonitrile were refluxed over standard drying agents (benzene/hexane over sodium and benzophenone, acetonitrile over CaH_2), distilled and deoxygenated prior to use. Deuterated acetonitrile (CD_3CN) and benzene (C_6D_6) were dried by short refluxing over CaH_2 (CD_3CN) and/or storage over activated 3 Å molecular sieves (CD_3CN and C_6D_6). All NMR samples were prepared under argon in J. Young PTFE tubes. *m*TerSiHCl$_2$, chlorosilylene **C** and ImMe$_4$ were synthesized according to procedures described in literature [54,73,74]. NMR spectra were recorded on Bruker AV-400 spectrometer (Rheinstetten, Germany) at ambient temperature (300 K). ^{1}H, ^{13}C, and ^{29}Si NMR spectroscopic chemical shifts δ are reported in ppm relative to tetramethylsilane. δ(^{1}H) and δ(^{13}C) were referenced internally to the relevant residual solvent resonances. δ(^{29}Si) was referenced to the signal of tetramethylsilane (TMS) (δ = 0 ppm) as the external standard. Elemental analyses (EA) were conducted with a EURO EA (HEKA tech, Wegberg, Germany) instrument equipped with a CHNS combustion analyzer. Details on XRD data are given in the supplementary materials.

*3.2. Improved and Upscaled Synthesis of Silyliumylidene **A***

*m*TerSiHCl$_2$ (1.00 g, 2.42 mmol, 1.0 eq.) and ImMe$_4$ (901 mg, 7.26 mmol, 3.0 eq.) were each dissolved in 17.5 mL of dry benzene in two different flasks. The ImMe$_4$ solution was added very slowly to the silane solution to generate a layer of immediately formed imidazolium hydrogenchloride salt separating both solutions without stirring. After complete addition/overlaying stirring was switched on, both solutions mixed thoroughly as fast as possible and the precipitated imidazolium hydrogenchloride salt was allowed to settle down for a short time. The supernatant dark red solution was filtered into a new flask, the residue was washed with 2 mL of dry benzene and the combined solutions were allowed to stand overnight for complete crystallization of the orange silyliumylidene. The yellow supernatant was separated from the orange crystalline solid, washed four times with 5 mL dry hexane to remove residues of white imidazolium hydrogenchloride salt and dried in vacuo. An orange crystalline product was obtained in 66% yield (1.00 g). Analytical data are the same as previously published [44].

*3.3. Synthesis of Thiosilaaldehyde **B***

Silyliumylidene **A** (150 mg, 221 µmol, 1.0 eq.) was dissolved in MeCN (3.0 mL), cooled to −20 °C and an excess of H_2S solution (approx. 0.8 M) in THF was added. The solution quickly turned from orange to yellow to blue-green while a white precipitate was formed. The solution was allowed to warm to RT upon which the precipitate redissolved. The solution was concentrated to halve the volume and stored in the fridge for crystallization overnight. The supernatant was filtered off and the white residue was washed with MeCN (0.5 mL) at 0 °C. The solid was dried in vacuo. **B** was obtained as a white crystalline solid in 54% yield (59.0 mg, 118 µmol). Storage of a crude reaction mixture at 8 °C yield single crystals of **B** suitable for X-ray diffraction analysis.

^{1}H-NMR (400 MHz, 298 K, CD_3CN) δ 7.45 (t, *J* = 7.6 Hz, 1H, C^4H, C^6H^3), 6.98 (s, 2H, $C^{3/5}H$, Mes), 6.91 (d, *J* = 7.6 Hz, 2H, $C^{3,5}H$, C_6H_3), 6.76 (s, 2H, $C^{3/5}H$, Mes), 5.36 (s, 1H, SiH, $^{1}J_{SiH}$ = 209.0 Hz), 3.46 (s, 6H, NCH_3, $ImMe_4$), 2.36 (s, 6H, $C^{1/3/5}CH_3$, Mes), 2.31 (s, 6H, $C^{1/3/5}CH_3$, Mes), 1.98 (s, 6H, CCH_3, $ImMe_4$), 1.93 (s, 6H, $C^{1/3/5}CH_3$, Mes); ^{13}C-NMR (126 MHz, 298 K, CD_3CN) δ 149.84, 148.75, 141.06, 138.76, 137.45, 137.42, 137.05, 130.08, 129.63, 128.45, 34.12 (NCH_3, $ImMe_4$), 22.21 ($C^{2/4/6}CH_3$, Mes), 21.76 ($C^{2/4/6}CH_3$, Mes), 21.23 ($C^{2/4/6}CH_3$, Mes), 8.68 (CCH_3, $ImMe_4$); ^{29}Si-INEPT-NMR (99 MHz, 298 K, CD_3CN) δ −39.58; EA experimental (calculated): C 74.27 (74.65), H 7.66 (7.68), N 5.61 (5.62), S 6.25 (6.43) %.

3.4. Conversion of Chlorosilylene **C** *to Silyliumylidene* **A**

Chlorosilylene **C** (40.0 mg, 80 μmol, 1.0 eq.) and $ImMe_4$ (10.1 mg, 80 μmol, 1.0 eq.) were dissolved in 1.5 mL of dry benzene in a Schlenk tube. The tube was placed in an oil bath and heated to 40 °C for 18 h. After this time, a large amount of orange crystals was formed with some white precipitate ($ImMe_4$·HCl) and a slightly yellow supernatant, which was removed via the syringe. The orange crystals were washed two times with 2 mL benzene and three times with 2 mL hexane to remove the white precipitate. The crystalline material was dried in vacuo to give **A** in 58% yield (29.0 mg). Analytical data are the same as previously published [44].

3.5. DFT Calculations

Geometry optimizations and harmonic frequency calculations have been performed using *Gaussian*09 [75] employing the M06-L/6-31+G(d,p) [76–78] level of density functional theory. The SMD polarizable continuum model was used to account for solvent effects of acetonitrile and benzene [79]. The 'ultrafine' grid option was used for numerical integrations [80]. Stationary points were characterized as minima or transition states by analysis of computed Hessians. The connectivity between minima and transition states was validated by IRC calculations [81] or displacing the geometry along the transition mode, followed by unconstrained optimization. For improved energies, single point calculations were conducted at the SMD-M06-L/6-311+G(d,p) [82,83] level of theory; wave functions used for bonding analysis were obtained at the M06-L/6-311++G(2d,2p) [82,83] level. Natural bond orbital (NBO) and natural resonance theory (NRT) analyses were performed using the NBO 6.0 program [84], interfaced with Gaussian09 [85,86]. The AIMALL [87] program was used for QTAIM analyses [66,67]. Unscaled zero-point vibrational energies, as well as thermal and entropic correction terms, were obtained from Hessians computed at the M06-L/6-31+G(d,p) level using standard procedures. Pictures of molecular structures were generated with the ChemCraft [88] program.

Supplementary Materials: The following are available online at http://www.mdpi.com/2304-6740/6/2/54/s1, Figures S1–S4: NMR spectra of **B**, Figures S5 and S6, Tables S1 and S2: Crystallographic details of **B** (CCDC 1839062), Table S3: Comparison of calc. and exp. Structures, Tables S4-S7: Details of NBO and QTAIM analyses, Figures S7–S8: Relaxed potential energy scans along the Si–C^{NHC} bonds in **10**, Table S9: Energies of all calculated compounds, Tables S10–S35: Cartesian coordinates of all calculated compounds.

Author Contributions: A.P. and R.B. performed the experiments. A.P. and J.I.S. conducted the calculations. P.J.A. measured and solved the SC-XRD data. M.C.H. and S.I. supervised the complete project. All authors discussed the results and commented on the manuscript.

Acknowledgments: We are exceptionally grateful to the WACKER Chemie AG and European Research Council (SILION 63794) for financial support. We thank Samuel Powley, Technische Universität München, for helpful discussion and proofreading the manuscript and Alexander Pöthig for advice pertaining to crystallography. Quantum-chemical calculations were performed at the Center for Scientific Computing (CSC) Frankfurt on the FUCHS and the LOEWE-CSC high-performance compute clusters and at the Leibniz Supercomputing Center of the Bavarian Academy of Science and Humanities.

Conflicts of Interest: The authors declare no conflict of interest.

References

1. Bayne, J.M.; Stephan, D.W. Phosphorus Lewis acids: Emerging reactivity and applications in catalysis. *Chem. Soc. Rev.* **2016**, *45*, 765–774. [CrossRef] [PubMed]

2. Hadlington, T.J.; Driess, M.; Jones, C. Low-valent group 14 element hydride chemistry: Towards catalysis. *Chem. Soc. Rev.* **2018**. [CrossRef] [PubMed]
3. Mandal, S.K.; Roesky, H.W. Group 14 Hydrides with Low Valent Elements for Activation of Small Molecules. *Acc. Chem. Res.* **2012**, *45*, 298–307. [CrossRef] [PubMed]
4. Power, P.P. Main-group elements as transition metals. *Nature* **2010**, *463*, 171–177. [CrossRef] [PubMed]
5. Roy, M.M.D.; Rivard, E. Pushing Chemical Boundaries with *N*-Heterocyclic Olefins (NHOs): From Catalysis to Main Group Element Chemistry. *Acc. Chem. Res.* **2017**, *50*, 2017–2025. [CrossRef] [PubMed]
6. Yadav, S.; Saha, S.; Sen, S.S. Compounds with Low-Valent p-Block Elements for Small Molecule Activation and Catalysis. *ChemCatChem* **2016**, *8*, 486–501. [CrossRef]
7. Yao, S.; Xiong, Y.; Driess, M. Zwitterionic and Donor-Stabilized *N*-Heterocyclic Silylenes (NHSis) for Metal-Free Activation of Small Molecules. *Organometallics* **2011**, *30*, 1748–1767. [CrossRef]
8. Alvarado-Beltran, I.; Rosas-Sanchez, A.; Baceiredo, A.; Saffon-Merceron, N.; Branchadell, V.; Kato, T. A Fairly Stable Crystalline Silanone. *Angew. Chem. Int. Ed.* **2017**, *56*, 10481–10485. [CrossRef] [PubMed]
9. Arz, M.I.; Geiß, D.; Straßmann, M.; Schnakenburg, G.; Filippou, A.C. Silicon(i) chemistry: The NHC-stabilised silicon(i) halides $Si_2X_2(Idipp)_2$ (X = Br, I) and the disilicon(i)-iodido cation $[Si_2(I)(Idipp)_2]^+$. *Chem. Sci.* **2015**, *6*, 6515–6524. [CrossRef]
10. Arz, M.I.; Schnakenburg, G.; Meyer, A.; Schiemann, O.; Filippou, A.C. The Si_2H radical supported by two *N*-heterocyclic carbenes. *Chem. Sci.* **2016**, *7*, 4973–4979. [CrossRef]
11. Boehme, C.; Frenking, G. Electronic Structure of Stable Carbenes, Silylenes, and Germylenes. *J. Am. Chem. Soc.* **1996**, *118*, 2039–2046. [CrossRef]
12. Burchert, A.; Müller, R.; Yao, S.; Schattenberg, C.; Xiong, Y.; Kaupp, M.; Driess, M. Taming Silicon Congeners of CO and CO_2: Synthesis of Monomeric Si^{II} and Si^{IV} Chalcogenide Complexes. *Angew. Chem. Int. Ed.* **2017**, *56*, 6298–6301. [CrossRef] [PubMed]
13. Denk, M.; Lennon, R.; Hayashi, R.; West, R.; Belyakov, A.V.; Verne, H.P.; Haaland, A.; Wagner, M.; Metzler, N. Synthesis and Structure of a Stable Silylene. *J. Am. Chem. Soc.* **1994**, *116*, 2691–2692. [CrossRef]
14. Ghana, P.; Arz, M.I.; Das, U.; Schnakenburg, G.; Filippou, A.C. Si=Si Double Bonds: Synthesis of an NHC-Stabilized Disilavinylidene. *Angew. Chem. Int. Ed.* **2015**, *54*, 9980–9985. [CrossRef] [PubMed]
15. Kira, M.; Ishida, S.; Iwamoto, T.; Kabuto, C. The First Isolable Dialkylsilylene. *J. Am. Chem. Soc.* **1999**, *121*, 9722–9723. [CrossRef]
16. Mondal, K.C.; Roesky, H.W.; Schwarzer, M.C.; Frenking, G.; Tkach, I.; Wolf, H.; Kratzert, D.; Herbst-Irmer, R.; Niepotter, B.; Stalke, D. Conversion of a Singlet Silylene to a stable Biradical. *Angew. Chem. Int. Ed.* **2013**, *52*, 1801–1805. [CrossRef] [PubMed]
17. Mondal, K.C.; Roy, S.; Dittrich, B.; Andrada, D.M.; Frenking, G.; Roesky, H.W. A Triatomic Silicon(0) Cluster Stabilized by a Cyclic Alkyl(amino) Carbene. *Angew. Chem. Int. Ed.* **2016**, *55*, 3158–3161. [CrossRef] [PubMed]
18. Nieder, D.; Yildiz, C.B.; Jana, A.; Zimmer, M.; Huch, V.; Scheschkewitz, D. Dimerization of a marginally stable disilenyl germylene to tricyclic systems: Evidence for reversible NHC-coordination. *Chem. Commun.* **2016**, *52*, 2799–2802. [CrossRef] [PubMed]
19. Protchenko, A.V.; Birjkumar, K.H.; Dange, D.; Schwarz, A.D.; Vidovic, D.; Jones, C.; Kaltsoyannis, N.; Mountford, P.; Aldridge, S. A Stable Two-Coordinate Acyclic Silylene. *J. Am. Chem. Soc.* **2012**, *134*, 6500–6503. [CrossRef] [PubMed]
20. Rekken, B.D.; Brown, T.M.; Fettinger, J.C.; Tuononen, H.M.; Power, P.P. Isolation of a Stable, Acyclic, Two-Coordinate Silylene. *J. Am. Chem. Soc.* **2012**, *134*, 6504–6507. [CrossRef] [PubMed]
21. Wang, Y.; Chen, M.; Xie, Y.; Wei, P.; Schaefer, H.F., III; Schleyer, P.V.R.; Robinson, G.H. Stabilization of elusive silicon oxides. *Nat. Chem.* **2015**, *7*, 509–513. [CrossRef] [PubMed]
22. Wendel, D.; Reiter, D.; Porzelt, A.; Altmann, P.J.; Inoue, S.; Rieger, B. Silicon and Oxygen's Bond of Affection: An Acyclic Three-Coordinate Silanone and Its Transformation to an Iminosiloxysilylene. *J. Am. Chem. Soc.* **2017**, *139*, 17193–17198. [CrossRef] [PubMed]
23. Xiong, Y.; Yao, S.; Inoue, S.; Epping, J.D.; Driess, M. A Cyclic Silylone ("Siladicarbene") with an Electron-Rich Silicon(0) Atom. *Angew. Chem. Int. Ed.* **2013**, *52*, 7147–7150. [CrossRef] [PubMed]
24. Xiong, Y.; Yao, S.; Inoue, S.; Irran, E.; Driess, M. The Elusive Silyliumylidene $[ClSi:]^+$ and Silathionium $[ClSi{=}S]^+$ Cations Stabilized by Bis(Iminophosphorane) Chelate Ligand. *Angew. Chem. Int. Ed.* **2012**, *51*, 10074–10077. [CrossRef] [PubMed]

25. Yamaguchi, T.; Sekiguchi, A.; Driess, M. An *N*-Heterocyclic Carbene−Disilyne Complex and Its Reactivity toward $ZnCl_2$. *J. Am. Chem. Soc.* **2010**, *132*, 14061–14063. [CrossRef] [PubMed]
26. Cowley, M.J.; Huch, V.; Rzepa, H.S.; Scheschkewitz, D. Equilibrium between a cyclotrisilene and an isolable base adduct of a disilenyl silylene. *Nat. Chem.* **2013**, *5*, 876–879. [CrossRef] [PubMed]
27. Filippou, A.C.; Chernov, O.; Schnakenburg, G. $SiBr_2$(Idipp): A Stable *N*-Heterocyclic Carbene Adduct of Dibromosilylene. *Angew. Chem. Int. Ed.* **2009**, *48*, 5687–5690. [CrossRef] [PubMed]
28. Filippou, A.C.; Lebedev, Y.N.; Chernov, O.; Straßmann, M.; Schnakenburg, G. Silicon(II) Coordination Chemistry: *N*-Heterocyclic Carbene Complexes of Si^{2+} and SiI^{+}. *Angew. Chem. Int. Ed.* **2013**, *52*, 6974–6978. [CrossRef] [PubMed]
29. Ghadwal, R.S.; Pröpper, K.; Dittrich, B.; Jones, P.G.; Roesky, H.W. Neutral Pentacoordinate Silicon Fluorides Derived from Amidinate, Guanidinate, and Triazapentadienate Ligands and Base-Induced Disproportionation of Si_2Cl_6 to Stable Silylenes. *Inorg. Chem.* **2011**, *50*, 358–364. [CrossRef] [PubMed]
30. Ghadwal, R.S.; Roesky, H.W.; Merkel, S.; Henn, J.; Stalke, D. Lewis Base Stabilized Dichlorosilylene. *Angew. Chem. Int. Ed.* **2009**, *48*, 5683–5686. [CrossRef] [PubMed]
31. Rivard, E. Donor-acceptor chemistry in the main group. *Dalton Trans.* **2014**, *43*, 8577–8586. [CrossRef] [PubMed]
32. Schweizer, J.I.; Meyer, L.; Nadj, A.; Diefenbach, M.; Holthausen, M.C. Unraveling the Amine-Induced Disproportionation Reaction of Perchlorinated Silanes—A DFT Study. *Chem. Eur. J.* **2016**, *22*, 14328–14335. [CrossRef] [PubMed]
33. Sinhababu, S.; Kundu, S.; Paesch, A.N.; Herbst-Irmer, R.; Stalke, D.; Fernández, I.; Frenking, G.; Stückl, A.C.; Schwederski, B.; Kaim, W.; et al. A Route to Base Coordinate Silicon Difluoride and the Silicon Trifluoride Radical. *Chem. Eur. J.* **2018**, *24*, 1264–1268. [CrossRef] [PubMed]
34. Schweizer, J.I.; Scheibel, M.G.; Diefenbach, M.; Neumeyer, F.; Würtele, C.; Kulminskaya, N.; Linser, R.; Auner, N.; Schneider, S.; Holthausen, M.C. A Disilene Base Adduct with a Dative Si–Si Single Bond. *Angew. Chem. Int. Ed.* **2016**, *55*, 1782–1786. [CrossRef] [PubMed]
35. Tillmann, J.; Meyer, L.; Schweizer, J.I.; Bolte, M.; Lerner, H.W.; Wagner, M.; Holthausen, M.C. Chloride-Induced Aufbau of Perchlorinated Cyclohexasilanes from Si2Cl6: A Mechanistic Scenario. *Chem. Eur. J.* **2014**, *20*, 9234–9239. [CrossRef] [PubMed]
36. Meyer-Wegner, F.; Nadj, A.; Bolte, M.; Auner, N.; Wagner, M.; Holthausen, M.C.; Lerner, H.W. The Perchlorinated Silanes Si_2Cl_6 and Si_3Cl_8 as Sources of $SiCl_2$. *Chem. Eur. J.* **2011**, *17*, 4715–4719. [CrossRef] [PubMed]
37. Gaspar, P.P. Learning from silylenes and supersilylenes. In *Organosilicon Chemistry VI: From Molecules to Materials*, *1*; Auner, N., Weis, J., Eds.; Wiley-VCH: Weinheim, Germany, 2005; Volume 2, pp. 10–24. ISBN 9783527618224.
38. Müller, T. Stability, Reactivity, and Strategies for the Synthesis of Silyliumylidenes, RSi:$^{+}$. A Computational Study. *Organometallics* **2010**, *29*, 1277–1283. [CrossRef]
39. Jutzi, P.; Mix, A.; Rummel, B.; Schoeller, W.W.; Neumann, B.; Stammler, H.-G. The $(Me_5C_5)Si^{+}$ Cation: A Stable Derivative of HSi^{+}. *Science* **2004**, *305*, 849–851. [CrossRef] [PubMed]
40. Driess, M.; Yao, S.; Brym, M.; van Wüllen, C. Low-Valent Silicon Cations with Two-Coordinate Silicon and Aromatic Character. *Angew. Chem. Int. Ed.* **2006**, *45*, 6730–6733. [CrossRef] [PubMed]
41. Hudnall, T.W.; Ugarte, R.A.; Perera, T.A. Main group complexes with *N*-Heterocyclic carbenes: Bonding, stabilization and applications in catalysis. In *N-Heterocyclic Carbenes: From Laboratory Curiosities to Efficient Synthetic Tools (2)*; The Royal Society of Chemistry: London, UK, 2017; pp. 178–237. ISBN 978-1-78262-423-3.
42. Melaimi, M.; Jazzar, R.; Soleilhavoup, M.; Bertrand, G. Cyclic (Alkyl)(amino)carbenes (CAACs): Recent Developments. *Angew. Chem. Int. Ed.* **2017**, *56*, 10046–10068. [CrossRef] [PubMed]
43. Agou, T.; Hayakawa, N.; Sasamori, T.; Matsuo, T.; Hashizume, D.; Tokitoh, N. Reactions of Diaryldibromodisilenes with N-Heterocyclic Carbenes: Formation of Formal Bis-NHC Adducts of Silyliumylidene Cations. *Chem. Eur. J.* **2014**, *20*, 9246–9249. [CrossRef] [PubMed]
44. Ahmad, S.U.; Szilvási, T.; Inoue, S. A facile access to a novel NHC-stabilized silyliumylidene ion and C-H activation of phenylacetylene. *Chem. Commun.* **2014**, *50*, 12619–12622. [CrossRef] [PubMed]
45. Hayakawa, N.; Sadamori, K.; Mizutani, S.; Agou, T.; Sugahara, T.; Sasamori, T.; Tokitoh, N.; Hashizume, D.; Matsuo, T. Synthesis and Characterization of *N*-Heterocyclic Carbene-Coordinated Silicon Compounds Bearing a Fused-Ring Bulky Eind Group. *Inorganics* **2018**, *6*, 30. [CrossRef]
46. Li, Y.; Chan, Y.-C.; Li, Y.; Purushothaman, I.; De, S.; Parameswaran, P.; So, C.-W. Synthesis of a Bent 2-Silaallene with a Perturbed Electronic Structure from a Cyclic Alkyl(amino) Carbene-Diiodosilylene. *Inorg. Chem.* **2016**, *55*, 9091–9098. [CrossRef] [PubMed]

47. Li, Y.; Chan, Y.-C.; Leong, B.-X.; Li, Y.; Richards, E.; Purushothaman, I.; De, S.; Parameswaran, P.; So, C.-W. Trapping a Silicon(I) Radical with Carbenes: A Cationic cAAC–Silicon(I) Radical and an NHC–Parent-Silyliumylidene Cation. *Angew. Chem. Int. Ed.* **2017**, *56*, 7573–7578. [CrossRef] [PubMed]
48. Yeong, H.-X.; Xi, H.-W.; Li, Y.; Lim, K.H.; So, C.-W. A Silyliumylidene Cation Stabilized by an Amidinate Ligand and 4-Dimethylaminopyridine. *Chem. Eur. J.* **2013**, *19*, 11786–11790. [CrossRef] [PubMed]
49. Leszczyńska, K.; Mix, A.; Berger, R.J.F.; Rummel, B.; Neumann, B.; Stammler, H.-G.; Jutzi, P. The Pentamethylcyclopentadienylsilicon(II) Cation as a Catalyst for the Specific Degradation of Oligo(ethyleneglycol) Diethers. *Angew. Chem. Int. Ed.* **2011**, *50*, 6843–6846. [CrossRef] [PubMed]
50. Meltzer, A.; Inoue, S.; Präsang, C.; Driess, M. Steering S–H and N–H Bond Activation by a Stable *N*-Heterocyclic Silylene: Different Addition of H_2S, NH_3, and Organoamines on a Silicon(II) Ligand versus Its Si(II)→$Ni(CO)_3$ Complex. *J. Am. Chem. Soc.* **2010**, *132*, 3038–3046. [CrossRef] [PubMed]
51. Präsang, C.; Stoelzel, M.; Inoue, S.; Meltzer, A.; Driess, M. Metal-Free Activation of EH_3 (E=P, As) by an Ylide-like Silylene and Formation of a Donor-Stabilized Arsasilene with a HSi=AsH Subunit. *Angew. Chem. Int. Ed.* **2010**, *49*, 10002–10005. [CrossRef] [PubMed]
52. Yao, S.; Brym, M.; van Wüllen, C.; Driess, M. From a Stable Silylene to a Mixed-Valent Disiloxane and an Isolable Silaformamide–Borane Complex with Considerable Silicon–Oxygen Double-Bond Character. *Angew. Chem. Int. Ed.* **2007**, *46*, 4159–4162. [CrossRef] [PubMed]
53. Szilvási, T.; Nyíri, K.; Veszprémi, T. Unique Insertion Mechanisms of Bis-dehydro-β-diketiminato Silylene. *Organometallics* **2011**, *30*, 5344–5351. [CrossRef]
54. Filippou, A.C.; Chernov, O.; Blom, B.; Stumpf, K.W.; Schnakenburg, G. Stable N-Heterocyclic Carbene Adducts of Arylchlorosilylenes and Their Germanium Homologues. *Chem. Eur. J.* **2010**, *16*, 2866–2872. [CrossRef] [PubMed]
55. Filippou, A.C.; Chernov, O.; Stumpf, K.W.; Schnakenburg, G. Metal–Silicon Triple Bonds: The Molybdenum Silylidyne Complex $[Cp(CO)_2Mo{\equiv}Si\text{-}R]$. *Angew. Chem. Int. Ed.* **2010**, *49*, 3296–3300. [CrossRef] [PubMed]
56. Hansen, K.; Szilvási, T.; Blom, B.; Driess, M. A Persistent 1,2-Dihydrophosphasilene Adduct. *Angew. Chem. Int. Ed.* **2015**, *54*, 15060–15063. [CrossRef] [PubMed]
57. Hansen, K.; Szilvási, T.; Blom, B.; Irran, E.; Driess, M. From an Isolable Acyclic Phosphinosilylene Adduct to Donor-Stabilized Si=E Compounds (E=O, S, Se). *Chem. Eur. J.* **2015**, *21*, 18930–18933. [CrossRef] [PubMed]
58. Arz, M.I.; Hoffmann, D.; Schnakenburg, G.; Filippou, A.C. NHC-stabilized Silicon(II) Halides: Reactivity Studies with Diazoalkanes and Azides. *Z. Anorg. Allg. Chem.* **2016**, *642*, 1287–1294. [CrossRef]
59. Ahmad, S.U.; Szilvási, T.; Irran, E.; Inoue, S. An NHC-Stabilized Silicon Analogue of Acylium Ion: Synthesis, Structure, Reactivity, and Theoretical Studies. *J. Am. Chem. Soc.* **2015**, *137*, 5828–5836. [CrossRef] [PubMed]
60. Sarkar, D.; Wendel, D.; Ahmad, S.U.; Szilvasi, T.; Pothig, A.; Inoue, S. Chalcogen-atom transfer and exchange reactions of NHC-stabilized heavier silaacylium ions. *Dalton Trans.* **2017**, *46*, 16014–16018. [CrossRef] [PubMed]
61. Baceiredo, A.; Kato, T. Multiple Bonds to Silicon (Recent Advances in the Chemistry of Silicon Containing Multiple Bonds). In *Organosilicon Compounds: Theory and Experiment (Synthesis)*; Lee, V.Y., Ed.; Academic Press: London, UK, 2017; pp. 533–618. ISBN 978-0-12-801981-8.
62. Lutters, D.; Merk, A.; Schmidtmann, M.; Müller, T. The Silicon Version of Phosphine Chalcogenides: Synthesis and Bonding Analysis of Stabilized Heavy Silaaldehydes. *Inorg. Chem.* **2016**, *55*, 9026–9032. [CrossRef] [PubMed]
63. Pyykkö, P.; Atsumi, M. Molecular Double-Bond Covalent Radii for Elements Li–E112. *Chem. Eur. J.* **2009**, *15*, 12770–12779. [CrossRef] [PubMed]
64. Roberts, J.D.; Webb, R.L.; McElhill, E.A. The Electrical Effect of the Trifluoromethyl Group. *J. Am. Chem. Soc.* **1950**, *72*, 408–411. [CrossRef]
65. Von Ragué Schleyer, P.; Kos, A.J. The importance of negative (anionic) hyperconjugation. *Tetrahedron* **1983**, *39*, 1141–1150. [CrossRef]
66. Bader, R.F.W. *Atoms in Molecules: A Quantum Theory*; Oxford University Press: Oxford, UK, 1990; ISBN 0198558651.
67. Matta, C.F.; Boyd, R.J. *An Introduction to the Quantum Theory of Atoms in Molecule*; Wiley-VCH: Weinheim, Germany, 2007; ISBN 3527610707.
68. Macchi, P.; Sironi, A. Chemical bonding in transition metal carbonyl clusters: Complementary analysis of theoretical and experimental electron densities. *Coord. Chem. Rev.* **2003**, *238*, 383–412. [CrossRef]

69. Macchi, P.; Sironi, A. Interactions involving metals—From 'Chemical Categories' to QTAIM, and Backwards. In *The Quantum Theory of Atoms in Molecules*; Matta, C.F., Boyd, R.J., Eds.; Wiley-VCH: Weinheim, Germany, 2007.
70. Bader, R.F.W.; Slee, T.S.; Cremer, D.; Kraka, E. Description of conjugation and hyperconjugation in terms of electron distributions. *J. Am. Chem. Soc.* **1983**, *105*, 5061–5068. [CrossRef]
71. Cremer, D.; Kraka, E.; Slee, T.S.; Bader, R.F.W.; Lau, C.D.H.; Nguyen Dang, T.T.; MacDougall, P.J. Description of homoaromaticity in terms of electron distributions. *J. Am. Chem. Soc.* **1983**, *105*, 5069–5075. [CrossRef]
72. Mandado, M.; Mosquera, R.A.; Graña, A.M. On the effects of electron correlation and conformational changes on the distortion of the charge distribution in alkyl chains. *Chem. Phys. Lett.* **2002**, *355*, 529–537. [CrossRef]
73. Simons, R.S.; Haubrich, S.T.; Mork, B.V.; Niemeyer, M.; Power, P.P. The Syntheses and Characterization of the Bulky Terphenyl Silanes and Chlorosilanes 2,6-$Mes_2C_6H_3SiCl_3$, 2,6-$Trip_2C_6H_3SiCl_3$, 2,6-$Mes_2C_6H_3SiHCl_2$, 2,6-$Trip_2C_6H_3SiHCl_2$, 2,6-$Mes_2C_6H_3SiH_3$, 2,6-$Trip_2C_6H_3SiH_3$and 2,6-$Mes_2C_6H_3SiCl_2SiCl_3$. *Main Group Chem.* **1998**, *2*, 275–283. [CrossRef]
74. Kuhn, N.; Kratz, T. Synthesis of Imidazol-2-ylidenes by Reduction of Imidazole-2(3*H*)-thiones. *Synthesis* **1993**, *1993*, 561–562. [CrossRef]
75. Frisch, M.J.; Trucks, G.W.; Schlegel, H.B.; Scuseria, G.E.; Robb, M.A.; Cheeseman, J.R.; Scalmani, G.; Barone, V.; Petersson, G.A.; Nakatsuji, H.; Revision, D.; et al. *Gaussian 09*; Revision D.01; Gaussian, Inc.: Wallingford, CT, USA, 2009.
76. Zhao, Y.; Truhlar, D.G. The M06 suite of density functionals for main group thermochemistry, thermochemical kinetics, noncovalent interactions, excited states, and transition elements: Two new functionals and systematic testing of four M06-class functionals and 12 other functionals. *Theor. Chem. Acc.* **2008**, *120*, 215–241. [CrossRef]
77. Ditchfield, R.; Hehre, W.J.; Pople, J.A. Self-Consistent Molecular-Orbital Methods. IX. An Extended Gaussian-Type Basis for Molecular-Orbital Studies of Organic Molecules. *J. Chem. Phys.* **1971**, *54*, 724–728. [CrossRef]
78. Hehre, W.J.; Ditchfield, R.; Pople, J.A. Self—Consistent Molecular Orbital Methods. XII. Further Extensions of Gaussian—Type Basis Sets for Use in Molecular Orbital Studies of Organic Molecules. *J. Chem. Phys.* **1972**, *56*, 2257–2261. [CrossRef]
79. Marenich, A.V.; Cramer, C.J.; Truhlar, D.G. Universal Solvation Model Based on Solute Electron Density and on a Continuum Model of the Solvent Defined by the Bulk Dielectric Constant and Atomic Surface Tensions. *J. Phys. Chem. B* **2009**, *113*, 6378–6396. [CrossRef] [PubMed]
80. Wheeler, S.E.; Houk, K.N. Integration Grid Errors for Meta-GGA-Predicted Reaction Energies: Origin of Grid Errors for the M06 Suite of Functionals. *J. Chem. Theory Comput.* **2010**, *6*, 395–404. [CrossRef] [PubMed]
81. Fukui, K. The path of chemical reactions—The IRC approach. *Acc. Chem. Res.* **1981**, *14*, 363–368. [CrossRef]
82. Krishnan, R.; Binkley, J.S.; Seeger, R.; Pople, J.A. Self-consistent molecular orbital methods. XX. A basis set for correlated wave functions. *J. Chem. Phys.* **1980**, *72*, 650–654. [CrossRef]
83. McLean, A.D.; Chandler, G.S. Contracted Gaussian basis sets for molecular calculations. I. Second row atoms, Z = 11–18. *J. Chem. Phys.* **1980**, *72*, 5639–5648. [CrossRef]
84. Glendening, E.D.; Badenhoop, J.K.; Reed, A.E.; Carpenter, J.E.; Bohmann, J.A.; Morales, C.M.; Landis, C.R.; Weinhold, F. *NBO 6.0*; Theoretical Chemistry Institute, University of Wisconsin: Madison, WI, USA, 2013.
85. Glendening Eric, D.; Landis Clark, R.; Weinhold, F. Natural bond orbital methods. *WIRES Ccomput. Mol. Sci.* **2011**, *2*, 1–42. [CrossRef]
86. Glendening Eric, D.; Landis Clark, R.; Weinhold, F. NBO 6.0: Natural bond orbital analysis program. *J. Chem. Theory Comput.* **2013**, *34*, 1429–1437. [CrossRef] [PubMed]
87. Keith, T.A. *AIMAll (Version 17. 01. 25)*; TK Gristmill Software: Overland Park, KS, USA, 2017.
88. Andrienko, G.A. *ChemCraf*—graphical software for visualization of quantum chemistry computations. Available online: http://www.chemcraftprog.com (accessed on 3 January 2015).

6.8. Transition Metal Carbonyl Complexes of an *N*-Heterocyclic Carbene Stabilized Silyliumylidene Ion

Title: Transition Metal Carbonyl Complexes of an *N*-Heterocyclic Carbene Stabilized Silyliumylidene Ion

Status: Article, published online October 22, 2019

Journal: Inorganic Chemistry, 2019, 58 (21), 14931-14937.

Publisher: American Chemical Society

DOI: 10.1021/acs.inorgchem.9b02772

Authors: Philipp Frisch, Tibor Szilvási, Amelie Porzelt, Shigeyoshi Inoue

Content: This report is an extension of the silyliumylidene project (see chapter 6.7). We aimed at determining the donor strength of our NHC-stabilised aryl-substituted silyliumylidene ions **1a-Cl**/**1b-Cl** *via* their application as a donor in transition-metal carbonyl complexes. Initial conversions were hampered by the interfering chloride anion as well as its limited solubility in solvents other than acetonitrile. The exchange of the anion to triflate (OTf) enabled homogeneous reaction mixtures, but the steric demand of **1a-OTf** prevented reaction with the metal carbonyls. Changing to the Tipp-substituted **1b-OTf** allowed for clean conversion with $M(CO)_5THF$ (M = Cr, Mo, W) and $Fe_2(CO)_9$ to obtain the silyliumylidene transition metal complexes **2**, **3**, **4** and **5**. SC-XRD analysis revealed that the Si–M bonds in **3** and **5** are located at the upper end of typical Si–M bond lengths. IR spectroscopy was used to deduce the σ-donor properties of the silyliumylidene ions, as the empty p-orbitals of the silicon centre are partially occupied due to the coordinated NHCs, which thus reduces possible π-acceptor properties to a minimum. DFT calculations showed a low proton affinity for **1b-OTf**, possibly due to its positive charge. NBO analysis revealed solely σ-donation being present in **2**-**4** and only a small contribution of π-back donation in **5**. To summarise, we prepared four different silyliumylidene transition-metal carbonyl complexes, made possible by anion exchange from **1-OTf**. Combined experimental and theoretical investigations revealed **1b-OTf** bearing only poor σ-donor abilities possibly due to its positive charge.

Contributions to the publication:

- Execution of the anion exchange experiments for **1a-Cl**/**1b-Cl** to enhance the solubility and usability of the NHC-stabilised silyliumylidene ions (in parts together with Korbinian Huber during his internship)
- Co-writing of the manuscript

Inorganic Chemistry
Article
Cite This: Inorg. Chem. 2019, 58, 14931−14937
pubs.acs.org/IC

Transition Metal Carbonyl Complexes of an N-Heterocyclic Carbene Stabilized Silyliumylidene Ion

Philipp Frisch,[†] Tibor Szilvási,[‡] Amelie Porzelt,[†] and Shigeyoshi Inoue*[,†]

[†]Department of Chemistry, WACKER-Institute of Silicon Chemistry and Catalysis Research Center, Technische Universität München, Lichtenbergstraße 4, 85748 Garching bei München, Germany

[‡]Department of Chemical and Biological Engineering, University of Wisconsin−Madison, 1415 Engineering Drive, Madison, Wisconsin 53706-1607, United States

Supporting Information

ABSTRACT: Silyliumylidene ions—Si(II) cations with a stereochemically active lone pair of electrons—can act as ligands in transition metal complexes comparable to silylenes. However, no investigations concerning their donor abilities have been carried out. Carbonyl complexes lend themselves exceptionally well to determine the donor/acceptor strength of various ligand systems. We now report the synthesis of novel group 6 and group 8 transition metal carbonyl complexes **2**−**5** of N-heterocyclic carbene (NHC) stabilized silyliumylidene ion **1b**, including the first Cr, Mo, and Fe complexes of a Si(II) cation. The complexes were fully characterized by multinuclear NMR and IR spectroscopy and SC-XRD studies. A combination of experimentally determined IR bands together with theoretical calculations revealed weak σ-donor properties and a negligible π-acceptor ability of NHC-stabilized Si(II) cation **1b**.

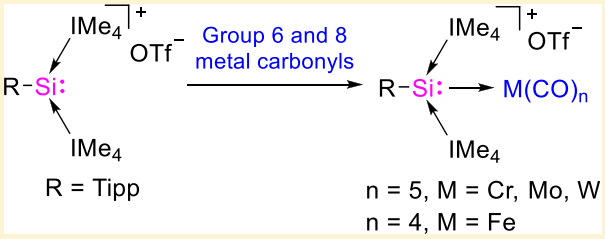

INTRODUCTION

Since Jutzi's initial report on the pentamethylcyclopentadiene-silicon(II) cation $[Cp^*Si:]^+$ in 2004,[1] silyliumylidene ions have gained increasing scientific interest. Because of their unique electronic structure—a silicon center with a lone pair of electrons, a positive charge, and two vacant orbitals[2]—they are promising candidates for the facile activation of various bond types, as well as small molecules and, importantly, main-group catalysis. These highly reactive species can also give new access routes to novel low-valent silicon compounds, such as silylones.[3] Their potential in the activation of small molecules has already been shown with the isolation of sila-acylium ions through the activation of CO_2,[4] and their heavier homologues directly from S_8, Se, and Te.[5] Other reported reactivities include the activation of O−H,[6] S−H,[7] and C−H[8] bonds and even the catalytic degradation of oligoethers to dioxane.[9]

Another possible application of Si(II) cations is their use as ligands in transition metal complexes. Because of the presence of a lone pair of electrons on the silicon center, silyliumylidene ions can function as ligands just like silylenes and carbenes. However, one-coordinate silyliumylidene ions $[R{-}Si:]^+$ (i.e., without donor-stabilization) have not been isolated so far due to their instability and high reactivity.[8b] Hence, isolation of these Si(II) cations necessitates their kinetic and thermodynamic stabilization through generally sterically demanding substituents as well as electron donating ligands, such as NHCs.[2b,10] On the other hand, introduction of these moieties generally hampers their reactivity and in the case of the stabilization through Lewis bases also (partially) fills the vacant orbitals on the silicon center, therefore reducing their π-acceptor ability.

Understandably, the reported transition metal coordination chemistry of silyliumylidene ions is significantly more limited than the related silylene coordination chemistry: our group described formal Pd_2 and Pt_2 silyliumylidene-phosphide complexes, obtained from a rearrangement reaction of a phosphasilene.[11] So et al. reported a Rh- and W-complex (**I**) (Chart 1) of a DMAP-stabilized silyliumylidene ion.[12] Recently, we described the first coinage metal complexes **II** of Si(II) cations, synthesized directly from an NHC-stabilized silyliumylidene ion.[13] The synthesis of a silylidyne molybdenum complex from $[Cp^*Si:]^+$ was also recently accomplished.[14] It is important to note that the donor strength of silyliumylidene ions as ligands in transition metal complexes has not been studied so far.

In contrast, a variety of group 6 and group 8 metal carbonyl complexes with silylenes as ligands have been isolated.[15] For example, West et al. reported a series of saturated and unsaturated bis(*N*-heterocyclic silylene) (NHSi) complexes **III** of group 6 carbonyls.[16] Related group 8 complexes with Fe and Ru,[16] as well as monosilylene complexes,[17] were also described. Complexes **IV** of an amidinate-stabilized chlorosilylene were prepared and utilized for the isolation of the corresponding fluorosilylene derivatives.[18] Furthermore, related amidinate-stabilized hydrosilylene complexes of $Fe(CO)_4$[19] and various $Fe(CO)_4$ complexes **VI**[20] from NHC-stabilized silylenes have

Received: September 17, 2019
Published: October 22, 2019

DOI: 10.1021/acs.inorgchem.9b02772
Inorg. Chem. 2019, 58, 14931−14937

Chart 1. Examples of Reported Silyliumylidene Transition Metal Complexes (I, II) and Silylene Transition Metal Carbonyl Complexes (III–VI)[a]

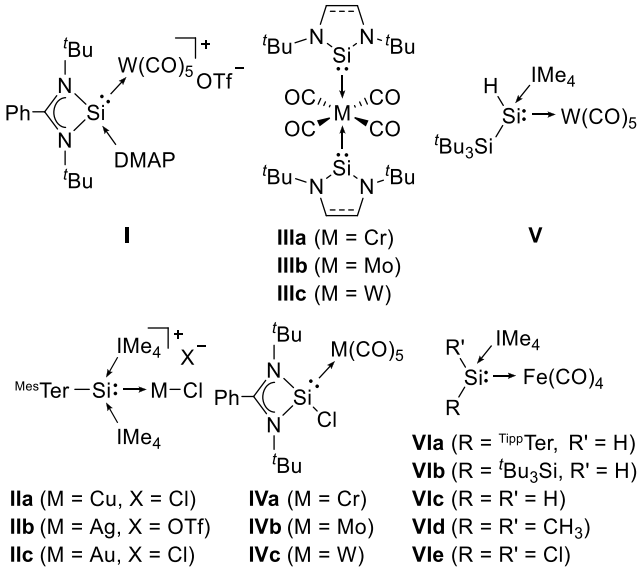

[a]DMAP = 4-dimethylaminopyridine, IMe_4 = 1,3,4,5-tetramethylimidazol-2-ylidene, $^{Mes/Tipp}$Ter = 2,6-(Mes/Tipp)$_2$-C_6H_3, Mes = 2,4,6-Me_3-C_6H_2, Tipp = 2,4,6-^{i}Pr$_3$-C_6H_2.

been reported in recent years. The electronic properties of silylenes as ligands have also been investigated computationally.[16,21]

Therefore, to start of any investigation into the donor strength of NHC-stabilized silyliumylidene ions and to determine their donor ability, we set out to synthesize transition metal carbonyl complexes utilizing our previously described NHC-stabilized silyliumylidene ions[8a] as ligands. Herein, we report the synthesis and full characterization of several novel group 6 (Cr, Mo, W) and group 8 (Fe) transition metal carbonyl complexes of NHC-stabilized Si(II) cations and an investigation of the donor ability of the silyliumylidene ligand by experimental as well as theoretical means.

RESULTS AND DISCUSSION

Synthesis and NMR Analysis. In an initial attempt, we reacted the group 6 transition metal carbonyl $W(CO)_6$ with the bulky *m*-terphenyl (*m*-Ter = 2,6-(2,4,6-Me_3-C_6H_2)$_2$-C_6H_3) substituted silyliumylidene chloride[8a] **1a-Cl** as a suspension in THF. However, no reaction occurred, even at elevated temperatures and prolonged reaction times. Irradiation of the mixture with UV light led to the full consumption of $W(CO)_6$ accompanied by complete dissolution of the Si(II) cation, however, no change in the ^{1}H and ^{29}Si NMR could be observed. Interestingly, the ^{13}C NMR indicated formation of the chloropentacarbonyltungstate anion[22] $[W(CO)_5Cl]^-$. This prompted us to exchange the chloride counteranion from the silyliumylidene ion **1a-Cl** to a triflate anion via reaction with KOTf to prevent any undesired anion formation (Scheme 1).

Introduction of the OTf^- anion also brings the additional benefit of increased solubility in THF, allowing for a homogeneous reaction. Unfortunately, even with the triflate anion, the steric bulk of the *m*-terphenyl substituent in **1a-OTf** seemed to prevent any reaction with $W(CO)_6$ or $W(CO)_5(THF)$. Hence, we moved our efforts to the sterically

Scheme 1. Synthesis of Silyliumylidene Triflates 1-OTf

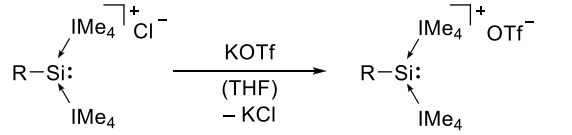

1a-Cl (R = *m*-Ter)
1b-Cl (R = Tipp)

1a-OTf (R = *m*-Ter, 92%)
1b-OTf (R = Tipp, 94%)

less demanding Tipp substituent (**1b-Cl**, Tipp = 2,4,6-^{i}Pr$_3$-C_6H_2) and, consequently, introduced the OTf^- anion. Finally, reaction of a THF solution of silyliumylidene triflate **1b-OTf** with a freshly prepared solution of $M(CO)_5(THF)$ (M = Cr, Mo, W) in THF allowed us to isolate the desired $[Tipp–Si(IMe_4)_2 \rightarrow M(CO)_5]^+$ complexes **2**–**4** in high yield (80–86%) as pale to bright yellow solids (Scheme 2). The successful complex formation can be observed by a visible color change from bright orange (**1b-OTf** in THF) to pale to bright yellow (**2**–**4**).

Scheme 2. Synthesis of Group 6 Carbonyl Complexes 2–4

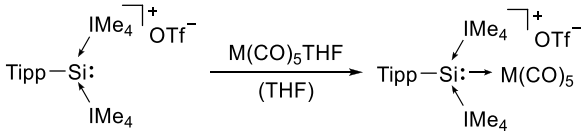

1b-OTf

2 (M = Cr, 80%)
3 (M = Mo, 83%)
4 (M = W, 86%)

While no direct reaction could be observed with $M(CO)_6$, initial preparation of $M(CO)_5(THF)$ is not necessary, as irradiation of a simple mixture of the starting materials with UV light led to formation of the same complexes, albeit slightly less clean. The complexes are well soluble in THF, C_6H_5F, acetonitrile, and pyridine and are slightly soluble in Et_2O. They are stable for about 2 days in THF, Et_2O, and C_6H_5F solution at room temperature, but after 48 h, small amounts of unidentified decomposition products can be observed in the ^{1}H NMR. They decompose rapidly in acetonitrile to an unidentified mixture of products.

Coordination of the silicon center to the transition metal is accompanied by marked downfield shift in the ^{29}Si NMR (−69.5 ppm for **1b-OTf**), which gets progressively weaker with an increasing atomic number of the group 6 metal. The $Cr(CO)_5$ complex **2** resonates at +6.3 ppm, whereas the $Mo(CO)_5$ and $W(CO)_5$ complexes (**3** and **4**) are shifted upfield to −17.3 and −30.5 ppm, respectively. The same trend was also observed for the related group 6 silylene complexes **III** (unsat./sat.; Cr, 136.9/170.3 ppm; Mo, 119.3/155.3 ppm; W, 97.8/137.1 ppm)[16] and **IV** (Cr, 92.3 ppm; Mo, 72.8 ppm; W, 53.0 ppm).[18] However, this is in stark contrast to the coinage metal silyliumylidene complexes **II**, where an increasing atomic number resulted in a stronger downfield shift (Cu, −48.8 ppm; Ag, −46.6 ppm; Au, −38.0 ppm).[13] For comparison, the only other silyliumylidene ion $W(CO)_5$ complex **I** shows a significantly stronger downfield shift of the ^{29}Si NMR resonance from −82.3 ppm in the uncoordinated silyliumylidene ion[5b] to +51.6 ppm in the complex.[12] We were also able to observe the coupling of the central Si atom with ^{183}W (~14% natural abundance, S = $^1/_2$; cf., Figure S28),

DOI: 10.1021/acs.inorgchem.9b02772
Inorg. Chem. 2019, 58, 14931–14937

resulting in a doublet with $^{1}J_{SiW}$ = 123.0 Hz, which is in line with other reported Si(II) → $W(CO)_5$ complexes.[17] No coupling with $^{95/97}$Mo (^{95}Mo, ~16%; ^{97}Mo, ~10% natural abundance; S = $^{5}/_{2}$) could be observed, even with a high concentration and significantly increased number of scans. ^{29}Si NMR shifts as well as other important analytical parameters are summed up in Table 1.

Table 1. Comparison of ^{29}Si NMR & ^{13}C NMR (THF-d_8) and Si−M Bond Lengths of Silyliumylidene Ion 1b-OTf and Its Transition Metal Complexes 2−5

	M	^{29}Si NMR [ppm]	^{13}C NMR (CO) [ppm]	Si1−M1 [Å]
1b		−69.5		
2	Cr	6.3	225.2, 222.0	
3	Mo	−17.3	210.0, 202.2	2.673(1)/2.740(1)
4	W	−30.5	201.9, 192.4	
5	Fe	5.4	217.4	2.349(1)

The ^{1}H NMR spectra of complexes **2**−**4** are very similar, showing a single set of resonances for the Tipp-substituent and the NHCs. The biggest difference, also compared to silyliumylidene **1b-OTf**, is the broadening of the septet corresponding to the *iso*-propyl groups in ortho-position to the central silicon atom. The ^{13}C NMR spectra show one set of resonances for the Tipp-substituent and the coordinated NHCs and two separate resonances for the metal-bound CO ligands, presumably due to the trans effect,[22] which is consistent with other low-valent silicon complexes.[17,18] The CO resonances can be observed in the expected range, with a gradual upfield shift going from Cr (225.5/222.0 ppm) to Mo (210.0/202.2 ppm) to W (201.9/192.4 ppm).

To further expand the coordination chemistry of silyliumylidene ions, we also attempted the synthesis of group 8 carbonyl complexes. No reaction could be observed between $Fe(CO)_5$ and **1b-OTf**. However, addition of one equivalent of the more reactive iron carbonyl compound $Fe_2(CO)_9$ to **1b-OTf** in THF resulted in the formation of $Fe(CO)_4$ complex **5**, which unfortunately was accompanied by slow polymerization of the solvent. We, therefore, switched to fluorobenzene, which allowed us to isolate complex **5** in good yield (72%) and purity as a colorless solid (Scheme 3). $Fe(CO)_5$ as the byproduct can

Scheme 3. Synthesis of Iron Carbonyl Complex 5

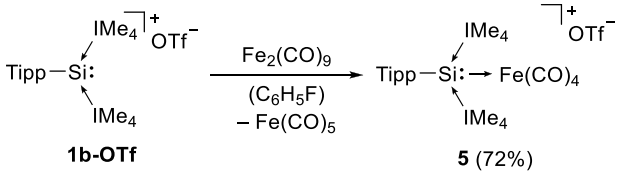

be easily removed under reduced pressure and no further polymerization occurred when the NMR measurements of the purified product where carried out in THF-d_8. As expected, coordination of iron to the silicon center once again causes a significant downfield shift of the ^{29}Si NMR resonance from −69.5 ppm (**1b-OTf**) to +5.4 ppm (**5**) (cf., Table 1). For comparison, the hydrosilylene complexes **VIa** and **VIb** show resonances at −11.1 ppm and −48.3 ppm, respectively (downfield from −80.5 ppm and −137.8 ppm in the free silylenes). The ^{1}H NMR spectrum is comparable to **2**−**4**, with a key difference being the significant upfield shift of the septet corresponding to the ortho ^{i}Pr groups to 3.14 ppm (for **5**) compared to 4.10−4.24 ppm observed for **2**−**4** (and 3.74 ppm for **1b-OTf**). Interestingly, no signal broadening of this septet occurs in this case. It is important to note that the ^{13}C NMR of complex **5** only shows a single resonance for the CO ligands at 217.5 ppm compared to the two resonances observed for the group 6 complexes.

Single-Crystal X-ray Diffraction (SC-XRD) Structure Determination. Single crystals suitable for XRD measurements of $Mo(CO)_5$ complex **3** were obtained by cooling a concentrated solution of **3** in Et_2O to −35 °C and single crystals of $Fe(CO)_4$ complex **5** were obtained by cooling a concentrated solution of **5** in C_6H_5F to −35 °C. The complexes are monomers in the solid state and feature a four-coordinate Si(II) center with a distorted tetrahedral geometry (Figure 1). As expected, the Mo atom in **3** features an octahedral coordination sphere with five terminal carbonyl ligands. The Si1−Mo1 bond lengths in **3** (2.673(1)/2.740(1) Å) are at the upper end of the reported Si−Mo bond lengths (2.41−2.71 Å).[23] In fact, 2.740(1) Å is the longest reported Mo−Si bond to date. They are much longer than the Si−Mo bonds in the silylene complexes **IIIb** (unsat./sat. = 2.471/2.480 Å)[16] and **IVb** (2.455(1) Å).[18] The bond is also significantly longer than the Si−W bond in silyliumylidene $W(CO)_5$ complex **I** (2.497(1) Å).[12] The Si1−C_{NHC} (avg. 1.956 Å) bond lengths, as well as the Mo1−C (avg. 2.035 Å) and C−O (avg. 1.142 Å) bond lengths, are in the expected range. So far, we were unable to obtain single crystals of the analogous Cr and W complexes, but because of their very similar NMR data and reactivity, they should exhibit comparable structures. The solid-state structure of iron complex **5** is very similar to that of tungsten complex **3**, except that the Fe atom adopts a trigonal bipyramidal structure with four terminal CO ligands (Figure 1, right) instead of five. Similarly, the Si1−Fe1 bond (2.349(1) Å) is also quite long. It is only slightly shorter than the longest reported Si−Fe bond to date (**VIb**, 2.372(1) Å).[20b] Similar to those in complex **3**, the Si1−C_{NHC}, Fe1−C, and C−O bonds are in the expected range.

IR Spectroscopic Analysis. All complexes **2**−**5** were characterized by IR spectroscopy. Experimentally determined values (solid state, neat) of CO stretching frequencies and the calculated bands of complexes **2**−**5** are listed in Table 2. Conclusions about the σ-donor or π-acceptor ability of silyliumylidene ion **1b** as a ligand can be drawn from the characteristic CO stretching frequencies in these complexes. To put the relative donor/acceptor strength of **1b** into perspective, we selected multiple literature known complexes and compared the CO stretching frequencies: strong(er) σ-donors/weak(er) π-acceptors increase the π-backbonding from the metal to the CO ligand and therefore strengthen the M−C bond while simultaneously weakening the C−O bond (which results in lower wave numbers of the CO stretching frequency, i.e., a bathochromic shift). Conversely, ligands with weak(er) σ-donor/strong(er) π-acceptor properties lead to higher wave numbers observed in the IR spectrum (i.e., a hypsochromic shift). In general, strong σ-donors are weaker π-acceptors and vice versa. However, in the case of **1**, the two coordinated NHC moieties occupy the p-orbitals, significantly reducing the π-acceptor ability of the central silicon atom. This drastically reduces the π-backbonding contribution from the metal fragment to the silicon center. Hence, any changes of the carbonyl stretching frequency observed in the IR spectrum

DOI: 10.1021/acs.inorgchem.9b02772
Inorg. Chem. 2019, 58, 14931−14937

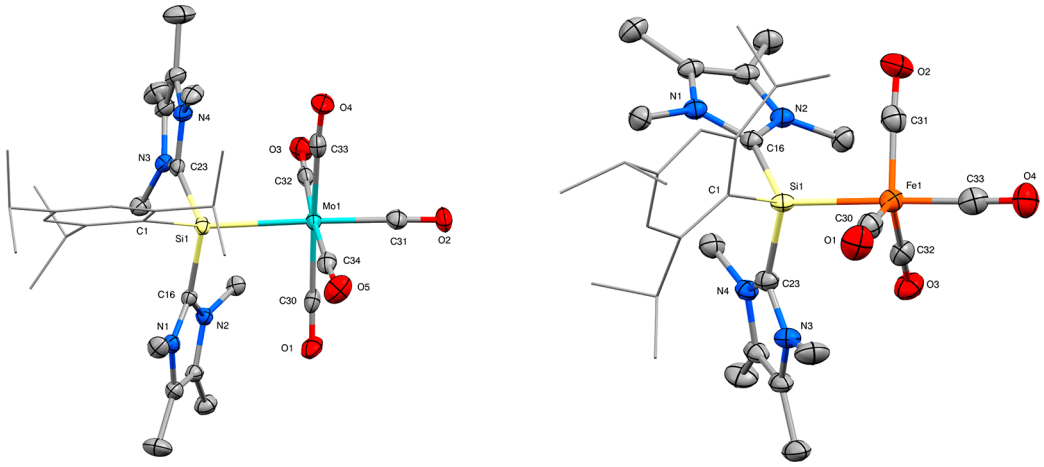

Figure 1. Ellipsoid plot (50% probability level) of the molecular structure of $Mo(CO)_5$ complex **3** (one out of two independent molecules in the asymmetric unit shown) and $Fe(CO)_4$ complex **5**. Tipp-substituents are simplified as wireframes. Hydrogen atoms, solvent molecules, and anions are omitted for clarity. Selected bond lengths [Å] and angles [°]: **3** Si1−Mo1 2.673(1)/2.740(1), Si1−C1 1.942(3)/1.966(3), Si1−C16 1.951(2)/1.950(3), Si1−C23 1.962(4)/1.960(3), Mo1−C30 2.037(3)/2.040(3), Mo1−C31 2.004(3)/1.998(3), Mo1−C32 2.043(4)/2.018(3), Mo1−C33 2.052(3)/2.057(3), Mo1−C34 2.041(4)/2.056(4), C30−O1 1.143(4)/1.140(4), C31−O2 1.140(4)/1.146(4), C32−O3 1.144(5)/1.154(5), C33−O4 1.140(3)/1.139(4), C34−O5 1.142(5)/1.142(4), Mo1−Si1−C1 132.7(1)/131.2(1), Mo1−Si1−C16 103.1(1)/102.2(1), Mo1−Si1−C23 108.1(1)/109.3(1), C1−Si1−C16 104.3(1)/108.6(1), C1−Si1−C23 98.9(1)/98.5(1), C16−Si1−C23 108.1(1)/104.8(1), Si1−Mo1−C31 169.4(1)/171.5(1); **5** Si1−Fe1 2.349(1), Si1−C1 1.91(2), Si1−C16 1.949(2), Si1−C23 1.956(2), Fe1−C30 1.768(2), Fe1−C31 1.775(2), Fe1−C32 1.781(3), Fe1−C33 1.790(3), C30−O1 1.160(3), C31−O2 1.157(3), C32−O3 1.154(3), C33−O4 1.146(3), Fe1−Si1−C1 115.5(6), Fe1−Si1−C16 116.5(1), Fe1−Si1−C23 106.4(1)), C1−Si1−C16 104.9(6), C1−Si1−C23 112.1(6), C16−Si1−C23 100.6(1), Si1−Fe1−C33 176.5(1).

Table 2. Experimentally Determined (Solid State, Neat) and Calculated CO Stretching Frequencies of Complexes 2−5 and Relevant IR Data for Reported Complexes I,[12] V,[20b] and VI[20]

		CO stretching frequencies $\delta_{C\equiv O}$ [cm^{-1}][a]	
	M	experimental	calculated
2	Cr	2037, 1965, 1889	2026, 1964, 1946, 1915, 1907
3	Mo	2054, 1969, 1897	2039, 1967, 1961, 1921, 1916
4	W	2052, 1963, 1891	2034, 1961, 1954, 1913, 1907
I	W	2070, 1991, 1921	
V	W	2042, 1952, 1879	
5	Fe	2021, 1943, 1887	2030, 1962, 1919, 1903
VIa	Fe	2009, 1922, 1884	
VIb	Fe	2002, 1919, 1878	
VIc	Fe	2011, 1904, 1855	
VId	Fe	1999, 1911, 1855	
VIe	Fe	2029, 1950, 1893	

[a]The difference in the number of observed and calculated IR bands can most likely be attributed to the overlap of close bands in the IR spectra.

should be mainly attributable to the σ-donor ability of Si(II) cation **1b**.

In general, common ligand classes like phosphines (e.g., $Ph_3P \rightarrow W(CO)_5$ $\delta_{C\equiv O}$ = 2060, 1914, 1887 cm^{-1})[24] or NHCs (e.g., IMes → $W(CO)_5$ $\delta_{C\equiv O}$ = 2057, 1911, 1876 cm^{-1})[25] are (significantly) stronger σ-donors than Si(II) cation **1b**, presumably because of the cationic nature of the silyliumylidene, as well as stronger π-acceptors, because of the presence of two NHC ligands on the central silicon atom reducing its π-acceptor ability. However, as this was expected, a comparison to other (donor-stabilized) low-valent silicon species is more fitting and interesting: the IR bands of silyliumylidene $W(CO)_5$ complexes **I**[12] and **4** (Table 2) show that silyliumylidene **1** is a stronger σ-donor/weaker π-acceptor than the corresponding DMAP-stabilized silyliumylidene ion.[5b] An increased σ-donor ability might be attributable to the two coordinated NHC moieties in **1** (vs the weaker N-donors in **I**), as it has been predicted that coordination of strong donors to silylenes actually increases their σ-donor strength considerably.[21] The substantial difference in bond lengths (cf., SC-XRD discussion) of these complexes could stem from the bulkier ligand framework present in our system. Comparison to complex **V**[20b] shows **1** to be a slightly weaker σ-donor than the respective hydrosilylene, presumably attributable to the cationic nature of **1**.[26]

Since no $Fe(CO)_4$ complexes of a Si(II) cation have been reported so far, we chose various related silylene complexes **VI**[20] for comparison. From this data, we can see that the σ-donor ability of silyliumylidene **1b** is very similar to the NHC-stabilized aryl-hydrosilylene ligand in **VIa** and, again, slightly lower than the NHC-stabilized silyl-hydrosilylene ligand in **VIb** (cf., $W(CO)_5$ complex). Considering that silyl groups have an increased σ-electron donating ability compared to aryl substituents, this is not surprising. Complex **VIe** ($IMe_4 \rightarrow SiCl_2 \rightarrow Fe(CO)_4$) shows comparable IR bands and with that should be very similar in relative σ-donor/π-acceptor strength. Furthermore, we have calculated the Tolman Electronic Parameters (TEPs) of the $[Tipp{-}Si(IMe_4)_2 \rightarrow Ni(CO)_3]^+$ complex (TEPs: 2063, 2017, 2001 cm^{-1}), which support the weak σ-donor/π-acceptor strength of **1b**.[20b,27]

Computational Studies. Density functional theory (DFT) calculations were performed to gain further insight into the ligand properties of silyliumylidene **1b** and the electronic structure and bonding situation in complexes **2**-**5**. We calculated the proton affinity (PA) of silyliumylidene **1**, which can be used to quantify its σ-donor ability.[28] For easy comparability, we employed the same method and basis set (B97-D/Def2-TZVP//B97-D/6-31G*) utilized in our previous publication discussing σ-donor/π-acceptor strength and ligand properties of various silylenes.[21] Expectedly, the

DOI: 10.1021/acs.inorgchem.9b02772
Inorg. Chem. 2019, 58, 14931−14937

predicted PA of 917 kJ/mol for **1b** was found to be rather low, which can most likely be attributed to the cationic nature of the silyliumylidene ion. This value does take the zwitterionic mesomeric structures of **1b** into consideration.[8a] Driess et al. reported a zwitterionic β-diketiminate silyliumylidene[29] that exhibits a similarly low PA (888 kJ/mol), which also stems from the cationic charge in the π-system of the ligand framework.[21] For comparison, these PAs are significantly lower than model phosphine compounds (Ph_3P, 1031 kJ/mol; Cy_3P, 1072 kJ/mol), NHCs (IDipp, 1176 kJ/mol), and donor-stabilized NHSis (~1200 kJ/mol) and slightly lower than nonstabilized NHSis (~980 kJ/mol).[21] These results agree well with those derived from the IR analysis.

Additionally, we calculated the frontier orbitals of all complexes: as expected, the HOMO and LUMO of **2**–**5** are very similar (as an example, see Figure 2 for HOMO and LUMO of **5**, cf., Figures S39–S41 for complexes **2**–**4**). While the HOMO of **5** is localized on the transition metal fragment, the LUMO is mainly located on the silicon center and the adjacent NHC framework. Furthermore, we also calculated the Wiberg Bond Indices (WBI) (Table 3). The low values for the WBIs (i.e., 0.63–0.78) correlate well with the long Si–M bond distances observed for the complexes. Investigation of the atomic charge distribution in complexes **2**–**5** via natural population analysis (NPA) shows a substantial positive charge located on the silyliumylidene silicon with a significant negative charge on the transition metal center. The negative charge located on the metal center decreases considerably with increasing atomic number of the metal (i.e., Cr (−2.61) → Mo (−2.25) → W (−1.66)), which is most likely the consequence of the orbital size differences that makes donation of the silicon-centered lone pair to the metal more difficult with its increasing size. Additionally, this conclusion is in line with the obtained bond polarization values and the increasing s character of silicon, which also indicate a decreasing donation of the silicon centered lone pair.

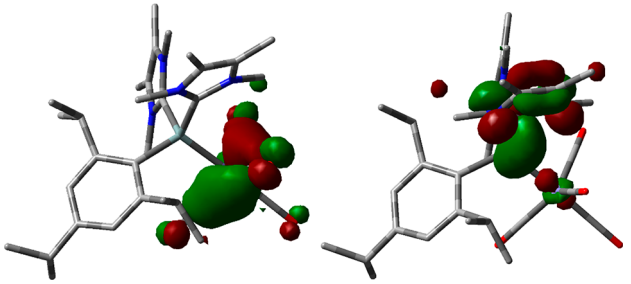

Figure 2. DFT-calculated frontier orbitals of silyliumylidene $Fe(CO)_4$ complex **5**: HOMO (left, −7.08 eV) and LUMO (right, −4.76 eV).

Interestingly, the calculated bond dissociation energies (BDEs) of **2**–**4** follow an opposite trend, showing the strongest binding for **4** (51.9 kcal/mol) and the weakest binding for **2** (41.5 kcal/mol). We presume that this trend can be traced back to an increased ionic nature of the Si → M bond with an increasing atomic number. This results in an increased bond strength with a decreasing covalent character, which is also reflected in the calculated WBI values. Finally, we note that **5** has both a much larger BDE than **2**–**4**, as well as an increased covalent character (WBI = 0.78). These results are comparable to the results of our previous study where we have systematically investigated Fe-carbonyl silylene complexes.[20b] Additionally, NBO analysis (cf., Table S2–S5) of iron complex **5** revealed a small contribution of π-backdonation from a metal d-orbital to the central silicon atom, while no π-backdonation for the group 6 complexes **2**–**4** was found. These substantial differences are also reflected in the thermal stability of the complexes: whereas the group 6 complexes **2**–**4** melt under decomposition between 74 and 83 °C, solid **5** only decomposes at temperatures higher than 195 °C.

CONCLUSIONS

In summary, we have synthesized and fully characterized a series of novel group 6 (Cr, Mo, W) and group 8 (Fe) carbonyl complexes **2**–**5** of an NHC-stabilized silyliumylidene ion, which includes the first reported Fe, Cr and Mo complexes of a silyliumylidene ion, by directly reacting silyliumylidene triflate **1b-OTf** with transition metal carbonyl precursors. Coordination of the Si(II) cation to the metal is accompanied by a significant downfield shift of the ^{29}Si NMR resonance. SC-XRD analysis revealed surprisingly long Si–M bond lengths. Analysis of the complexes via carbonyl IR stretching frequencies together with DFT calculations give insight into the σ-donor ability of the Si(II) cation, which is significantly lower than in model NHC or phosphine complexes, most likely because of the positive charge located on the silicon center. Further coordination chemistry of NHC-stabilized Si(II) cations toward other metals and their application in organometallic transformations is currently under investigation in our laboratory.

ASSOCIATED CONTENT

Supporting Information

The Supporting Information is available free of charge on the ACS Publications website at DOI: 10.1021/acs.inorgchem.9b02772.

Experimental details, crystallographic data, NMR spectra, IR spectra, and computational details (PDF)

Accession Codes

CCDC 1949742–1949745 contain the supplementary crystallographic data for this paper. These data can be obtained free of charge via www.ccdc.cam.ac.uk/data_request/cif, or by emailing data_request@ccdc.cam.ac.uk, or by contacting The

Table 3. Summary of the Calculated Si–M Bond Lengths, Bond Dissociation Energies (BDEs), Percentage of s Character on the Silicon Center, NPA Atomic Charges, Wiberg Bond Index (WBI) for Complexes 2–5

					bond polarization		NPA atomic charge		WBI
	M	theor. Si–M [Å]	BDE Si–M [kcal/mol]	s character of silicon [%]	Si [%]	M [%]	Si	M	Si–M
2	Cr	2.541	41.5	33.4	60.4	39.6	+1.24	−2.61	0.69
3	Mo	2.686	45.2	35.3	64.7	35.3	+1.18	−2.25	0.66
4	W	2.679	51.9	36.9	69.0	31.0	+1.12	−1.66	0.63
5	Fe	2.340	62.1	31.8	53.0	47.0	+1.32	−1.59	0.78

DOI: 10.1021/acs.inorgchem.9b02772
Inorg. Chem. 2019, 58, 14931–14937

Cambridge Crystallographic Data Centre, 12 Union Road, Cambridge CB2 1EZ, UK; fax: +44 1223 336033.

AUTHOR INFORMATION

Corresponding Author

*E-mail: s.inoue@tum.de.

ORCID

Tibor Szilvási: 0000-0002-4218-1570

Shigeyoshi Inoue: 0000-0001-6685-6352

Notes

The authors declare no competing financial interest.

ACKNOWLEDGMENTS

The authors are exceptionally grateful to the WACKER Chemie AG and the European Research Council (SILION 637394) for continued financial support. We are also thankful to Dr A. Pöthig and Dr C. Jandl for advice regarding crystallography and K. Huber for his experimental work concerning the anion exchange reactions.

REFERENCES

(1) Jutzi, P.; Mix, A.; Rummel, B.; Schoeller, W. W.; Neumann, B.; Stammler, H.-G. The Me_5C_5Si Cation: A Stable Derivative of HSi^+. *Science* **2004**, *305*, 849−851.

(2) (a) Bertrand, G. The Modest Undressing of a Silicon Center. *Science* **2004**, *305*, 783−785. (b) Powley, S. L.; Inoue, S. NHC-Stabilised Silyliumylidene Ions. *Chem. Rec.* **2019**, DOI: 10.1002/tcr.201800188.

(3) Xiong, Y.; Yao, S.; Inoue, S.; Epping, J. D.; Driess, M. A Cyclic Silylone ("Siladicarbene") with an Electron-Rich Silicon(0) Atom. *Angew. Chem., Int. Ed.* **2013**, *52*, 7147−7150.

(4) Ahmad, S. U.; Szilvási, T.; Irran, E.; Inoue, S. An NHC-Stabilized Silicon Analogue of Acylium Ion: Synthesis, Structure, Reactivity, and Theoretical Studies. *J. Am. Chem. Soc.* **2015**, *137*, 5828−5836.

(5) (a) Xiong, Y.; Yao, S.; Inoue, S.; Irran, E.; Driess, M. The Elusive Silyliumylidene $[ClSi:]^+$ and Silathionium $[ClSi{=}S]^+$ Cations Stabilized by Bis(Iminophosphorane) Chelate Ligand. *Angew. Chem., Int. Ed.* **2012**, *51*, 10074−10077. (b) Yeong, H.-X.; Xi, H.-W.; Li, Y.; Lim, K. H.; So, C.-W. A Silyliumylidene Cation Stabilized by an Amidinate Ligand and 4-Dimethylaminopyridine. *Chem. - Eur. J.* **2013**, *19*, 11786−11790. (c) Sarkar, D.; Wendel, D.; Ahmad, S. U.; Szilvási, T.; Pöthig, A.; Inoue, S. Chalcogen-atom transfer and exchange reactions of NHC-stabilized heavier silaacylium ions. *Dalton Trans* **2017**, *46*, 16014−16018.

(6) Sarkar, D.; Nesterov, V.; Szilvási, T.; Altmann, P. J.; Inoue, S. The Quest for Stable Silaaldehydes: Synthesis and Reactivity of a Masked Silacarbonyl. *Chem. - Eur. J.* **2019**, *25*, 1198−1202.

(7) Porzelt, A.; Schweizer, J.; Baierl, R.; Altmann, P.; Holthausen, M.; Inoue, S. S-H Bond Activation in Hydrogen Sulfide by NHC-Stabilized Silyliumylidene Ions. *Inorganics* **2018**, *6*, 54.

(8) (a) Ahmad, S. U.; Szilvási, T.; Inoue, S. A facile access to a novel NHC-stabilized silyliumylidene ion and C-H activation of phenylacetylene. *Chem. Commun.* **2014**, *50*, 12619−12622. (b) Gerdes, C.; Saak, W.; Haase, D.; Müller, T. Dibenzosilanorbornadienyl Cations and Their Fragmentation into Silyliumylidenes. *J. Am. Chem. Soc.* **2013**, *135*, 10353−10361.

(9) Leszczyńska, K.; Mix, A.; Berger, R. J. F.; Rummel, B.; Neumann, B.; Stammler, H.-G.; Jutzi, P. The Pentamethylcyclopentadienylsilicon(II) Cation as a Catalyst for the Specific Degradation of Oligo(ethyleneglycol) Diethers. *Angew. Chem., Int. Ed.* **2011**, *50*, 6843−6846.

(10) Nesterov, V.; Reiter, D.; Bag, P.; Frisch, P.; Holzner, R.; Porzelt, A.; Inoue, S. NHCs in Main Group Chemistry. *Chem. Rev.* **2018**, *118*, 9678−9842.

(11) Breit, N. C.; Szilvási, T.; Suzuki, T.; Gallego, D.; Inoue, S. From a Zwitterionic Phosphasilene to Base Stabilized Silyliumylidene-Phosphide and Bis(silylene) Complexes. *J. Am. Chem. Soc.* **2013**, *135*, 17958−17968.

(12) Yeong, H.-X.; Li, Y.; So, C.-W. A Base-Stabilized Silyliumylidene Cation as a Ligand for Rhodium and Tungsten Complexes. *Organometallics* **2014**, *33*, 3646−3648.

(13) Frisch, P.; Inoue, S. Coinage metal complexes of NHC-stabilized silyliumylidene ions. *Chem. Commun.* **2018**, *54*, 13658−13661.

(14) Ghana, P.; Arz, M. I.; Schnakenburg, G.; Straßmann, M.; Filippou, A. C. Metal-Silicon Triple Bonds: Access to $[Si(\eta^5\text{-}C_5Me_5)]^+$ from SiX_2(NHC) and its Conversion to the Silylidyne Complex $[TpMe(CO)_2MoSi(\eta^3\text{-}C_5Me_5)]$ (TpMe = κ^3-*N*,*N*',*N*''-hydridotris(3,5-dimethyl-1-pyrazolyl)borate). *Organometallics* **2018**, *37*, 772−780.

(15) Iwamoto, T.; Ishida, S. Stable Silylenes and Their Transition Metal Complexes. In *Organosilicon Compounds*; Lee, V. Y., Ed.; Academic Press, 2017; Chapter 8, pp 361−532.

(16) Schmedake, T. A.; Haaf, M.; Paradise, B. J.; Millevolte, A. J.; Powell, D. R.; West, R. Electronic and steric properties of stable silylene ligands in metal(0) carbonyl complexes. *J. Organomet. Chem.* **2001**, *636*, 17−25.

(17) Zark, P.; Schäfer, A.; Mitra, A.; Haase, D.; Saak, W.; West, R.; Müller, T. Synthesis and reactivity of N-aryl substituted N-heterocyclic silylenes. *J. Organomet. Chem.* **2010**, *695*, 398−408.

(18) Azhakar, R.; Ghadwal, R. S.; Roesky, H. W.; Wolf, H.; Stalke, D. Stabilization of Low Valent Silicon Fluorides in the Coordination Sphere of Transition Metals. *J. Am. Chem. Soc.* **2012**, *134*, 2423−2428.

(19) Blom, B.; Pohl, M.; Tan, G.; Gallego, D.; Driess, M. From Unsymmetrically Substituted Benzamidinato and Guanidinato Dichlorohydridosilanes to Novel Hydrido N-Heterocyclic Silylene Iron Complexes. *Organometallics* **2014**, *33*, 5272−5282.

(20) (a) Lutters, D.; Severin, C.; Schmidtmann, M.; Müller, T. Activation of 7-Silanorbornadienes by N-Heterocyclic Carbenes: A Selective Way to N-Heterocyclic-Carbene-Stabilized Silylenes. *J. Am. Chem. Soc.* **2016**, *138*, 6061−6067. (b) Eisenhut, C.; Szilvási, T.; Dübek, G.; Breit, N. C.; Inoue, S. Systematic Study of N-Heterocyclic Carbene Coordinate Hydrosilylene Transition-Metal Complexes. *Inorg. Chem.* **2017**, *56*, 10061−10069.

(21) Benedek, Z.; Szilvási, T. Can low-valent silicon compounds be better transition metal ligands than phosphines and NHCs? *RSC Adv.* **2015**, *5*, 5077−5086.

(22) Buchner, W.; Schenk, W. A. ^{13}C NMR spectra of monosubstituted tungsten carbonyl complexes. NMR trans influence in octahedral tungsten (0) compounds. *Inorg. Chem.* **1984**, *23*, 132−137.

(23) Ghana, P.; Arz, M. I.; Chakraborty, U.; Schnakenburg, G.; Filippou, A. C. Linearly Two-Coordinated Silicon: Transition Metal Complexes with the Functional Groups M≡Si—M and M═Si═M. *J. Am. Chem. Soc.* **2018**, *140*, 7187−7198.

(24) Yih, K.-H.; Lee, G.-H.; Wang, Y. Synthesis and Structural Characterization of Configurational Isomers of Tungsten-Palladium Complexes with Bridging Diphenyl(dithioalkoxycarbonyl)phosphine as a Ligand and Phosphine Transfer from Tungsten to Palladium. *Inorg. Chem.* **2000**, *39*, 2445−2451.

(25) Wang, Z.; Li, S.; Teo, W. J.; Poh, Y. T.; Zhao, J.; Hor, T. S. A. Molybdenum (0) and tungsten (0) carbonyl N-heterocyclic carbene complexes as catalyst for olefin epoxidation. *J. Organomet. Chem.* **2015**, *775*, 188−194.

(26) Inoue, S.; Eisenhut, C. A Dihydrodisilene Transition Metal Complex from an N-Heterocyclic Carbene-Stabilized Silylene Monohydride. *J. Am. Chem. Soc.* **2013**, *135*, 18315−18318.

(27) Ardizzoia, G. A.; Brenna, S. Interpretation of Tolman electronic parameters in the light of natural orbitals for chemical valence. *Phys. Chem. Chem. Phys.* **2017**, *19*, 5971−5978.

(28) (a) Fey, N.; Tsipis, A. C.; Harris, S. E.; Harvey, J. N.; Orpen, A. G.; Mansson, R. A. Development of a Ligand Knowledge Base, Part 1: Computational Descriptors for Phosphorus Donor Ligands. *Chem. - Eur. J.* **2006**, *12*, 291−302. (b) Jover, J.; Fey, N.; Harvey, J. N.; Lloyd-

DOI: 10.1021/acs.inorgchem.9b02772
Inorg. Chem. 2019, 58, 14931−14937

Jones, G. C.; Orpen, A. G.; Owen-Smith, G. J. J.; Murray, P.; Hose, D. R. J.; Osborne, R.; Purdie, M. Expansion of the Ligand Knowledge Base for Monodentate P-Donor Ligands (LKB-P). *Organometallics* **2010**, *29*, 6245−6258.
(29) Driess, M.; Yao, S.; Brym, M.; van Wüllen, C. Low-Valent Silicon Cations with Two-Coordinate Silicon and Aromatic Character. *Angew. Chem., Int. Ed.* **2006**, *45*, 6730−6733.

DOI: 10.1021/acs.inorgchem.9b02772
Inorg. Chem. 2019, 58, 14931−14937

7. Summary and Outlook

Acyclic silylenes

With the limited number of reported examples, we used a combination of NHI and silyl ligands to access new donor-free acyclic silylenes. Formation of a green acyclic imino(silyl)silylene **1** (Scheme 9, chapter 6.1) was achieved at low-temperatures and verified by combined experimental and theoretical studies. Its isolable resting state was found to be a yellow silacycloheptatriene **1'** (silepin, Si +IV), which is a direct result of the high *Lewis* acidic character of **1**. As such it is capable of insertion into the C=C bonds of the ligand phenyl ring, resulting in the dearomatised silepin complex (**1'**). Theoretical studies revealed these two complexes to be close in energy and thermal rearrangement of **1'** to **1** is accessible, thus enabling **1'** to be used as a 'masked' silylene. **1'** can also be converted with BCF to yield the adduct of the silylene (**2**) and was further examined towards the activation of small molecules. The Si(+IV) compound (**1'**) activates H_2 and ethylene under mild conditions and furthermore conversion with CO_2 yields the first monomeric silicon carbonate complex **3** under release of CO.

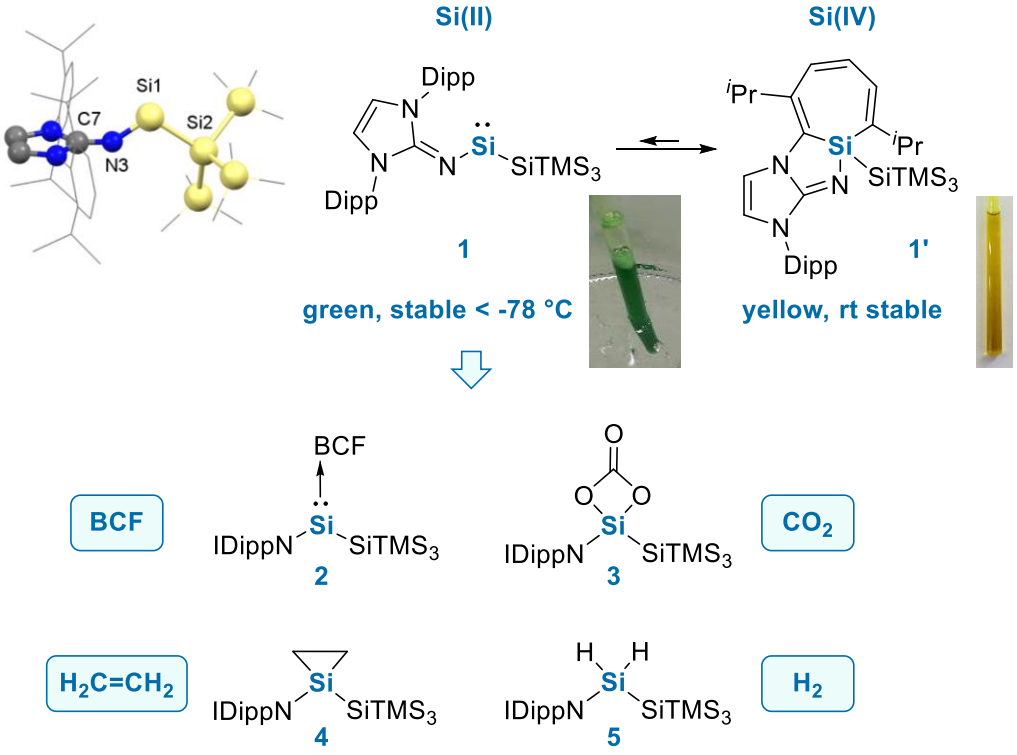

Scheme 9: Summary of the reactivity of imino-hypersilyl-silepin acting as a masked silylene including the calculated structure of **1** (chapter 6.1).[308]

Formation of **3** was assumed to proceed *via* an intermediary silanone. Silanones are three coordinate silicon species which bear a Si–O double bond, thus representing the heavier congeners of ketones and are often referred to as "Kipping's dream".[309-310] Changing the oxygenation agent to N_2O, gave rise to formation of the first acyclic three-coordinate silanone **6a** (Scheme 10, chapter 6.2). Unsurprisingly, it bears limited stability in solution. However, silyl ligand exchange enhanced the stability and enabled the SC-XRD characterisation of **6b**. NBO analysis of **6b,** including representative smaller model systems, revealed both ligands crucial for the stabilisation of this species: Firstly, the strong electron-donating NHI group forces overlap of the lone pair of the exocyclic nitrogen with the Si–O π-bond (HOMO-10). Secondly, the polarisation of the silicon oxygen bond is reduced due to the attached electropositive silyl group. The similarities and differences between **2a** and **2b** were examined, with both compounds providing access to

carbonates **3a**/**3b** and methanol quenching products **7a**/**7b**. For the hypersilyl-substituted **6a** rearrangement to a disilene, *via* TMS-migration to the oxygen, was proposed and verified by reaction of the intermediary disilene with ethylene (compound **9**). Furthermore, the NHC-disilene adduct **8** was isolated, which is best represented by its zwitterionic structure according to NBO analysis. In the case of **6b**, a different rearrangement to imino-siloxy-substituted silylene **10** was observed. This silylene represents the first reported oxygen-substituted acyclic silylene, which bears an increased HOMO-LUMO gap and ΔE_{ST} compared to **1a**. However, it was still able to activate ethylene to give **11** at rt. Since this report, silanone **6b** was further shown to enable sila-Wittig reactions.[311]

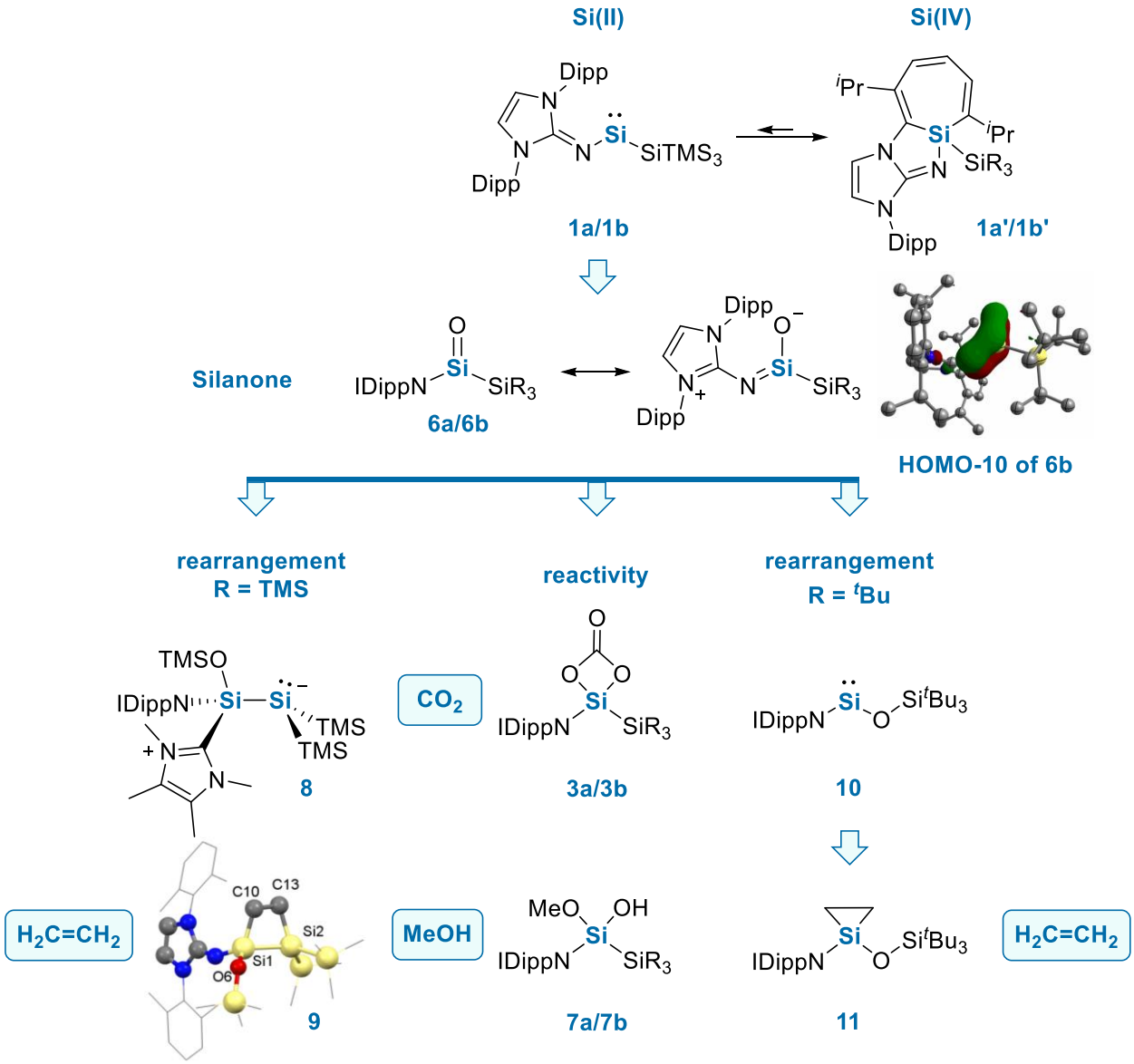

Scheme 10: Summary of the reactivity of silanones **6a**/**6b** (chapter 6.2).[312]

Inspired by the TMS group migration occurring for **6a**, we studied this rearrangement in an acyclic bis(silyl)silylene (chapter 6.3). Combination of the hypersilyl and supersilyl groups in one molecule provided access to disilene **12'**, which according to extended calculations bears a *trans*-bent and twisted structure, comparable to **L36** and **L40** (Figure 14). Mechanistic theoretical studies revealed the equilibrium between disilene **12'** and bis(silyl)silylene **12** is accessible whereas deactivation of the equilibrium mixture *via* C–H activation of **12** (yielding **13**) is connected with a substantially higher barrier. These calculations revealed a triplet state of **12** to be lower in energy compared to the singlet state. However, experimental

proof for the triplet silylene could not be found, although several siliranes where obtained from [2 + 1] cycloaddition reactions. Additionally, efficient activation of H_2 by **12**/**12'** at mild conditions was found to yield compound **15**. This conversion is connected with a low activation barrier of only 4.2 kcal/mol. For the previously reported acyclic silylenes, activation of H_2 at mild conditions was thought to be connected to the low HOMO-LUMO gaps of these species. However, **12** bears a rather high $\Delta E_{HOMO\text{-}LUMO}$ of 4.18 eV, thus the general assumption of low HOMO-LUMO gaps being a requirement for H_2 activation (*via* a low activation barrier) does not hold true for bis(silyl)silylenes. Additional high level calculations by Holthausen revealed the singlet state of **12** being lower in energy, supporting the assumed activation of H_2 *via* the singlet bis(silyl)silylene. Furthermore, reaction of **12'** with ammonia yielded compound **16**, verified by combined experimental and theoretical methods.

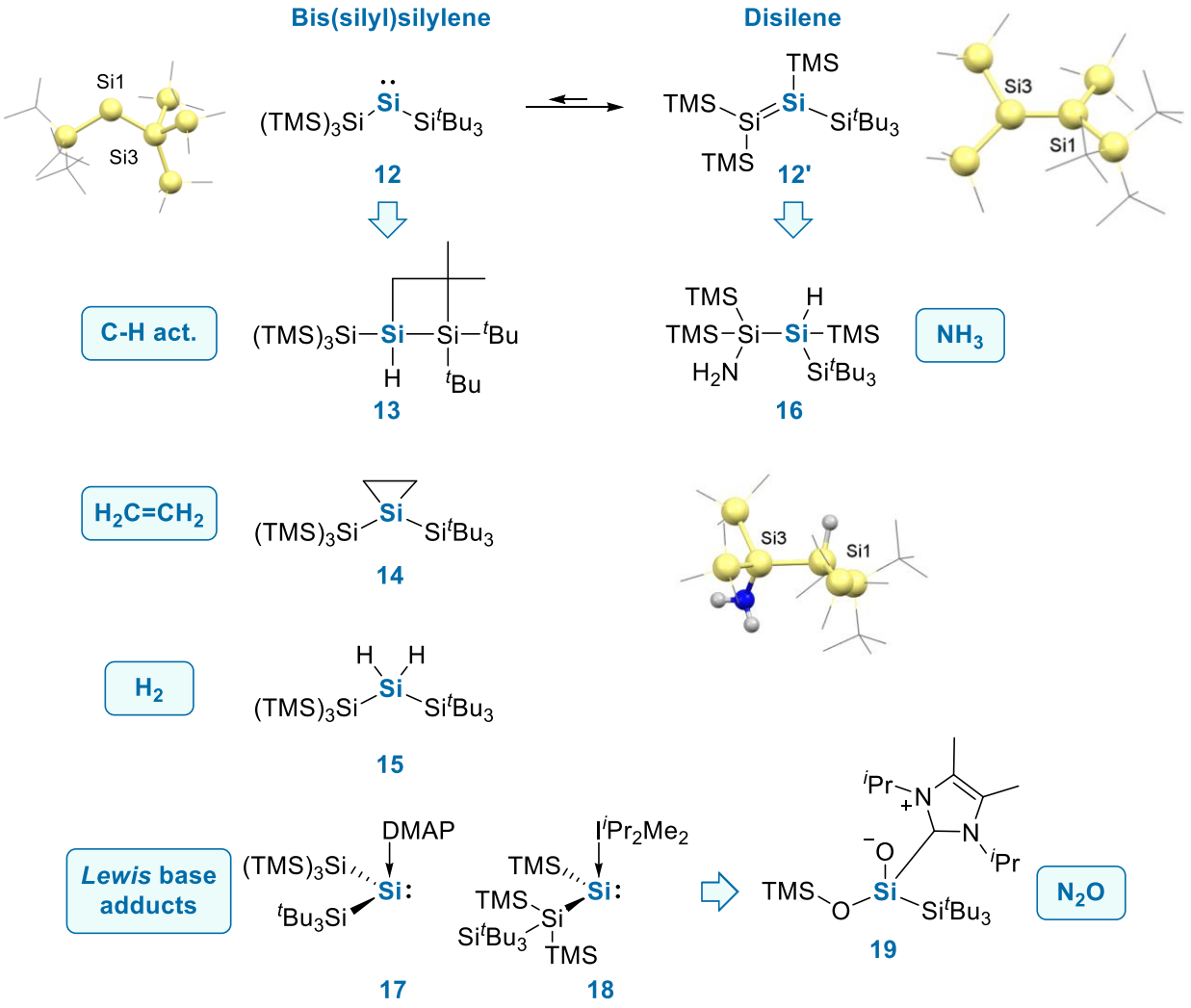

Scheme 11: Reactivity of the equilibrium mixture **12**/**12'** including calculated structures.[313]

Furthermore, this study was successful in the isolation of the different accessible silylenes by stabilisation with *Lewis* bases (compounds **17** and **18**). Rearrangement of **18** and *Lewis* base exchange reactions (in the order DMAP ⟶ I^{i}Pr$_2$Me$_2$ ⟶ IMe$_4$) were observed, which is in line with increased donor strength and *Gibbs* free energies of bond dissociation. In addition, NHC-stabilised silylene **18** was shown to selectively react with N_2O to yield silyl ester **19**. NBO analysis of **19** revealed a zwitterionic formulation as the most appropriate *Lewis* structure with additional negative hyperconjugation from the oxygen lone pairs into the Si–C^{NHC} and the second Si–O bonds rationalising the rather short Si–O bonds observed within SC-XRD analysis.

In the last silylene chapter (6.4), the bent silicon carbonyl complex **20** (Scheme 12) was studied in detail. Combined NBO and QTAIM analysis revealed a major contribution of the donor-acceptor bonding motif (chapter Donor-stabilised Silylenes, Figure 9), bearing donation from the carbonyl to the silicon centre and back-donation from the silicon centre to the carbonyl unit, which is reminiscent of transition-metal carbonyl complexes. Furthermore, the bis(silyl)-substitution was found to be critical for the high stability of **20** *via* comparative calculations on a variety of smaller model systems.

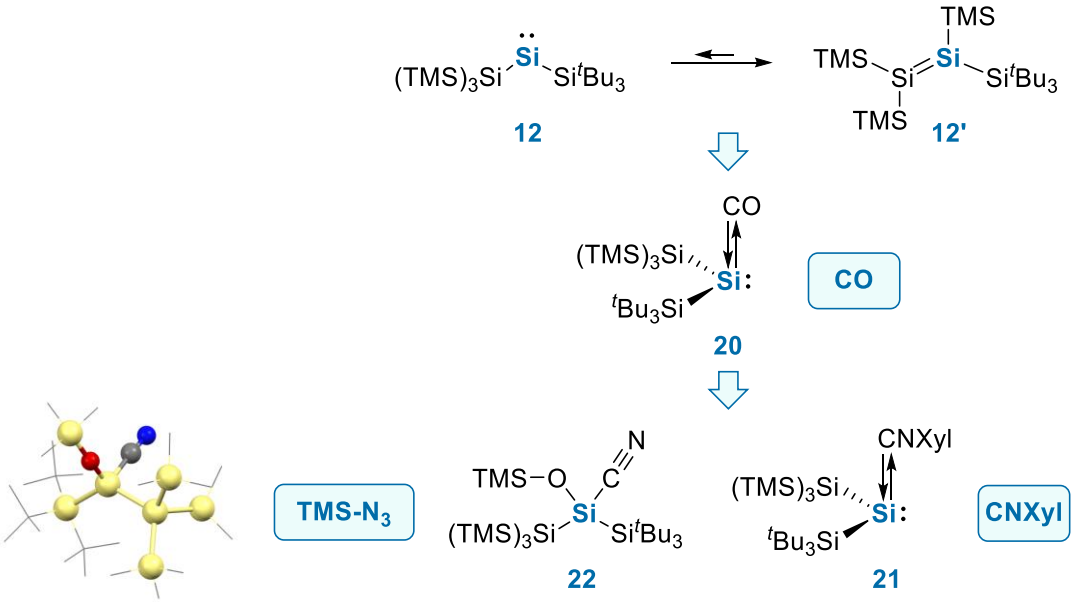

Scheme 12: Reactivity of disilene/bis(silyl)silylene equilibrium mixture towards CO, exchange with isocyanide and functionalisation of the CO moiety with TMS-N_3.[314]

Akin to transition-metal complexes, the CO unit in **20** can be exchanged with isocyanides to give **21**. To elucidate the high resemblance to transition-metal carbonyl complexes further, the CO unit in **20** was successfully reacted with TMS-azide. In contrast to transition metal-carbonyls, which result in isocyanide formation, a silyl cyanide **22** was obtained. This was attributed to the high oxophilicity of silicon compared to transition-metals.

In conclusion, this thesis has succeeded in broadening the scope of donor-free acyclic silylenes bearing NHI- and/or silyl ligands as well as insight into new reactivity pathways. The experimental work was supported by a variety of computational methods providing in-depth insight into the underlying mechanisms and bonding situations, which are not obtainable by experimental work alone. This includes the first reversible Si(II)/Si(IV) redox couple, which gave access to two silanones, the heavier analogues of ketones, with the choice of silyl ligand found to be influential in their rearrangement pathways. Thorough investigations into key parameters, e.g. electronic and mechanistic insights, aided molecular design which resulted in the first acyclic bis(silyl)silylene, accessible from its rearranged disilene. Furthermore, silicon carbonyl complexes resembling transition-metal carbonyl complexes were achieved within this thesis. The first step of a catalytic cycle (Scheme 7) was shown to be possible for the investigated systems with a variety of reagents, yet challenges towards reductive elimination (i.e. last step in a catalytic cycle) still remain. In this regard, the reversible Si(II)/Si(IV) redox couple highlights that it is indeed possible to go from Si(IV) to Si(II) and back again, which is highly advantageous when considering the catalytic potential of main group compounds. Moreover, it was shown that the reactivity of acyclic silylenes cannot be judged from their HOMO-LUMO gap alone, as other factors yet to be identified influence their ability to activate enthalpically strong bonds like those present in H_2.

In view of catalysis, the large variety of acyclic silylenes should encourage further investigations in enabling the next steps towards a catalytic application, with a particular focus on reductive elimination

strategies. This might include further ligand modification to enable a more flexible nature of applied stabilising donors, i.e. labile donor ligands, as this could provide a vacant coordination site for further functionalisation of the oxidative addition products.

Dialumenes

As highlighted in chapter 3, low-valent aluminium compounds bearing multiple bond character were targeted for several years, but dialumenes remained elusive. Use of a combination of strong σ-donating silyl groups and NHCs allowed access to dialumene **23** (Scheme 13) which is the first of its kind (chapter 6.5). Dialumene **23** exhibits a completely *trans*-planar structure with the shortest Al–Al bond reported to date. NBO analysis revealed two bonds between the aluminium centres, which is reflected in HOMO and HOMO-1 of **23**. Reactivity evaluated the double bonding nature of **23** *via* reaction with C–C multiple bonds to give compounds **24**-**26**.

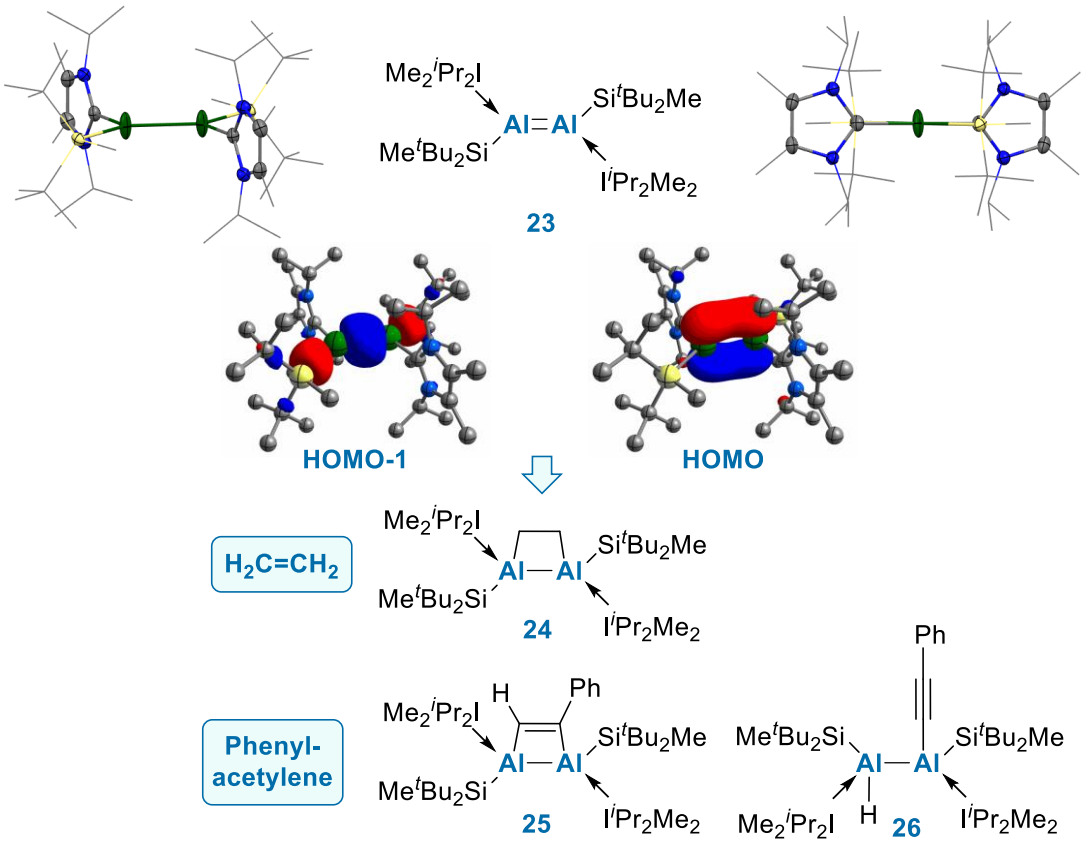

Scheme 13: Structure and frontier orbitals of dialumene **23** and reactivity towards C–C multiple bonds.[315]

Following this report, the reactivity of **23** was extended to CO_2, NO_2 and O_2 including the catalytic reduction of CO_2 by HBpin.[244]

Extension of this dialumene chemistry was achieved through isolation of an aryl-stabilised double bond (**27**, Scheme 14, chapter 6.6). This change in ligands highly influences the geometry at the aluminium centres as dialumene **27** exhibits a *trans*-bent and twisted structure. Theoretical evaluation of this structural difference involved examination of a variety of smaller model systems. This revealed the *trans*-planar structure of **23** as a direct result of the high steric demand and shape of the silyl ligand. In the case of Tipp-substitution (**27**), the steric demand is decreased and, therefore, delocalisation of the π-bond to the carbene carbon atoms is possible due to increased flexible coordination of NHCs. Furthermore, NBO analysis revealed the electronic effect on the Al_2 core as a change in polarisation accompanied with a

decreased HOMO-LUMO gap present in **27**. These differences were also addressed experimentally. Whereas reaction with ethylene and phenylacetylene affords the products akin to the silyl case, the increased flexibility of **27** allows for conversion with di(phenyl)acetylene to give **28**, which is inaccessible for **23**. Furthermore, clean conversion with Xylyl-isocyanide resulted in the formation of **29**, bearing a butterfly configuration. Comparison in the reactions towards small molecules (CO_2, O_2, N_2O) revealed enhanced reactivity of **27** including the characterisation of an inorganic epoxide (**30**) as a semi-stable intermediate. Furthermore, switching of ligands in dialumene **27** renders the activation of H_2 possible, yielding a mixture of the *trans*- and *cis*-products of **31**.

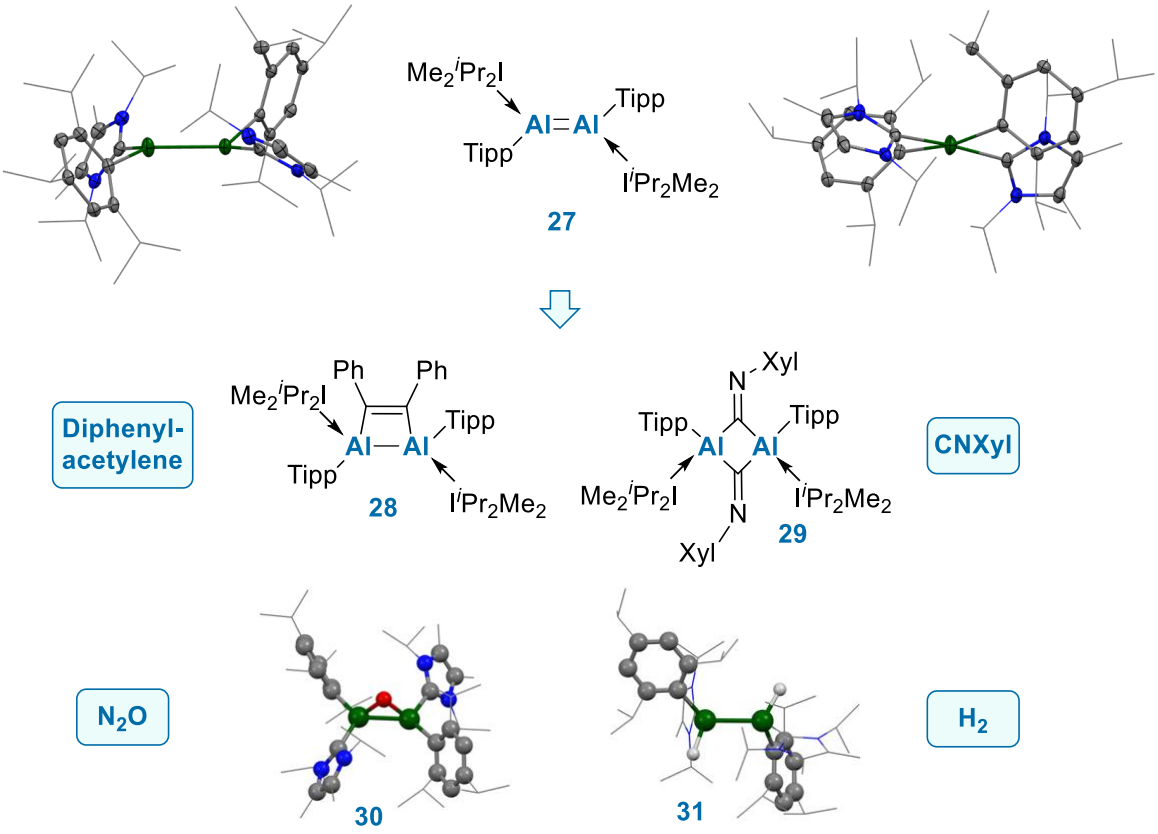

Scheme 14: *Trans*-bent and twisted structure of dialumene **27** including its enhanced reactivity and calculated structures.[316]

In the second part of this report, the activity of **23**/**27** in catalysis was compared experimentally, which revealed the analogous enhanced reactivity of **27** compared to **23**. In the hydroboration of CO_2 dialumene **27** allows for the reduction of catalyst loading and enables access to the higher reduced species. In amine-borane dehydrogenation catalysis, **27** clearly outperforms **23**, which only yields low conversions. This was attributed to the ability of **27** to form Al–H bonds.

To summarise, this thesis investigated the first two isolable NHC-stabilised dialumenes including the first study to include a direct comparison of silyl and aryl ligands in main group multiple bonds. This revealed important insights into the bonding situation of this new class of compounds and the influence of the attached ligands on the structural motif was disclosed. With dialumene chemistry in its infancy, future work should investigate the full potential of these systems particularly in regard to catalytic application. Utilisation of other stabilising ligands and/or different donors can further fine tune the reactivity of dialumenes to challenge the prosperous group of anionic aluminyls (chapter 3, Figure 26) that have been published recently.

Silyliumylidene Ions

The studies on aryl-substituted silyliumylidene ions began with optimisation of the existing synthetic procedure. Now NHC-stabilised silyliumylidene ion **32** (Scheme 15, chapter 6.7) is accessible on the gram scale as a prerequisite to study its reactivity in a broader context. Concerning its rather unexplored reactivity, treatment of **32** with H_2S yielded NHC-stabilised thiosilaaldehyde **34**. Combined bonding analysis using NBO and QTAIM revealed the zwitterionic representation as the most appropriate *Lewis* structure for **34** (Scheme 15), although enhanced interaction between silicon and sulphur is present due to negative hyperconjugation from the sulphur lone-pairs (Scheme 15). Computational mechanistic investigations revealed a stepwise addition of H_2S to the nucleophilic silicon centre. Thus, **32** bears reactivity better represented by the *Lewis* representation **A** in Scheme 15. This addition is followed by barrierless NHC dissociation and S-H abstraction by the now free NHC, which yields compound **34**. Hence, the lability of the coordinated NHCs represents an important step in this reaction.

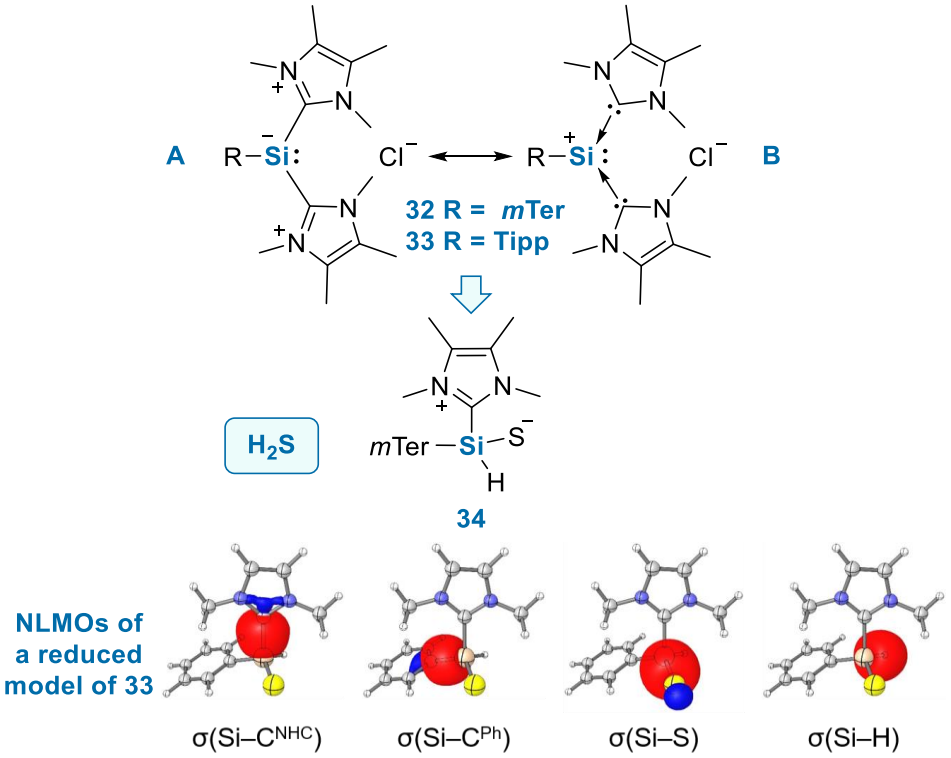

Scheme 15: Different *Lewis* structures for **32** and **33** as well as reactivity of silyliumylidene ion **32** towards hydrogen sulphide and NLMOs of **34**.[317]

Furthermore, the interconversion of **32** and NHC-stabilised chloro-silylene **L10** (Figure 8) was studied experimentally and theoretically, revealing them to be located close in energy but connected with a substantial barrier for interconversion by addition of one NHC. This also precluded the contribution of **L10** in reactions of **32** at low-temperature, thus providing a consistent mechanistic picture between experimental and theoretical observations.

Further reactivity studies towards a variety of reagents were hampered either by low solubility of **32** and **33** in solvents different to acetonitrile, instability of the reagents in acetonitrile or interference of the chloride counter anion. Hence, anion exchange was sought to mitigate these issues.

Reaction with KOTf in acetonitrile gave the anion exchanged silyliumylidene ions **35** and **36**, respectively, in good yields. Thus, providing an easy route to increased solubility across a range of routinely used polar and non-polar solvents. Compound **35** and **36** were reported along with the metal carbonyl adducts (**37**-

40) of **35** (Scheme 16, chapter 6.8). Notably, adduct formation was not possible with the sterically more demanding silyliumylidene ion **35**. Metal carbonyl complexes **38** and **40** possessed Si–M bonds located at the upper end of reported values for Si–M single bonds. IR spectroscopy along with DFT calculations revealed that **36** bears poor σ-donor abilities, which is probably connected to its positive charge.

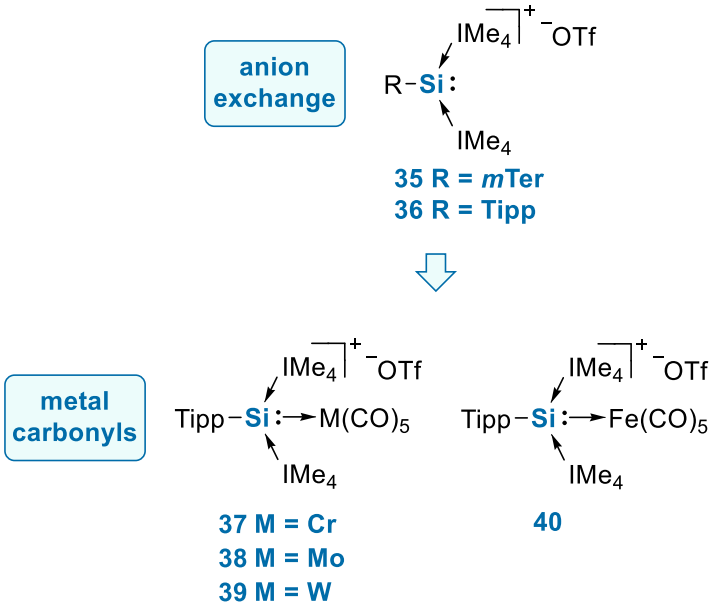

Scheme 16: Conversion of anion exchanged silyliumylidenes **35** and **36** with different metal carbonyls.[318]

Preliminarily studies on further application of **35** and **36** revealed the potential of these systems in bond activations and catalysis, which was reported in a short lecture in July 2019 at the ICHAC conference in Prague prior to the report of the group of So (Scheme 3 **D-F**).[211] Current ongoing investigations into the role of **35** and **36** in catalysis appear to be more intricate than the recent report of silyliumylidene catalysis by the group of So.

To summarise, this thesis revealed a rather nucleophilic reaction profile of NHC-stabilised silyliumylidene ions. Further reactivity studies using the anion-exchanged versions should provide further insight into the variety of accessible chemistry for these compounds, including their application in catalysis.[319] Prospective investigations demand for a more flexible coordination of the applied donor, to enable reactivity at the p-orbitals of the silicon centre, which have hitherto be shown to be blocked by coordination of the two NHC moieties.

In conclusion, this thesis features a series of silicon and aluminium compounds with ligands not solely responsible for stabilisation but also governing the reactivity of these compounds. Oxidative addition of challenging small molecules was achieved, representing the first step of a catalytic cycle. Yet, the challenge to also gain control of reductive elimination (i.e. the last step in a catalytic cycle) still remains. In this regard, the reversible Si(II)/Si(IV) redox couple highlights that this is possible for low-valent silicon compounds. To further develop the catalytic potential of some of the most abundant elements found within the Earth's crust, namely silicon and aluminium, a comprehensive understanding of their bonding and reaction mechanisms is required. This can be achieved upon the interplay of theoretical and experimental chemistry enabling insights into the structure-reactivity relationship. With this in hand, catalyst design can be improved to enable true catalytic application of low-valent main group complexes.

8. Licenses for Copyrighted Content

The published results are ordered according to the topics acyclic silylenes, dialumenes and silyliumylidene ions and further chronological based on online publication in the corresponding journal. The Supporting Information are not included in this thesis. Data are available free of charge on the websites of the journals connected to the publications DOI number.

8.1. From Si(II) to Si(IV) and Back: Reversible Intramolecular Carbon–Carbon Bond Activation by an Acyclic Iminosilylene

Authors: Daniel Wendel, Amelie Porzelt, Fabian A. D. Herz, Debotra Sarkar, Christian Jandl, Shigeyoshi Inoue, Bernhard Rieger

Journal: Journal of the American Chemical Society, 2017, 139 (24), 8134-8137.

Publisher: American Chemical Society

DOI: 10.1021/jacs.7b05136

License for Copyright Content:

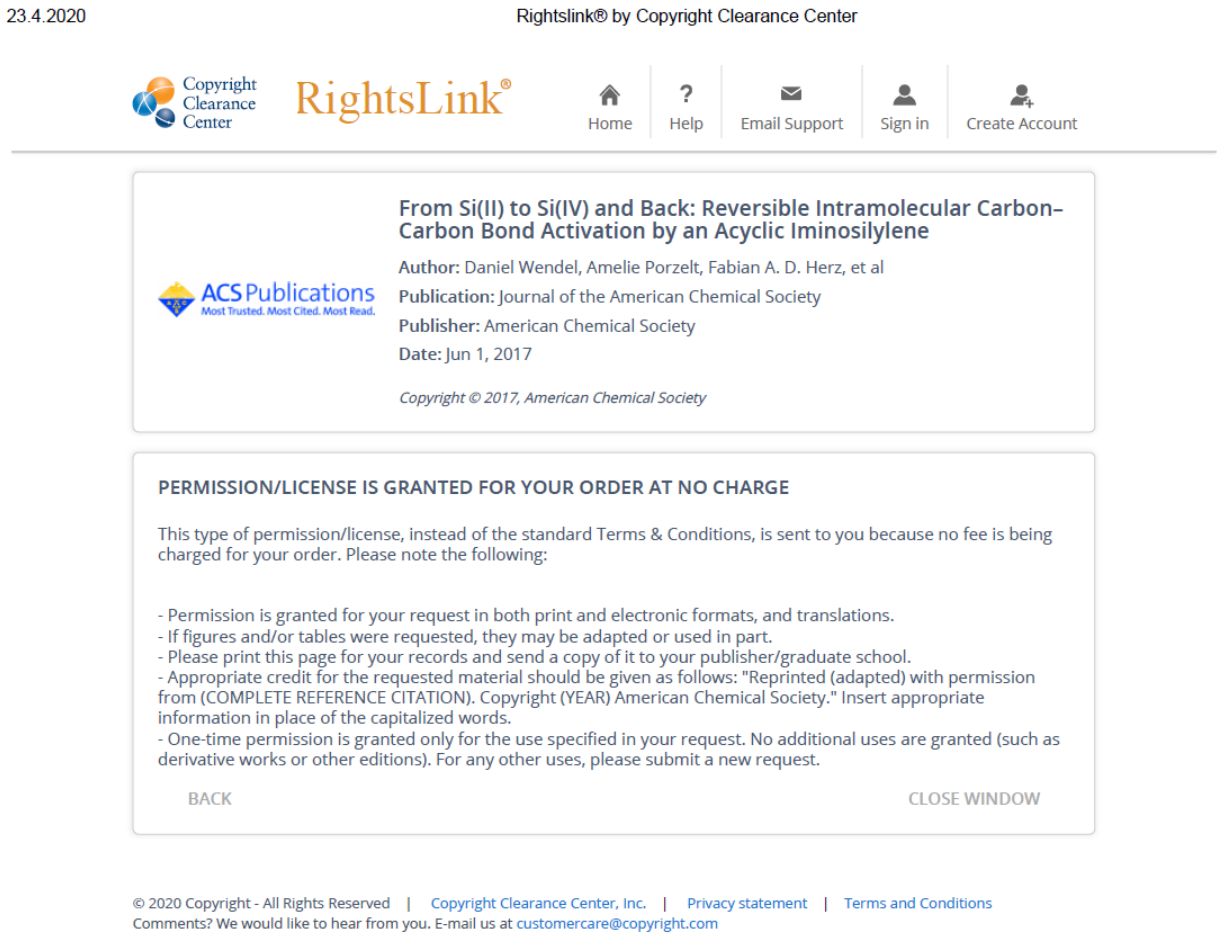

23.4.2020 Rightslink® by Copyright Clearance Center

Copyright Clearance Center RightsLink®

Home | Help | Email Support | Sign in | Create Account

From Si(II) to Si(IV) and Back: Reversible Intramolecular Carbon–Carbon Bond Activation by an Acyclic Iminosilylene

Author: Daniel Wendel, Amelie Porzelt, Fabian A. D. Herz, et al

Publication: Journal of the American Chemical Society

Publisher: American Chemical Society

Date: Jun 1, 2017

Copyright © 2017, American Chemical Society

PERMISSION/LICENSE IS GRANTED FOR YOUR ORDER AT NO CHARGE

This type of permission/license, instead of the standard Terms & Conditions, is sent to you because no fee is being charged for your order. Please note the following:

- Permission is granted for your request in both print and electronic formats, and translations.
- If figures and/or tables were requested, they may be adapted or used in part.
- Please print this page for your records and send a copy of it to your publisher/graduate school.
- Appropriate credit for the requested material should be given as follows: "Reprinted (adapted) with permission from (COMPLETE REFERENCE CITATION). Copyright (YEAR) American Chemical Society." Insert appropriate information in place of the capitalized words.
- One-time permission is granted only for the use specified in your request. No additional uses are granted (such as derivative works or other editions). For any other uses, please submit a new request.

BACK CLOSE WINDOW

© 2020 Copyright - All Rights Reserved | Copyright Clearance Center, Inc. | Privacy statement | Terms and Conditions

Comments? We would like to hear from you. E-mail us at customercare@copyright.com

8.2. Silicon and Oxygen's Bond of Affection: An Acyclic Three-Coordinate Silanone and Its Transformation to an Iminosiloxysilylene

Authors: Daniel Wendel, Dominik Reiter, Amelie Porzelt, Philipp J. Altmann, Shigeyoshi Inoue, Bernhard Rieger

Journal: Journal of the American Chemical Society, 2017, 139 (47), 17193-17198.

Publisher: American Chemical Society

DOI: 10.1021/jacs.7b10634

License for Copyright Content:

23.4.2020 Rightslink® by Copyright Clearance Center

Copyright Clearance Center RightsLink®

Home | Help | Email Support | Sign in | Create Account

Silicon and Oxygen's Bond of Affection: An Acyclic Three-Coordinate Silanone and Its Transformation to an Iminosiloxysilylene

ACS Publications Most Trusted. Most Cited. Most Read.

Author: Daniel Wendel, Dominik Reiter, Amelie Porzelt, et al
Publication: Journal of the American Chemical Society
Publisher: American Chemical Society
Date: Nov 1, 2017

Copyright © 2017, American Chemical Society

PERMISSION/LICENSE IS GRANTED FOR YOUR ORDER AT NO CHARGE

This type of permission/license, instead of the standard Terms & Conditions, is sent to you because no fee is being charged for your order. Please note the following:

- Permission is granted for your request in both print and electronic formats, and translations.
- If figures and/or tables were requested, they may be adapted or used in part.
- Please print this page for your records and send a copy of it to your publisher/graduate school.
- Appropriate credit for the requested material should be given as follows: "Reprinted (adapted) with permission from (COMPLETE REFERENCE CITATION). Copyright (YEAR) American Chemical Society." Insert appropriate information in place of the capitalized words.
- One-time permission is granted only for the use specified in your request. No additional uses are granted (such as derivative works or other editions). For any other uses, please submit a new request.

BACK CLOSE WINDOW

© 2020 Copyright - All Rights Reserved | Copyright Clearance Center, Inc. | Privacy statement | Terms and Conditions
Comments? We would like to hear from you. E-mail us at customercare@copyright.com

8.3. Disilene-Silylene Interconversion: A Synthetically Accessible Acyclic Bis(silyl)silylene

Authors: Dominik Reiter,† Richard Holzner,† Amelie Porzelt,† Philipp J. Altmann, Philipp Frisch, Shigeyoshi Inoue

Journal: Journal of the American Chemical Society, 2019, 141 (34), 13536-13546.

Publisher: American Chemical Society

DOI: 10.1021/jacs.9b05318

†authors contributed equally

License for Copyright Content:

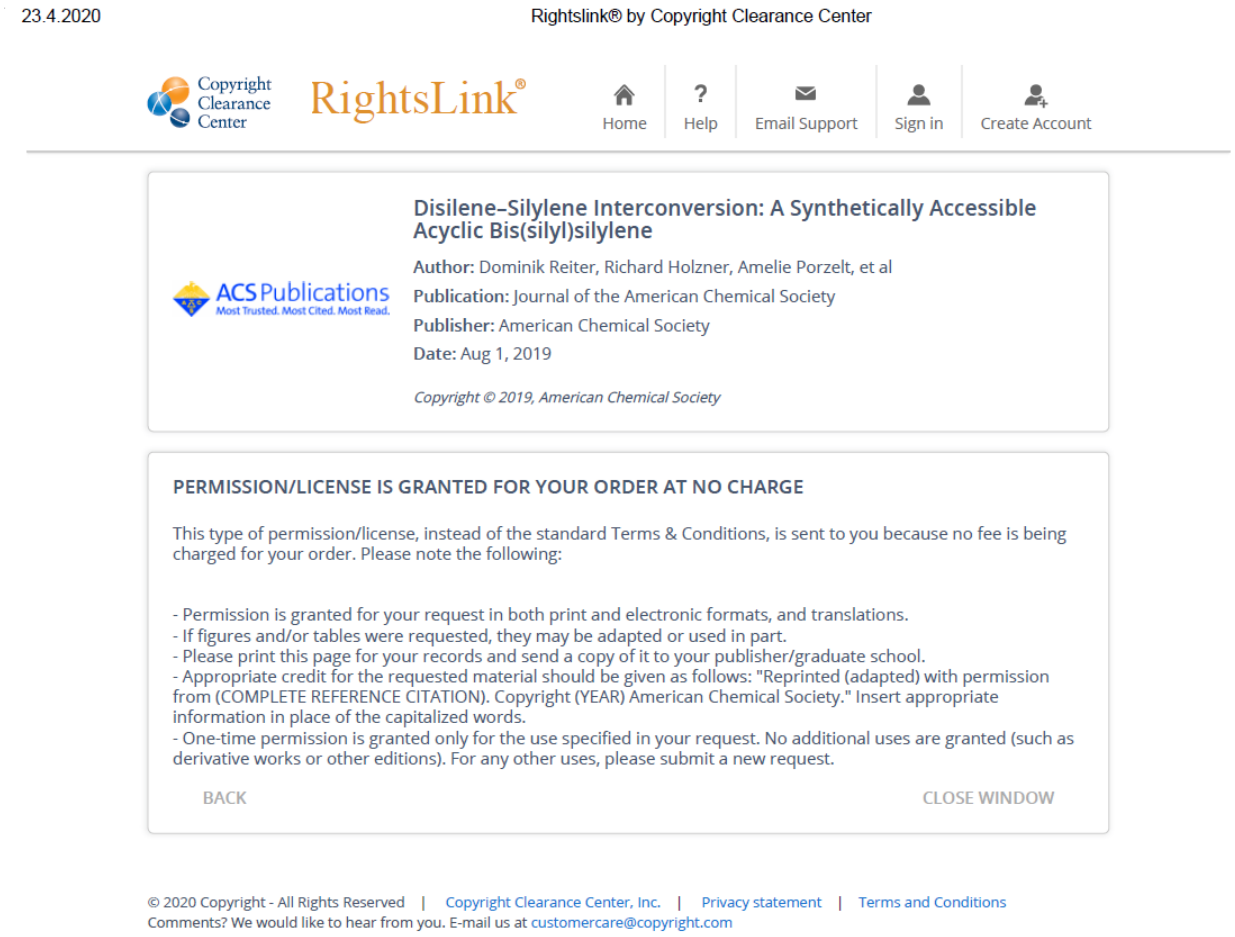

23.4.2020 Rightslink® by Copyright Clearance Center

Copyright Clearance Center RightsLink®

Home | Help | Email Support | Sign in | Create Account

ACS Publications
Most Trusted. Most Cited. Most Read.

Disilene–Silylene Interconversion: A Synthetically Accessible Acyclic Bis(silyl)silylene

Author: Dominik Reiter, Richard Holzner, Amelie Porzelt, et al
Publication: Journal of the American Chemical Society
Publisher: American Chemical Society
Date: Aug 1, 2019

Copyright © 2019, American Chemical Society

PERMISSION/LICENSE IS GRANTED FOR YOUR ORDER AT NO CHARGE

This type of permission/license, instead of the standard Terms & Conditions, is sent to you because no fee is being charged for your order. Please note the following:

- Permission is granted for your request in both print and electronic formats, and translations.
- If figures and/or tables were requested, they may be adapted or used in part.
- Please print this page for your records and send a copy of it to your publisher/graduate school.
- Appropriate credit for the requested material should be given as follows: "Reprinted (adapted) with permission from (COMPLETE REFERENCE CITATION). Copyright (YEAR) American Chemical Society." Insert appropriate information in place of the capitalized words.
- One-time permission is granted only for the use specified in your request. No additional uses are granted (such as derivative works or other editions). For any other uses, please submit a new request.

BACK CLOSE WINDOW

© 2020 Copyright - All Rights Reserved | Copyright Clearance Center, Inc. | Privacy statement | Terms and Conditions
Comments? We would like to hear from you. E-mail us at customercare@copyright.com

8.4. Silylated silicon-carbonyl complexes as mimics of ubiquitous transition-metal carbonyls

Authors: Dominik Reiter, Richard Holzner, Amelie Porzelt, Philipp Frisch, Shigeyoshi Inoue

Journal: Nature Chemistry, 2020, 12, 1131-1135.

Publisher: Springer Nature

DOI: 10.1038/s41557-020-00555-4

License for Copyright Content:

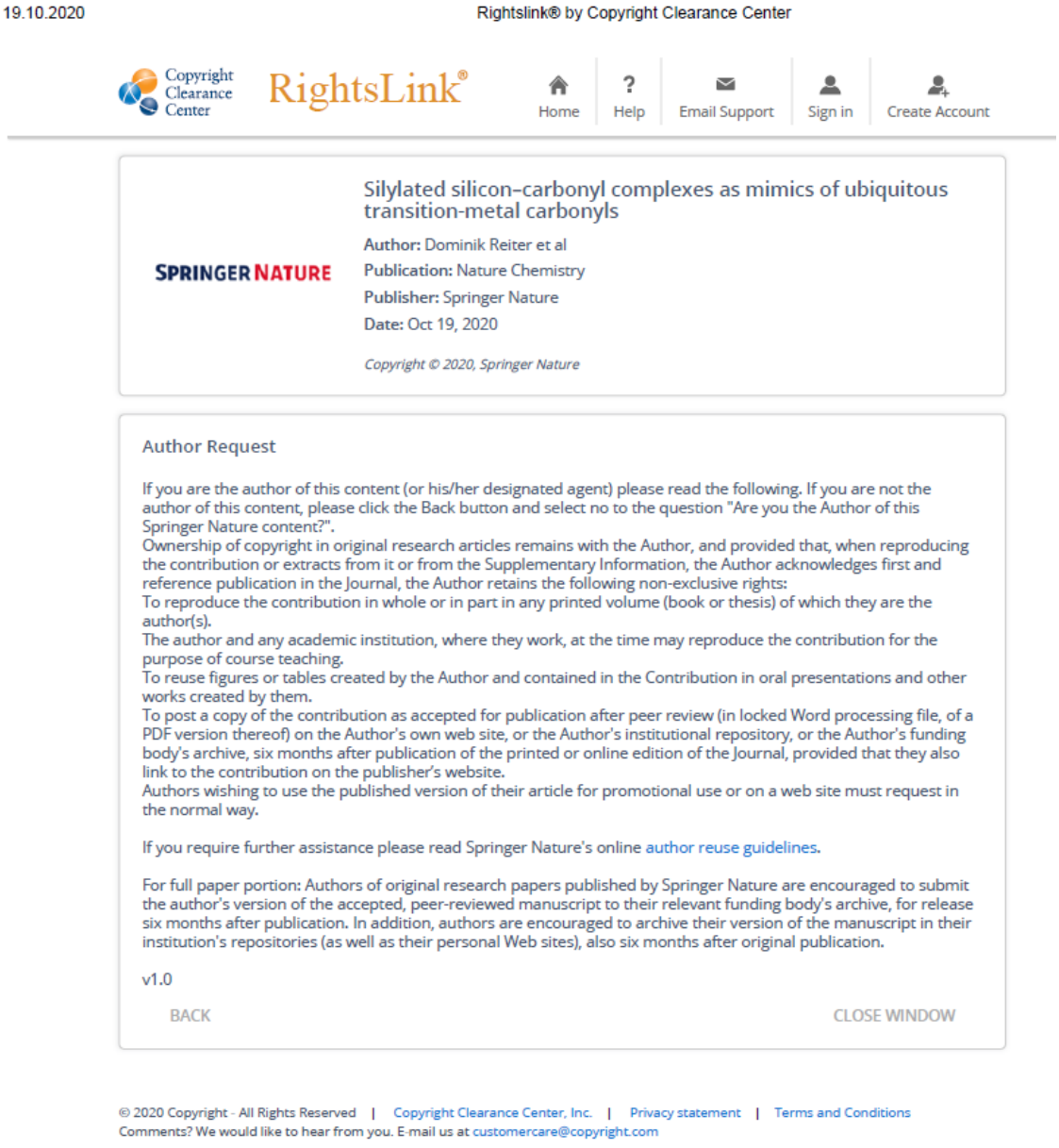

19.10.2020 Rightslink® by Copyright Clearance Center

Copyright Clearance Center RightsLink®

Home | Help | Email Support | Sign in | Create Account

SPRINGER NATURE

Silylated silicon–carbonyl complexes as mimics of ubiquitous transition-metal carbonyls

Author: Dominik Reiter et al
Publication: Nature Chemistry
Publisher: Springer Nature
Date: Oct 19, 2020

Copyright © 2020, Springer Nature

Author Request

If you are the author of this content (or his/her designated agent) please read the following. If you are not the author of this content, please click the Back button and select no to the question "Are you the Author of this Springer Nature content?".
Ownership of copyright in original research articles remains with the Author, and provided that, when reproducing the contribution or extracts from it or from the Supplementary Information, the Author acknowledges first and reference publication in the Journal, the Author retains the following non-exclusive rights:
To reproduce the contribution in whole or in part in any printed volume (book or thesis) of which they are the author(s).
The author and any academic institution, where they work, at the time may reproduce the contribution for the purpose of course teaching.
To reuse figures or tables created by the Author and contained in the Contribution in oral presentations and other works created by them.
To post a copy of the contribution as accepted for publication after peer review (in locked Word processing file, of a PDF version thereof) on the Author's own web site, or the Author's institutional repository, or the Author's funding body's archive, six months after publication of the printed or online edition of the Journal, provided that they also link to the contribution on the publisher's website.
Authors wishing to use the published version of their article for promotional use or on a web site must request in the normal way.

If you require further assistance please read Springer Nature's online author reuse guidelines.

For full paper portion: Authors of original research papers published by Springer Nature are encouraged to submit the author's version of the accepted, peer-reviewed manuscript to their relevant funding body's archive, for release six months after publication. In addition, authors are encouraged to archive their version of the manuscript in their institution's repositories (as well as their personal Web sites), also six months after original publication.

v1.0

BACK CLOSE WINDOW

© 2020 Copyright - All Rights Reserved | Copyright Clearance Center, Inc. | Privacy statement | Terms and Conditions
Comments? We would like to hear from you. E-mail us at customercare@copyright.com

8.5. A Stable Neutral Compound with an Aluminum-Aluminum Double Bond

Authors: Prasenjit Bag, Amelie Porzelt, Philipp J. Altmann, Shigeyoshi Inoue

Journal: Journal of the American Chemical Society, 2017, 139 (41), 14384-14387.

Publisher: American Chemical Society

DOI: 10.1021/jacs.7b08890

License for Copyright Content:

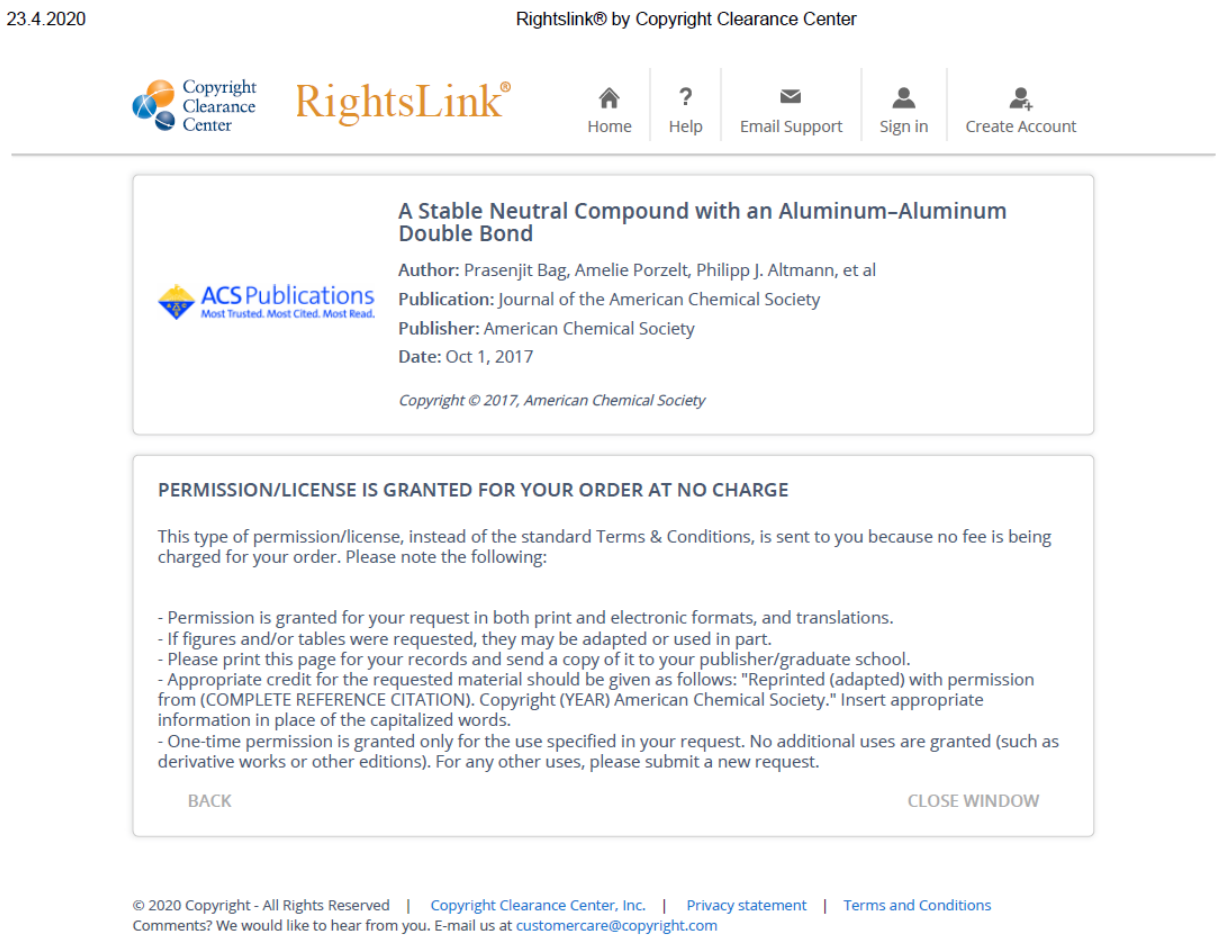

23.4.2020 Rightslink® by Copyright Clearance Center

Copyright Clearance Center RightsLink®

Home | Help | Email Support | Sign in | Create Account

ACS Publications
Most Trusted. Most Cited. Most Read.

A Stable Neutral Compound with an Aluminum–Aluminum Double Bond

Author: Prasenjit Bag, Amelie Porzelt, Philipp J. Altmann, et al
Publication: Journal of the American Chemical Society
Publisher: American Chemical Society
Date: Oct 1, 2017

Copyright © 2017, American Chemical Society

PERMISSION/LICENSE IS GRANTED FOR YOUR ORDER AT NO CHARGE

This type of permission/license, instead of the standard Terms & Conditions, is sent to you because no fee is being charged for your order. Please note the following:

- Permission is granted for your request in both print and electronic formats, and translations.
- If figures and/or tables were requested, they may be adapted or used in part.
- Please print this page for your records and send a copy of it to your publisher/graduate school.
- Appropriate credit for the requested material should be given as follows: "Reprinted (adapted) with permission from (COMPLETE REFERENCE CITATION). Copyright (YEAR) American Chemical Society." Insert appropriate information in place of the capitalized words.
- One-time permission is granted only for the use specified in your request. No additional uses are granted (such as derivative works or other editions). For any other uses, please submit a new request.

BACK CLOSE WINDOW

© 2020 Copyright - All Rights Reserved | Copyright Clearance Center, Inc. | Privacy statement | Terms and Conditions
Comments? We would like to hear from you. E-mail us at customercare@copyright.com

8.6. Dialumenes – Aryl vs. Silyl Stabilisation for Small Molecule Activation and Catalysis

Authors: Catherine Weetman, Amelie Porzelt, Prasenjit Bag, Franziska Hanusch, Shigeyoshi Inoue

Journal: Chemical Science, 2020, 11, 4817-4827

Publisher: Royal Society of Chemistry

DOI: 10.1039/D0SC01561J

License for Copyright Content:

8.7. S–H Bond Activation in Hydrogen Sulfide by NHC-Stabilized Silyliumylidene Ions

Title: Amelie Porzelt, Julia I. Schweizer, Ramona Baierl, Philipp J. Altmann, Max C. Holthausen, Shigeyoshi Inoue

Journal: Inorganics, 2018, 6, 54.

Publisher: MDPI

DOI: 10.3390/inorganics6020054

License for Copyright Content:

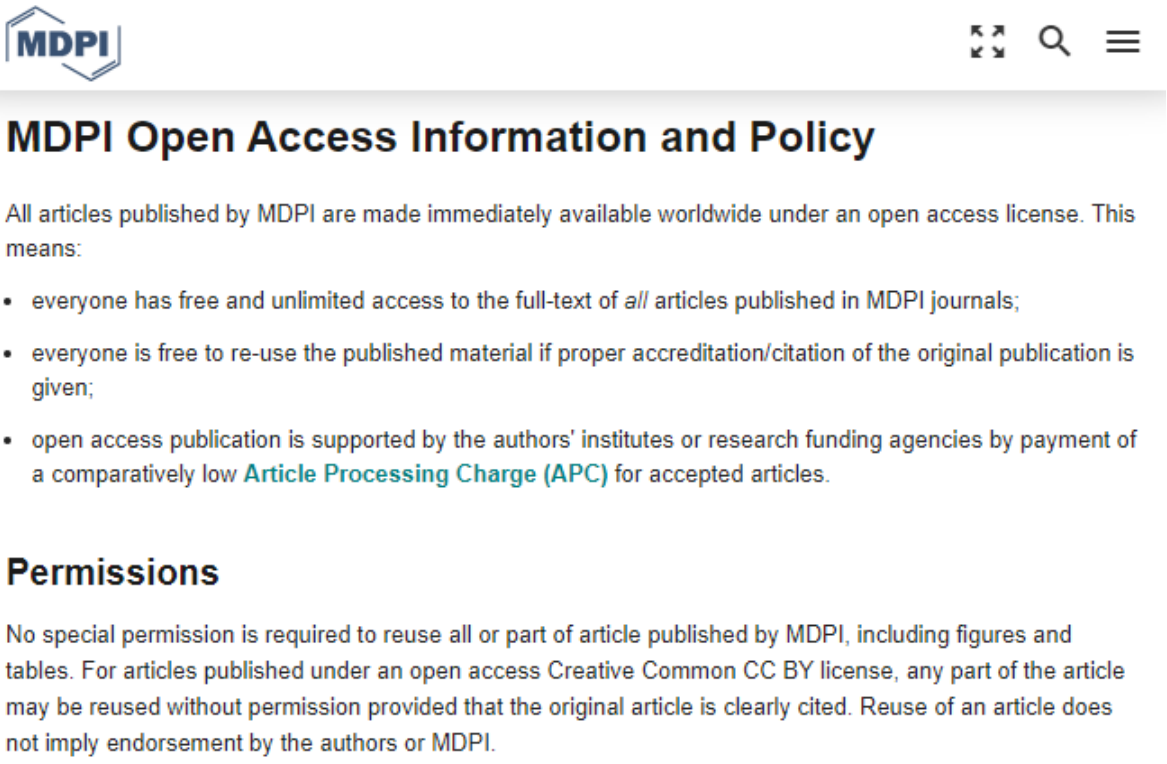

MDPI

MDPI Open Access Information and Policy

All articles published by MDPI are made immediately available worldwide under an open access license. This means:

- everyone has free and unlimited access to the full-text of *all* articles published in MDPI journals;
- everyone is free to re-use the published material if proper accreditation/citation of the original publication is given;
- open access publication is supported by the authors' institutes or research funding agencies by payment of a comparatively low **Article Processing Charge (APC)** for accepted articles.

Permissions

No special permission is required to reuse all or part of article published by MDPI, including figures and tables. For articles published under an open access Creative Common CC BY license, any part of the article may be reused without permission provided that the original article is clearly cited. Reuse of an article does not imply endorsement by the authors or MDPI.

8.8. Transition Metal Carbonyl Complexes of an *N*-Heterocyclic Carbene Stabilized Silyliumylidene Ion

Authors: Philipp Frisch, Tibor Szilvási, Amelie Porzelt, Shigeyoshi Inoue

Journal: Inorganic Chemistry, 2019, 58 (21), 14931-14937.

Publisher: American Chemical Society

DOI: 10.1021/acs.inorgchem.9b02772

License for Copyright Content:

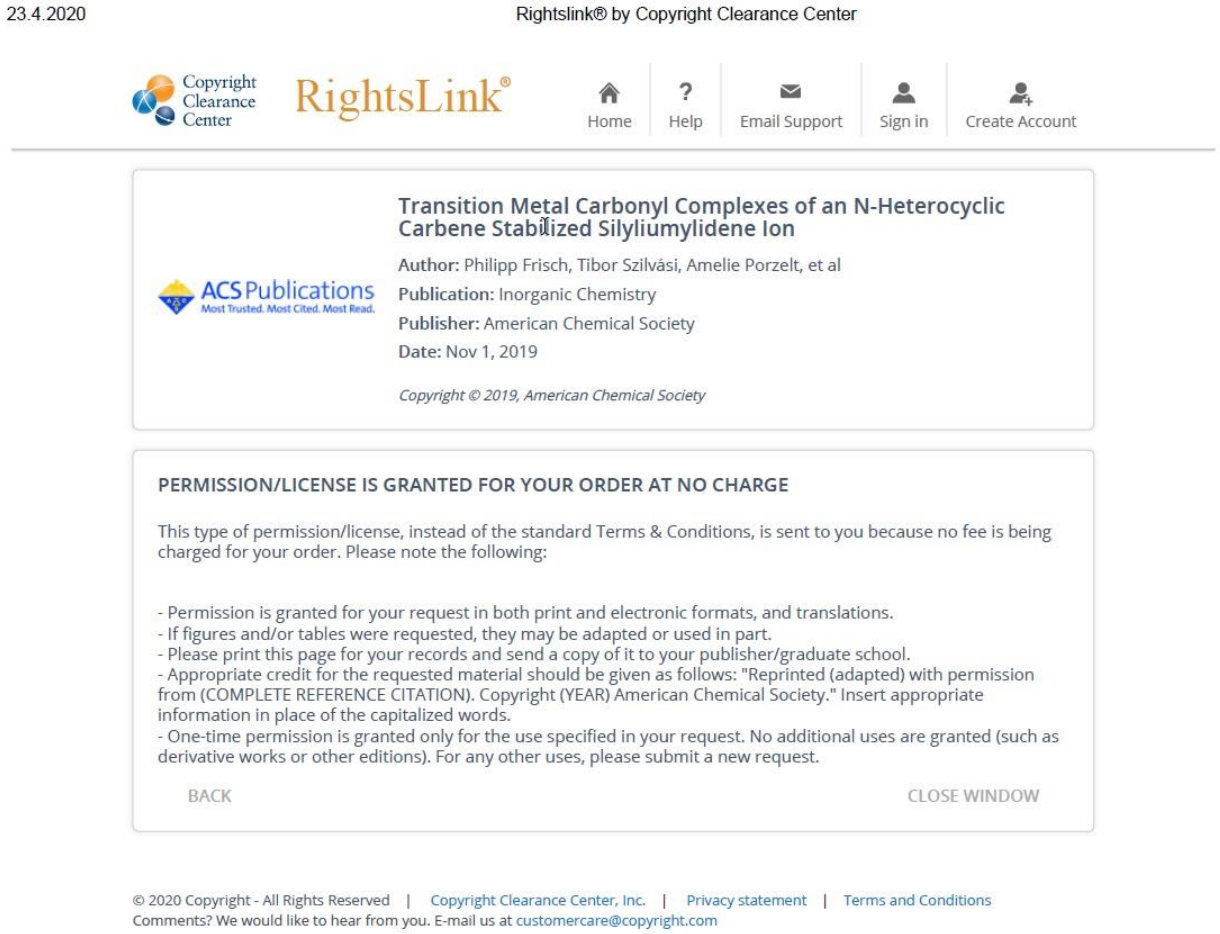

23.4.2020 Rightslink® by Copyright Clearance Center

Copyright Clearance Center RightsLink® Home Help Email Support Sign in Create Account

ACS Publications Most Trusted. Most Cited. Most Read.

Transition Metal Carbonyl Complexes of an N-Heterocyclic Carbene Stabilized Silyliumylidene Ion

Author: Philipp Frisch, Tibor Szilvási, Amelie Porzelt, et al
Publication: Inorganic Chemistry
Publisher: American Chemical Society
Date: Nov 1, 2019

Copyright © 2019, American Chemical Society

PERMISSION/LICENSE IS GRANTED FOR YOUR ORDER AT NO CHARGE

This type of permission/license, instead of the standard Terms & Conditions, is sent to you because no fee is being charged for your order. Please note the following:

- Permission is granted for your request in both print and electronic formats, and translations.
- If figures and/or tables were requested, they may be adapted or used in part.
- Please print this page for your records and send a copy of it to your publisher/graduate school.
- Appropriate credit for the requested material should be given as follows: "Reprinted (adapted) with permission from (COMPLETE REFERENCE CITATION). Copyright (YEAR) American Chemical Society." Insert appropriate information in place of the capitalized words.
- One-time permission is granted only for the use specified in your request. No additional uses are granted (such as derivative works or other editions). For any other uses, please submit a new request.

BACK CLOSE WINDOW

© 2020 Copyright - All Rights Reserved | Copyright Clearance Center, Inc. | Privacy statement | Terms and Conditions
Comments? We would like to hear from you. E-mail us at customercare@copyright.com

9. Appendix

9.1. Complete list of publications

D. Wendel, **A. Porzelt**, F. A. D. Herz, D. Sarkar, C. Jandl, S. Inoue, B. Rieger, From Si(II) to Si(IV) and Back: Reversible Intramolecular Carbon–Carbon Bond Activation by an Acyclic Iminosilylene, *J. Am. Chem. Soc.* **2017**, *139* (24), 8134-8137.

P. Bag, **A. Porzelt**, P. J. Altmann, S. Inoue, A Stable Neutral Compound with an Aluminum-Aluminum Double Bond, *J. Am. Chem. Soc.* **2017**, *139* (41), 14384-14387.

D. Wendel, D. Reiter, **A. Porzelt**, P. J. Altmann, S. Inoue, B. Rieger, Silicon and Oxygen's Bond of Affection: An Acyclic Three-Coordinate Silanone and Its Transformation to an Iminosiloxysilylene, *J. Am. Chem. Soc.* **2017**, *139* (47), 17193-17198.

A. Porzelt, J. Schweizer, R. Baierl, P. Altmann, M. Holthausen, S. Inoue, S-H Bond Activation in Hydrogen Sulfide by NHC-Stabilized Silyliumylidene Ions, *Inorganics* **2018**, *6*, 54.

D. Reiter, R. Holzner, **A. Porzelt**, P. J. Altmann, P. Frisch, S. Inoue, Disilene-Silylene Interconversion: A Synthetically Accessible Acyclic Bis(silyl)silylene, *J. Am. Chem. Soc.* **2019**, *141* (34), 13536-13546.

P. Frisch, T. Szilvási, **A. Porzelt**, S. Inoue, Transition Metal Carbonyl Complexes of an *N*-Heterocyclic Carbene Stabilized Silyliumylidene Ion, *Inorg. Chem.* **2019**, *58* (21), 14931-14937.

C. Weetman, **A. Porzelt**, P. Bag, F. Hanusch, S. Inoue , Dialumenes – Aryl vs. Silyl Stabilisation for Small Molecule Activation and Catalysis, *Chem. Sci.* **2020**, *11*, 4817-4827.

D. Reiter, R. Holzner, **A. Porzelt**, P. Frisch, S. Inoue, Silylated silicon–carbonyl complexes as mimics of ubiquitous transition-metal carbonyls, *Nat. Chem.* **2020**, *12*, 1131-1135.

Further publications:

V. Nesterov, D. Reiter, P. Bag, P. Frisch, R. Holzner, **A. Porzelt**, S. Inoue, NHCs in Main Group Chemistry, *Chem. Rev.* **2018**, *118* (19), 9678-9842.

9.2. Conference Contributions

Talks:

- **ICHAC** 2019 (International Conference on Heteroatom Chemistry) Prague – Short Lecture (30.06 - 05.07.2019) - Reactivity of NHC-Stabilized Silyliumylidene Ions towards Group 13 Compounds

Poster presentations:

- **IRIS** 2018 (International Symposium on Inorganic Ring Systems) Kyoto, Japan, S-H bond activation in Hydrogen Sulfide by NHC-stabilized Silyliumylidene Ions
- **9th European Silicon Days** 2019 Saarbrücken, Small Molecule Activation by NHC-stabilized Silyliumylidene Ions

10. References

[1] Mendelejew, D., Über die Beziehungen der Eigenschaften zu den Atomgewichten der Elemente (On the Relationship of the Properties of the Elements to their Atomic Weights). *Z. Chem.* **1869**, *12*, 405-406.

[2] Weyer, J., *Geschichte der Chemie, Band 2 – 19. und 20. Jahrhundert*. Springer Spectrum: Hamburg, **2018**; p 462.

[3] Meyer, L., Die Natur der chemischen Elemente als Function ihrer Atomgewichte. *Ann. Chem. Pharm.* **1870**, *Supplementband 7*, 354–364.

[4] Meyer, L., Die modernen Theorien der Chemie und ihre Bedeutung für die chemische Statik. Verlag von Maruschke & Berendt: Breslau, **1864**.

[5] Meyer, L., Zur Systematik der anorganischen Chemie. *Ber. Dtsch. Chem. Ges.* **1873**, *6* (1), 101-106.

[6] Shaik, S.; Cremades, E.; Alvarez, S., The Periodic-Table—A Universal Icon: Its Birth 150 Years Ago, and Its Popularization Through Literature Art and Music. *Angew. Chem., Int. Ed.* **2019**, *58* (38), 13194-13206.

[7] Graedel, T. E.; Allwood, J.; Birat, J.-P.; Buchert, M.; Hagelüken, C.; Reck, B. K.; Sibley, S. F.; Sonnemann, G., What Do We Know About Metal Recycling Rates? *J. Ind. Ecol.* **2011**, *15* (3), 355-366.

[8] Graedel, T. E.; Allwood, J.; Birat, J.-P.; Reck, B. K.; Sibley, S. F.; Sonneman, G.; Bucher, M.; Hagelüken, C. Recycling Rates of Metals - A Statuts Report of the Working Group on the Global Metal Flows to the International Ressource Panel; UNEP: **2011**.

[9] The 90 natural elements that make up everything, European Chemical Society. https://www.euchems.eu/euchems-periodic-table/.

[10] Nelson, J. J. M.; Schelter, E. J., Sustainable Inorganic Chemistry: Metal Separations for Recycling. *Inorg. Chem.* **2019**, *58* (2), 979-990.

[11] Critical Raw Material Closed Loop Recovery Project - Pan European Policy Recommendations; CRM Recovery: **2019**.

[12] Paulik, F. E.; Roth, J. F., Novel catalysts for the low-pressure carbonylation of methanol to acetic acid. *Chem. Commun.* **1968**, (24), 1578a-1578a.

[13] Roelen, O. Verfahren zur Herstellung von sauerstoffhaltigen Verbindungen. **1938/1952**.

[14] Smidt, J.; Hafner, W.; Jira, R.; Sedlmeier, J.; Sieber, R.; Rüttinger, R.; Kojer, H., Katalytische Umsetzungen von Olefinen an Platinmetall-Verbindungen Das Consortium-Verfahren zur Herstellung von Acetaldehyd. *Angew. Chem.* **1959**, *71* (5), 176-182.

[15] Hagen, J., Homogeneously Catalyzed Industrial Processes. In *Industrial Catalysis*, **2015**; pp 47-80.

[16] Falbe, J.; Bahrmann, H., Homogeneous catalysis-industrial applications. *J. Chem. Educ.* **1984**, *61* (11), 961.

[17] van Leeuwen, P. W. N. M., *Homogeneous Catalysis Understanding the Art*. Kluwer Academic Publishers: London, **2004**.

[18] Bhaduri, S.; Mukesh, D., *Homogeneous catalysis: mechanisms and industrial applications*. John Wiley & Sons: New Jersey, **2014**.

[19] Nakajima, Y.; Shimada, S., Hydrosilylation reaction of olefins: recent advances and perspectives. *RSC Advances* **2015**, *5* (26), 20603-20616.

[20] Harder, S., *Early Main Group Metal Catalysis: Concepts and Reactions* Wiley-VCH Verlag & Co. KGaA: Weinheim, **2020**.

[21] Bullock, M., *Catalysis without Precious Metals*. Wiley-VCH Verlag & Co. KGaA: Weinheim, **2010**.

[22] Teichert, J. F., *Homogeneous Hydrogenation with Non-Precious Catalysts*. Wiley-VCH Verlag GmbH & Co. KGaA.: Weinheim, **2019**.

[23] Gewirth, A. A.; Varnell, J. A.; DiAscro, A. M., Nonprecious Metal Catalysts for Oxygen Reduction in Heterogeneous Aqueous Systems. *Chem. Rev.* **2018**, *118* (5), 2313-2339.

[24] Lam, J.; Szkop, K. M.; Mosaferi, E.; Stephan, D. W., FLP catalysis: main group hydrogenations of organic unsaturated substrates. *Chem. Soc. Rev.* **2019**, *48* (13), 3592-3612.

[25] Power, P. P., Main-group elements as transition metals. *Nature* **2010**, *463* (7278), 171-177.

[26] Weetman, C.; Inoue, S., The Road Travelled: After Main-Group Elements as Transition Metals. *ChemCatChem* **2018**, *10* (19), 4213-4228.
[27] Melen, R. L., Frontiers in molecular p-block chemistry: From structure to reactivity. *Science* **2019**, *363* (6426), 479-484.
[28] Yadav, S.; Saha, S.; Sen, S. S., Compounds with Low-Valent p-Block Elements for Small Molecule Activation and Catalysis. *ChemCatChem* **2016**, *8* (3), 486-501.
[29] Hadlington, T. J.; Driess, M.; Jones, C., Low-valent group 14 element hydride chemistry: towards catalysis. *Chem. Soc. Rev.* **2018**, *47* (11), 4176-4197.
[30] Taylor, S. R., Abundance of chemical elements in the continental crust: a new table. *Geochim. Cosmochim. Acta* **1964**, *28* (8), 1273-1285.
[31] Slater, J. C., Atomic Radii in Crystals. *J. Chem. Phys.* **1964**, *41* (10), 3199-3204.
[32] A. F. Holleman; E. Wiberg; Wiberg, N., *Lehrbuch der anorganischen Chemie*. de Gruyther: Berlin, **2007**; Vol. 102.
[33] Kutzelnigg, W., Chemical Bonding in Higher Main Group Elements. *Angew. Chem., Int. Ed.* **1984**, *23* (4), 272-295.
[34] Michael E. Jung; Roman Lagoutte; Jahn, U., Triphenylcarbenium Tetrafluoroborate. In *Encyclopedia of Reagents for Organic Synthesis*, doi: 10.1002/047084289X.rt362.pub2, **2011**.
[35] Lambert, J. B.; Zhao, Y., The Trimesitylsilylium Cation. *Angew. Chem., Int. Ed.* **1997**, *36* (4), 400-401.
[36] Lee, V. Y., Organosilicon Compounds: Theory and experiment (synthesis). Academic Press: **2017**.
[37] Kim, K.-C.; Reed, C. A.; Elliott, D. W.; Mueller, L. J.; Tham, F.; Lin, L.; Lambert, J. B., Crystallographic Evidence for a Free Silylium Ion. *Science* **2002**, *297* (5582), 825-827.
[38] Pyykko, P., Relativistic effects in structural chemistry. *Chem. Rev.* **1988**, *88* (3), 563-594.
[39] McGuire, B. A., 2018 Census of Interstellar, Circumstellar, Extragalactic, Protoplanetary Disk, and Exoplanetary Molecules. *Astrophys. J., Suppl. Ser.* **2018**, *239* (2), 17.
[40] Stoffels, A.; Kluge, L.; Schlemmer, S.; Brünken, S., Laboratory rotational ground state transitions of NH_3D^+ and CF^+. *A&A* **2016**, *593*, A56.
[41] Morris, R. A.; Viggiano, A. A.; Van Doren, J. M.; Paulson, J. F., Chemistry of CF_n^+ (n = 1-3) ions with halocarbons. *J. Phys. Chem.* **1992**, *96* (6), 2597-2603.
[42] Pyykkö, P.; Riedel, S.; Patzschke, M., Triple-Bond Covalent Radii. *Chem. - Eur. J.* **2005**, *11* (12), 3511-3520.
[43] Kalescky, R.; Kraka, E.; Cremer, D., Are carbon—halogen double and triple bonds possible? *Int. J. Quantum Chem.* **2014**, *114* (16), 1060-1072.
[44] Jutzi, P.; Kanne, D.; Krüger, C., Decamethylsilicocene—Synthesis and Structure. *Angew. Chem., Int. Ed.* **1986**, *25* (2), 164-164.
[45] Kühler, T.; Jutzi, P., Decamethylsilicocene: Synthesis, Structure, Bonding and Chemistry. In *Adv. Organomet. Chem.*, Academic Press: **2003**; Vol. 49, pp 1-34.
[46] Denk, M.; Lennon, R.; Hayashi, R.; West, R.; Belyakov, A. V.; Verne, H. P.; Haaland, A.; Wagner, M.; Metzler, N., Synthesis and Structure of a Stable Silylene. *J. Am. Chem. Soc.* **1994**, *116* (6), 2691-2692.
[47] Arduengo, A. J.; Harlow, R. L.; Kline, M., A stable crystalline carbene. *J. Am. Chem. Soc.* **1991**, *113* (1), 361-363.
[48] Kira, M.; Ishida, S.; Iwamoto, T.; Kabuto, C., The First Isolable Dialkylsilylene. *J. Am. Chem. Soc.* **1999**, *121* (41), 9722-9723.
[49] Driess, M.; Yao, S.; Brym, M.; van Wüllen, C.; Lentz, D., A New Type of N-Heterocyclic Silylene with Ambivalent Reactivity. *J. Am. Chem. Soc.* **2006**, *128* (30), 9628-9629.
[50] So, C.-W.; Roesky, H. W.; Magull, J.; Oswald, R. B., Synthesis and Characterization of $[PhC(NtBu)_2]SiCl$: A Stable Monomeric Chlorosilylene. *Angew. Chem., Int. Ed.* **2006**, *45* (24), 3948-3950.
[51] Blom, B.; Stoelzel, M.; Driess, M., New Vistas in N-Heterocyclic Silylene (NHSi) Transition-Metal Coordination Chemistry: Syntheses, Structures and Reactivity towards Activation of Small Molecules. *Chem. - Eur. J.* **2013**, *19* (1), 40-62.
[52] Blom, B.; Gallego, D.; Driess, M., N-heterocyclic silylene complexes in catalysis: new frontiers in an emerging field. *Inorg. Chem. Front.* **2014**, *1* (2), 134-148.

[53] Nesterov, V.; Reiter, D.; Bag, P.; Frisch, P.; Holzner, R.; Porzelt, A.; Inoue, S., NHCs in Main Group Chemistry. *Chem. Rev.* **2018**, *118* (19), 9678-9842.
[54] Hopkinson, M. N.; Richter, C.; Schedler, M.; Glorius, F., An overview of N-heterocyclic carbenes. *Nature* **2014**, *510* (7506), 485-496.
[55] Sau, S. C.; Hota, P. K.; Mandal, S. K.; Soleilhavoup, M.; Bertrand, G., Stable abnormal N-heterocyclic carbenes and their applications. *Chem. Soc. Rev.* **2020**, *49* (4), 1233-1252.
[56] Melaimi, M.; Jazzar, R.; Soleilhavoup, M.; Bertrand, G., Cyclic (Alkyl)(amino)carbenes (CAACs): Recent Developments. *Angew. Chem., Int. Ed.* **2017**, *56* (34), 10046-10068.
[57] Lavallo, V.; Canac, Y.; Präsang, C.; Donnadieu, B.; Bertrand, G., Stable Cyclic (Alkyl)(Amino)Carbenes as Rigid or Flexible, Bulky, Electron-Rich Ligands for Transition-Metal Catalysts: A Quaternary Carbon Atom Makes the Difference. *Angew. Chem., Int. Ed.* **2005**, *44* (35), 5705-5709.
[58] Wang, Y.; Xie, Y.; Wei, P.; King, R. B.; Schaefer, H. F.; von R. Schleyer, P.; Robinson, G. H., A Stable Silicon(0) Compound with a Si=Si Double Bond. *Science* **2008**, *321* (5892), 1069-1071.
[59] Filippou, A. C.; Chernov, O.; Schnakenburg, G., $SiBr_2$(Idipp): A Stable N-Heterocyclic Carbene Adduct of Dibromosilylene. *Angew. Chem., Int. Ed.* **2009**, *48* (31), 5687-5690.
[60] Ghadwal, R. S.; Roesky, H. W.; Merkel, S.; Henn, J.; Stalke, D., Lewis Base Stabilized Dichlorosilylene. *Angew. Chem., Int. Ed.* **2009**, *48* (31), 5683-5686.
[61] Ghadwal, R. S.; Azhakar, R.; Roesky, H. W., Dichlorosilylene: A High Temperature Transient Species to an Indispensable Building Block. *Acc. Chem. Res.* **2013**, *46* (2), 444-456.
[62] Roesky, H. W., Chemistry of low valent silicon. *J. Organomet. Chem.* **2013**, *730*, 57-62.
[63] Xiong, Y.; Yao, S.; Inoue, S.; Epping, J. D.; Driess, M., A Cyclic Silylone ("Siladicarbene") with an Electron-Rich Silicon(0) Atom. *Angew. Chem., Int. Ed.* **2013**, *52* (28), 7147-50.
[64] Mondal, K. C.; Roesky, H. W.; Schwarzer, M. C.; Frenking, G.; Niepötter, B.; Wolf, H.; Herbst-Irmer, R.; Stalke, D., A Stable Singlet Biradicaloid Siladicarbene: $(L:)_2Si$. *Angew. Chem., Int. Ed.* **2013**, *52* (10), 2963-2967.
[65] Himmel, D.; Krossing, I.; Schnepf, A., Dative or Not Dative? *Angew. Chem., Int. Ed.* **2014**, *53* (24), 6047-6048.
[66] Frenking, G., Dative Bonds in Main-Group Compounds: A Case for More Arrows! *Angew. Chem., Int. Ed.* **2014**, *53* (24), 6040-6046.
[67] Himmel, D.; Krossing, I.; Schnepf, A., Dative Bonds in Main-Group Compounds: A Case for Fewer Arrows! *Angew. Chem., Int. Ed.* **2014**, *53* (2), 370-374.
[68] Filippou, A. C.; Chernov, O.; Blom, B.; Stumpf, K. W.; Schnakenburg, G., Stable N-Heterocyclic Carbene Adducts of Arylchlorosilylenes and Their Germanium Homologues. *Chem. - Eur. J.* **2010**, *16* (9), 2866-2872.
[69] Tanaka, H.; Ichinohe, M.; Sekiguchi, A., An Isolable NHC-Stabilized Silylene Radical Cation: Synthesis and Structural Characterization. *J. Am. Chem. Soc.* **2012**, *134* (12), 5540-5543.
[70] Stanford, M. W.; Schweizer, J. I.; Menche, M.; Nichol, G. S.; Holthausen, M. C.; Cowley, M. J., Intercepting the Disilene-Silylsilylene Equilibrium. *Angew. Chem., Int. Ed.* **2019**, *58* (5), 1329-1333.
[71] Inoue, S.; Eisenhut, C., A dihydrodisilene transition metal complex from an N-heterocyclic carbene-stabilized silylene monohydride. *J. Am. Chem. Soc.* **2013**, *135* (49), 18315-8.
[72] Dübek, G.; Hanusch, F.; Inoue, S., NHC-Stabilized Silyl-Substituted Chlorosilylene. *Inorg. Chem.* **2019**, *58* (23), 15700-15704.
[73] Lee, M. E.; Cho, H. M.; Ryu, M. S.; Kim, C. H.; Ando, W., A Stable Halosilylene at Room Temperature in THF Solution. *J. Am. Chem. Soc.* **2001**, *123* (31), 7732-7733.
[74] Azhakar, R.; Tavčar, G.; Roesky, H. W.; Hey, J.; Stalke, D., Facile Synthesis of a Rare Chlorosilylene–BH_3 Adduct. *Eur. J. Inorg* **2011**, *2011* (4), 475-477.
[75] Al-Rafia, S. M. I.; Malcolm, A. C.; McDonald, R.; Ferguson, M. J.; Rivard, E., Efficient generation of stable adducts of Si(II) dihydride using a donor–acceptor approach. *Chem. Commun.* **2012**, *48* (9), 1308-1310.
[76] Ghadwal, R. S.; Roesky, H. W.; Merkel, S.; Stalke, D., Ambiphilicity of Dichlorosilylene in a Single Molecule. *Chem. - Eur. J.* **2010**, *16* (1), 85-88.

[77] Al-Rafia, S. M. I.; McDonald, R.; Ferguson, M. J.; Rivard, E., Preparation of Stable Low-Oxidation-State Group 14 Element Amidohydrides and Hydride-Mediated Ring-Expansion Chemistry of N-Heterocyclic Carbenes. *Chem. - Eur. J.* **2012**, *18* (43), 13810-13820.
[78] Rivard, E., Donor-acceptor chemistry in the main group. *Dalt. Trans.* **2014**, *43* (23), 8577-8586.
[79] Hickox, H. P.; Wang, Y.; Xie, Y.; Wei, P.; Schaefer, H. F.; Robinson, G. H., Push–Pull Stabilization of Parent Monochlorosilylenes. *J. Am. Chem. Soc.* **2016**, *138* (31), 9799-9802.
[80] Ghadwal, R. S.; Rottschäfer, D.; Andrada, D. M.; Frenking, G.; Schürmann, C. J.; Stammler, H.-G., Normal-to-abnormal rearrangement of an N-heterocyclic carbene with a silylene transition metal complex. *Dalt. Trans.* **2017**, *46* (24), 7791-7799.
[81] Blom, B.; Driess, M.; Gallego, D.; Inoue, S., Facile Access to Silicon-Functionalized Bis-Silylene Titanium(II) Complexes. *Chem. - Eur. J.* **2012**, *18* (42), 13355-13360.
[82] Takeda, N.; Suzuki, H.; Tokitoh, N.; Okazaki, R.; Nagase, S., Reaction of a Sterically Hindered Silylene with Isocyanides: The First Stable Silylene−Lewis Base Complexes. *J. Am. Chem. Soc.* **1997**, *119* (6), 1456-1457.
[83] Takeda, N.; Kajiwara, T.; Suzuki, H.; Okazaki, R.; Tokitoh, N., Synthesis and Properties of the First Stable Silylene–Isocyanide Complexes. *Chem. - Eur. J.* **2003**, *9* (15), 3530-3543.
[84] Suzuki, H.; Tokitoh, N.; Okazaki, R., A Novel Reactivity of a Silylene: The First Examples of [1 + 2] Cycloaddition with Aromatic Compounds. *J. Am. Chem. Soc.* **1994**, *116* (25), 11572-11573.
[85] Staudinger, H., Ketene, eine neue Körperklasse. *Ber. Dtsch. Chem. Ges.* **1905**, *38* (2), 1735-1739.
[86] Tidwell, T. T., The First Century of Ketenes (1905–2005): The Birth of a Versatile Family of Reactive Intermediates. *Angew. Chem., Int. Ed.* **2005**, *44* (36), 5778-5785.
[87] Franke, R.; Selent, D.; Börner, A., Applied Hydroformylation. *Chem. Rev.* **2012**, *112* (11), 5675-5732.
[88] Kiss, G., Palladium-Catalyzed Reppe Carbonylation. *Chem. Rev.* **2001**, *101* (11), 3435-3456.
[89] Blanco-Urgoiti, J.; Añorbe, L.; Pérez-Serrano, L.; Domínguez, G.; Pérez-Castells, J., The Pauson–Khand reaction, a powerful synthetic tool for the synthesis of complex molecules. *Chem. Soc. Rev.* **2004**, *33* (1), 32-42.
[90] Knorn, M. Metal-Isonitriles - Synthesis, characterization and application in catalysis. Universität Regensburg, Regensburg, **2015**.
[91] Lang, S., Unravelling the labyrinth of palladium-catalysed reactions involving isocyanides. *Chem. Soc. Rev.* **2013**, *42* (12), 4867-4880.
[92] Protchenko, A. V.; Vasko, P.; Do, D. C. H.; Hicks, J.; Fuentes, M. Á.; Jones, C.; Aldridge, S., Reduction of Carbon Oxides by an Acyclic Silylene: Reductive Coupling of CO. *Angew. Chem., Int. Ed.* **2019**, *58* (6), 1808-1812.
[93] Wang, Y.; Kostenko, A.; Hadlington, T. J.; Luecke, M.-P.; Yao, S.; Driess, M., Silicon-Mediated Selective Homo- and Heterocoupling of Carbon Monoxide. *J. Am. Chem. Soc.* **2019**, *141* (1), 626-634.
[94] Xiong, Y.; Yao, S.; Szilvási, T.; Ruzicka, A.; Driess, M., Homocoupling of CO and isocyanide mediated by a *C,C'*-bis(silylenyl)-substituted ortho-carborane. *Chem. Commun.* **2020**, *56* (5), 747-750.
[95] Ganesamoorthy, C.; Schoening, J.; Wölper, C.; Song, L.; Schreiner, P. R.; Schulz, S., A silicon–carbonyl complex stable at room temperature. *Nat. Chem.* **2020**, *12* (7), 608-614.
[96] Weidenbruch, M.; Brand-Roth, B.; Pohl, S.; Saak, W., Ein cyclodimeres Silaketenimin. *Angew. Chem.* **1990**, *102* (1), 93-95.
[97] Abe, T.; Iwamoto, T.; Kabuto, C.; Kira, M., Synthesis, Structure, and Bonding of Stable Dialkylsilaketenimines. *J. Am. Chem. Soc.* **2006**, *128* (13), 4228-4229.
[98] Arrington, C. A.; Petty, J. T.; Payne, S. E.; Haskins, W. C. K., The reaction of dimethylsilylene with carbon monoxide in low-temperature matrices. *J. Am. Chem. Soc.* **1988**, *110* (18), 6240-6241.
[99] Hamilton, T. P.; Schaefer, H. F., III, Silaketene: A product of the reaction between silylene and carbon monoxide? *J. Chem. Phys.* **1989**, *90* (2), 1031-1035.
[100] Becerra, R.; Walsh, R., Silylene Does React with Carbon Monoxide. *J. Am. Chem. Soc.* **2000**, *122* (13), 3246-3247.
[101] Becerra, R.; Cannady, J. P.; Walsh, R., Silylene Does React with Carbon Monoxide: Some Gas-Phase Kinetic and Theoretical Studies. *J. Phys. Chem. A* **2001**, *105* (10), 1897-1903.

[102] Bornemann, H.; Sander, W., Reactions of methyl(phenyl)silylene with CO and PH_3—the formation of acid–base complexes. *J. Organomet. Chem.* **2002**, *641* (1-2), 156-164.
[103] Pearsall, M. A.; West, R., The reactions of diorganosilylenes with carbon monoxide. *J. Am. Chem. Soc.* **1988**, *110* (21), 7228-7229.
[104] Tacke, M.; Klein, C.; Stufkens, D. J.; Oskam, A.; Jutzi, P.; Bunte, A., Complexes of decamethylsilicocene: Cp_2*Si(CO) and Cp_2*Si(N_2). *Z. Anorg. Allg. Chem.* **1993**, *619* (5), 865-868.
[105] Mansikkamäki, A.; Power, P. P.; Tuononen, H. M., Computational Analysis of n→π* Back-Bonding in Metallylene − Isocyanide Complexes R_2MCNR' (M = Si, Ge, Sn; R = *t*Bu, Ph; R' = Me, *t*Bu, Ph). *Organometallics* **2013**, *32* (22), 6690-6700.
[106] Fischer, R. C.; Power, P. P., π-Bonding and the Lone Pair Effect in Multiple Bonds Involving Heavier Main Group Elements: Developments in the New Millennium. *Chem. Rev.* **2010**, *110* (7), 3877-3923.
[107] Kenkichi, S.; Shinobu, T.; Hideki, S.; Mitsuo, K., Generation and Trapping of Bis(dialkylamino)silylenes: Experimental Evidence for Bridged Structure of Diaminosilylene Dimers. *B. Chem. Soc. Jpn* **1997**, *70* (1), 253-260.
[108] Tsutsui, S.; Sakamoto, K.; Kira, M., Bis(diisopropylamino)silylene and Its Dimer. *J. Am. Chem. Soc.* **1998**, *120* (38), 9955-9956.
[109] Lee, G.-H.; West, R.; Müller, T., Bis[bis(trimethylsilyl)amino]silylene, an Unstable Divalent Silicon Compound. *J. Am. Chem. Soc.* **2003**, *125* (27), 8114-8115.
[110] Rekken, B. D.; Brown, T. M.; Fettinger, J. C.; Tuononen, H. M.; Power, P. P., Isolation of a Stable, Acyclic, Two-Coordinate Silylene. *J. Am. Chem. Soc.* **2012**, *134* (15), 6504-6507.
[111] Protchenko, A. V.; Birjkumar, K. H.; Dange, D.; Schwarz, A. D.; Vidovic, D.; Jones, C.; Kaltsoyannis, N.; Mountford, P.; Aldridge, S., A Stable Two-Coordinate Acyclic Silylene. *J. Am. Chem. Soc.* **2012**, *134* (15), 6500-6503.
[112] Lips, F.; Fettinger, J. C.; Mansikkamäki, A.; Tuononen, H. M.; Power, P. P., Reversible Complexation of Ethylene by a Silylene under Ambient Conditions. *J. Am. Chem. Soc.* **2014**, *136* (2), 634-637.
[113] Rekken, B. D.; Brown, T. M.; Fettinger, J. C.; Lips, F.; Tuononen, H. M.; Herber, R. H.; Power, P. P., Dispersion Forces and Counterintuitive Steric Effects in Main Group Molecules: Heavier Group 14 (Si–Pb) Dichalcogenolate Carbene Analogues with Sub-90° Interligand Bond Angles. *J. Am. Chem. Soc.* **2013**, *135* (27), 10134-10148.
[114] Protchenko, A. V.; Schwarz, A. D.; Blake, M. P.; Jones, C.; Kaltsoyannis, N.; Mountford, P.; Aldridge, S., A Generic One-Pot Route to Acyclic Two-Coordinate Silylenes from Silicon(IV) Precursors: Synthesis and Structural Characterization of a Silylsilylene. *Angew. Chem., Int. Ed.* **2013**, *52* (2), 568-571.
[115] Protchenko, A. V.; Blake, M. P.; Schwarz, A. D.; Jones, C.; Mountford, P.; Aldridge, S., Reactivity of Boryl- and Silyl-Substituted Carbenoids toward Alkynes: Insertion and Cycloaddition Chemistry. *Organometallics* **2015**, *34* (11), 2126-2129.
[116] Wendel, D.; Eisenreich, W.; Jandl, C.; Pöthig, A.; Rieger, B., Reactivity of an Acyclic Silylsilylene toward Ethylene: Migratory Insertion into the Si–Si Bond. *Organometallics* **2016**, *35* (1), 1-4.
[117] Harris, D. H.; Lappert, M. F., Monomeric, volatile bivalent amides of group IV elements, $M(NR^{12})_2$ and $M(NR^1R^2)_2$(M=Ge, Sn, or Pb; R^1=Me_3Si, R^2=Me_3C). *J. Am. Chem. Soc., Chem. Comm.* **1974**, (21), 895-896.
[118] Hadlington, T. J.; Abdalla, J. A. B.; Tirfoin, R.; Aldridge, S.; Jones, C., Stabilization of a two-coordinate, acyclic diaminosilylene (ADASi): completion of the series of isolable diaminotetrylenes, :$E(NR_2)_2$ (E = group 14 element). *Chem. Commun.* **2016**, *52* (8), 1717-1720.
[119] Ochiai, T.; Franz, D.; Inoue, S., Applications of N-heterocyclic imines in main group chemistry. *Chem. Soc. Rev.* **2016**, *45* (22), 6327-6344.
[120] Kuhn, N.; Fawzi, R.; Steinmann, M.; Wiethoff, J.; Bläser, D.; Boese, R., Synthese und Struktur von 2-Imino-l,3-dimethylimidazolin. *Z. Naturforsch.* **1995**, *50b*, 1779-1784.
[121] Back, O.; Donnadieu, B.; von Hopffgarten, M.; Klein, S.; Tonner, R.; Frenking, G.; Bertrand, G., *N*-Heterocyclic carbenes versus transition metals for stabilizing phosphinyl radicals. *Chem. Sci.* **2011**, *2* (5), 858-861.

[122] Kinjo, R.; Donnadieu, B.; Bertrand, G., Isolation of a Carbene-Stabilized Phosphorus Mononitride and Its Radical Cation ($PN^{+\cdot}$). *Angew. Chem., Int. Ed.* **2010**, *49* (34), 5930-5933.
[123] Dielmann, F.; Back, O.; Henry-Ellinger, M.; Jerabek, P.; Frenking, G.; Bertrand, G., A Crystalline Singlet Phosphinonitrene: A Nitrogen Atom–Transfer Agent. *Science* **2012**, *337* (6101), 1526-1528.
[124] Franz, D.; Irran, E.; Inoue, S., Isolation of a three-coordinate boron cation with a boron-sulfur double bond. *Angew. Chem., Int. Ed.* **2014**, *53* (51), 14264-8.
[125] Franz, D.; Szilvasi, T.; Irran, E.; Inoue, S., A monotopic aluminum telluride with an Al=Te double bond stabilized by *N*-heterocyclic carbenes. *Nat. Commun.* **2015**, *6*, 10037.
[126] Ochiai, T.; Szilvási, T.; Inoue, S., Facile Access to Stable Silylium Ions Stabilized by *N*-Heterocyclic Imines. *Molecules* **2016**, *21* (9), 1155.
[127] Lui, M. W.; Merten, C.; Ferguson, M. J.; McDonald, R.; Xu, Y.; Rivard, E., Contrasting Reactivities of Silicon and Germanium Complexes Supported by an *N*-Heterocyclic Guanidine Ligand. *Inorg. Chem.* **2015**, *54* (4), 2040-2049.
[128] Inoue, S.; Leszczyńska, K., An Acyclic Imino-Substituted Silylene: Synthesis, Isolation, and its Facile Conversion into a Zwitterionic Silaimine. *Angew. Chem., Int. Ed.* **2012**, *51* (34), 8589-8593.
[129] Loh, Y. K.; Ying, L.; Ángeles Fuentes, M.; Do, D. C. H.; Aldridge, S., An N-Heterocyclic Boryloxy Ligand Isoelectronic with N-Heterocyclic Imines: Access to an Acyclic Dioxysilylene and its Heavier Congeners. *Angew. Chem., Int. Ed.* **2019**, *58* (15), 4847-4851.
[130] Roy, M. M. D.; Ferguson, M. J.; McDonald, R.; Zhou, Y.; Rivard, E., A Vinyl Silylsilylene and its Activation of Strong Homo- and Heteroatomic Bonds. *Chem. Sci.* **2019**, *10* (26), 6476-6481.
[131] Crocker, R. D.; Nguyen, T. V., The Resurgence of the Highly Ylidic N-Heterocyclic Olefins as a New Class of Organocatalysts. *Chem. - Eur. J.* **2016**, *22* (7), 2208-2213.
[132] Roy, M. M. D.; Rivard, E., Pushing Chemical Boundaries with *N*-Heterocyclic Olefins (NHOs): From Catalysis to Main Group Element Chemistry. *Acc. Chem. Res.* **2017**, *50* (8), 2017-2025.
[133] Chu, T.; Nikonov, G. I., Oxidative Addition and Reductive Elimination at Main-Group Element Centers. *Chem. Rev.* **2018**, *118* (7), 3608-3680.
[134] Jordan, P. C., Lower Electronic Levels of the Radicals SiH, SiH_2, and SiH_3. *J. Chem. Phys.* **1966**, *44* (9), 3400-3406.
[135] Holthausen, M. C.; Koch, W.; Apeloig, Y., Theory Predicts Triplet Ground-State Organic Silylenes. *J. Am. Chem. Soc.* **1999**, *121* (11), 2623-2624.
[136] Gaspar, P. P.; Xiao, M.; Pae, D. H.; Berger, D. J.; Haile, T.; Chen, T.; Lei, D.; Winchester, W. R.; Jiang, P., The quest for triplet ground state silylenes. *J. Organomet. Chem.* **2002**, *646* (1), 68-79.
[137] Gordon, M. S., Potential-energy surfaces in singlet and triplet silylene. *Chem. Phys. Lett.* **1985**, *114* (4), 348-352.
[138] Yoshida, M.; Tamaoki, N., DFT Study on Triplet Ground State Silylenes Revisited: The Quest for the Triplet Silylene Must Go On. *Organometallics* **2002**, *21* (13), 2587-2589.
[139] Apeloig, Y.; Pauncz, R.; Karni, M.; West, R.; Steiner, W.; Chapman, D., Why Is Methylene a Ground State Triplet while Silylene Is a Ground State Singlet? *Organometallics* **2003**, *22* (16), 3250-3256.
[140] Skell, P. S.; Woodworth, R. C., Structure of Carbene, CH_2. *J. Am. Chem. Soc.* **1956**, *78* (17), 4496-4497.
[141] Kosa, M.; Karni, M.; Apeloig, Y., Were Reactions of Triplet Silylenes Observed? *J. Am. Chem. Soc.* **2013**, *135* (24), 9032-9040.
[142] Jiang, P.; Trieber, D.; Gaspar, P. P., Kinetic Studies on the Thermal Decomposition of trans-2,3-Dimethyl-1-tri-tert-butylsilyl-1-triisopropylsilylsilirane and the Mechanism of Silylene Generation. *Organometallics* **2003**, *22* (11), 2233-2239.
[143] Sekiguchi, A.; Tanaka, T.; Ichinohe, M.; Akiyama, K.; Tero-Kubota, S., Bis(tri-tert-butylsilyl)silylene: Triplet Ground State Silylene. *J. Am. Chem. Soc.* **2003**, *125* (17), 4962-4963.
[144] Sekiguchi, A.; Tanaka, T.; Ichinohe, M.; Akiyama, K.; Gaspar, P. P., Tri-tert-butylsilylsilylenes with Alkali Metal Substituents ($^tBu_3Si$)SiM (M = Li, K): Electronically and Sterically Accessible Triplet Ground States. *J. Am. Chem. Soc.* **2008**, *130* (2), 426-427.
[145] Riplinger, C.; Neese, F., An efficient and near linear scaling pair natural orbital based local coupled cluster method. *J. Chem. Phys.* **2013**, *138* (3), 034106.

[146] Riplinger, C.; Sandhoefer, B.; Hansen, A.; Neese, F., Natural triple excitations in local coupled cluster calculations with pair natural orbitals. *J. Chem. Phys.* **2013**, *139* (13), 134101.
[147] Kendall, R. A.; Jr., T. H. D.; Harrison, R. J., Electron affinities of the first-row atoms revisited. Systematic basis sets and wave functions. *J. Chem. Phys.* **1992**, *96* (9), 6796-6806.
[148] Woon, D. E.; Dunning Jr., T. H., Gaussian basis sets for use in correlated molecular calculations. III. The atoms aluminum through argon. *J. Chem. Phys.* **1993**, *98* (2), 1358-1371.
[149] Grimme, S.; Brandenburg, J. G.; Bannwarth, C.; Hansen, A., Consistent structures and interactions by density functional theory with small atomic orbital basis sets. *J. Chem. Phys.* **2015**, *143* (5), 054107.
[150] Holthausen, M. C., Personal communication. **2019**.
[151] Jutzi, P., New Element-Carbon (p-p)π Bonds. *Angew. Chem., Int. Ed.* **1975**, *14* (4), 232-245.
[152] Gusel'nikov, L. E.; Nametkin, N. S., Formation and properties of unstable intermediates containing multiple p_{π}-p_{π} bonded Group 4B metals. *Chem. Rev.* **1979**, *79* (6), 529-577.
[153] Becker, G.; Gresser, G.; Uhl, W., Acyl-und Alkylidenphosphane, XV 2.2-Dimethylpropylidinphosphan, eine stabile Verbindung mit einem Phosphoratom der Koordinationszahl 1/ Acyl- and Alkylidenephosphines, XV 2,2-Dimethylpropvlidynephosphine, a Stable Compound with a Phosphorus Atom of Coordination Number 1. *Z. Naturforsch. B* **1981**, *36* (1), 16-19.
[154] Brook, A. G.; Abdesaken, F.; Gutekunst, B.; Gutekunst, G.; Kallury, R. K., A solid silaethene: isolation and characterization. *J. Am. Chem. Soc., Chem. Comm.* **1981**, (4), 191-192.
[155] Yoshifuji, M.; Shima, I.; Inamoto, N.; Hirotsu, K.; Higuchi, T., Synthesis and Structure of Bis(2,4,6-tri-*tert*-butylphenyl)diphosphene: Isolation of a True Phosphobenzene. *J. Am. Chem. Soc.* **1981**, *103* (15), 4587-4589.
[156] West, R.; Fink, M. J.; Michl, J., Tetramesityldisilene, a Stable Compound Containing a Silicon-Silicon Double Bond. *Science* **1981**, *214* (4527), 1343-1344.
[157] Carter, E. A.; Goddard, W. A., Relation between singlet-triplet gaps and bond energies. *J. Phys. Chem.* **1986**, *90* (6), 998-1001.
[158] Trinquier, G.; Malrieu, J. P.; Riviere, P., Unusual bonding in trans-bent digermene. *J. Am. Chem. Soc.* **1982**, *104* (17), 4529-4533.
[159] Trinquier, G.; Malrieu, J. P., Nonclassical distortions at multiple bonds. *J. Am. Chem. Soc.* **1987**, *109* (18), 5303-5315.
[160] Malrieu, J. P.; Trinquier, G., Trans-bending at double bonds. Occurrence and extent. *J. Am. Chem. Soc.* **1989**, *111* (15), 5916-5921.
[161] Pearson, R. G., Symmetry rule for predicting molecular structures. *J. Am. Chem. Soc.* **1969**, *91* (18), 4947-4955.
[162] Levin, C. C., Qualitative molecular orbital picture of electronegativity effects on XH_3 inversion barriers. *J. Am. Chem. Soc.* **1975**, *97* (20), 5649-5655.
[163] Kira, M., Distortion Modes of Heavy Ethylenes and Their Anions: π–σ* Orbital Mixing Model. *Organometallics* **2011**, *30* (16), 4459-4465.
[164] P. Power, P., Homonuclear multiple bonding in heavier main group elements. *J. Am. Chem. Soc., Dalt. Trans.* **1998**, (18), 2939-2951.
[165] Lee, V. Y.; Fukawa, T.; Nakamoto, M.; Sekiguchi, A.; Tumanskii, B. L.; Karni, M.; Apeloig, Y., $(^tBu_2MeSi)_2Sn{=}Sn(SiMe^tBu_2)_2$: A Distannene with a >Sn=Sn< Double Bond That Is Stable Both in the Solid State and in Solution. *J. Am. Chem. Soc.* **2006**, *128* (35), 11643-11651.
[166] Weidenbruch, M., Recent Advances in the Chemistry of Silicon–Silicon Multiple Bonds. In *The Chemistry of Organic Silicon Compounds*, Rappoport, Z.; Apeloig, Y., Eds. John Wiley & Sons: Chichester, U. K., 2001; Vol. 3, pp 391-428.
[167] Renji, O.; West, R., Chemistry of Stable Disilenes. In *Adv. Organomet. Chem.*, Gordon, F.; Stone, A.; West, R., Eds. Academic Press: 1996; Vol. 39, pp 231-273.
[168] Kira, M.; Iwamoto, T., Progress in the Chemistry of Stable Disilenes. In *Adv. Organomet. Chem.*, West, R.; Hill, A. F., Eds. Academic Press: 2006; Vol. 54, pp 73-148.
[169] Kira, M., Bonding and structure of disilenes and related unsaturated group-14 element compounds. *Proc. Jpn. Acad., Ser. B* **2012**, *88* (5), 167-191.

[170] Iwamoto, T.; Ishida, S., Multiple Bonds with Silicon: Recent Advances in Synthesis, Structure, and Functions of Stable Disilenes. In *Functional Molecular Silicon Compounds II: Low Oxidation States*, Scheschkewitz, D., Ed. Springer International Publishing: Cham, **2014**; pp 125-202.

[171] Schmedake, T. A.; Haaf, M.; Apeloig, Y.; Müller, T.; Bukalov, S.; West, R., Reversible Transformation between a Diaminosilylene and a Novel Disilene. *J. Am. Chem. Soc.* **1999**, *121* (40), 9479-9480.

[172] Sekiguchi, A.; Inoue, S.; Ichinohe, M.; Arai, Y., Isolable Anion Radical of Blue Disilene $(^tBu_2MeSi)_2Si{=}Si(SiMe^tBu_2)_2$ Formed upon One-Electron Reduction: Synthesis and Characterization. *J. Am. Chem. Soc.* **2004**, *126* (31), 9626-9629.

[173] Inoue, S.; Ichinohe, M.; Sekiguchi, A., The Isolable Cation Radical of Disilene: Synthesis, Characterization, and a Reversible One-Electron Redox System. *J. Am. Chem. Soc.* **2008**, *130* (19), 6078-6079.

[174] Suzuki, K.; Matsuo, T.; Hashizume, D.; Tamao, K., Room-Temperature Dissociation of 1,2-Dibromodisilenes to Bromosilylenes. *J. Am. Chem. Soc.* **2011**, *133* (49), 19710-19713.

[175] Sasamori, T.; Hironaka, K.; Sugiyama, Y.; Takagi, N.; Nagase, S.; Hosoi, Y.; Furukawa, Y.; Tokitoh, N., Synthesis and Reactions of a Stable 1,2-Diaryl-1,2-dibromodisilene: A Precursor for Substituted Disilenes and a 1,2-Diaryldisilyne. *J. Am. Chem. Soc.* **2008**, *130* (42), 13856-13857.

[176] Ichinohe, M.; Kinjo, R.; Sekiguchi, A., The First Stable Methyl-Substituted Disilene: Synthesis, Crystal Structure, and Regiospecific MeLi Addition. *Organometallics* **2003**, *22* (23), 4621-4623.

[177] Wendel, D.; Szilvási, T.; Jandl, C.; Inoue, S.; Rieger, B., Twist of a Silicon–Silicon Double Bond: Selective *Anti*-Addition of Hydrogen to an Iminodisilene. *J. Am. Chem. Soc.* **2017**, *139* (27), 9156-9159.

[178] Wendel, D.; Szilvási, T.; Henschel, D.; Altmann, P. J.; Jandl, C.; Inoue, S.; Rieger, B., Precise Activation of Ammonia and Carbon Dioxide by an Iminodisilene. *Angew. Chem., Int. Ed.* **2018**, *57* (44), 14575-14579.

[179] Leszczyńska, K.; Abersfelder, K.; Mix, A.; Neumann, B.; Stammler, H. G.; Cowley, M. J.; Jutzi, P.; Scheschkewitz, D., Reversible Base Coordination to a Disilene. *Angew. Chem., Int. Ed.* **2012**, *51* (27), 6785-6788.

[180] Cowley, M. J.; Huch, V.; Rzepa, H. S.; Scheschkewitz, D., Equilibrium between a cyclotrisilene and an isolable base adduct of a disilenyl silylene. *Nat. Chem.* **2013**, *5*, 876-879.

[181] Schweizer, J. I.; Scheibel, M. G.; Diefenbach, M.; Neumeyer, F.; Würtele, C.; Kulminskaya, N.; Linser, R.; Auner, N.; Schneider, S.; Holthausen, M. C., A Disilene Base Adduct with a Dative Si–Si Single Bond. *Angew. Chem., Int. Ed.* **2016**, *55* (5), 1782-1786.

[182] Douglas, A. E.; Lutz, B. L., Spectroscopic identification of the SiH^+ molecule: The $A^1\Pi$–$X^1\Sigma^+$ system. *Can. J. Phys.* **1970**, *48* (3), 247-253.

[183] Grevesse, N.; Sauval, A. J., Identification of SiH^+ in the Solar Photospheric Spectrum. *A&A* **1970**, *9*, 232.

[184] Singh, P. D.; Vanlandingham, F. G., Line positions and oscillator strengths of rotation-vibration band of possible interstellar SiH and SiH^+. *A&A* **1978**, *66*, 87.

[185] Sannigrahi, A. B.; Buenker, R. J.; Hirsch, G.; Gu, J.-p., Ab initio configuration interaction study of the electronic spectrum of SiH^+. *Chem. Phys. Lett.* **1995**, *237* (3), 204-211.

[186] Gaspar, P. P., Learning from silylenes and supersilylenes. In *Organosilicon Chemistry VI: From molecules to materials, 1*, Auner, N.; Weis, J., Eds. Wiley-VCH: Weinheim, 2005; Vol. 2, pp 10-24.

[187] Gerdes, C.; Saak, W.; Haase, D.; Müller, T., Dibenzosilanorbornadienyl cations and their fragmentation into silyliumylidenes. *J. Am. Chem. Soc.* **2013**, *135* (28), 10353-61.

[188] Jutzi, P.; Mix, A.; Rummel, B.; Schoeller, W. W.; Neumann, B.; Stammler, H.-G., The $(Me_5C_5)Si^+$ Cation: A Stable Derivative of HSi^+. *Science* **2004**, *305* (5685), 849-851.

[189] Driess, M.; Yao, S.; Brym, M.; van Wüllen, C., Low-Valent Silicon Cations with Two-Coordinate Silicon and Aromatic Character. *Angew. Chem., Int. Ed.* **2006**, *45* (40), 6730-6733.

[190] Filippou, A. C.; Lebedev, Y. N.; Chernov, O.; Straßmann, M.; Schnakenburg, G., Silicon(II) Coordination Chemistry: N-Heterocyclic Carbene Complexes of Si^{2+} and SiI^+. *Angew. Chem., Int. Ed.* **2013**, *52* (27), 6974-6978.

[191] Xiong, Y.; Yao, S.; Inoue, S.; Irran, E.; Driess, M., The elusive silyliumylidene [ClSi:]$^{+}$ and silathionium [ClSi=S]$^{+}$ cations stabilized by bis(iminophosphorane) chelate ligand. *Angew. Chem., Int. Ed.* **2012**, *51* (40), 10074-7.

[192] Yeong, H.-X.; Xi, H.-W.; Li, Y.; Lim, K. H.; So, C.-W., A Silyliumylidene Cation Stabilized by an Amidinate Ligand and 4-Dimethylaminopyridine. *Chem. - Eur. J.* **2013**, *19* (35), 11786-11790.

[193] Takahiro, S.; Joon Soo, H.; Koji, H.; Nozomi, T.; Shigeru, N.; Norihiro, T., Synthesis and structure of stable 1,2-diaryldisilyne. *Pure and Applied Chemistry* **2010**, *82* (3), 603-612.

[194] Müller, T., Stability, Reactivity, and Strategies for the Synthesis of Silyliumylidenes, RSi:$^{+}$. A Computational Study. *Organometallics* **2010**, *29* (5), 1277-1283.

[195] Power, P. P., π-Bonding and the Lone Pair Effect in Multiple Bonds between Heavier Main Group Elements. *Chem. Rev.* **1999**, *99* (12), 3463-3504.

[196] Rivard, E.; Power, P. P., Multiple Bonding in Heavier Element Compounds Stabilized by Bulky Terphenyl Ligands. *Inorg. Chem.* **2007**, *46* (24), 10047-10064.

[197] Tsukasa, M.; Katsunori, S.; Tomohide, F.; Baolin, L.; Mikinao, I.; Yoshiaki, S.; Takashi, O.; Liangchun, L.; Megumi, K.; Makoto, H.; Yoshiyuki, T.; Daisuke, H.; Takeo, F.; Aiko, F.; Yongming, L.; Hayato, T.; Kohei, T., Synthesis and Structures of a Series of Bulky "Rind-Br" Based on a Rigid Fused-Ring s-Hydrindacene Skeleton. *B. Chem. Soc. Jpn* **2011**, *84* (11), 1178-1191.

[198] Agou, T.; Hayakawa, N.; Sasamori, T.; Matsuo, T.; Hashizume, D.; Tokitoh, N., Reactions of Diaryldibromodisilenes with N-Heterocyclic Carbenes: Formation of Formal Bis-NHC Adducts of Silyliumylidene Cations. *Chem. - Eur. J.* **2014**, *20* (30), 9246-9249.

[199] Ahmad, S. U.; Szilvási, T.; Inoue, S., A facile access to a novel NHC-stabilized silyliumylidene ion and C-H activation of phenylacetylene. *Chem. Commun.* **2014**, *50* (84), 12619-12622.

[200] Hayakawa, N.; Sadamori, K.; Mizutani, S.; Agou, T.; Sugahara, T.; Sasamori, T.; Tokitoh, N.; Hashizume, D.; Matsuo, T., Synthesis and Characterization of *N*-Heterocyclic Carbene-Coordinated Silicon Compounds Bearing a Fused-Ring Bulky Eind Group. *Inorganics* **2018**, *6* (1), 30.

[201] Frisch, P.; Inoue, S., NHC-stabilized Silyl-substituted Silyliumylidene Ions. *Dalt. Trans.* **2019**, *48* (28), 10403-10406.

[202] Li, Y.; Chan, Y.-C.; Leong, B.-X.; Li, Y.; Richards, E.; Purushothaman, I.; De, S.; Parameswaran, P.; So, C.-W., Trapping a Silicon(I) Radical with Carbenes: A Cationic cAAC–Silicon(I) Radical and an NHC–Parent-Silyliumylidene Cation. *Angew. Chem., Int. Ed.* **2017**, *56* (26), 7573-7578.

[203] Jutzi, P., The Pentamethylcyclopentadienylsilicon(II) Cation: Synthesis, Characterization, and Reactivity. *Chem. - Eur. J.* **2014**, *20* (30), 9192-9207.

[204] Ahmad, S. U.; Szilvási, T.; Irran, E.; Inoue, S., An NHC-Stabilized Silicon Analogue of Acylium Ion: Synthesis, Structure, Reactivity, and Theoretical Studies. *J. Am. Chem. Soc.* **2015**, *137* (17), 5828-36.

[205] Sarkar, D.; Wendel, D.; Ahmad, S. U.; Szilvási, T.; Pöthig, A.; Inoue, S., Chalcogen-atom transfer and exchange reactions of NHC-stabilized heavier silaacylium ions. *Dalt. Trans.* **2017**, *46* (46), 16014-16018.

[206] Lutters, D.; Merk, A.; Schmidtmann, M.; Müller, T., The Silicon Version of Phosphine Chalcogenides: Synthesis and Bonding Analysis of Stabilized Heavy Silaaldehydes. *Inorg. Chem.* **2016**, *55* (17), 9026-9032.

[207] Sarkar, D.; Nesterov, V.; Szilvási, T.; Altmann, P. J.; Inoue, S., The Quest for Stable Silaaldehydes: Synthesis and Reactivity of a Masked Silacarbonyl. *Chem. Eur. J.* **2019**, *25* (5), 1198-1202.

[208] Frisch, P.; Inoue, S., Lewis base-stabilized silyliumylidene ions in transition metal coordination chemistry. *Dalton Transactions* **2020**.

[209] Leszczyńska, K.; Mix, A.; Berger, R. J. F.; Rummel, B.; Neumann, B.; Stammler, H.-G.; Jutzi, P., The Pentamethylcyclopentadienylsilicon(II) Cation as a Catalyst for the Specific Degradation of Oligo(ethyleneglycol) Diethers. *Angew. Chem., Int. Ed.* **2011**, *50* (30), 6843-6846.

[210] Fritz-Langhals, E., Silicon(II) Cation Cp*Si:$^{+}$ X^{-}: A New Class of Efficient Catalysts in Organosilicon Chemistry. *Org. Process Res. Dev.* **2019**, *23* (11), 2369-2377.

[211] Leong, B.-X.; Lee, J.; Li, Y.; Yang, M.-C.; Siu, C.-K.; Su, M.-D.; So, C.-W., A Versatile NHC-Parent Silyliumylidene Cation for Catalytic Chemo- and Regioselective Hydroboration. *J. Am. Chem. Soc.* **2019**, *141* (44), 17629-17636.

[212] Rubin, M.; Schwier, T.; Gevorgyan, V., Highly Efficient $B(C_6F_5)_3$-Catalyzed Hydrosilylation of Olefins. *J. Org. Chem.* **2002**, *67* (6), 1936-1940.
[213] Simonneau, A.; Oestreich, M., 3-Silylated Cyclohexa-1,4-dienes as Precursors for Gaseous Hydrosilanes: The $B(C_6F_5)_3$-Catalyzed Transfer Hydrosilylation of Alkenes. *Angew. Chem., Int. Ed.* **2013**, *52* (45), 11905-11907.
[214] Oestreich, M.; Hermeke, J.; Mohr, J., A unified survey of Si–H and H–H bond activation catalysed by electron-deficient boranes. *Chem. Soc. Rev.* **2015**, *44* (8), 2202-2220.
[215] Brook, M. A., New Control Over Silicone Synthesis using SiH Chemistry: The Piers–Rubinsztajn Reaction. *Chem. - Eur. J.* **2018**, *24* (34), 8458-8469.
[216] Shannon, R., Revised effective ionic radii and systematic studies of interatomic distances in halides and chalcogenides. *Acta Cryst. A* **1976**, *32* (5), 751-767.
[217] Uhl, W., Terakis[bis(trimethylsilyl)methyl]dialan(4), eine Verbingung mit Aluminium-Aluminium-Bindung. *Z. Naturforsch.* **1988**, *43b*, 1113-1118.
[218] Roesky, H. W., The Renaissance of Aluminum Chemistry. *Inorg. Chem.* **2004**, *43* (23), 7284-7293.
[219] Dohmeier, C.; Robl, C.; Tacke, M.; Schnöckel, H., The Tetrameric Aluminum(I) Compound $[\{Al(\eta^5\text{-}C_5Me_5)\}_4]$. *Angew. Chem., Int. Ed.* **1991**, *30* (5), 564-565.
[220] Gauss, J.; Schneider, U.; Ahlrichs, R.; Dohmeier, C.; Schnoeckel, H., 27Al NMR spectroscopic investigation of aluminum(I) compounds: ab initio calculations and experiment. *J. Am. Chem. Soc.* **1993**, *115* (6), 2402-2408.
[221] Hofmann, A.; Tröster, T.; Kupfer, T.; Braunschweig, H., Monomeric $Cp^{3t}Al(I)$: synthesis, reactivity, and the concept of valence isomerism. *Chem. Sci.* **2019**, *10* (11), 3421-3428.
[222] Urwin, S. J.; Rogers, D. M.; Nichol, G. S.; Cowley, M. J., Ligand coordination modulates reductive elimination from aluminium(III). *Dalt. Trans.* **2016**, *45* (35), 13695-13699.
[223] Ganesamoorthy, C.; Loerke, S.; Gemel, C.; Jerabek, P.; Winter, M.; Frenking, G.; Fischer, R. A., Reductive elimination: a pathway to low-valent aluminium species. *Chem. Commun.* **2013**, *49* (28), 2858-2860.
[224] Cui, C.; Roesky, H. W.; Schmidt, H.-G.; Noltemeyer, M.; Hao, H.; Cimpoesu, F., Synthesis and Structure of a Monomeric Aluminum(I) Compound $[\{HC(CMeNAr)_2\}Al]$ (Ar=2,6–iPr$_2$C$_6$H$_3$): A Stable Aluminum Analogue of a Carbene. *Angew. Chem., Int. Ed.* **2000**, *39* (23), 4274-4276.
[225] Sudheendra Rao, M. N.; Roesky, H. W.; Anantharaman, G., Organoaluminum chemistry with low valent aluminum—recent developments. *J. Organomet. Chem.* **2002**, *646* (1), 4-14.
[226] Wehmschulte, R. J., The Chemistry of Low-Valent Organoaluminum Species. In *PATAI'S Chemistry of Functional Groups*, 2016; pp 1-30.
[227] Bonyhady, S. J.; Collis, D.; Frenking, G.; Holzmann, N.; Jones, C.; Stasch, A., Synthesis of a stable adduct of dialane(4) (Al_2H_4) via hydrogenation of a magnesium(I) dimer. *Nat. Chem.* **2010**, *2*, 865.
[228] Li, B.; Kundu, S.; Zhu, H.; Keil, H.; Herbst-Irmer, R.; Stalke, D.; Frenking, G.; Andrada, D. M.; Roesky, H. W., An open route to asymmetric substituted Al–Al bonds using Al(I)- and Al(III)-precursors. *Chem. Commun.* **2017**, *53* (17), 2543-2546.
[229] Tan, G.; Szilvási, T.; Inoue, S.; Blom, B.; Driess, M., An Elusive Hydridoaluminum(I) Complex for Facile C–H and C–O Bond Activation of Ethers and Access to Its Isolable Hydridogallium(I) Analogue: Syntheses, Structures, and Theoretical Studies. *J. Am. Chem. Soc.* **2014**, *136* (27), 9732-9742.
[230] Mellerup, S. K.; Cui, Y.; Fantuzzi, F.; Schmid, P.; Goettel, J. T.; Bélanger-Chabot, G.; Arrowsmith, M.; Krummenacher, I.; Ye, Q.; Engel, V.; Engels, B.; Braunschweig, H., Lewis-Base Stabilization of the Parent Al(I) Hydride under Ambient Conditions. *J. Am. Chem. Soc.* **2019**, *141* (42), 16954-16960.
[231] Bag, P.; Weetman, C.; Inoue, S., Experimental Realisation of Elusive Multiple-Bonded Aluminium Compounds: A New Horizon in Aluminium Chemistry. *Angew. Chem., Int. Ed.* **2018**, *57* (44), 14394-14413.
[232] Pluta, C.; Pörschke, K.-R.; Krüger, C.; Hildenbrand, K., An Al–Al One-Electron π Bond. *Angew. Chem., Int. Ed.* **1993**, *32* (3), 388-390.
[233] Uhl, W.; Vester, A.; Kaim, W.; Poppe, J., Dialan-Radikalanionen $[R_2Al\text{-}AlR_2]^{\cdot-}$. *J. Organomet. Chem.* **1993**, *454* (1), 9-13.

[234] Wehmschulte, R. J.; Ruhlandt-Senge, K.; Olmstead, M. M.; Hope, H.; Sturgeon, B. E.; Power, P. P., Reduction of a Tetraaryldialane to Generate Al–Al π-bonding. *Inorg. Chem.* **1993**, *32* (14), 2983-2984.
[235] Wright, R. J.; Brynda, M.; Power, P. P., Synthesis and Structure of the "Dialuminyne" Na_2[Ar'AlAlAr'] and Na_2[(Ar"Al)$_3$]: Al–Al Bonding in Al_2Na_2 and Al_3Na_2 Clusters. *Angew. Chem., Int. Ed.* **2006**, *45* (36), 5953-5956.
[236] Su, J.; Li, X.-W.; Crittendon, R. C.; Robinson, G. H., How Short is a -Ga≡Ga- Triple Bond? Synthesis and Molecular Structure of Na_2[Mes*$_2$C$_6$H$_3$-Ga≡Ga-C$_6$H$_3$Mes*$_2$] (Mes* = 2,4,6-*i*-Pr$_3$C$_6$H$_2$): The First Gallyne. *J. Am. Chem. Soc.* **1997**, *119* (23), 5471-5472.
[237] Wright, R. J.; Phillips, A. D.; Power, P. P., The [2 + 4] Diels−Alder Cycloadditon Product of a Probable Dialuminene, Ar'AlAlAr' (Ar' = C$_6$H$_3$- 2,6-Dipp$_2$; Dipp = C$_6$H$_3$-2,6-^{i}Pr$_2$), with Toluene. *J. Am. Chem. Soc.* **2003**, *125* (36), 10784-10785.
[238] Cui, C.; Li, X.; Wang, C.; Zhang, J.; Cheng, J.; Zhu, X., Isolation of a 1,2-Dialuminacyclobutene. *Angew. Chem., Int. Ed.* **2006**, *45* (14), 2245-2247.
[239] Agou, T.; Nagata, K.; Tokitoh, N., Synthesis of a Dialumene-Benzene Adduct and Its Reactivity as a Synthetic Equivalent of a Dialumene. *Angew. Chem., Int. Ed.* **2013**, *52* (41), 10818-10821.
[240] Nagata, K.; Agou, T.; Sasamori, T.; Tokitoh, N., Formation of a Diaminoalkyne Derivative by Dialumane-mediated Homocoupling of t-Butyl Isocyanide. *Chem. Lett.* **2015**, *44* (11), 1610-1612.
[241] Nagata, K.; Murosaki, T.; Agou, T.; Sasamori, T.; Matsuo, T.; Tokitoh, N., Activation of Dihydrogen by Masked Doubly Bonded Aluminum Species. *Angew. Chem., Int. Ed.* **2016**, *55* (41), 12877-12880.
[242] Moilanen, J.; Power, P. P.; Tuononen, H. M., Nature of Bonding in Group 13 Dimetallenes: a Delicate Balance between Singlet Diradical Character and Closed Shell Interactions. *Inorg. Chem.* **2010**, *49* (23), 10992-11000.
[243] Holzmann, N.; Stasch, A.; Jones, C.; Frenking, G., Structures and Stabilities of Group 13 Adducts [(NHC)(EX$_3$)] and [(NHC)$_2$(E$_2$X$_n$)] (E=B to In; X=H, Cl; n=4, 2, 0; NHC=N-Heterocyclic Carbene) and the Search for Hydrogen Storage Systems: A Theoretical Study. *Chem. - Eur. J.* **2011**, *17* (48), 13517-13525.
[244] Weetman, C.; Bag, P.; Szilvási, T.; Jandl, C.; Inoue, S., CO_2 Fixation and Catalytic Reduction by a Neutral Aluminum Double Bond. *Angew. Chem., Int. Ed.* **2019**, *58* (32), 10961-10965.
[245] Hicks, J.; Vasko, P.; Goicoechea, J. M.; Aldridge, S., Synthesis, structure and reaction chemistry of a nucleophilic aluminyl anion. *Nature* **2018**, *557* (7703), 92-95.
[246] Schwamm, R. J.; Anker, M. D.; Lein, M.; Coles, M. P., Reduction vs. Addition: The Reaction of an Aluminyl Anion with 1,3,5,7-Cyclooctatetraene. *Angew. Chem., Int. Ed.* **2019**, *58* (5), 1489-1493.
[247] Schwamm, R. J.; Coles, M. P.; Hill, M. S.; Mahon, M. F.; McMullin, C. L.; Rajabi, N. A.; Wilson, A. S. S., A Stable Calcium Alumanyl. *Angew. Chem., Int. Ed.* **2020**, *59* (10), 3928-3932.
[248] Kurumada, S.; Takamori, S.; Yamashita, M., An alkyl-substituted aluminium anion with strong basicity and nucleophilicity. *Nat. Chem.* **2020**, *12* (1), 36-39.
[249] Sugita, K.; Nakano, R.; Yamashita, M., Cycloaddition of Dialkylalumanyl Anion toward Unsaturated Hydrocarbons in (1+2) and (1+4) Modes. *Chem. - Eur. J.* **2020**, *26* (10), 2174-2177.
[250] Koshino, K.; Kinjo, R., Construction of σ-aromatic AlB_2 ring via Borane Coupling with a Dicoordinate Cyclic (Alkyl)(Amino)Aluminyl Anion. *J. Am. Chem. Soc.* **2020**, *142* (19), 9057-9062.
[251] Jensen, F., *Introduction to Computational Chemistry* John Wiley & Sons Ltd: Chichester, England, **2009**.
[252] Koch, W.; Holthausen, M. C., *A Chemist's Guide to Density Functional Theory, Second Edition*. Wily-VCH Verlag GmbH: Weinheim, **2001**.
[253] Lewars, E. G., Computational Chemistry Introduction to the Theory and Applications of Molecular and Quantum Mechanics. Springer International Publishing: **2016**; Vol. 3, p 728.
[254] Glendening, E. D.; Badenhoop, J. K.; Reed, A. E.; Carpenter, J. E.; Bohmann, J. A.; Morales, C. M.; Landis, C. R.; Weinhold, F. *NBO 6.0*, Theoretical Chemistry Institute, University of Wisconsin, Madison, **2013**.
[255] Glendening Eric, D.; Landis Clark, R.; Weinhold, F., NBO 6.0: Natural bond orbital analysis program. *J. Chem. Theory Comput.* **2013**, *34* (16), 1429-1437.

[256] Glendening Eric, D.; Landis Clark, R.; Weinhold, F., Natural bond orbital methods. *WIREs Comput Mol Sci* **2011**, *2* (1), 1-42.
[257] Matta, C. F.; Boyd, R. J., *The Quantum Theory of Atoms in Molecules*. Wiley -VCH, Weinheim: **2007**.
[258] Macchi, P.; Sironi, A., Chemical bonding in transition metal carbonyl clusters: complementary analysis of theoretical and experimental electron densities. *Coord. Chem. Rev.* **2003**, *238-239* (Supplement C), 383-412.
[259] Macchi, P.; Sironi, A., Interactions involving Metals - From 'Chemical Categories' to QTAIM, and Backwards. In *The Quantum Theory of Atoms in Molecules*, Matta, C. F.; Boyd, R. J., Eds. Wiley-VCH: Weinheim, **2007**.
[260] Sousa, S. F.; Fernandes, P. A.; Ramos, M. J., General Performance of Density Functionals. *J. Phys. Chem. A* **2007**, *111* (42), 10439-10452.
[261] Perdew, J. P.; Ruzsinszky, A.; Tao, J.; Staroverov, V. N.; Scuseria, G. E.; Csonka, G. I., Prescription for the design and selection of density functional approximations: More constraint satisfaction with fewer fits. *J. Chem. Phys.* **2005**, *123* (6), 062201.
[262] Perdew, J. P.; Schmidt, K., Jacob's ladder of density functional approximations for the exchange-correlation energy. *AIP Conf. Proc.* **2001**, *577* (1), 1-20.
[263] Vosko, S. H.; Wilk, L.; Nusair, M., Accurate spin-dependent electron liquid correlation energies for local spin density calculations: a critical analysis. *Can. J. Phys.* **1980**, *58* (8), 1200-1211.
[264] Stephens, P. J.; Devlin, F. J.; Chabalowski, C. F.; Frisch, M. J., Ab Initio Calculation of Vibrational Absorption and Circular Dichroism Spectra Using Density Functional Force Fields. *J. Phys. Chem.* **1994**, *98* (45), 11623-11627.
[265] Becke, A. D., Density-functional thermochemistry. III. The role of exact exchange. *J. Chem. Phys.* **1993**, *98* (7), 5648-5652.
[266] Lee, C.; Yang, W.; Parr, R. G., Development of the Colle-Salvetti correlation-energy formula into a functional of the electron density. *Phys. Rev. B* **1988**, *37* (2), 785-789.
[267] Zhao, Y.; Truhlar, D. G., Density Functionals with Broad Applicability in Chemistry. *Acc. Chem. Res.* **2008**, *41* (2), 157-167.
[268] Grimme, S.; Antony, J.; Ehrlich, S.; Krieg, H., A consistent and accurate ab initio parametrization of density functional dispersion correction (DFT-D) for the 94 elements H-Pu. *J. Chem. Phys.* **2010**, *132* (15), 154104.
[269] Arp, H.; Baumgartner, J.; Marschner, C.; Zark, P.; Müller, T., Dispersion Energy Enforced Dimerization of a Cyclic Disilylated Plumbylene. *J. Am. Chem. Soc.* **2012**, *134* (14), 6409-6415.
[270] Liptrot, D. J.; Power, P. P., London dispersion forces in sterically crowded inorganic and organometallic molecules. *Nat. Rev. Chem.* **2017**, *1*, 0004.
[271] Zhao, Y.; Schultz, N. E.; Truhlar, D. G., Exchange-correlation functional with broad accuracy for metallic and nonmetallic compounds, kinetics, and noncovalent interactions. *J. Chem. Phys.* **2005**, *123* (16), 161103.
[272] Scuseria, G. E.; Van Voorhis, T., Exchange energy functionals based on the density matrix expansion of the Hartree-Fock exchange term. *Molecular Physics* **1997**, *92* (3), 601-608.
[273] Voorhis, T. V.; Scuseria, G. E., A novel form for the exchange-correlation energy functional. *J. Chem. Phys.* **1998**, *109* (2), 400-410.
[274] Perdew, J. P.; Burke, K.; Ernzerhof, M., Generalized Gradient Approximation Made Simple. *Physical Review Letters* **1996**, *77* (18), 3865-3868.
[275] Stoll, H.; Pavlidou, C. M. E.; Preuß, H., On the calculation of correlation energies in the spin-density functional formalism. *Theor. Chim. Acta* **1978**, *49* (2), 143-149.
[276] Zhao, Y.; Truhlar, D. G., A new local density functional for main-group thermochemistry, transition metal bonding, thermochemical kinetics, and noncovalent interactions. *J. Chem. Phys.* **2006**, *125* (19), 194101.
[277] Mardirossian, N.; Head-Gordon, M., How Accurate Are the Minnesota Density Functionals for Noncovalent Interactions, Isomerization Energies, Thermochemistry, and Barrier Heights Involving Molecules Composed of Main-Group Elements? *J. Chem. Theory Comput.* **2016**, *12* (9), 4303-4325.

[278] Arrowsmith, M.; Schweizer, J. I.; Heinz, M.; Härterich, M.; Krummenacher, I.; Holthausen, M. C.; Braunschweig, H., Synthesis and reduction chemistry of mixed-Lewis-base-stabilised chloroborylenes. *Chem. Sci.* **2019**, *10* (19), 5095-5103.

[279] Lutters, D.; Severin, C.; Schmidtmann, M.; Müller, T., Activation of 7-Silanorbornadienes by N-Heterocyclic Carbenes: A Selective Way to N-Heterocyclic-Carbene-Stabilized Silylenes. *J. Am. Chem. Soc.* **2016**, *138* (18), 6061-6067.

[280] Wheeler, S. E.; Houk, K. N., Integration Grid Errors for Meta-GGA-Predicted Reaction Energies: Origin of Grid Errors for the M06 Suite of Functionals. *J. Chem. Theory Comput.* **2010**, *6* (2), 395-404.

[281] Ditchfield, R.; Hehre, W. J.; Pople, J. A., Self-Consistent Molecular-Orbital Methods. IX. An Extended Gaussian-Type Basis for Molecular-Orbital Studies of Organic Molecules. *J. Chem. Phys.* **1971**, *54* (2), 724-728.

[282] Hehre, W. J.; Ditchfield, R.; Pople, J. A., Self—Consistent Molecular Orbital Methods. XII. Further Extensions of Gaussian—Type Basis Sets for Use in Molecular Orbital Studies of Organic Molecules. *J. Chem. Phys.* **1972**, *56* (5), 2257-2261.

[283] Krishnan, R.; Binkley, J. S.; Seeger, R.; Pople, J. A., Self-consistent molecular orbital methods. XX. A basis set for correlated wave functions. *J. Chem. Phys.* **1980**, *72* (1), 650-654.

[284] McLean, A. D.; Chandler, G. S., Contracted Gaussian basis sets for molecular calculations. I. Second row atoms, Z=11–18. *J. Chem. Phys.* **1980**, *72* (10), 5639-5648.

[285] Schlegel, H. B., Optimization of equilibrium geometries and transition structures. *J. Comput. Chem.* **1982**, *3* (2), 214-218.

[286] Optimization in Gaussian16. https://gaussian.com/opt/ (accessed 04.04.2020).

[287] Frisch, M. J.; Trucks, G. W.; Schlegel, H. B.; Scuseria, G. E.; Robb, M. A.; Cheeseman, J. R.; Scalmani, G.; Barone, V.; Petersson, G. A.; Nakatsuji, H.; Caricato, M.; Li, X.; Hratchian, H. P.; Izmaylov, A. F.; Bloino, J.; Zheng, G.; Sonnenberg, J. L.; Hada, M.; Ehara, M.; Toyota, K.; Fukuda, R.; Hasegawa, J.; Ishida, M.; Nakajima, T.; Honda, Y.; Kitao, O.; Nakai, H.; Vreven, T.; Montgomery, J. A., Jr. ; Peralta, J. E.; Ogliaro, F.; Bearpark, M.; Heyd, J. J.; Brothers, E.; Kudin, K. N.; Staroverov, V. N.; Kobayashi, R.; Normand, J.; Raghavachari, K.; Rendell, A.; Burant, J. C.; Iyengar, S. S.; Tomasi, J.; Cossi, M.; Rega, N.; Millam, J. M.; Klene, M.; Knox, J. E.; Cross, J. B.; Bakken, V.; Adamo, C.; Jaramillo, J.; Gomperts, R.; Stratmann, R. E.; Yazyev, O.; Austin, A. J.; Cammi, R.; Pomelli, C.; Ochterski, J. W.; Martin, R. L.; Morokuma, K.; Zakrzewski, V. G.; Voth, G. A.; Salvador, P.; Dannenberg, J. J.; Dapprich, S.; Daniels, A. D.; Farkas, Ö.; Foresman, J. B.; Ortiz, J. V.; Cioslowski, J.; Fox, D. J. *Gaussian 09, Revision D.01*, Gaussian, Inc. : Wallingford, CT, USA, **2009**.

[288] Frisch, M. J.; Trucks, G. W.; Schlegel, H. B.; Scuseria, G. E.; Robb, M. A.; Cheeseman, J. R.; Scalmani, G.; Barone, V.; Mennucci, B.; Petersson, G. A.; Nakatsuji, H.; Caricato, M.; Li, X.; Hratchian, H. P.; Izmaylov, A. F.; Bloino, J.; Zheng, G.; Sonnenberg, J. L.; Hada, M.; Ehara, M.; Toyota, K.; Fukuda, R.; Hasegawa, J.; Ishida, M.; Nakajima, T.; Honda, Y.; Kitao, O.; Nakai, H.; Vreven, T.; Montgomery, J. A., Jr. ; Peralta, J. E.; Ogliaro, F.; Bearpark, M.; Heyd, J. J.; Brothers, E.; Kudin, K. N.; Staroverov, V. N.; Kobayashi, R.; Normand, J.; Raghavachari, K.; Rendell, A.; Burant, J. C.; Iyengar, S. S.; Tomasi, J.; Cossi, M.; Rega, N.; Millam, J. M.; Klene, M.; Knox, J. E.; Cross, J. B.; Bakken, V.; Adamo, C.; Jaramillo, J.; Gomperts, R.; Stratmann, R. E.; Yazyev, O.; Austin, A. J.; Cammi, R.; Pomelli, C.; Ochterski, J. W.; Martin, R. L.; Morokuma, K.; Zakrzewski, V. G.; Voth, G. A.; Salvador, P.; Dannenberg, J. J.; Dapprich, S.; Daniels, A. D.; Farkas, Ö.; Foresman, J. B.; Ortiz, J. V.; Cioslowski, J.; Fox, D. J. *Gaussian 09, Revision E.01*, Gaussian, Inc. : Wallingford CT, **2009**.

[289] Frisch, M. J.; Trucks, G. W.; Schlegel, H. B.; Scuseria, G. E.; Robb, M. A.; Cheeseman, J. R.; Scalmani, G.; Barone, V.; Petersson, G. A.; Nakatsuji, H.; Li, X.; Caricato, M.; Marenich, A. V.; Bloino, J.; Janesko, B. G.; Gomperts, R.; Mennucci, B.; Hratchian, H. P.; Ortiz, J. V.; Izmaylov, A. F.; Sonnenberg, J. L.; Williams; Ding, F.; Lipparini, F.; Egidi, F.; Goings, J.; Peng, B.; Petrone, A.; Henderson, T.; Ranasinghe, D.; Zakrzewski, V. G.; Gao, J.; Rega, N.; Zheng, G.; Liang, W.; Hada, M.; Ehara, M.; Toyota, K.; Fukuda, R.; Hasegawa, J.; Ishida, M.; Nakajima, T.; Honda, Y.; Kitao, O.; Nakai, H.; Vreven, T.; Throssell, K.; Montgomery Jr., J. A.; Peralta, J. E.; Ogliaro, F.; Bearpark, M. J.; Heyd, J. J.; Brothers, E. N.; Kudin, K. N.; Staroverov, V. N.; Keith, T. A.; Kobayashi, R.; Normand, J.; Raghavachari, K.; Rendell, A. P.; Burant, J. C.;

Iyengar, S. S.; Tomasi, J.; Cossi, M.; Millam, J. M.; Klene, M.; Adamo, C.; Cammi, R.; Ochterski, J. W.; Martin, R. L.; Morokuma, K.; Farkas, O.; Foresman, J. B.; Fox, D. J. *Gaussian 16 Rev. B.01*, Gaussian, Inc. : Wallingford, CT, **2016**.

[290] Minkin, V. I., Glossary of terms used in theoretical organic chemistry. *Pure and Applied Chemistry* **1999**, *71* (10), 1919-1981.

[291] Fukui, K., The path of chemical reactions - the IRC approach. *Acc. Chem. Res.* **1981**, *14* (12), 363-368.

[292] Ditchfield, R., Self-consistent perturbation theory of diamagnetism. *Molecular Physics* **1974**, *27* (4), 789-807.

[293] Wolinski, K.; Hinton, J. F.; Pulay, P., Efficient implementation of the gauge-independent atomic orbital method for NMR chemical shift calculations. *J. Am. Chem. Soc.* **1990**, *112* (23), 8251-8260.

[294] Dreuw, A.; Head-Gordon, M., Single-Reference ab Initio Methods for the Calculation of Excited States of Large Molecules. *Chem. Rev.* **2005**, *105* (11), 4009-4037.

[295] Weinhold, F.; Landis, C. R., *Valency and Bonding: A Natural Bond Orbital Donor-Acceptor Perspective*. Cambridge University Press: Cambridge, **2005**.

[296] Weinhold, F.; Landis Clark, R., *Discovering Chemistry with Natural Bond Orbitals*. John Wiley & Sons, Inc.: New Jersey, **2012**; p 51-91.

[297] Wiberg, K. B., Application of the pople-santry-segal CNDO method to the cyclopropylcarbinyl and cyclobutyl cation and to bicyclobutane. *Tetrahedron* **1968**, *24* (3), 1083-1096.

[298] Andrienko, G. A. *ChemCraft - graphical software for visualization of quantum chemistry computations*, http://www.chemcraftprog.com, **2015**.

[299] Glendening, E. D.; Badenhoop, J. K.; Weinhold, F., Natural resonance theory: III. Chemical applications. *J. Comput. Chem.* **1998**, *19* (6), 628-646.

[300] Glendening, E. D.; Weinhold, F., Natural resonance theory: I. General formalism. *J. Comput. Chem.* **1998**, *19* (6), 593-609.

[301] Glendening, E. D.; Weinhold, F., Natural resonance theory: II. Natural bond order and valency. *J. Comput. Chem.* **1998**, *19* (6), 610-627.

[302] Cremer, D.; Kraka, E., Chemische Bindungen ohne Bindungselektronendichte – reicht die Differenzdichteanalyse zur Bindungsbeschreibung aus? *Angew. Chem.* **1984**, *96* (8), 612-614.

[303] Keith, T. A. *AIMAll (Version 17.01.25)*, TK Gristmill Software, Overland Park KS, USA, **2017**.

[304] Keith, T. A. *AIMAll (Version 19.02.13)*, TK Gristmill Software, Overland Park KS, USA, **2019**.

[305] Lu, T., Multiwfn 3.3.7 - A Multifunctional Wave function Analyzer School of Chemical and Biological Engineering, University of Science and Technology, Beijing, China **2013**.

[306] Lu, T., Multiwfn 3.5 - A Multifunctional Wavefunction Analyzer. School of Chemical and Biological Engineering, University of Science and Technology, Beijing **2018**.

[307] Lu, T.; Chen, F., Multiwfn: A multifunctional wavefunction analyzer. *J. Comput. Chem.* **2012**, *33* (5), 580-592.

[308] Wendel, D.; Porzelt, A.; Herz, F. A. D.; Sarkar, D.; Jandl, C.; Inoue, S.; Rieger, B., From Si(II) to Si(IV) and Back: Reversible Intramolecular Carbon–Carbon Bond Activation by an Acyclic Iminosilylene. *J. Am. Chem. Soc.* **2017**, *139* (24), 8134-8137.

[309] Yao, S.; Brym, M.; van Wüllen, C.; Driess, M., From a Stable Silylene to a Mixed-Valent Disiloxane and an Isolable Silaformamide–Borane Complex with Considerable Silicon–Oxygen Double-Bond Character. *Angew. Chem., Int. Ed.* **2007**, *46* (22), 4159-4162.

[310] Sen, S. S., A Stable Silanone with a Three-Coordinate Silicon Atom: A Century-Long Wait is Over. *Angew. Chem., Int. Ed.* **2014**, *53* (34), 8820-8822.

[311] Reiter, D.; Frisch, P.; Szilvási, T.; Inoue, S., Heavier Carbonyl Olefination: The Sila-Wittig Reaction. *J. Am. Chem. Soc.* **2019**, *141* (42), 16991-16996.

[312] Wendel, D.; Reiter, D.; Porzelt, A.; Altmann, P. J.; Inoue, S.; Rieger, B., Silicon and Oxygen's Bond of Affection: An Acyclic Three-Coordinate Silanone and Its Transformation to an Iminosiloxysilylene. *J. Am. Chem. Soc.* **2017**, *139* (47), 17193-17198.

[313] Reiter, D.; Holzner, R.; Porzelt, A.; Altmann, P. J.; Frisch, P.; Inoue, S., Disilene-Silylene Interconversion: A Synthetically Accessible Acyclic Bis(silyl)silylene. *J. Am. Chem. Soc.* **2019**, *141* (34), 13536-13546.

[314] Reiter, D.; Holzner, R.; Porzelt, A.; Frisch, P.; Inoue, S., Silylated silicon–carbonyl complexes as mimics of ubiquitous transition-metal carbonyls. *Nat. Chem.* **2020**, *12* (12), 1131-1135.

[315] Bag, P.; Porzelt, A.; Altmann, P. J.; Inoue, S., A Stable Neutral Compound with an Aluminum–Aluminum Double Bond. *J. Am. Chem. Soc.* **2017**, *139* (41), 14384-14387.

[316] Weetman, C.; Porzelt, A.; Bag, P.; Hanusch, F.; Inoue, S., Dialumenes – Aryl vs. Silyl Stabilisation for Small Molecule Activation and Catalysis. *Chem. Sci.* **2020**, *11* (18), 4817-4827.

[317] Porzelt, A.; Schweizer, J.; Baierl, R.; Altmann, P.; Holthausen, M.; Inoue, S., S–H Bond Activation in Hydrogen Sulfide by NHC-Stabilized Silyliumylidene Ions. *Inorganics* **2018**, *6* (2), 54.

[318] Frisch, P.; Szilvasi, T.; Porzelt, A.; Inoue, S., Transition Metal Carbonyl Complexes of an N-Heterocyclic Carbene Stabilized Silyliumylidene Ion. *Inorg. Chem.* **2019**, *58* (21), 14931-14937.

[319] Porzelt, A.; Inoue, S., Reactivity of NHC-stabilised silyliumylidene ions, Unpublished results. **2020**.